ZooKeys 859: 1–15 (2019)
doi: 10.3897/zookeys.859.34117
http://zookeys.pensoft.net

RESEARCH ARTICLE

A peer-reviewed open-access journal
ZooKeys
Launched to accelerate biodiversity research

Guess who? On the importance of using appropriate name: case study of *Marphysa sanguinea* (Montagu, 1813)

Nicolas Lavesque[1,2], Guillemine Daffe[3], Jacques Grall[4], Joana Zanol[5], Benoit Gouillieux[1,2], Pat Hutchings[6,7]

1 *Université de Bordeaux, EPOC, UMR 5805, Station Marine d'Arcachon, 33120 Arcachon, France* **2** *CNRS, EPOC, UMR 5805, Station Marine d'Arcachon, 33120 Arcachon, France* **3** *CNRS, Université de Bordeaux, Observatoire Aquitain des Sciences de l'Univers, UMS 2567 POREA, 33615 Pessac, France* **4** *Université de Brest, CNRS, UMS 3113, Observatoire, Séries Faune-Flore, OSU-IUEM, 29280 Plouzané, France* **5** *Laboratório de Biodiversidade de Annelida, Departamento de Invertebrados, Museu Nacional, Universidade Federal do Rio de Janeiro, Rio de Janeiro, Brazil* **6** *Australian Museum Research Institute, Australian Museum, Sydney, Australia* **7** *Department of Biological Sciences, Macquarie University, North Ryde 2109, Australia*

Corresponding author: *Nicolas Lavesque* (nicolas.lavesque@u-bordeaux.fr)

Academic editor: *Chris Glasby* | Received 26 February 2019 | Accepted 14 May 2019 | Published 2 July 2019

http://zoobank.org/1EBB6796-08EB-4F12-83FB-4CE146055DFC

Citation: Lavesque N, Daffe G, Grall J, Zanol J, Gouillieux B, Hutchings P (2019) Guess who? On the importance of using appropriate name: case study of *Marphysa sanguinea* (Montagu, 1813). ZooKeys 859:1–15. https://doi.org/10.3897/zookeys.859.34117

Abstract

The common bait worm *Marphysa sanguinea* (Montagu, 1813), originally described from the south coast of England, is the type species of the genus. This species has been widely reported from all around the world and has been considered as cosmopolitan until recently. This is partly because the original description was very brief and poorly illustrated, and also because all species superficially look similar. In order to clarify the situation, *M. sanguinea* was redescribed and a neotype was designated by Hutchings and Karageorgpoulos in 2003. Recently, specimens from Cornwall, close to the type locality, were sampled, examined morphologically, and used to obtain COI gene sequences for this species. Molecular results permitted us to confirm the identity and presence of *M. sanguinea* along the French coasts and to highlight the presence of inaccurate sequences of this species on GenBank. Use of this "false" cosmopolitan species at a worldwide scale by many biologists is also discussed in this paper.

Keywords
Bait worms, cosmopolitan species, misidentification, molecular, taxonomy

Introduction

Eunicidae Berthold, 1827 is a very speciose family with eleven recent genera and more than 400 valid species distributed worldwide (Read and Fauchald 2019a). The genus *Marphysa* de Quatrefages, 1866 comprises approximately 70 valid species (Read and Fauchald 2019b) and many of these have similar general morphology. *Marphysa sanguinea* (Montagu, 1813), type species of the genus, has a brief and poorly illustrated original description, which could fit most species of the genus. Thus, *M. sanguinea* has been considered for decades as a cosmopolitan species (Hutchings and Kupriyanova 2017). Indeed, this species was reported from Europe (Fauvel 1923; Parapar et al. 1993; Lewis and Karageorgopoulos 2008; Hutchings et al. 2012), Grand Caribbean Region (Salazar-Vallejo and Carrera-Parra 1998), Pacific and Atlantic coasts of North America (Leidy 1855; Webster 1879; Hartman 1944; Fauchald 1970), Atlantic Coast of South America (Morgado and Tanaka 2001), Red Sea (Fauvel 1953), Africa (Day 1967; Kouadio et al. 2008; Lamptey and Armah 2008), Asia (Miura 1977), and Australia (Day 1967).

In the absence of type material, Hutchings and Karageorgopoulos (2003) decided to clarify the status of this species and described a neotype. They provided a complete description of specimens from the type locality (Cornwall, England) together with SEM plates and data about habitat and reproduction. Subsequent to this work, several species previously identified as *M. sanguinea* at a worldwide scale were carefully checked and some described as new species: *Marphysa mullawa* Hutchings & Karageorgopoulos, 2003 (from Australia), *Marphysa elityeni* Lewis & Karageorgopoulos, 2008 (from South Africa), *Marphysa kristiani* Zanol, da Silva & Hutchings, 2016 (from Australia), *Marphysa victori* Lavesque, Daffe, Bonifácio & Hutchings, 2017 (from France), *Marphysa hongkongensa* Wang, Zhang & Qiu, 2018 (from Hong-Kong), *Marphysa aegypti* Elgetany, El-Ghobashy, Ghoneim & Struck, 2018 (from Egypt), and also a suite of species from China where most previous records recorded *M. sanguinea* as being present: *Marphysa multipectinata*, *Marphysa tribranchiata* and *Marphysa tripectinata* Liu, Hutchings & Sun, 2017, *Marphysa bulla* Liu, Hutchings & Kupriyanova, 2018, *Marphysa maxidenticulata* Liu, Hutchings & Kupriyanova, 2018. Molina-Acevedo and Carrera-Parra (2015) also refuted the presence of *M. sanguinea* in the Grand Caribbean region. All these works confirm the absence of *M. sanguinea* outside European waters. Most of these recent studies provide molecular data for type specimens and compare them to sequences stored in GenBank (NCBI), including sequences of *M. sanguinea* from several localities, but none from the type locality.

In this study, we test the identification of *M. sanguinea* cytochrome oxidase I (COI) sequences in GenBank, comparing them with those of specimens from the type locality (Cornwall, UK). We have also carefully checked and described the studied material.

Materials and methods

Sampling and morphological analyses

Specimens were collected in subtidal turf slabs in Arcachon Bay, in intertidal soft rocks in Bay of Brest (France) and in rocks easily split to extract the worms in Plymouth Sound (Cornwall, UK), close to the type locality. Specimens from Brest and Cornwall were fixed and preserved in 96% ethanol. For the Arcachon specimen, several posterior parapodia were removed and fixed in 96% ethanol for molecular studies. The rest of specimen was fixed in 4% formaldehyde seawater solution, then transferred to 70% ethanol for morphological analyses. Preserved specimens were examined under a Nikon SMZ25 stereomicroscope and a Nikon Eclipse E400 microscope and photographed with a Nikon DS-Ri 2 camera. Measurements were made with the NIS-Elements Analysis software. Selected parapodia along the body were removed from one specimen from Brest (AM W.49086) and examined under the scanning electron microscope (JEOL JSM 6480LA) and imaged with a secondary detector at Macquarie University, Sydney, Australia.

Morphological terminology is based on previous studies of Paxton (2000) and Zanol et al. (2014) for general terms and pattern of subacicular hook colour, and Molina-Acevedo and Carrera-Parra (2015, 2017) for jaw morphology and for description of chaetae.

The studied material is deposited at the Australian Museum, Sydney (**AM**), National Museum of Brazil, Rio de Janeiro (**MNRJ**) and the Muséum National d'Histoire Naturelle, Paris (**MNHN**).

Molecular data and analyses

Sub-samples for DNA analysis were removed from specimens, placed in ethanol 96% and frozen at -20 °C. Extraction of DNA was done with QIAamp DNA Micro Kit (QIAGEN) following protocol supplied by the manufacturers. Approximately 600 bp of COI (cytochrome c oxidase subunit I) gene was amplified, using primers polyLCO and polyHCO COI (Carr et al. 2011). PCR (Polymerase Chain Reaction) occurred in 50 µL mixtures containing: 10µL of 5X Colorless GoTaq Reaction Buffer (final concentration of 1X), 1.5 µL of $MgCl_2$ solution (final concentration of 1.5mM), 1 µL of PCR nucleotide mix (final concentration of 0.2 mM each dNTP), 0.5 µl of each primer (final concentration of 1µM), 0.2 µl of GoTaq G2 Flexi DNA Polymerase (5U/µl), 1 µl template DNA and 33.8 µL of nuclease-free water. The temperature profile was as follows for 16S: 94 °C/600s - (94 °C/60s-59 °C/30s-72 °C/90s)*40 cycles - 72 °C/600s - 4 °C, for COI: 94 °C/600s - (94 °C/40s-44 °C/40s-72 °C/60s)*5 cycles - (94 °C/40s-51 °C/40s-72 °C/60s)*35 cycles - 72 °C/300s - 4 °C. PCR success was verified by electrophoresis in a 1 % p/v agarose gel stained with ethidium bromide.

Amplified products were sent to GATC Biotech Company to complete double strain sequencing, using same set of primers as used for PCR.

Overlapping sequence (forward and reverse) fragments were merged into consensus sequences and aligned using Clustal Omega. COI sequences were translated into amino acid alignment and checked for stop codons in order to avoid pseudogenes. The minimum length coverage was around 590 bp.

Pairwise Kimura 2-parameter (K2P) genetic distance and Maximum Likelihood tree using K2P model and non-parametric bootstrap branch support (1000 replicates) was performed using MEGA version 7.0.26. Tree-based analysis was obtained with all *Marphysa* species and available (and exploitable) sequences of *M. sanguinea* in GenBank. Other genera of Eunicidae were considered as outgroup.

Results

Taxonomic Account

Family Eunicidae Berthold, 1827

Genus *Marphysa* Quatrefages, 1866

Type species. *Nereis sanguinea* Montagu, 1813

***Marphysa sanguinea* (Montagu, 1813)**
Figs 1–3

Material examined. MNHN-IA-TYPE 1856, one complete specimen, Mount Edgcumbe, Plymouth Sound, Cornwall, UK (50°20'59"N, 4°09'52"W), intertidal in soft rocks, 04 November 2017. MNRJP002048, one complete specimen, Mount Edgcumbe, Plymouth Sound, Cornwall (UK) (50°20'59"N, 4°09'52"W), intertidal in soft rocks, 04 November 2017. AM W.51410, one complete specimen, Mount Edgcumbe, Plymouth Sound, Cornwall (UK) (50°20'59"N, 4°09'52"W), intertidal in soft rocks, 04 November 2017. MNHN-IA-TYPE 1857, one complete specimen, Pyla, Arcachon Bay, France (44°33'57"N, 1°14'16"W), subtidal in turf slab (8m depth), 29 October 2017. AM W. 49085, one complete specimen, Logonna-Daoulas, Bay of Brest, France (48°19'37"N, 4°19'27"W), intertidal in soft rocks, 18 October 2016. AM W.49086, Logonna-Daoulas, Bay of Brest, France (48°19'37"N, 4°19'27"W), intertidal in soft rocks, 18 October 2016, several parapodia mounted for SEM. AM W. 27392, one complete specimen, Devon, Plymouth, Mount Edgcumbe (50°21'10"N, 4°09'30"W), intertidal from burrows in rock crevices, 25 October 1999.

Description. Body relatively long, with complete individuals ranging from 48.1 (ca. 138 chaetigers) to 163.1 mm (ca. 270 chaetigers) in length and from 3.7 to 6.6 mm in width (chaetiger 10 with parapodia), with same width throughout, slightly tapering

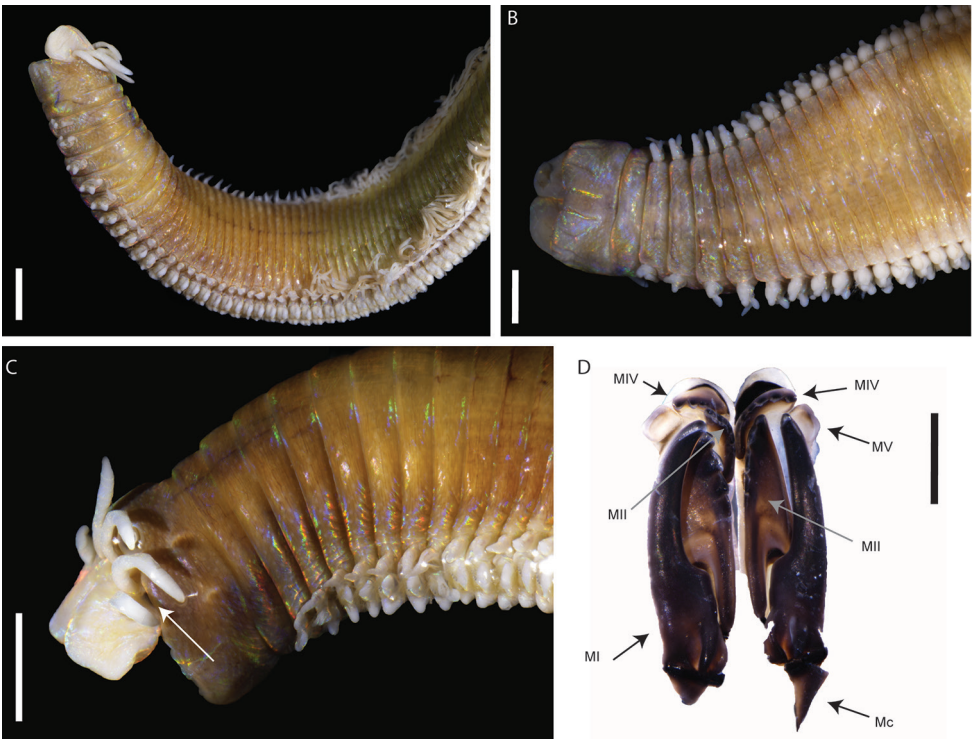

Figure 1. *Marphysa sanguinea*: **A** anterior part, dorsolateral view (MNHN-IA-TYPE 1856) **B** anterior part, ventral view (MNHN-IA-TYPE 1856) **C** anterior part, lateral view (MNRJP002048) **D** Maxillae, dorsal view (MNHN-IA-TYPE 1856). Key: white arrow showing eye; MI to MV, maxillae I to V, Mc, maxillary carriers. Scale bars: 2 mm (**A–C**), 1mm (**D**).

at anterior end and abruptly tapering at posterior end. Body cylindrical on anterior chaetigers, becoming dorsoventrally flattened. Prostomium slightly shorter than anterior ring of peristomium, as wide as peristomium, bilobed with buccal lips separated by deep ventral and dorsal notch with each lobe rounded (Fig. 1B, C). Anterior ring of peristomium longer than posterior ring (2 to 3 times) (Fig. 1B, C). Eyes present, positioned posteriorly between palps and lateral antennae (Fig. 1C). Prostomial appendages slightly wrinkled, arranged in arc on the posterior margin of the prostomium; median antenna longer than lateral antennae reaching first chaetiger (Fig. 1A), palps shortest appendages (Fig. 1A, C). MI more than three times as long as carrier and five times longer than closing system. MIII located ventroanterior to MII. Attachment lamella of MIII long and thin, placed at the middle of the plate. Left MIV with attachment lamella semicircular, thin, situated along anterior edge. Right MIV with attachment lamella semicircular, larger than left one, situated along anterior edge. Maxillary formula: I=1+1, II=3−4+5, III=6-7+0, IV=4+5−6, V=1+1 (Fig. 1D).

First few parapodia smaller than subsequent ones but all similar in structure. Notopodial cirri elongate and triangular (Figs 1C, 2A), digitiform in last chaetigers (Fig. 2C); longer than chaetal lobe. Ventral cirri from chaetiger 1 to 4–5 conical to tapering,

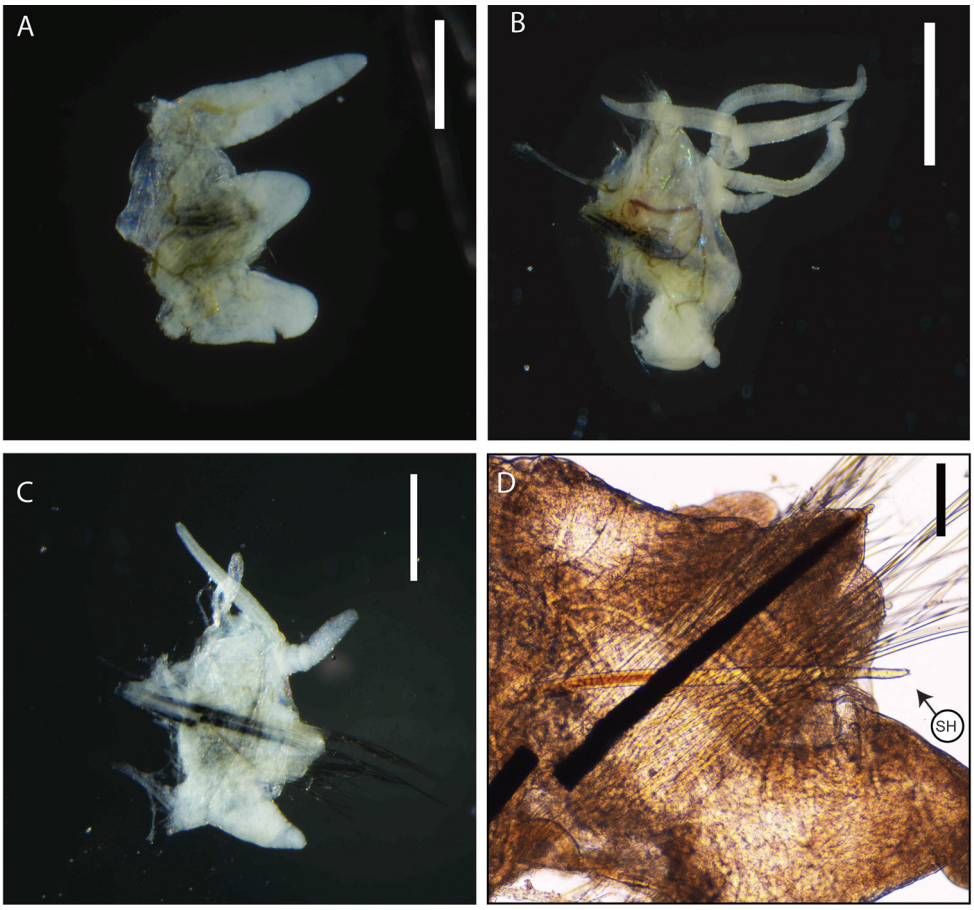

Figure 2. *Marphysa sanguinea* (MNHN-IA-TYPE 1856): **A** parapodium from anterior chaetiger **B** parapodium from mid-body **C** parapodia from posterior chaetiger **D** parapodium from posterior chaetiger. Abbreviation: SH, Subacicular hook. Scale bars: 1 mm (**B**), 500µm (**A, C**), 100µm (**D**).

with round wide tips, shorter than notopodial cirri (Fig. 2A); basally inflated from chaetiger 5–6, inflated base of round shape with round tip (Figs 1B, 2B); last chaetigers with triangular cirri (Fig. 2C). Pre-chaetal lobe inconspicuous; post-chaetal lobe from first chaetigers triangular swollen (Fig. 2A), longer than chaetal lobe, becoming inconspicuous from ca. chaetigers 15–20 (Figs 2B, C). Branchiae pectinate, from chaetiger 21 (from chaetiger 13 for small specimens) (Figs 1A, 2B), extending posteriorly by last 5–15 chaetigers; number of branchial filaments increasing from one in first chaetigers to maximum four in mid-body (Fig. 2B), posterior chaetigers with two filaments; filaments slightly annulated.

Chaetae arranged in two bundles: supra-acicular and sub-acicular, separated by a row of aciculae. Aciculae dark, tapering, very protruding, 1–4 per parapodium in anterior chaetigers and 2–3 in mid and posterior chaetigers. Single subacicular bifid hook present from chaetiger 21–25 to nearly end of body, dark on base to middle

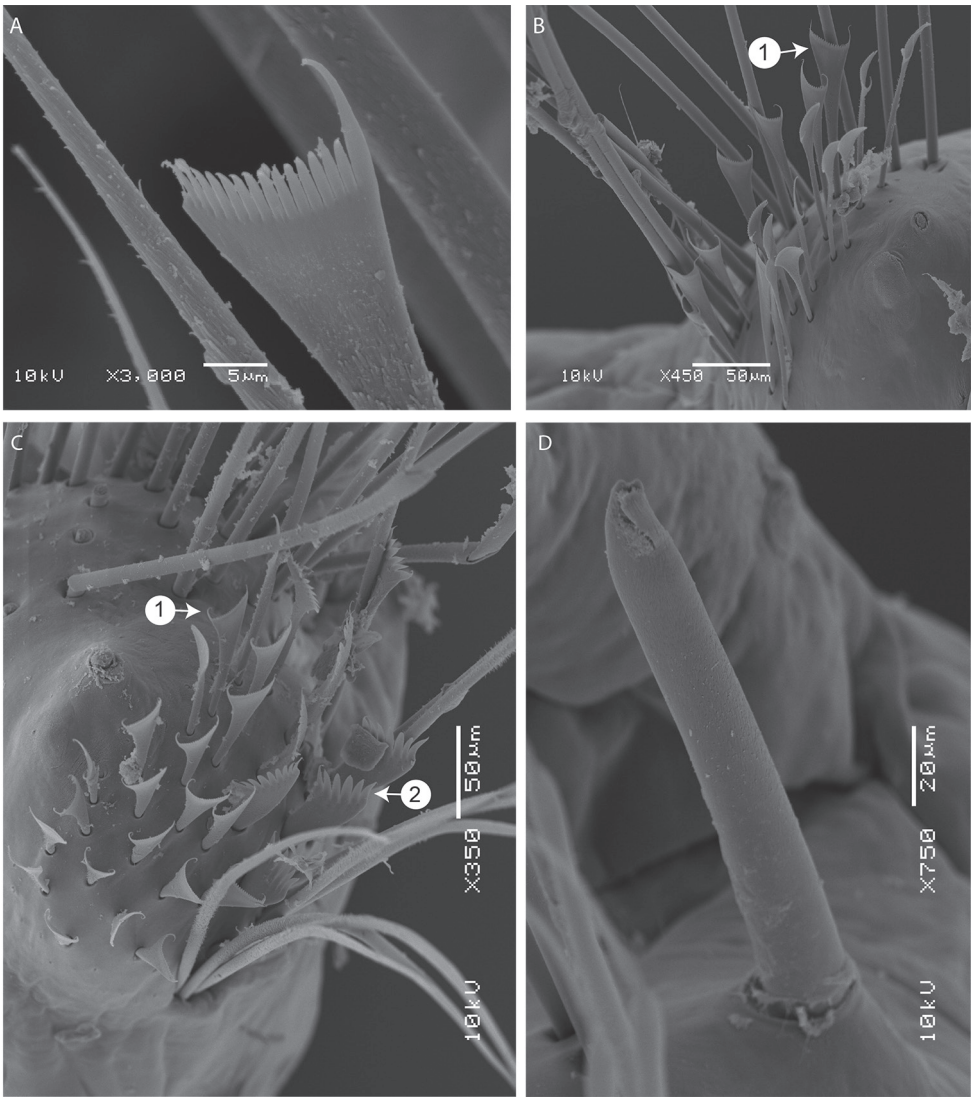

Figure 3. SEM images of *Marphysa sanguinea*: **A** isodont, symmetrical pectinate chaetae from anterior chaetiger (AM W.49086, 3rd chaetiger) **B** isodont, symmetrical pectinate chaetae from mid-body chaetiger (AM W.49086, chaetiger 108) **C** the two types of pectinate chaetae (AM W.49086, far posterior chaetiger) **D** subacicular bifid hook (AM W.49086, chaetiger 142). Numbers in white circles indicate the type of pectinate chaetae.

and translucent at the distal end (Figs 2D, 3D). Supra-acicular bundle with limbate and pectinate chaetae; sub-acicular with compound spiniger chaetae. Between 10 to 20 limbate chaetae, chaetae of different lengths with hirsute blades, similar to each other. Pectinate chaetae present from chaetiger 2–3 (with up to 28 pectinate chaetae within a single parapodia), restricted to supra-acicular fascicle. Pectinate chaetae of two types. In anterior parapodia, isodonts narrow (n < 10) with long internal teeth (with

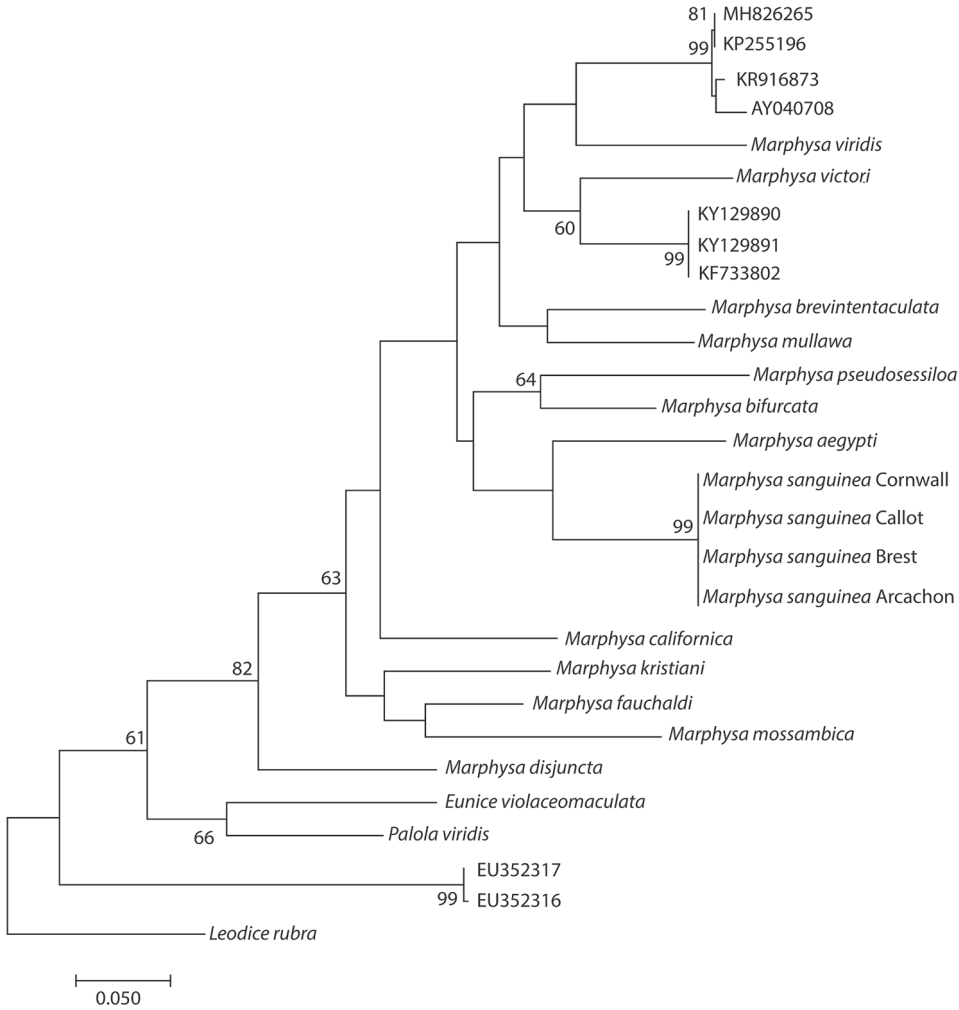

Figure 4. Maximum Likelihood tree of valid species of *Marphysa* and different *Marphysa sanguinea* available in GenBank, based on cytochrome oxidase I (COI) sequences and Kimura-2-parameters model. Bootstrap values on nodes if >50. Sequence accession numbers refer to Table 1.

ca. 14–15 tapering teeth) and two long outer winged teeth (nearly 2–3 times longer than inner teeth) (type 1) (Fig. 3A). Median and posterior parapodia with two types of pectinate chaetae (Fig. 2C): thin, isodonts narrow, with ca. 25 short teeth (type 1) (Fig. 3B, C); anodonts wide pectinate chaetae with long and thick teeth (n = 6–14) (type 2) (Fig. 3C); Type 2 less numerous (3–7) than type 1 (16–22). Compound spinigers with hirsute shafts and "socket-like" articulations (Fig. 2A), present along whole body, with more than 30 spinigers within a parapodia. Compound falcigers absent.

Pygidium with only one pair of relatively short pygidial cirri on ventral margin (approximately as long as last five chaetigers), anus slightly crenulated.

Table 1. List of terminal taxa used in molecular analysis, GenBank accession numbers, status of the species, locality of analysed specimen, and voucher specimen catalogue numbers.

Species	GenBank accession number	Status	Locality	Voucher specimen
Eunice cf. *violaceomaculata* Ehlers, 1887	GQ497542	valid	Carrie Bow Cay, Belize	
Palola viridis Gray in Stair, 1847	GQ497556	valid	Kosrae, Micronesia	
Leodice rubra (Grube, 1856)	GQ497528	valid	Ceará, Brazil	
M. aegypti Elgetany, El-Ghobashy, Ghoneim & Struck, 2018	MF196968	valid	Suez Canal, Egypt	
M. bifurcata Kott, 1951	KX172177	valid	Lizard Island, Australia	
M. brevitentaculata Treadwell, 1921	GQ497548	valid	Quintana Roo, Mexico	
M. californica Moore, 1909	GQ497552	valid	California, USA	
M. disjuncta Hartman, 1961	GQ497549	valid	California, USA	
M. fauchaldi Glasby & Hutchings, 2010	KX172165	valid	North Australia	
M. kristiani Zanol et al., 2016	KX172141	valid	Cowan Creek, Australia	
M. mossambica (Peters, 1854)	KX172164	valid	Australia	
M. mullawa Hutchings & Karageorgopoulos, 2003	KX172166	valid	Careel Bay, Australia	
M. pseudosessiloa Zanol, da Silva & Hutchings, 2017	KY605405	valid	Careel Bay, Australia	
M. victori Lavesque, Daffe, Bonifácio & Hutchings, 2017	MG384997	valid	Arcachon, France	
M. viridis Treadwell, 1917	GQ497553	valid	Ceará, Brazil	
M. sanguinea (Montagu, 1813)	GQ497547	valid	Callot Island, France	
	MK541904	valid	Cornwall, UK	AM W.51410
	MK950851	valid	Cornwall, UK	MNHN-IA-TYPE 1856
	MK950852	valid	Cornwall, UK	MNRJP002048
	MK950853	valid	Arcachon, France	MNHN-IA-TYPE 1857
	MK967470	valid	Brest, France	AM W. 49085
	MH826265	invalid	USA	
	KP255196	invalid	USA	
	KR916873	invalid	Portugal	
	AY040708	invalid	?	
	KY129890	invalid	East China Sea	
	KY129891	invalid	East China Sea	
	KF733802	invalid	Yellow Sea, China	
	EU352317	invalid	China?	
	EU352316	invalid	China?	

Remarks. Specimens both from British and French coasts agree with the description of the neotype and with voucher AM W.27392 which was also compared in the neotype description by Hutchings and Karageorgopoulos (2003). Most morphological characteristics are within the variation range of those observed by Hutchings and Karageorgopoulos (2003). However, few differences can be noticed: (1) larger number of pectinate chaetae (up to 28, instead of 10–14) beginning from chaetiger 2–3 (instead of chaetiger 1–2), (2) presence of coarsely denticulate chaetae with less teeth (6–14 teeth instead of ca. 14). These variations are typical within a species in the *Marphysa* genus.

Molecular data. COI gene was successfully sequenced and published at NCBI GenBank for the tree specimens sampled in Cornwall near the locality type (Table 1). COI was also successfully sequenced for specimens sampled in Brest and in Arcachon (Table 1).

First of all, molecular analysis distinguished *M. sanguinea* from other species with sequences available in GenBank (Fig. 4). Analysis permitted the grouping of specimens of *M. sanguinea* from Cornwall together with specimens from French Atlantic coast

(Arcachon, Brest) but also from southern English Channel, Callot Island (Zanol et al. 2014) (Fig. 4). Intraspecific pairwise genetic distances for COI were zero among these specimens. This tree clearly emphasised the presence of different species among this *sanguinea* complex. Especially, some specimens registered as *M. sanguinea* did not belong even to the *Marphysa* genus (EU352317 and EU352316).

Finally, a comparison of sequences of COI of a specimen from the type locality (AM W.51410) with specimen used to sequence the complete mitochondrial genome of *M. sanguinea* (accession number: KF733802, specimen from China) (Li et al. 2016) was performed. Unsurprisingly, these sequences were very different; the interspecific pairwise genetic distance was 18.5%.

Discussion

This study provides a molecular baseline for future taxonomic works. Among the *M. sanguinea sequences* in GenBank, molecular analyses only confirmed the identification of sequence GQ497547 (Zanol et al. 2014) from coarse sand near a *Zostera marina* seagrass bed in Callot Island (English Channel, northern Bretagne, France). All other sequences are not *M. sanguinea* and K2P genetic distance between these sequences and the specimen from the type locality varied from 13.6% (with KR916873) to 35.1% (with EU352316).

This study, therefore, confirms the presence of *M. sanguinea* along the French coasts, from the English Channel to the Bay of Biscay. Except for specimens from the French part of the English Channel (Zanol et al. 2014), which were sampled in coarse sand, all the confirmed records of *M. sanguinea* indicate that they are often associated with hard substrates. Specimens from the type locality (this study, Hutchings and Karageorgopoulos 2003) lived intertidally, in deep burrows in crevices in rocks at low watermark. In Arcachon Bay, they were found subtidally, inside turf slabs. Finally, in the Bay of Brest, specimens were also sampled from intertidal soft rocks. Except for specimens from Callot, all studied specimens were sampled in hard substrates. Actually, *Marphysa* species are known to occur in a range of specific habitats: muddy seagrass beds (e.g., *M. mullawa* (Hutchings and Karageorgopolous 2003, Zanol et al. 2016)), muddy flats (e.g., *M. kristiani* (Zanol et al. 2016)), sandy shores (*M. hongkongensa* (Wang et al. 2018), aquaculture fish ponds (e.g., *M. fauchaldi* (Glasby and Hutchings 2010)), oyster reefs (e.g., *M. victori* (Lavesque et al. 2017)).

Among the GenBank sequences that have been misidentified as *M. sanguinea*, the most astonishing is the sequence that is part of the complete mitochondrial genome of a species from the coast of the Yellow Sea (China) (GenBank accession number: KF733802) (Li et al. 2016). This species forms a monophyletic clade with other sequences from East China, suggesting that either a new species is present in this area or specimens belong to a described species for which there is no sequence identified as such in GenBank. Moreover, we also found an alarming result with the presence in

GenBank of sequences registered as *M. sanguinea* which did not even belong to the genus *Marphysa* (EU352317 and EU352316). This finding confirms the necessity of cautiously using these sequences, because these sequences come from specimens that clearly do not belong to *M. sanguinea*, and inevitably continues the confusion regarding the identity of this species. Furthermore, no vouchers were deposited in a museum that would allow for examination and comparison with other close species, or allow corroboration that it might be a new species for science. We strongly recommend verification of sequence publication in an international journal, whether a polychaete taxonomist has been associated with the study and whether a voucher specimen has been deposited in an official collection, before using the sequences.

As well as being (wrongly) considered as a cosmopolitan species for decades (Hutchings and Kupriyanova 2017), specimens identified as *M. sanguinea* are also widely used as a biological model by many scientists, but never with specimens originating from the type locality or its vicinity. Thus, many studies use specimen under the name *M. sanguinea* as a model in biochemistry, such as studies on galactosylceramides (Noda et al. 1992; Noda et al. 1994, specimens from fishing shops, Japan), erythrocruorin (Chew et al. 1965, specimens from Swan River, Australia; Weber et al. 1978, specimens from Pivers Island, North Carolina), lectins (Ozeki et al. 1997, specimens from fishing shops, Japan), phenols (Whitfield et al. 1999, specimens from Sydney, Australia), or acetylcholine (Horiuchi et al. 2003, specimens from commercial sources, Japan). Biology and physiology from so-called *M. sanguinea* specimens are also largely studied by scientists worldwide. From the literature, we identified works on development regarding sex gonad (Yu et al. 2005, specimens from Shandong Province, China), reproduction cycle (Yu et al. 2005; Ouassas et al. 2015, specimens from Saharan area, Morocco), metabolism and excretion (Yang et al. 2015, specimens from Dalian, China). Several papers also study rearing of so-called *M. sanguinea* with effects of density on growth (Parandavar et al. 2015, specimens from South Korea) or appropriate feeding for early juvenile stages (Kim et al. 2017, specimens from South Korea). Besides Li et al. (2016), several papers focus on genetic elements of this species, such as purification, characterisation and cDNA cloning of opine dehydrogenases (Endo et al. 2007, specimens from fishing shops, Japan) or genetic diversity from different geographical populations (Zhao et al. 2016, specimens from China). Finally, a recent study deals with microplastics and the formation of plastic fragments by *M. sanguinea* inhabiting marine polystyrene debris (Jang et al. 2018, specimens from Geoje Island, South Korea). While one could consider these as anecdotal, their conclusions are likely completely wrong when it comes to the species they refer to Even closely similar morphological species might have very different life-history traits (Cole et al. 2018), internal biology and of course, DNA. Such misidentifications could also lead to management and economic problems since *Marphysa* spp. are widely harvested as bait worldwide (Cole et al. 2018). In conclusion, we highly encourage marine biologists and ecologists to collaborate with confirmed taxonomists when assigning species names to marine invertebrate specimen.

Acknowledgments

Authors wish to thank sailors of 'Planula IV' for their help during sampling. We would like to thank Sue Lindsay who mounted the parapodia for the SEM and took the images, and Ingo Burghardt for his support with molecular analysis. We also deeply thank Keith Hiscock (Marine Biological Association UK) and Jason Hall-Spencer (Plymouth University) for their essential help during the sampling in Cornwall. Finally, we also thank Chris Glasby, Idris Izwandy, and an anonymous reviewer to provide helpful comments on the submitted manuscript.

References

Berthold AA (1827) Latreille's Natürliche Familien des Thierreichs. Aus dem Französischen, mit Anmerkungen und Zusätzen. Verlage Landes-Industrie-Comptoirs, Weimar, 606 pp. https://doi.org/10.5962/bhl.title.11652

Carr CM, Hardy SM, Brown TM, Macdonald T, Hebert PDN (2011) A tri-oceanic perspective: DNA barcoding reveals geographic structure and cryptic diversity in Canadian polychaetes. PLoS ONE 6: e22232. https://doi.org/10.1371/journal.pone.0022232

Chew MY, Scutt PB, Oliver IT, Lugg JWH (1965) Erythrocruorin of *Marphysa sanguinea*: Isolation and some physical, physiochemical and other properties. Biochemestry Journal 94: 378–383. https://doi.org/10.1042/bj0940378

Cole VJ, Chick RC, Hutchings PA (2018) A review of global fisheries for polychaete worms as a resource for recreational fishers: diversity, sustainability and research needs. Reviews in Fish Biology and Fisheries 28: 543–565. https://doi.org/10.1007/s11160-018-9523-4

Day JH (1967) A Monograph on the Polychaeta of Southern Africa. Part I. Errantia. British Museum (Natural History), London, 458 pp. https://doi.org/10.5962/bhl.title.8596

Elgetany AH, El-Ghobashy AE, Ghoneim AM, Struck TH (2018) Description of a new species of the genus *Marphysa* (Eunicidae), *Marphysa aegypti* sp. n., based on molecular and morphological evidence. Invertebrate Zoology 15(1): 71–84.

Endo N, Kan-No N, Nagahisa E (2007) Purification, characterization, and cDNA cloning of opine ehydrogenases from the polychaete rockworm *Marphysa sanguinea*. Comparative Biochemistry and Physiology Part B: Biochemistry and Molecular Biology 147: 293–307. https://doi.org/10.1016/j.cbpb.2007.01.018

Fauchald K (1970) Polychaetous annelids of the families Eunicidae, Lumbrineridae, Iphitimidae, Arabellidae, Lysaretidae and Dorvilleidae from Western Mexico. Allan Hancock Monographs in Marine Biology 5: 1–335. https://doi.org/10.5479/si.00810282.221

Fauvel P (1923) Polychètes errantes. Faune de France. Librairie de la Faculté des Sciences, Paris, 488 pp.

Fauvel P (1953) The fauna of India including Pakistan, Ceylon, Burma and Malaya: Annelida, Polychaeta. The Indian Press, Ltd, Allahabad, 507 pp.

Glasby CJ, Hutchings PA (2010) A new species of *Marphysa* Quatrefages, 1865 (Polychaeta: Eunicida: Eunicidae) from northern Australia and a review of similar taxa from the In-

do-West Pacific, including the genus *Nauphanta* Kinberg, 1865. Zootaxa 2352: 29–45. https://doi.org/10.11646/zootaxa.2352.1.2

Hartman O (1944) Polychaetous Annelids, 5. Eunicea. Allan Hancock Pacific Expeditions 10: 1–238.

Horiuchi Y, Kimura R, Kato N, Fujii T, Seki M, Endo T, Kato T, Kawashima K (2003) Evolutional study on acetylcholine expression. Life Sciences 72: 1745–1756. https://doi.org/10.1016/S0024-3205(02)02478-5

Hutchings PA, Karageorgopoulos P (2003) Designation of a neotype of *Marphysa sanguinea* (Montagu, 1813) and a description of a new species of *Marphysa* from Eastern Australia. Hydrobiologia 496: 87–94. https://doi.org/10.1023/A:1026124310552

Hutchings PA, Glasby CJ, Wijnhoven S (2012) Note on additional diagnostic characters of *Marphysa sanguinea* (Montagu, 1813) (Annelida: Eunicida: Eunicidae), a recently introduced species in Netherlands. Aquatic Invasions 7: 277–282. https://doi.org/10.3391/ai.2012.7.2.014

Hutchings PA, Kupriyanova E (2017) Cosmopolitan polychaetes – fact or fiction? Personal and historical perspectives. Invertebrate Systematics. https://doi.org/10.1071/IS17035

Jang M, Shima WJ, Myung GH, Song YK, Hong SH (2018) Formation of microplastics by polychaetes (*Marphysa sanguinea*) inhabiting expanded polystyrene marine debris. Marine Pollution Bulletin 131: 365–369. https://doi.org/10.1016/j.marpolbul.2018.04.017

Kim KH, Kim BK, Kim SK, Phoo WW, Maran BAV, Kim CH (2017) Appropriate feeding for early juvenile stages of eunicid polychaete *Marphysa sanguinea*. Fisheries and Aquatic Sciences 18: 57–63. https://doi.org/10.1186/s41240-017-0064-x

Kouadio KN, Diomande D, Ouattara A, Kone YJM, Gourene G (2008) Taxonomic diversity and structure of benthic macroinvertebrates in Aby Lagoon (Ivory Coast, West Africa). Pakistan Journal of Biological Sciences 20: 19. https://doi.org/10.3923/pjbs.2008.2224.2230

Lamptey E, Armah AK (2008) Factors affecting macrobenthic fauna in a tropical hypersaline coastal lagoon in Ghana, West Africa; 31: 1006–1019. https://doi.org/10.1007/s12237-008-9079-y

Lavesque N, Daffe G, Bonifácio P, Hutchings PA (2017) A new species of the *Marphysa sanguinea* complex from French waters (Bay of Biscay, NE Atlantic) (Annelida, Eunicidae). ZooKeys 716: 1–17. https://doi.org/10.3897/zookeys.716.14070

Leidy J (1855) Contributions towards a knowledge of the marine Invertebrate fauna of the coasts of Rhode Island and New Jersey. Journal of the Academy of Natural Sciences of Philadelphia, New Series 3: 135–152.

Lewis C, Karageorgopoulos P (2008) A new species of *Marphysa* (Eunicidae) from the Western Cape of South Africa. Journal of the Marine Biological Association of the United Kingdom 88: 277–287. https://doi.org/10.1017/S002531540800009X

Li S, Chen Y, Zhang M, Bao X, Li Y, Teng W, Liu Z, Fu C, Wang Q, Liu W (2016) Complete mitochondrial genome of the marine polychaete, *Marphysa sanguinea* (Polychaeta, Eunicida). Mitochondrial DNA Part A 27: 42–43. https://doi.org/10.3109/19401736.2013.869686

Liu Y, Hutchings PA, Sun S (2017) Three new species of *Marphysa* Quatrefages, 1865 (Polychaeta: Eunicida: Eunicidae) from the south coast of China and redescription of *Mar-*

physa sinensis Monro, 1934. Zootaxa 4263(2): 228–250. https://doi.org/10.11646/zootaxa.4377.2.3

Liu Y, Hutchings P, Kupriyanova E (2018) Two new species of *Marphysa* Quatrefages, 1865 (Polychaeta: Eunicida: Eunicidae) from northern coast of China and redescription for *Marphysa orientalis* Treadwell, 1936. Zootaxa 4377(2): 191–215. https://doi.org/10.11646/zootaxa.4377.2.3

Miura T (1977) Eunicid polychaetous annelids from Japan part II. Mer (Tokyo) 15: 11–31.

Molina-Acevedo IC, Carrera-Parra LF (2015) Reinstatement of three Grand Caribbean species of the *Marphysa sanguinea* complex (Polychaeta: Eunicidae). Zootaxa 3925(1): 37–55. https://doi.org/10.11646/zootaxa.3925.1.3

Molina-Acevedo IC, Carrera-Parra LF (2017) Revision of *Marphysa* de Quatrefages, 1865 and some species of *Nicidion* Kinberg, 1865 with the erection of a new genus (Polychaeta: Eunicidae) from the Grand Caribbean. Zootaxa 4241: 1–62. https://doi.org/10.11646/zootaxa.4241.1.1

Morgado EH, Tanaka MO (2001) The macrofauna associated with the bryozoan *Schizoporella errata* (Walters) in southeastern Brazil. Scienta Marina 65: 173–181. https://doi.org/10.3989/scimar.2001.65n3173

Montagu G (1813) Descriptions of several new or rare animals, principally marine, found on the south coast of Devonshire. Transactions of the Linnean Society of London 11: 18–21. https://doi.org/10.1111/j.1096-3642.1813.tb00035.x

Noda N, Ryuichiro T, Kazumoto M, Kawasaki T (1992) Two novel Galactosylceramides from *Marphysa sanguinea*. Tetrahedron Letters 33: 7527–7530. https://doi.org/10.1016/S0040-4039(00)60815-8

Noda N, Tanaka R, Tsujino K, Takasaki Y, Nakano M, Nishi M, Miyahara K (1994) Phosphocholine-Bonded Galactosylceramides Having a Tri-Unsaturated Long-Chain Base from the Clam Worm, *Marphysa sanguinea*. Journal of Biochemistry 116: 435–442. https://doi.org/10.1093/oxfordjournals.jbchem.a124543

Ouassas M, Lefrere L, Ait Alla A, Agnaou M, Gillet P, Moukrim A (2015) Reproductive cycle of *Marphysa sanguinea* (Polychaeta: Eunicidae) in a Saharan wetland: Khnifiss Lagoon (South of Morocco). Journal of Materials and Environmental Science 6: 246–253.

Ozeki Y, Tazawa E, Matsui T (1997) d-Galactoside-Specific Lectins from the Body Wall of an Echiuroid (*Urechis unicinctus*) and Two Annelids (*Neanthes japonica* and *Marphysa sanguinea*). Comparative Biochemistry and Physiology Part B: Biochemistry and Molecular Biology 118: 1–6. https://doi.org/10.1016/S0305-0491(97)00014-X

Parapar J, Besteiro C, Urgorri V (1993) Taxonomy and Ecology of Annelida of the Iberian Peninsula – Polychaeta from the Ria-De-Ferrol. Cahiers de Biologie Marine 34: 411–432.

Parandavar H, Kim KH, Kim CH (2015) Effects of rearing density on growth of the polychaete rockworm *Marphysa sanguinea*. Fisheries and Aquatic Sciences 18: 57–63. https://doi.org/10.5657/FAS.2015.0057

Quatrefages A (1866) Histoire naturelle des Annelés marins et d'eau douce. Annélides et Géphyriens. Tome second. Librairie Encyclopédique de Rôret, Paris, 337–794. https://doi.org/10.5962/bhl.title.122818

Read G, Fauchald K (2019a) World Polychaeta database. Eunicidae Berthold, 1827. World Register of Marine Species. http://www.marinespecies.org/aphia.php?p=taxdetails&id=966 [Accessed on 2019-04-25]

Read G, Fauchald K (2019b) World Polychaeta database. *Marphysa* Quatrefages, 1866. World Register of Marine Species. http://www.marinespecies.org/aphia.php?p=taxdetails&id=129281 [Accessed on 2019-02-25]

Salazar-Vallejo SI, Carrera-Parra LF (1998) Eunicids (Polychaeta) from the Mexican Caribbean with keys to Great Caribbean species: *Fauchaldius*, *Lysidice*, *Marphysa*, *Nematonereis* and *Palola*. Revista de Biologia Tropical 45: 1481–1498.

Wang Z, Zhang Y, Qiu JW (2018) A New Species in the *Marphysa sanguinea* complex (Annelida, Eunicidae) from Hong Kong. Zoological Studies 57(48): 1–13.

Weber RE, Bonaventura J, Sullivan B, Bonaventura C (1978) Oxygen equilibria and ligand-binding kinetics of erythrocruorins from two burrowing Polychaetes of different modes of life, *Marphysa sanguinea* and *Diopatra cuprea*. Journal of Comparative Physiology 123: 177–184. https://doi.org/10.1007/BF00687847

Webster HE (1879) The Annelida Chaetopoda of the Virginian coast. Transactions of the Albany Institute 9: 202–272. https://doi.org/10.5962/bhl.title.11296

Whitfield FB, Drew M, Helidoniotis F, Svoronos D (1999) Distribution of bromophenols in species of marine polychaetes and bryozoans from Eastern Australia and the role of such animals in the flavor of edible ocean fish and prawns (shrimp). Journal of Agricultural and Food Chemistry 47: 4756–4762. https://doi.org/10.1021/jf9904719

Yang D, Chan F, Zhou Y, Xiu Z (2015) Diel variation in metabolism and ammonia excretion of *Marphysa sanguinea* (Polychaeta: Eunicidae). Chinese Journal of Oceanology and Limnology. https://doi.org/10.1007/s00343-016-4340-x

Yu HZ, Zhu LY, Zheng JS (2005) Development of sex gonad and reproduction cycle of *Marphysa sanguinea*. Journal of Fishery Sciences of China 12: 669–674.

Zhao H, Wang X, Yang D, Zhao X, Li N, Zhou Y (2016) An analysis of genetic diversity in *Marphysa sanguinea* from different geographic populations using ISSR polymorphisms. Biochemical Systematics and Ecology 64: 65–69. https://doi.org/10.1016/j.bse.2015.11.002

Zanol J, Halanych KM, Fauchald K (2014) Reconciling taxonomy and phylogeny in the bristleworm family Eunicidae (polychaete, Annelida). Zoologica Scripta 43: 79–100. https://doi.org/10.1111/zsc.12034

Zanol J, da Silva T dos SC, Hutchings P (2016) Integrative taxonomy of *Marphysa* (Eunicidae, Polychaeta, Annelida) species of the Sanguinea-group from Australia. Invertebrate Biology 135(4): 328–344. https://doi.org/10.1111/ivb.12146

Zanol J, da Silva T dos SC, Hutchings P (2017) One new species and two redescriptions of *Marphysa* (Eunicidae, Annelida) species of the Aenea-group from Australia. Zootaxa 4268(3): 411–426. https://doi.org/10.11646/zootaxa.4268.3.6

ZooKeys 859: 17–29 (2019)
doi: 10.3897/zookeys.859.33284
http://zookeys.pensoft.net

RESEARCH ARTICLE

A peer-reviewed open-access journal
ZooKeys
Launched to accelerate biodiversity research

A new species of *Aciconula* (Amphipoda, Senticauda, Caprellidae) from Sultan Iskandar Marine Park, Malaysia

Jacqueline H.C. Lim[1], B. Abdul Rahim Azman[1,2], B.H. Ross Othman[3]

1 *School of Environmental & Natural Resource Sciences, Faculty of Science and Technology, Universiti Kebangsaan Malaysia, 43600 UKM Bangi, Selangor, Malaysia* **2** *Marine Ecosystem Research Centre (EKOMAR), Faculty of Science and Technology, Universiti Kebangsaan Malaysia, 43600 UKM Bangi, Selangor, Malaysia* **3** *School of Marine and Environmental Sciences, Universiti Malaysia Terengganu, 21030 Kuala Nerus, Terengganu, Malaysia*

Corresponding author: *B. Abdul Rahim Azman* (abarahim@gmail.com)

Academic editor: *Alan Myers* | Received 23 January 2019 | Accepted 14 May 2019 | Published 2 July 2019

http://zoobank.org/F293A34B-5874-4E69-B991-DAB74038FB00

Citation: Lim JHC, Azman BAR, Othman BHR (2019) A new species of *Aciconula* (Amphipoda, Senticauda, Caprellidae) from Sultan Iskandar Marine Park, Malaysia. ZooKeys 859: 17–29. https://doi.org/10.3897/zookeys.859.33284

Abstract

A new species of caprellid, *Aciconula tinggiensis* (Amphipoda, Senticaudata, Caprellidae) was discovered from Pulau Tinggi, Sultan Iskandar Marine Park (SIMP), South China Sea, Malaysia. The new Malaysian species can be distinguished from the other *Aciconula* species by the combination of the following characters: 1. the presence of a very small suture between head and pereonite 1; 2. antenna 1 flagellum with 4 articles; 3. inner lobe of lower lip unilobed; 4. gnathopod 2 palm of propodus with a large proximal projection (stretching from the proximal margin of the palm to nearly mid-way of palm); 5. pereopods 3–4 with 2 articles (article 1 subrectangular, article 2 conical or tapering at the tip with 1 plumose seta and 2 normal setae) and; 6. pereopod 5 covered with relatively dense and long setae. An updated identification key for the five known species in the genus, including information on the respective geographical distribution and habitat, is presented.

Keywords

Aciconula tinggiensis sp. nov., caprellid, new species, taxonomy, South China Sea

Introduction

The amphipod genus *Aciconula* was established by Mayer (1903) with *A. miranda* Mayer, 1903 as its type species. However, the exact diagnostic characteristics of this genus were unclear because the types described by Mayer (1903) for this genus were both females (that were collected from three different localities: Singapore, Malaysia and Koh Krau, Thailand) and only figures of the whole body, pereopod 3, pereopod 4, pereopod 5, mandibular palp article 3 and maxilliped were drawn. Mayer (1912) then described a male but the abdomen and mouthparts were also not included. Nevertheless, general morphology of the male specimen agrees well with the type and the rest of the appendages such as pereopods 3 to 7 are also similar to the female. The abdomen was also left out. Following that, Arimoto (1976) referred to Utinomi's (1969) description based on specimens collected from Kii Peninsula, Japan and revised its generic diagnosis. Subsequently, three more species of *Aciconula* were reported; *Aciconula acanthosoma* Chess, 1989 from southern California; *A. australiensis* Guerra-García, 2004 from Western Australia and most recently *A. tridentata* Guedes-Silva & Souza-Filho, 2013 described from Pernambuco, Brazil.

The Sultan Iskandar Marine Park (SIMP) is one of Malaysia's marine protected areas located 15–65 km from Mersing, off the north-east coast of the Johor State, Malaysia in the South China Sea. This body of water covering an area of about 8000 hectares holds one of the most diverse marine ecosystems on the east coast of Peninsular Malaysia, ranging from sandy shores, coral reefs, mangroves, estuaries, mudflats to seagrass and open water habitats (see Harborne et al. 2000; Japar Sidik and Muta Harah 2003; Maritime Institute of Malaysia 2006; Japar Sidik et al. 2006; Azman et al. 2008; Japar Sidik and Muta Harah 2011; Lim et al. 2015). The SIMP (Fig. 1) consists of 13 main islands namely Pulau Harimau, Pulau Mensirip, Pulau Goal, Pulau Besar, Pulau Tengah, Pulau Hujung, Pulau Rawa, Pulau Tinggi, Pulau Mentinggi, Pulau Sibu, Pulau Sibu Hujung, Pulau Pemanggil and Pulau Aur. This paper continues the previous significant contributions on the biodiversity of SIMP and its vicinity including Othman and Azman (2007), Lim et al. (2010), Gan et al. (2010), Azman and Melvin (2011), Lim et al. (2012), Azman and Othman (2013), Chew et al. (2014), Tan et al. (2014, 2015), Lim et al. (2015), Chew et al. (2016) Lim et al. (2017) and Tan and Azman (2017, 2018) on marine crustaceans. The present paper also deals with the detailed description of this new species; an updated identification key to all the known *Aciconula* species is also given.

Material and methods

Sampling

The caprellids examined in this study were collected from an artificial reef of Kampung Pasir Panjang, Pulau Tinggi, Sultan Iskandar Marine Park (SIMP) at 9–11 m water depth (Fig. 1). Collections were made by SCUBA; hosts (stinging hydroids) together with attached caprellids were put into fine mesh bags. Specimens used for morphological descriptions were preserved in 4% formaldehyde before examination.

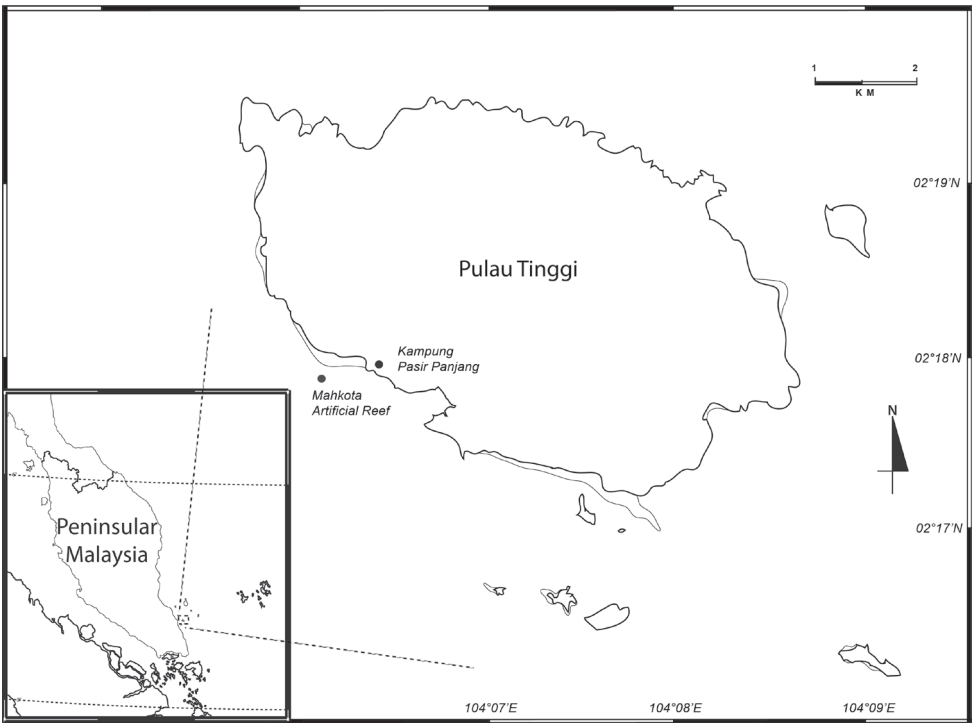

Figure 1. Pulau Tinggi of Sultan Iskandar Marine Park (SIMP), Malaysia.

Laboratory procedures

Appendages were dissected from the right side of the specimens and stored in several semi-permanent slides mounted in glycerol and then drawn under an optical microscope (Olympus BX43) and a stereomicroscope with a camera lucida. The drawings were digitized on Adobe Illustrator CS3 using the methods described in Coleman (2003). All materials are deposited at the South China Sea Research and Repository Centre, Institute of Oceanography and Environment, Universiti Malaysia Terengganu, 21030 Kuala Nerus, Terengganu, Malaysia (UMT Crus). The following abbreviations are used in the figures: **A**, antenna; **ABD(L)**, abdomen lateral view; **ABD(V)**, abdomen ventral view; **G**, gnathopod; LL, lower lip; **MD**, mandible; **MX**, maxilla; **MXP**, maxilliped; **P**, pereopod; **UL**, upper lip; **R**, right; **L**, left; ♂, male; ♀, female.

Systematics

Order AMPHIPODA Latreille, 1816
Suborder COROPHIIDEA Leach, 1814
Family CAPRELLIDAE Leach, 1814
Genus *Aciconula* Mayer, 1903

***Aciconula tinggiensis* sp. nov.**
http://zoobank.org/DEE62918-DA9C-4090-9245-872B7D982DBD
Figs 2–5

Etymology. Named after the type locality, Pulau Tinggi in SIMP, Malaysia.

Material examined. Holotype: male, 2.2 mm, UMT Crus 01003, Mahkota artificial reef Pulau Tinggi, SIMP, Johor, 02°17.637'N, 104°05.817'E, SCUBA diving, 9 June 2009, 12.31 PM, depth 10.7 m, coll. Azman, B.A.R., Gan, S.Y., Lim, J.H.C., Chew, M.W.H. & Shamsul, B.

Paratypes: 1 female, UMT Crus 01004 (Fig. 4); 2 males, 1 female, UMT Crus 01005; 2 males, 2 females, UMT Crus 01006; 2 males, 2 females, 1 juvenile, UMT Crus 01007; same station data.

Type locality. Mahkota artificial reef, Pulau Tinggi, SIMP, Malaysia.

Description. [Based mostly on holotype (UMT Crus 01003), 2.2 mm, supplemented by paratype (UMT Crus 01004), 1.8 mm for female and (UMT Crus 01005) for lower lip and maxilliped]

Adult male. Body length, 2.2 mm. UMT Crus 01003. Head/pereonite 1 without dorsal projection. Head length 0.2 mm; pereonite 1, 0.07 mm; head and pereonite 1 partially fused (suture clear); pereonite 2, 0.34 mm with an acute mid-dorsal projection; pereonite 3 longest, 0.53 mm; pereonite 4, 0.44 mm; pereonite 5, 0.41 mm, subequal in length to pereonite 4; pereonite 6, 0.16 mm; pereonite 7 short, 0.12 mm. Eye small. Antenna 1 about 0.4× body length; peduncular article 1 with tuft of plumose setae; peduncular article 2 longest; peduncular article 3 lobed at posterodistal margin; flagellum approximately half of peduncular length with 4 articles, proximal article composed of 2 articles. Antenna 2 about 0.4× the length of antenna 1; peduncular articles lobus; flagellum 2-articulate.

Lower lip outer lobes with pair of ducts; inner lobes unilobed. Mandible left incisor with 6 teeth; lacinia mobilis plate like and serrated distally; accessory setal row with 3 setae; mandibular molar present without robust teeth; palp 3-articulate with distal article comprising a row of 5 teeth and setal formula of 1-3-1, second article of palp without seta on inner distal margin; right incisor with 5 teeth; lacinia mobilis with 7 teeth; accessory setal row with 2 setae; palp 3-articulate with distal article comprising a row of 5 teeth and setal formula of 1-3-1, second article of palp with one seta on inner distal margin. Maxilla 1 outer plate with 5 cuspidate and denticulate spines (robust apical setal-teeth); palp article 2 long, 4× length of article 1 with 3 setae apically. Maxilla 2 inner plate with 4 short and long setae distally; outer plate 1.3× length of inner plate with 5 slender setae apically. Maxilliped inner plate small, with one short and one long apical setae; outer plate about 2.5× inner plate with 3 setae at distal margin; palp 4-articulate, scarcely setose, article 2 with 1 seta at inner distal margin, article 3 with 5 distal setae; article 4 tapering to a tip with 2 setae distally and 1 seta at outer proximal margin.

Pereon. Gnathopod 1 basis longer than ischium, merus and carpus combined; propodus subtriangular, longer than wide, scarcely setose, palm with a pair of grasping spines; dactylus falcate, provided with fine setae along lateral margin, tip of dactylus bifid. Gnathopod 2 begins ¼-way along anterior margin of pereonite 2; basis about

0.7 × pereonite 2; ischium and merus subquadrate; carpus triangular; propodus 1.6 × as long as wide, 1.3× length of basis, palm with large proximal projection (stretching from proximal margin of palm to nearly mid-way of palm), provided with one robust grasping spine proximally, a small triangular projection medially and ending with a triangular projection provided with 1 seta, distal margin of palm with 1 triangular projection; dactylus falcate, fitting on palm.

Gill 3 length 0.2× corresponding pereonite, oval. Pereopod 3 reduced, about 0.5× gill length, 2-articulate, second article with one plumose seta and two simple setae apically. Gill 4 slightly larger than gill 3, 0.3 × corresponding pereonite, oval. Pereopod 4 reduced, about 0.5 × gill length, 2-articulate, second article of pereopod 4 more slender than article 2 of pereopod 3 with one plumose seta and two simple setae apically. Pereopod 5, 6-articulate, curved upwards anterodorsally and extending past pereonite 4, setose entire margin comprising short and very long setae, carpus and propodus subequal in length, dactylus reduced to a small cone with one plumose seta apically. Pereopod 6 propodus with a pair of grasping spines proximally, dactylus falcate with one plumose seta on anterior margin at proximal region. Pereopod 7 similar with pereopod 6 but more robust than pereopod 6.

Pleon. Uropod 1 vestigial with 4 setae; Uropod 2 vestigial with 2 setae distally and one facial seta on inner margin. Telson with one seta apically.

Adult female. Body length, 1.8 mm. UMT Crus 01004. Head length 0.2 mm; pereonite 1, 0.04 mm; head/pereonite 1 without dorsal projection; pereonite 2, 0.29 mm with rounded mid-dorsal projection; pereonite 3, 0.39 mm; pereonite 4, 0.32 mm with acute dorsodistal projection; pereonite 5, 0.38 mm, subequal in length to pereonite 3; pereonite 6, 0.13 mm; pereonite 7 short, 0.08 mm. Eye small. Antenna 1 about 0.4 × body length; peduncular article 1 with tuft of setae; peduncular article 2 longest; peduncular article 3-lobed at posterodistal margin; flagellum approximately 1.8 × peduncular length with 4 articles. Antenna 2 about 0.4 × the length of antenna 1; peduncular articles lobus; flagellum 2-articulate.

Mouthparts of the female are similar to those of male (refer to male mouthparts).

Pereon. Gnathopod 2 basis begins ¼-way along anterior margin of pereonite 2; basis about 0.7 × pereonite 2; ischium and merus subquadrate; carpus subtriangular; propodus 2.4 × as long as wide, 1.2 × length of basis, palm without large proximal projection, provided with one robust grasping spine distally; dactylus falcate, fitting on palm. Gill 3 length 0.3 × corresponding pereonite, oval. Pereopod 3 reduced, about 0.5 × gill length, 2-articulate, similar with the male, second article with one plumose setae and two simple setae apically. Gill 4 subequal with gill 3, 0.4 × corresponding pereonite, oval. Pereopod 4 reduced, about 0.4 × gill length, 2-articulate, subequal with pereopod 3 with one plumose setae and two simple setae apically. Oostegites on pereonite 3 and 4 with setae. Pereopod 5, 6-articulate, curved upwards anterodorsally and extending past pereonite 4, more slender than male pereopod 5, setose entire margin comprising short and very long setae, propodus longest, dactylus reduced to a small cone with one plumose seta apically.

Pleon. Uropod 1 vestigial with 1 simple setae; Uropod 2 vestigial with 1 setae distally. Telson with one plumose seta apically.

Remarks. Considering the four reported species from the genus *Aciconula*, *A. tinggiensis* sp. nov. is most similar to *A. australiensis* in terms of antenna 1 and 2, gnathopod 1, mouthparts (maxilliped and maxillas) and abdomen. Pereopods 3 and 4 of the male are also similar except for the presence of a seta on article 1 of *A. australiensis*. The Malaysian specimen differs from the Australian counterpart in terms of the absence of 1) a head projection (present in *A. australiensis*); 2) inner lobe of lower lip unilobed (*A. australiensis* bilobed); 3) gnathopod 2 propodus proximal projection shallow and wide, about 1/2 of palm (*A. australiensis* more pronounced, about 1/3 of palm); 4) pereopod 3 of female similar to the male with only 2 articles while *A. australiensis* shows sexual dimorphism with 3 articles; 5) longer (articles 4 and 5 about 2 × longer) pereopod 5, 0.43 × body length, terminal article with one plumose seta and generally more setose (*A. australiensis* only 0.23 × body length; terminal articles with one normal seta); 6) mandibles with setal formula of 1-3-1 (setal formula 1-4-1 in *A. australiensis*).

Aciconula acanthosoma Chess, 1989 clearly differs from the Malaysian specimen firstly by its numerous dorsal projections throughout its body, maxilliped inner lobes more robust and wide, terminally with one tooth and three setae (slender with two normal setae in *A. tinggiensis* sp. nov.), maxilla 2 with very short terminal setae and mandibles with large, well-developed molar and palp with setal formula of 1-6-1. Apart from its body armature and mouthparts, it also varies in terms of appendages such as gnathopod 2 (basis with a distolateral projection, palmar margin of propodus with a proximal projection followed by a strong spine and a deep sinus), pereopod 5 with short and fine dense setae (setae longer and less extensive in *A. tinggiensis* sp. nov.), and abdomen with one pair of well-developed, 1-articulate abdominal appendage. The species from southern California is also much larger than the present specimen (3.3 × longer) and the other two existing species from the Indo-Pacific. In spite of this, *A. acanthosoma* does have a few similarities in pereopods 3 and 4 with 2 articles and article 2 conical (except for the 3 terminal plumose setae) and pereopods 6 and 7 with 7 articles and grasping structure on article 6. There is more dissimilarity in these two species than similarities. According to Guerra-García (2004), *A. acanthosoma* could be placed in a new genus based on the abdominal appendages and several mouthparts but presently there is only one genus, which exhibits the soft and flexible character of pereopod 5, therefore it is retained in the genus *Aciconula*.

The female specimen of *A. tinggiensis* sp. nov. was primarily used to compare with Mayer's (1903) type and Mayer's (1912) account of *A. miranda* because he only provided more detailed description and figures of females compared to males. Females of *A. tinggiensis* sp. nov. are similar to *A. miranda* Mayer, 1903 based on a single dorsal projection on pereonite 2, antenna 1 flagellum with 4 articles, pereopod 4 with 2 articles (similar in shape and terminally with one plumose seta), and its gill shape. However, the present species (female) differs from *A. miranda* Mayer, 1903 in its pereopod 5 which has longer but less dense setae (more densely setose in *A. miranda*); pereopod 3 with 2 articles (3 articles in *A. miranda*); and pereopod 3 article 2 is conical and short (article 2 is subcylindrical with several seta marginally). Mouthparts of *A. tinggiensis*

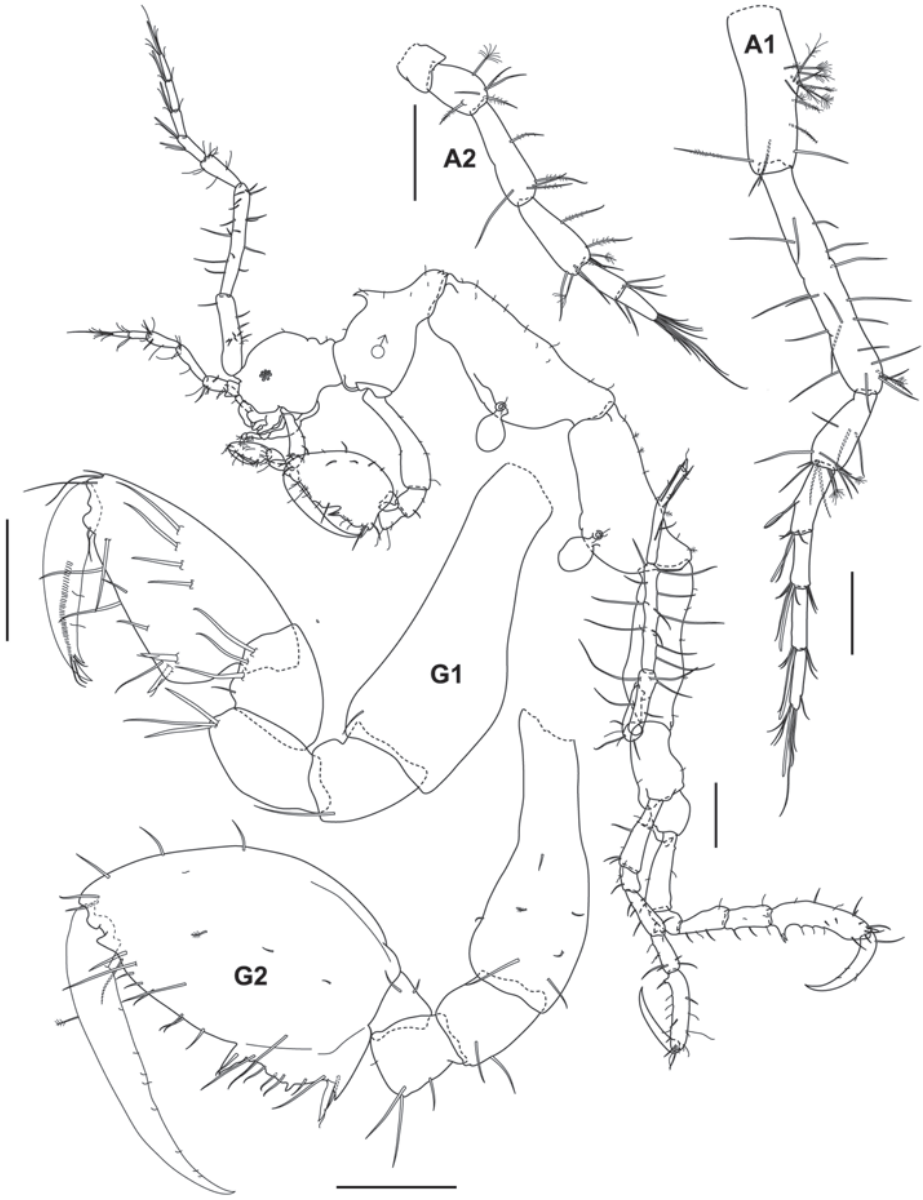

Figure 2. *Aciconula tinggiensis* sp. nov., male holotype, 2.2 mm, UMT Crus 01003, Mahkota artificial reef, Pulau Tinggi, SIMP. Scales bars: 0.1 mm (A1, A2, G2); 0.05 mm (G1); 0.2 mm (whole body).

sp. nov. for males and females are similar therefore only the male mouthparts are used for comparison with Mayer's (1903) description and figures. *Aciconula tinggiensis* sp. nov. differs from *A. miranda* in terms of the setal formula of the mandibular palp 1-3-1 (setal formula 1-7-1 in *A. miranda*) and maxilliped outer plate with only 3 distal setae (maxilliped entire inner margin lined with setae in *A. miranda*).

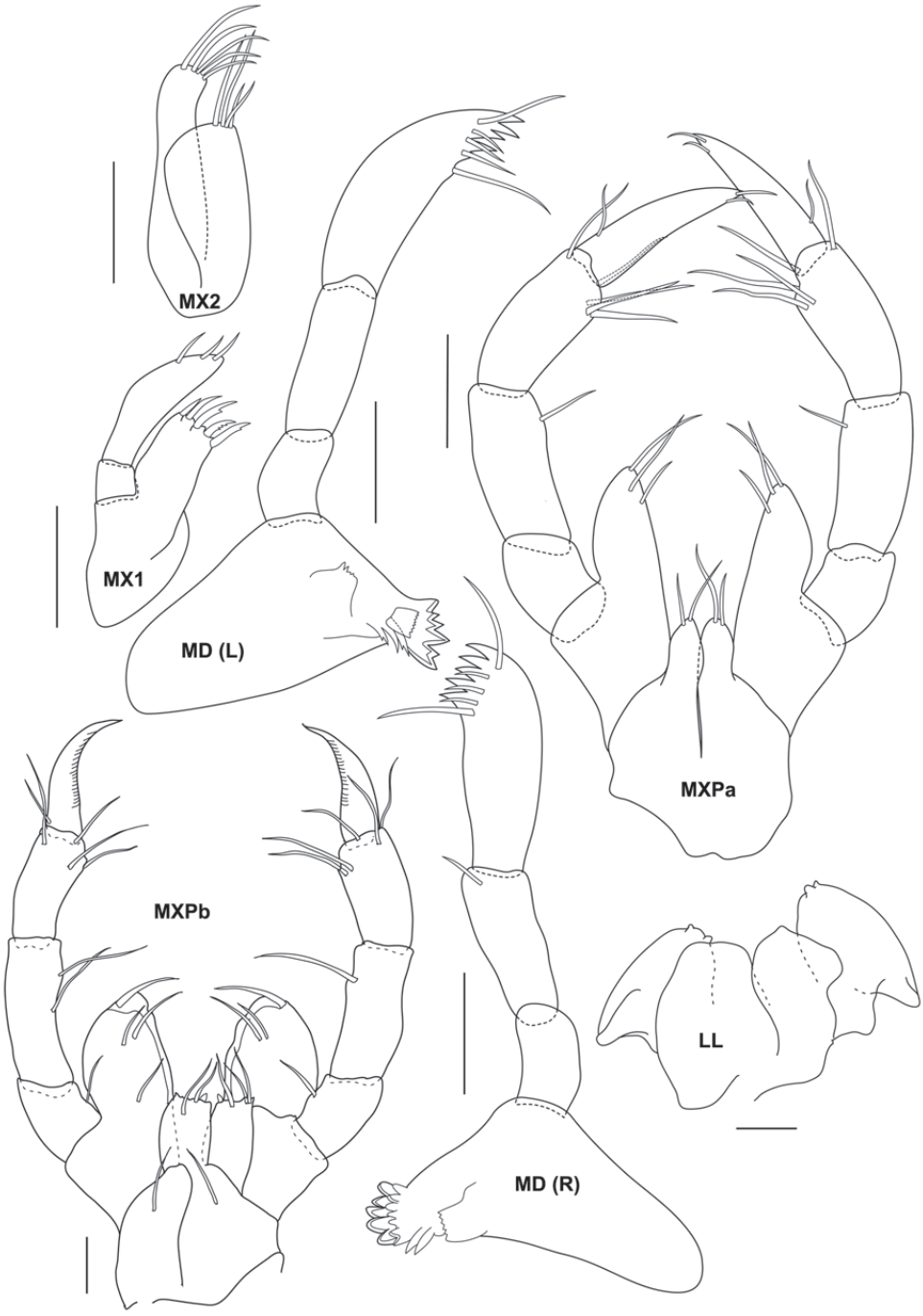

Figure 3. *Aciconula tinggiensis* sp. nov., male holotype, 2.2 mm, UMT Crus 01003, Mahkota artificial reef, Pulau Tinggi, SIMP. Lower lip (LL) and MXPb from male paratype, UMT Crus 01005. Scale bars: 0.025 mm

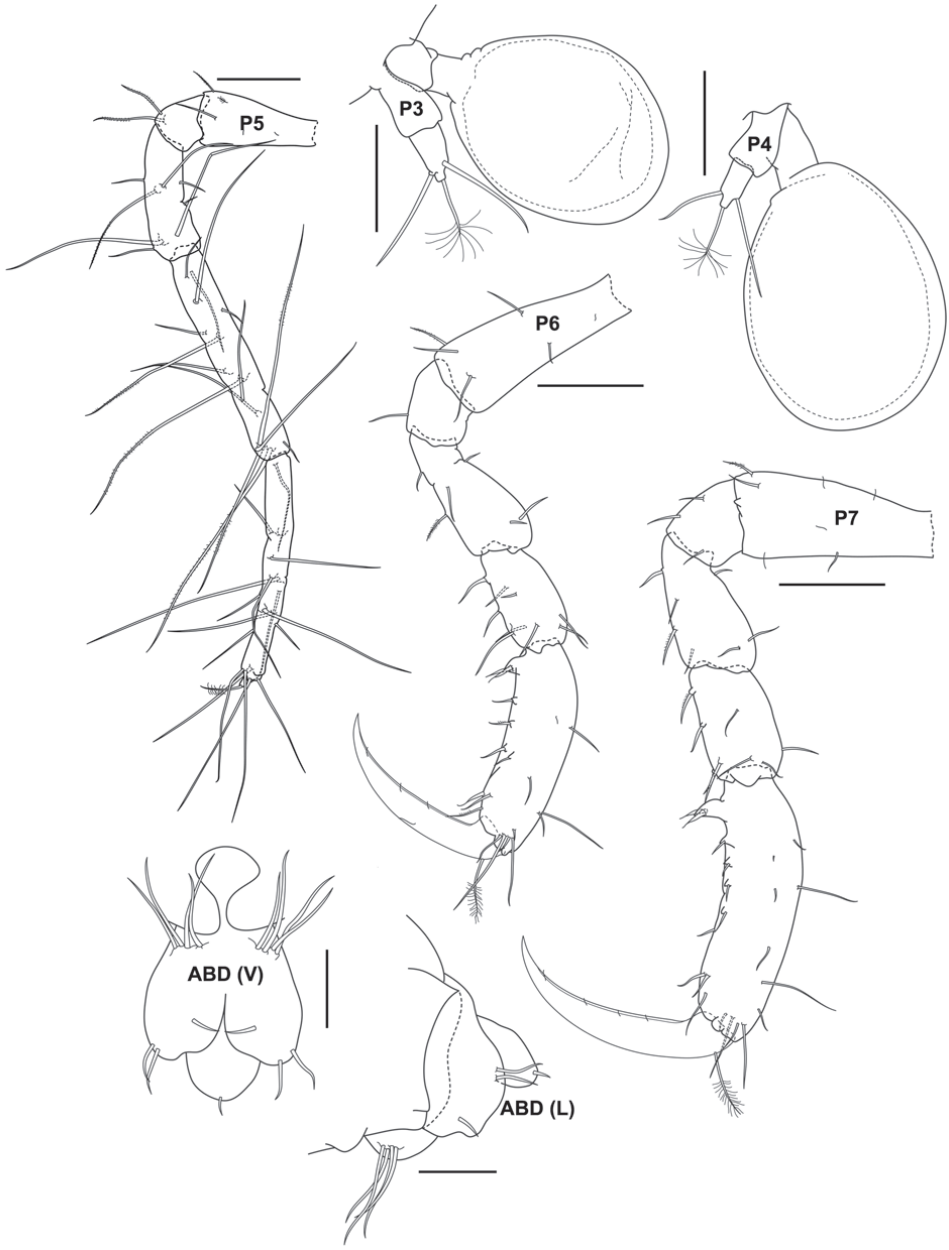

Figure 4. *Aciconula tinggiensis* sp. nov., male holotype, 2.2 mm, UMT Crus 01003, Mahkota artificial reef, Pulau Tinggi, SIMP. Scale bars: 0.025 mm (ABD); 0.05 mm (P3, P4); 0.1 mm (P5, P6, P7).

Aciconula tridentata Guedes-Silva & Souza-Filho, 2013 reported from Brazil, is similar to the present species in the: 1) presence of a small sharp median forward projection of the head; 2) pereopods 3 and 4 of male with two-articles, and absence of abdominal

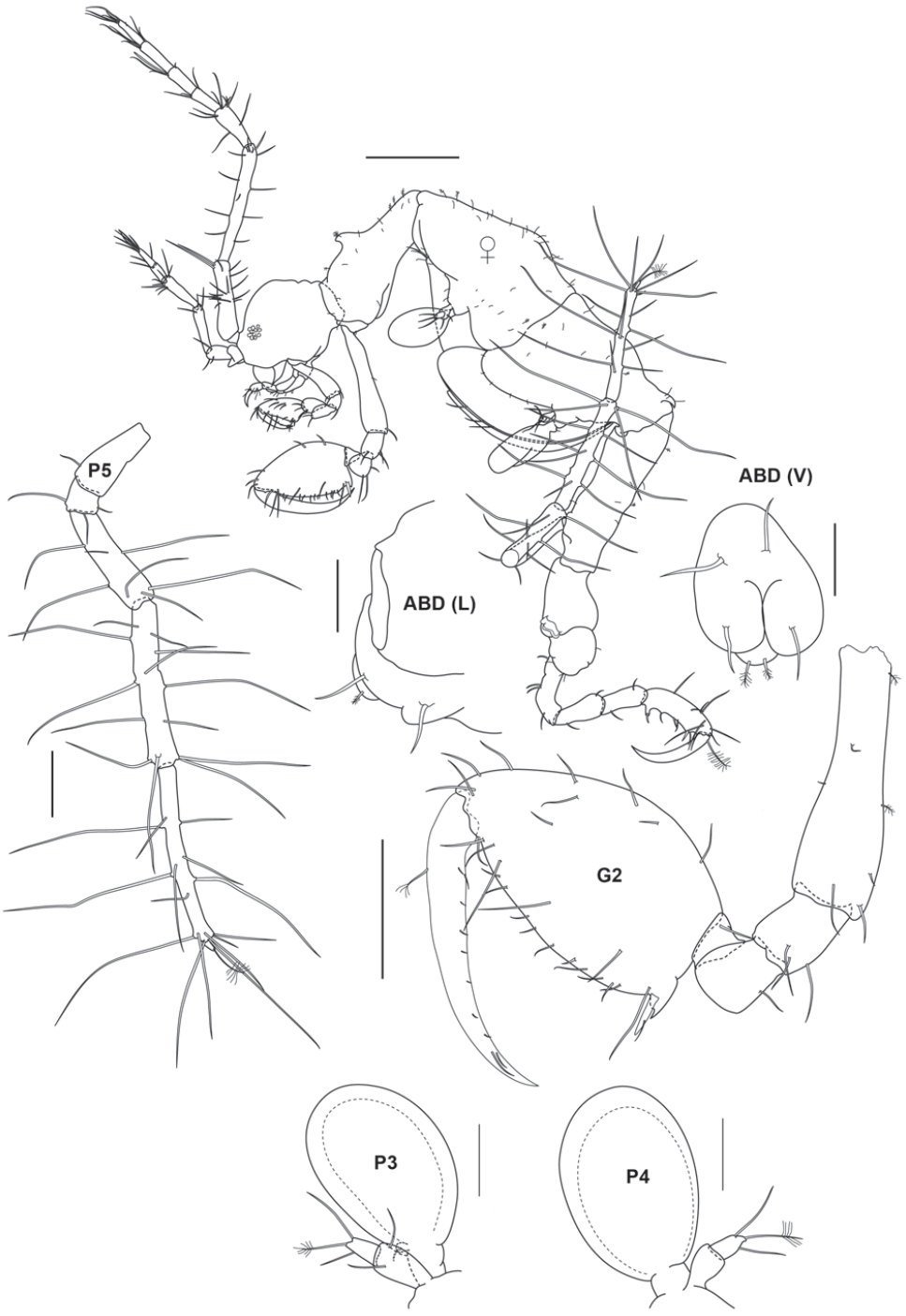

Figure 5. *Aciconula tinggiensis* sp. nov., female paratype, 1.8 mm, UMT Crus 01004, Mahkota artificial reef, Pulau Tinggi, SIMP. Scale bars: 0.025 mm (ABD); 0.1 mm (G2, P5); 0.05 mm (P3, P4); 0.2 mm (whole body).

appendages but differs in the length of the outer plate of maxilliped (longer in *Aciconula tinggiensis* sp. nov. reaching the mid-length of palp article 2), the sculpturing on the palm of male gnathopod 2, (with a 3-dentate projection, followed by a large excavation leading to a projection with two sharp processes in *A. tridentata*) and number or articles in female pereopods 3 and 4 (pereopod 3 4-articulate and pereopod 4 3-articulate in *A. tridentata*)

In conclusion, *Aciconula tinggiensis* sp. nov. described here is recognized as distinct from the four existing species of this genus based on these combination of characters; 1) a very small suture between head and pereonite 1; 2) antenna 1 flagellum with 4 articles, its setal formula of 1-3-1; 3) unilobed inner lobe of lower lip with pair of ducts on outer lobe; 4) gnathopod 2 palm of propodus with a large proximal projection, (stretching from the proximal margin of the palm to nearly mid-way of palm) provided with one robust grasping spine proximally, a small triangular projection medially and ending with a triangular projection provided with 1 seta; 5) pereopods 3 and 4 with 2 articles (article 1 subrectangular, article 2 conical or tapering at the tip with 1 plumose seta and 2 normal setae); 6) pereopod 5 covered with relatively dense and long setae; and 7) abdomen region with penes situated medially, uropod 2 degenerated into 4 setae, uropod 2 degenerated into 1 seta medially and 2 setae distally.

Habitat. The specimens have been found from 10–12 meters deep, living on stinging hyroids.

Distribution. Currently only known from Pulau Tinggi, Johor, Malaysia.

Key to the species of the genus *Aciconula* Mayer, 1903

1 Body dorsally strongly spinose, abdominal appendages present ..... ***A. acanthosoma* Chess, 1989**

– Body dorsally not spinose, abdominal appendages absent **2**

2 Head lacking a small sharp median forward projection ..... ***A. miranda* Mayer, 1903**

– Head with a small sharp median forward projection **3**

3 Antenna 1 article 1 bearing a setose hump proximally..... ***A. australiensis* Guerra-Garcia, 2004**

– Antenna 1 article 1 lacking setose hump proximally..... **4**

4 Gnathopod 2 male first half of propodus palm bearing a 3-dentate followed by a large excavation ..... ***A. tridentata* Guedes-Silva & Souza-Filho, 2013**

– Gnathopod 2 male first half of propodus palm without dentation ..... ***A. tinggiensis* sp. nov.**

Acknowledgments

The authors would like to thank Shamsul B., Melvin C.W.H. and Ms. Gan S.Y. for their assistance in the field. Many thanks are also due to Sultan Iskandar Marine Park

and Marine Park Section, Department of Fisheries, Malaysia. This study was supported by the Universiti Kebangsaan Malaysia research grant (LIV-2015-02) and the Japan Society for the Promotion of Science (JSPS) Core-to-Core Program (B.Asia-Africa Science Platforms).

References

Arimoto I (1976) Taxonomic studies of caprellids (Crustacea, Amphipoda, Caprellidae) found in the Japanese and adjacent waters. Special Publications from the Seto Marine Biological Laboratory 3: 1–229. https://doi.org/10.5134/176456

Azman BAR, Ramlan O, Wan-Lotfi WM, Zaidi C, Othman BHR (2008) Seagrass biodiversity of Pulau Tinggi, Johor. In: Mohamed CAR, Sahrani FK, Ali MM, Zaidi CC, Norhayati A (Eds) Malaysia marine ecosystem: The studies of Johor Darul Takzim east coast. Research and Information Series of Malaysian Coasts, Malaysia, 1–176.

Azman BAR, Melvin CWH (2011) Two new species of *Urothoe* (Crustacea, Amphipoda, Gammaridea) from the east Johor Islands Archipelago, Malaysia. Zookeys 87: 43–62. https://doi.org/10.3897/zookeys.87.817

Azman BAR, Othman BHR (2013) Shallow water marine gammaridean amphipods of Pulau Tioman, Malaysia, with the description of a new species. ZooKeys 335: 1–31. https://doi.org/10.3897/zookeys.335.5567

Chess JR (1989) *Aciconula acanthosoma*, new species, a caprellid amphipod from Southern California, with notes on its ecology. Journal of Crustacean Biology 9: 662–665. https://doi.org/10.2307/1548595

Chew M, Abdul Rahim A, Haji Ross OB (2014) *Tinggianthura alba*: A new genus and species of Anthuridae (Isopoda, Cymothoida, Anthuroidea) from Pulau Tinggi, Johor, Malaysia with an updated key to the genera of Anthuridae. PLoS One 9: e99072. https://doi.org/10.1371/journal.pone.0099072

Chew M, Rahim ABA, Mohd Yusof NYB (2016) Two new species of *Pendanthura* (Isopoda, Cymothoida, Anthuroidea) from the east coast of Peninsular Malaysia with an identification key to the species of Pendanthura. Bulletin Marine Science 92: 229–242. https://doi.org/10.5343/bms.2015.1056

Coleman CO (2003) "Digital inking": How to make perfect line drawings on computers. Organisms Diversity and Evolution 3(14): 1–14. https://doi.org/10.1078/1439-6092-00081

Gan SY, Azman BAR, Yoshida T, Majid AM, Toda T, Takahashi K, Othman BHR (2010) Comparison of day and night mysid assemblages in a seagrass bed by using emergence traps, with key to species occuring at Pulau Tinggi, Malaysia. Coastal Marine Science 34: 74–81.

Guedes-Silva E, Souza-Filho J (2013) A new species of *Aciconula* (Amphipoda: Corophiidea) from Brazilian waters. Journal of the Marine Biological Association of the United Kingdom 93(7): 1835-1841. https://doi.org/10.1017/S0025315413000155

Guerra-García JM (2004) The Caprellidea (Crustacea: Amphipoda) from Western Australia and Northern Territory, Australia. Hydrobiologia 522: 1–74. https://doi.org/10.1023/B:HYDR.0000029929.07691.a7

Harbone A, Fenner D, Barnes D, Beger A, Harding M, Roxburgh ST (2000) Status report on the coral reefs of the east coast of Peninsular Malaysia. Coral Cay Conservation Limited, London, 89 pp.

Japar Sidik B, Muta Harah Z (2003) The seagrasses of Malaysia. In: Green EP, Short FT (Eds) World Atlas of Seagrasses. University of California Press, Berkeley, 152–160.

Japar Sidik B, Muta Harah Z (2011) Seagrasses – diversity, values and why they are declining. In: Ibrahim K, Mohamed CAR, Jamaludin MR, Kee AAA, Zulkifli FA, Lee JN (Eds) Malaysia's Marine Biodiversity: Inventory and Current Status. Department of Marine Park Malaysia, Putrajaya, 71–89.

Japar Sidik B, Muta Harah Z, Arshad A (2006) Distribution and significance of seagrass ecosystems in Malaysia. Aquatic Ecosystem Health & Management 9: 203–214. https://doi.org/10.1080/14634980600705576

Latreille PA (1816) Chevrolle. Nouveau dictionnaire d'histoire naturelle Paris 6: 433–4.

Leach WE (1814) Article Crustaceology. The Edinburgh Encyclopaedia 7: 429–437.

Lim JHC, Azman BAR, Othman BHR (2010) Melitoid amphipods of the genera *Ceradocus* Costa, 1853 and *Victoriopisa* Karaman and Barnard, 1979 (Crustacea: Amphipoda: Maeridae) from the South China Sea, Malaysia. Zootaxa 2384: 23–39 https://doi.org/10.11646/zootaxa.2348.1.2

Lim JHC, Rahim ABA, Takeuchi I (2012) *Microtripus tinggiensis*, new genus and species (Amphipoda: Caprellidea: Phtisicidae) from Pulau Tinggi, East Johor Islands Archipelago, Malaysia. Proceedings of the Biological Society of Washington 125: 241–251. https://doi.org/10.2988/11-40.1

Lim JHC, Othman BHR, Takeuchi I (2015) Description of *Orthoprotella bicornis*, new species, and *Paraprotella teluksuang*, new species (Crustacea: Amphipoda) from Johor, Malaysia with special reference to unusual sexual bias towards females in *Paraprotella*. Raffles Bulletin of Zoology 63: 33–48.

Lim JHC, Azman BAR, Takeuchi I, Othman BHR (2017) *Pseudaeginella telukrimau* sp. nov., a new species of caprellid (Crustacea: Amphipoda) from Malaysia. Zootaxa 4282: 62–72. https://doi.org/10.11646/zootaxa.4282.1.3

Mayer P (1903) Die Caprelliden der Siboga-Expedition. Siboga-Expeditie 34: 1–160. https://doi.org/10.5962/bhl.title.53742

Mayer P (1912) Caprellidae. In: Michaelsen W, Hartmeyer R (Eds) Die Fauna Sudwest-Australiens 4: 1–14.

Maritime Institute of Malaysia (2006) Malaysia national coral reef report. UNEP-GEF South China Sea Project and Marine Park Section. Ministry of Natural Resources and Environment, Malaysia, 83 pp.

Othman BHR, Azman BAR (2007) A new species of Talitridae (Amphipod: Gammaridea) from Tioman Island, Malaysia. Zootaxa 1454: 59–68. https://doi.org/10.11646/zootaxa.1454.1.5

Soler-Hurtado MM, Guerra-García JM (2016) The Caprellid *Aciconula acanthosoma* (Crustacea: Amphipoda) Associated with Gorgonians from Ecuador, Eastern Pacific. Pacific Science 70: 73–82. https://doi.org/10.2984/70.1.6

Utinomi H (1969) Caprellids from Kamae Bay, northeastern Kyushu (Amphipoda; Caprellidae). Publications of the Seto Marine Biological Laboratory 16(5): 295– 306. https://doi.org/10.5134/175557

ZooKeys 859: 31–48 (2019)
doi: 10.3897/zookeys.859.33069
http://zookeys.pensoft.net

RESEARCH ARTICLE

A peer-reviewed open-access journal
ZooKeys
Launched to accelerate biodiversity research

A new species of the genus *Centruroides* Marx (Scorpiones, Buthidae) from western Michoacán State, México using molecular and morphological evidence

Ana F. Quijano-Ravell[1], Luis F. de Armas[2], Oscar F. Francke[3], Javier Ponce-Saavedra[4*]

1 *Instituto de Ciencias Básicas e Ingeniería. Laboratorio de Interacciones Biológicas. Centro de Investigaciones Biológicas. Universidad Autónoma del Estado de Hidalgo, Km. 4.5 carretera Pachuca-Tulancingo, Pachuca, 42184, Hidalgo, México* **2** *P.O. Box 4327, San Antonio de los Baños, Artemisa 38100, Cuba* **3** *Colección Nacional de Arácnidos, Instituto de Biología, Universidad Nacional Autónoma de México, Apartado Postal 70-153, México 04510, D.F., México* **4** *Laboratorio de Entomología "Biol. Sócrates Cisneros Paz", Facultad de Biología, Universidad Michoacana de San Nicolás de Hidalgo, Edificio B-4, 2do piso, Ciudad Universitaria, Morelia 58060, Michoacán, México*

Corresponding author: *Javier Ponce-Saavedra* (ponce.javier0691@gmail.com)

Academic editor: *J.O. Camara* | Received 14 January 2019 | Accepted 20 May 2019 | Published 2 July 2019

http://zoobank.org/C9EC1D32-5229-49A5-A857-C720EBA1FE69

Citation: Quijano-Ravell AF, de Armas LF, Francke OF, Ponce-Saavedra J (2019) A new species of the genus *Centruroides* Marx (Scorpiones, Buthidae) from western Michoacán State, México using molecular and morphological evidence. ZooKeys 859: 31–48. https://doi.org/10.3897/zookeys.859.33069

Abstract

A new species of scorpion belonging to the genus *Centruroides* Marx, 1890 is described from the Coalcomán mountain range, western Michoacán State, Mexico. Its general aspect resembles *Centruroides ruana* Quijano-Ravell & Ponce-Saavedra, 2016, and *C. infamatus* (C. L. Koch, 1844), but it is a smaller species having lower pectinal tooth counts; also, males of *C. ruana* have the pedipalp chelae slightly thicker, whereas *C. infamatus* has a subaculear tubercle nearer to the base of the aculeus. Another species with similar aspect is *Centruroides ornatus* Pocock, 1902; however, a preliminary molecular analysis of the mitochondrial gene mRNA 16S showed genetic divergence (measured as p-distance) near to 10% between these species, and lower differences between the new species with respect to *C. infamatus* (4.63%) and *C. ruana* (5.07%). The molecular evidence together with the morphological characters (integrative taxonomy) are sufficient for recognizing the Coalcomán population as a separate and valid species.

Keywords

bark scorpions, Coalcomán Range, North America, striped scorpions, taxonomy

Introduction

Buthid scorpions of the genus *Centruroides* Marx, 1890 (Buthidae) are widely distributed in Mexican territory, from which 45 nominal species and two subspecies have been recognized (Ponce-Saavedra and Francke 2019), some of them with medical importance (Ponce-Saavedra and Moreno-Barajas 2005, Ponce-Saavedra and Francke 2013a, b, Ponce-Saavedra et al. 2016, Quijano-Ravell and Ponce-Saavedra 2016).

From Michoacán State, eight species belonging to this genus have been described or recorded (Ponce-Saavedra et al. 2016): *Centruroides balsasensis* Ponce-Saavedra & Francke, 2004; *C. bertholdii* (Thorell, 1876); *C. infamatus* (C. L. Koch, 1844); *C. limpidus* (Karsch, 1879); *C. nigrescens* (Pocock, 1898); *C. ornatus* Pocock, 1902; *C. ruana* Quijano-Ravell & Ponce-Saavedra, 2016 and *C. tecomanus* Hoffmann, 1932. Only *C. ruana* is endemic to Michoacán.

Centruroides elegans (Thorell, 1876) and *C. pallidiceps* Pocock, 1902 were mentioned from Michoacán by Beutelspacher-Baigts (2000), but those records were seemingly based on misidentified specimens. The first one is only known from Jalisco and Nayarit; whereas the second species seems to be restricted to Sinaloa and Sonora (Ponce-Saavedra and Francke 2013a, b; Santibañez-Lopez et al. 2016).

The Coalcomán Range is located in the west of Michoacán and forms part of the western-most region of the Sierra Madre del Sur. Its highest elevations reach almost 2900 m a.s.l. and contain well conserved areas with high levels of endemism for animals and plants (Arriaga et al. 2000).

In the present contribution we describe a new species of the genus *Centruroides* from the Coalcomán Range, based on several specimens of both sexes under an integrative taxonomic perspective, using morphological and molecular evidence.

Material and methods

Material examined

The examined specimens are deposited in 75% ethanol in the following institutions: CAFBUM: Colección Aracnológica del Laboratorio de Entomología "Biol. Sócrates Cisneros Paz", Facultad de Biología, Universidad Michoacana de San Nicolás de Hidalgo, Morelia, Michoacán, México; CNAN: Colección Nacional de Arácnidos, Instituto de Biología, Universidad Nacional Autónoma de México, D.F; and IESC: Instituto de Ecología y Sistemática, La Habana, Cuba.

Morphological analysis

The specimens were examined and measured with a Zeiss Stemi DV4 stereomicroscope, equipped with a 0.1 mm ocular micrometer. Photographs were obtained with a

microscope eyepiece camera 3.1mp AmScope MU300. Digital images obtained were processed and edited with Adobe Photoshop CS5.The distribution map was generated with ESRI ArcGIS online. We obtained two hemispermatophores from one male of the new species as a complementary structure for the description.

Nomenclature and measurements follow Stahnke (1970), except for trichobothriotaxy (Vachon 1974, 1975), metasomal carinae (Francke 1977), pedipalp chela carinae (Acosta et al. 2008, as interpreted by Armas et al. 2011), and sternum (Soleglad and Fet 2003).

Molecular analyses

In addition to the morphological diagnostic characters, a molecular analysis using sequences of mitochondrial gene RNAm 16S was carried out with specimens of four populations of *C. ornatus*, one of *C. balsasensis* and two localities of *C. infamatus*. Also, included was one sequence of the type population of *C. ruana* (Quijano-Ravell & Ponce-Saavedra 2016). All sequences were obtained from specimens captured at different dates by several collectors that were found in the CNAN, CAFBUM and IESC collections, except the one of *C. infamatus* from Uruapan which was downloaded from GenBank (AF439753).

For the genetic analyses, DNA was extracted from muscle tissue preserved at 96% ethanol (pedipalps and legs fragments) using the FitzSimmons protocol (FitzSimmons 1997). A fragment of the mRNA 16S was amplified by polymerase chain reaction (PCR) with the primers previously used for scorpions of the *Centruroides* genus by some authors (Gantenbein et al. 1999; Gantenbein et al. 2000; Gantenbein et al. 2001, Towler et al. 2001, Teruel et al. 2006, Ponce-Saavedra et al. 2009), 5'-GCATTTGAACTCAGATCA-3' and 3'-GTGCAAAGGTAAGCATAATCA-5'. The PCR conditions were established according to the protocol for arthropods of Simon et al. (1994) with modifications using 25 µl as a final volume. The cycle parameters were: initial denaturation at 94 °C (5 min), denaturation at 94 °C (30 s), annealing at 50 °C (30 s) and extension at 72 °C (30 s and 7 min) repeated for 30 cycles. The amplified products were observed in an agarose gel with UV light for verify their quality. DNA samples were sent to Macrogen Inc. USA for sequencing.

DNA sequences were aligned with MEGA X: Molecular Evolutionary Genetics Analysis software (Kumar et al. 2018) and a p-distances matrix was generated using the Jukes-Cantor model.

The analysis involved 11 nucleotide sequences (Table 5); all ambiguous positions were removed for each sequence pair (pairwise deletion option). There were 350 positions in the final dataset. The percentage of replicate trees in which the associated taxa clustered together in the bootstrap test (500 replicates) are shown next to the branches. The evolutionary distances were computed using the p-distance method and are in the units of the number of base-pair differences per site. For the Maximum Likelihood method we used the Tamura-Nei model. Initial tree(s) for the heuristic search

were obtained automatically by applying Neighbor-Joining and BioNJ algorithms to a matrix of pairwise distances estimated using the Maximum Composite Likelihood (MCL) approach, and then selecting the topology with the superior log likelihood value. Due to small number of species in this analysis, the most parsimonious tree was obtained using the Subtree-Pruning-Regrafting (SPR) algorithm (Nei and Kumar 2000) with search level 1 in which the initial trees were obtained by the random addition of sequences (10 replicates). The evolutionary history using both methods was inferred from the Bootstrap consensus tree obtained from 500 replicates. Analyses were conducted in MEGA X: Molecular Evolutionary Genetics Analysis across computing platforms (Kumar et al. 2018).

Taxonomy

Family Buthidae C. L. Koch, 1837
Genus *Centruroides* Marx, 1890

***Centruroides romeroi* sp. nov.**
http://zoobank.org/6528884A-5A64-4CC7-B99A-73D5D1BB645F
Figs 1–20; 29, 30a, e, i, 31a, e. Tables 1–3.

Type material. Male **holotype** (CNAN-T01315), Michoacán: Coalcomán de Vázquez Pallares municipality: La Nieve (18°49.070'N, 103°02.653'W, 2230−2260 m a.s.l.), 07-VIII-2002, O. Francke, E. González S. y S. Reynaud colls, determined as *Centruroides infamatus ornatus* by R. J. Moreno B., 02-VII-2004. **Paratypes**: 17 ♂♂, 38 ♀♀ Michoacán: Coalcomán de Vázquez Pallares municipality: La Nieve, 10.VII.2006, 2246 m, O. Francke, J. Ponce, M. Córdova, A. Jaimes, G. O. Francke & V. Capovilla, colls: 1 male (peines 22-21) 1 female (18-18). (CNAN-T01316), 3 ♂♂, 5 ♀♀ (CAFBUM S0150), 3 ♂♂ adult, 1 ♂ juvenile, 3 ♀♀ (IESC-3.3796 to. 3.3802). Michoacán: Coalcomán de Vázquez Pallares municipality: La Nieve, 7. VIII. 2002, 2265 m, O. Francke, E. Gonzalez-Santillán & S. Reynaud colls.

Distribution. Only known from the type locality (Fig. 1).

Etymology. The proposed name is a patronym honoring Biol. Mario Manuel Romero Tinoco, who has dedicated his life to increasing our knowledge of the "hot land" in Michoacán State, and for his relevant and continued contributions to the people that inhabit those beautiful places.

Diagnosis. A medium-sized species belonging to the *Centruroides infamatus* subgroup (as defined by Ponce-Saavedra and Francke 2019) of the "striped" group. Pectines with 16–18 (mode 18) teeth in females and 20–22 (mode 21) in males (Table 3). Hemispermatophore flagelliform, internal lobe (il) slightly developed, moderately sclerotized and almost straight; medial lobe (ml) scarcely developed but sclerotized; external lobe spiniform hook-like; trunk broad, fusiform and expanded towards the pedal flexure region; truncal flexure is conspicuous; pedicel with margins strongly

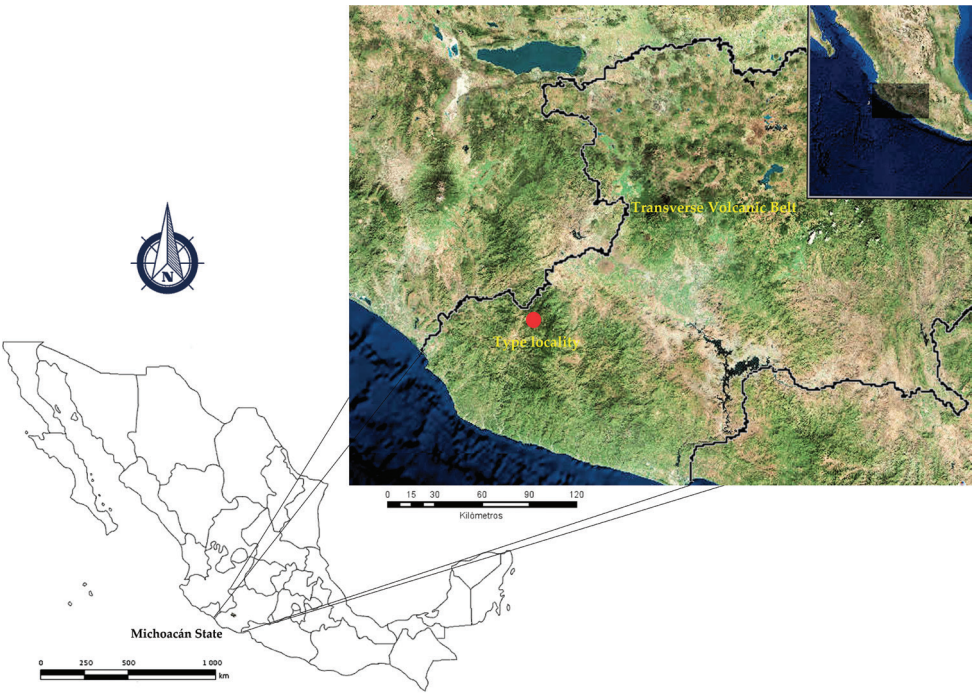

Figure 1. *Centruroides romeroi* sp. nov., geographic position of the type locality in Mexico.

sclerotized at inner margin that is less sclerotized towards the pedal flexure which is well developed (Fig. 29).

Centruroides romeroi sp. nov. closely resembles *C. ruana* and *C. infamatus*, (Quijano-Ravell and Ponce-Saavedra 2016) but it is noticeably smaller (33–45 mm in *C. romeroi* sp. nov., 63–70.7 mm in *C. ruana* and 54–66 mm in *C. infamatus*) having a lower pectinal tooth count and paler coloration pattern. Also, males of *C. ruana* have pedipalp chelae slightly thicker (Fig. 30b), whereas *C. infamatus* has subaculear tubercle nearer to the base of the aculeus (Fig. 30k). The most similar species to *Centruroides romeroi* sp nov. is *C. ornatus* but the new species differs as follows: It has pedipalps moderately elongated (Fig. 30a); femur with dorsal, external and ventral intercarinal spaces finely and densely granulose and the internal face with many coarser scattered granules, some of which are large and conical; dorsal internal, dorsal external and ventral internal carinae on the manus dentate and well developed and the ventral external carina strong, serrate. Pedipalps of *C. ornatus* moderately elongated (Fig. 30d); manus oval; femur with intercarinal spaces coriaceous, except dorsally where they are finely granulose; all carinae strong, coarsely granulose to subdentate. Segment V of *Centruroides romeroi* sp. nov. (Fig. 30a) almost entirely acarinate except for subtle vestiges of dorsal supramedians (basal one-third only), ventral lateral and ventral median carinae. Segment V of *C. ornatus* (Fig. 30h) with ventral lateral carinae very weakly subgranulose, the submedian carinae absent and ventral median carina weakly subgranulose. Pectinal

Table 1. Measurements (in mm) of the holotype and four paratype males of *Centruroides romeroi* sp. nov. Abbreviations: L=Length; W=Width; D= Depth; Ca = Carapace; MeS= Mesosomal segment; MS= Metasomal segment; Ves=Vesicle; Fmr=Femur; Ptla= Patella; Hand= hand of chelae of pedipalp; Fix F= Fixed finger; MovF= Movable finger; BP= Basal plate of pectines; P.C.= Pectinal tooth count.

Measurement	Holotype	Paratypes				
		Male 1	Male 2	Male 3	Male 4	Male 5
L Ca	4.60	4.40	4.40	4.40	4.60	4.60
LMeSVII	4.00	3.80	3.20	4.00	4.40	3.80
W MeSVII	4.10	4.20	4.00	4.20	4.20	4.20
L MSI	4.00	3.80	3.60	3.80	4.20	3.80
L MSII	4.60	4.60	4.20	4.40	5.00	4.60
L MSIII	5.20	5.00	4.80	5.00	5.80	5.20
L MSIV	5.80	5.80	5.40	5.60	6.40	5.60
L MSV	6.60	6.60	6.20	6.20	7.20	6.20
W MSI	2.20	2.20	2.20	2.20	2.20	2.20
W MSII	2.00	2.00	2.00	2.00	2.00	2.00
W MSIII	2.00	2.00	2.00	2.00	2.00	2.00
W MSIV	2.00	2.00	2.00	2.00	2.00	2.00
W MSV	2.20	2.20	2.20	2.20	2.20	2.00
D MSI	1.80	2.00	1.80	1.80	1.80	1.80
D MSII	1.80	2.00	1.80	1.80	1.80	1.80
D MSIII	1.80	2.00	1.80	1.80	1.80	1.80
D MSIV	1.80	2.00	1.80	1.80	1.80	1.80
D MSV	2.00	2.10	2.00	2.00	2.00	2.00
L Ves	3.00	2.90	3.00	2.80	3.00	3.00
W Ves	1.60	1.60	1.60	1.60	1.60	1.60
D Ves	1.60	1.40	1.60	1.60	1.60	1.60
L Fmr	4.80	4.80	4.60	4.60	4.90	4.60
W Fmr	1.20	1.20	1.20	1.20	1.20	1.20
L Ptla	5.00	5.00	4.80	4.80	5.20	4.80
W Ptla	1.60	1.60	1.60	1.60	1.60	1.60
L Hand	3.40	3.60	3.40	3.60	3.80	3.60
W Hand	1.60	1.60	1.60	1.80	1.80	1.80
D Hand	1.60	1.60	1.60	1.60	1.60	1.60
L Fix F	4.20	4.40	4.00	4.00	4.40	4.10
L Mov F	5.00	5.00	4.60	4.80	5.00	5.00
L BP	0.50	0.60	0.60	0.50	0.50	0.60
W BP	1.00	1.10	1.10	1.00	1.00	1.00
P.C.	21-21	21-22	21-22	22-23	20-20	22-22

tooth counts in *C. romeroi* sp. nov. male 18–22, female with 16–21 teeth, whereas *C. ornatus* males have 19–24 teeth, females 17–23. Basal pectinal plate of *C. romeroi* sp. nov. with anterior margin with a deep, narrow anteromedian notch, whereas on *C. ornatus* the anterior margin is almost straight, with small median V-shaped notch (Fig. 31d). Also, the distribution of *C. ornatus* is endemic to the Transverse Volcanic Belt whereas *C. romeroi* sp. nov. is distributed only in the Coalcomán mountain range which is part of the western-most region of the Sierra Madre del Sur (Fig. 1).

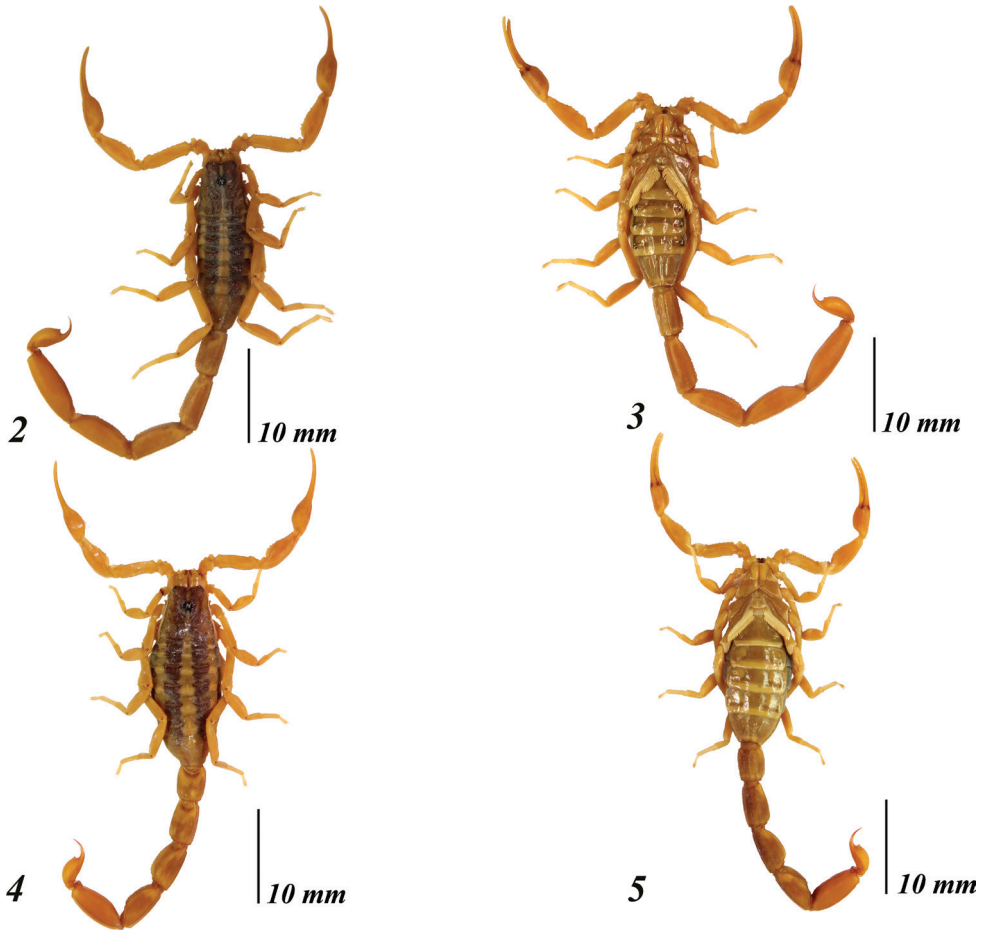

Figures 2–5. *Centruroides romeroi* sp. nov., habitus. **2–3** dorsal and ventral views of the male holotype **4–5** dorsal and ventral view of female paratype.

Description of the male holotype (Figs 2–20). A typical "striped scorpion", basically yellow, paler ventrally (Figs 2–5). Carapace with a broad dark brownish band that runs from the lateral eyes to the posterior median carinae, except on median furrow, two patches lateral to ocular tubercle, the ocular lateral furrows and the posterior median furrow, all which are immaculate (Fig. 6). Ocular tubercle and area around lateral eyes intensely infuscate. Lateral margins pale brown. Lateral submargins mostly immaculate, with vestigial brown pigment. Posterior margin with two short dark lines from which the tergites stripes originate. Mesosoma dorsally with two longitudinal blackish stripes on tergites I–VI, separated by a slightly narrower pale stripe; on VII the dark stripes become diffuse (Fig. 7). Median longitudinal carina immaculate on all tergites. Pedipalps mostly immaculate, chelae ventrally vestigially infuscate; the fingers have the same color as the manus (Figs 8, 9). Metasoma dorsally immaculate, ventrally and laterally with vestigial pigments on segments I–IV, and immaculate on V and telson (Figs 2–5, 10). Legs immaculate.

Table 2. Measurements (in mm) of six female paratypes of *Centruroides romeroi* sp. nov. Abbreviations: L=Length; W=Width; D= Depth; Ca = Carapace; MeS= Mesosomal segment; MS= Metasomal segment; Ves=Vesicle; Fmr=Femur; Ptla= Patella; Hand= hand of chelae of pedipalp; Fix F= Fixed finger; MovF= Movable finger; BP= Basal plate of pectines; P.C.= Pectinal tooth count.

Measurement	Paratypes					
	Female 1	Female 2	Female 3	Female 4	Female 5	Female 6
L Ca	4.60	4.80	4.40	4.20	4.20	4.60
LMeSVII	3.00	3.20	3.20	3.40	3.20	3.60
W MeSVII	5.00	4.60	4.60	5.00	4.60	5.00
L MSI	3.20	3.20	3.20	2.80	2.60	3.20
L MSII	3.60	3.60	3.80	3.40	3.20	3.80
L MSIII	4.00	4.00	4.00	3.80	3.40	4.20
L MSIV	4.60	4.40	4.60	4.20	3.80	4.60
L MSV	5.40	5.20	5.20	5.00	4.60	5.20
W MSI	2.60	2.60	2.60	2.40	2.40	2.60
W MSII	2.40	2.40	2.40	2.20	2.20	2.40
W MSIII	2.40	2.40	2.40	2.20	2.20	2.40
W MSIV	2.40	2.40	2.20	2.20	2.00	2.40
W MSV	2.20	2.40	2.20	2.00	2.00	2.40
D MSI	2.00	2.20	2.00	2.00	2.00	2.20
D MSII	2.00	2.20	2.00	2.00	2.00	2.20
D MSIII	2.00	2.20	2.00	2.00	2.00	2.20
D MSIV	1.80	2.00	1.80	1.80	1.80	2.00
D MSV	1.80	2.00	1.80	1.80	1.80	2.00
L Ves	2.40	2.40	2.40	2.20	2.30	2.40
W Ves	1.60	1.60	1.60	1.40	1.40	1.60
D Ves	1.40	1.40	1.40	1.40	1.40	1.60
L Fmr	4.40	4.20	4.40	4.20	4.00	4.60
W Fmr	1.20	1.20	1.20	1.20	1.20	1.20
L Ptla	4.80	4.80	4.80	4.60	4.20	5.00
W Ptla	1.60	1.60	1.60	1.40	1.60	1.60
L Hand	3.40	3.20	3.40	3.00	3.00	3.40
W Hand	1.80	1.60	1.80	1.40	1.40	1.80
D Hand	1.60	1.60	1.60	1.40	1.40	1.60
L Fix F	4.40	4.40	4.20	4.00	3.80	4.40
L Mov F	5.00	5.00	4.80	4.80	4.40	5.20
L BP	0.60	0.60	0.60	0.60	0.60	0.60
W BP	1.20	1.00	1.20	1.20	1.10	1.00
P.C.	18-16	18-18	18-18	17-17	18-18	19-18

Table 3. Variation of the pectinal tooth counts in *Centruroides romeroi* sp. nov. Abbreviations: n, sample by sex; N, total of examined combs; * Mode.

Sex	n	Pectinal tooth counts							Average	Standard Deviation
		16	17	18	19	20	21	22		
Female	90	2	22	**47***	16	2	1		17.96	0.84
Male	46			3	3	13	**21***	8	20.60	1.05
N	**136**									

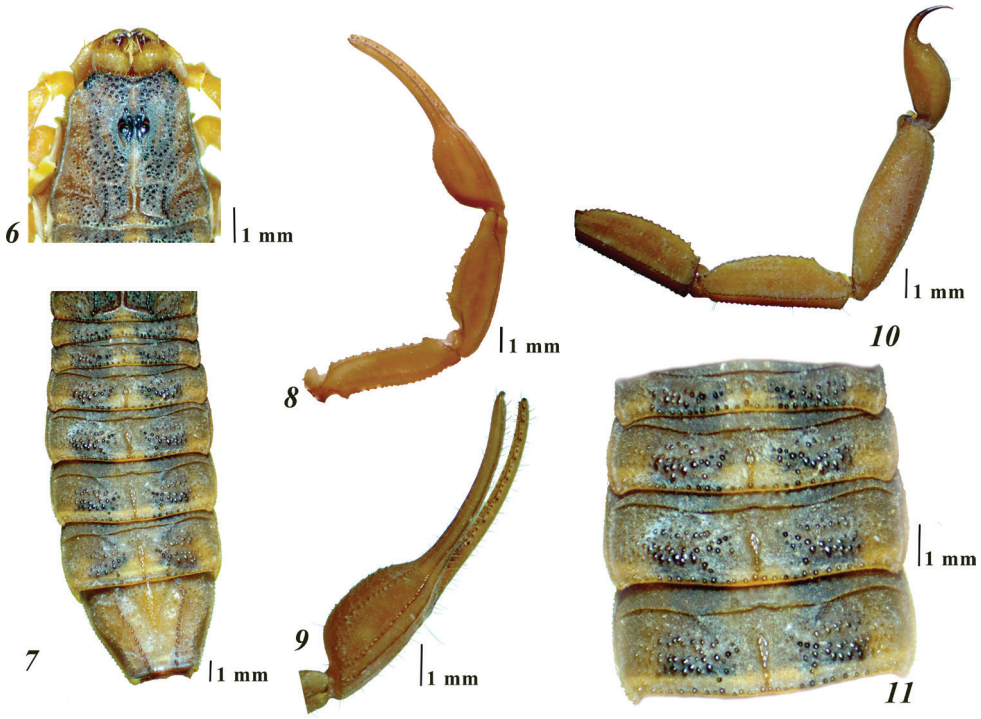

Figures 6–11. *Centruroides romeroi* sp. nov., male holotype: **6** carapace **7** dorsal aspect of mesosoma **8** dorsal aspect of pedipalp **9** manus **10** lateral aspect of metasomal segments III–V and telson **11** tergites I–IV.

Carapace. Anterior margin with median notch broadly "V" shaped, reaching the level of the posterior margin of the first pair of lateral eyes, weakly crenulate and scarcely setose; three pairs of lateral eyes subequal in size (Fig. 6). Lateral areas feebly granulose, margins finely granulate. Ocular tubercle smooth. Central pigmented area with medium-sized granules, but finely granulose around the ocular tubercle (Fig. 6). Posterior margin straight, granulose, with medium-sized granules and a shallow median indentation (Fig. 6). Carinae: anterior medians indistinct; superciliary crest smooth, with obsolete broad granules (Fig. 6); posterior medians well developed, granulose. Furrows: anterior median, median ocular, posterior median, and posterior marginal wide and moderately deep; laterals ocular narrow; posterior laterals wide, with disperse small granules; central laterals vestigial (Fig. 6).

Mesosoma. Tergites with moderate median longitudinal carina (Figs 7, 11); submedian and lateral carinae on VII strong and serrate. Pigmented areas are covered by small to medium-sized granules (Fig. 7). Sternites sparsely setose, spiracles oblique and slit-like; III – VI acarinate; III with a median triangular area which is smooth and glossy, and two lateral areas which are densely and finely granulose (Fig. 12); IV – VI with integument smooth and glossy, each with four short and smooth posterior carinae, with the submedian pair indistinct on IV – V; V with some coarse punctures medially, without translucent whitish patch; VII with two pairs of long and moderately

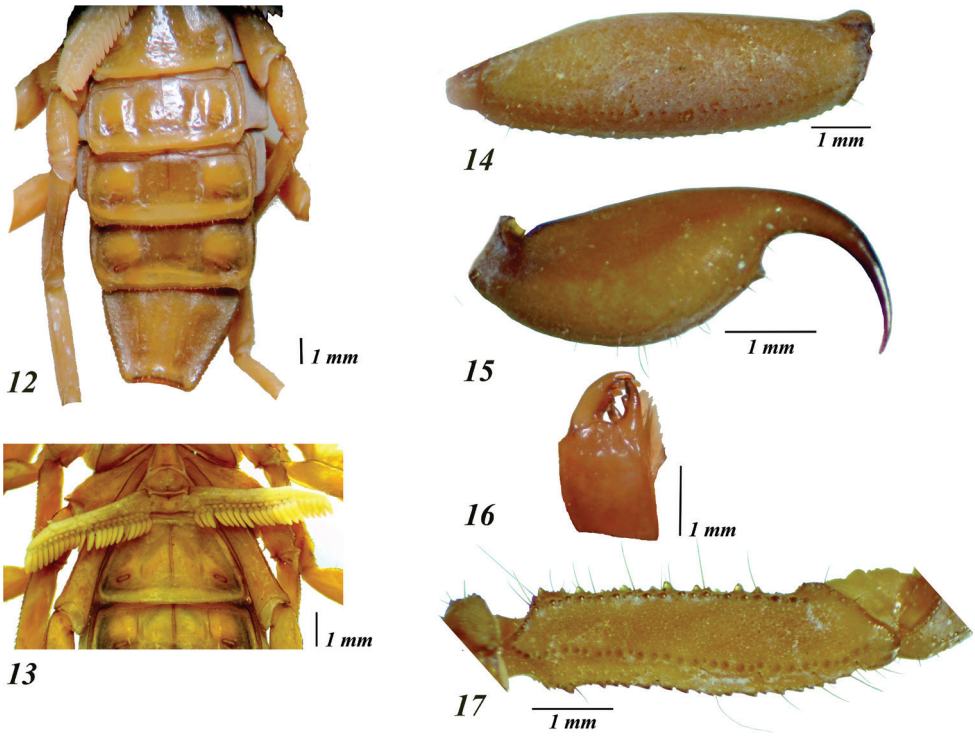

Figures 12–17. *Centruroides romeroi* sp. nov., male holotype: **12** sternites **13** coxoesternal region and sternite III **14** lateral view of metasomal segment V **15** lateral view of telson **16** right chelicera **17** dorsal aspect of pedipalp femur.

to strongly costate to subcrenulate submedian and lateral carinae, intercarinal spaces very finely and densely granulose (Fig. 12).

Sternum type 1, triangular, very finely granular, with two long, median subdistal macrosetae; posterior depression long, wide and deep (Fig. 13).

Genital operculum (Fig. 13) medium-sized (its width is slightly larger than the sternum length); each valve subtriangular, with four macrosetae and some shorter setae. Genital papillae do not protrude from the posterior margin of the valves. Prepectinal plate moderately sclerotized, with anterior margin concave.

Pectines. Tooth count 21/22. Basal plate rectangular, anterior margin almost straight, with small median V-shaped notch, posterior margin straight (Fig. 13).

Metasoma. Moderately elongated and not incrassate distally (Figs 2, 3, 10). Intercarinal spaces coriaceous, with scarce minute granules. Segments I–IV with the following carination: dorsal laterals, lateral supramedians and lateral inframedians (on I only) well developed, serrate, the dorsal lateral carinae become gradually stronger and dentate distally on each segment, mainly on II – III; ventral laterals and ventral submedians well developed, finely granulate and subserrate. Segment V rounded in cross-section, almost entirely acarinate except for subtle vestiges of dorsal supramedians (basal one-third only), ventral lateral and ventral median carinae (Fig. 14). Tel-

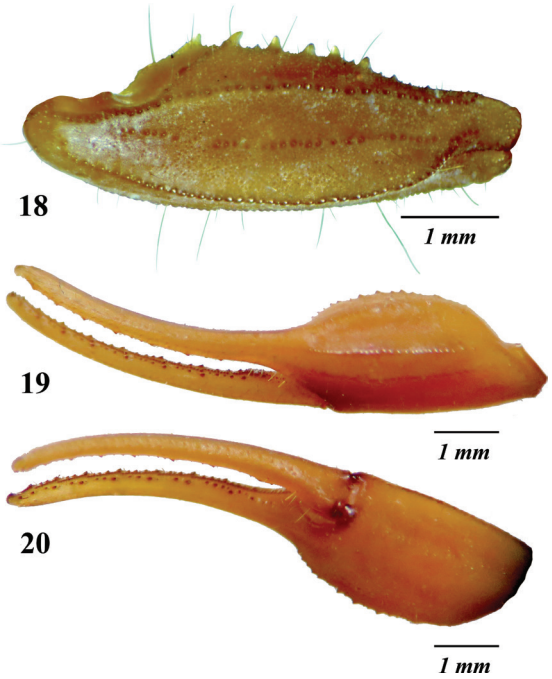

Figures 18–20. *Centruroides romeroi* sp. nov., male holotype: **18** dorsal aspect of pedipalp patella **19, 20** chelae.

son with vesicle slightly elongated (length/width ratio = 1.78, depth/width ratio = 1.00) and coriaceous; ventral median carina vestigial; subaculear tubercle short, widely conical and somewhat distant from the base of aculeus, which is shorter than vesicle and moderately curved (Fig. 15), moderately setose. Vesicle incrassate oval (1.81 times longer than wide, 1.07 times wider than deep), integument coriaceous; ventral median carina vestigial, ending in a small subaculear tubercle, widely conical, not particularly close nor separated from base of aculeus. Aculeus strongly curved, shorter than vesicle.

Chelicerae with dentition typical for the genus (Fig. 16). Tegument very finely and densely granulose, dorsodistal portion of manus with coarse and glossy granules arranged transversally, defining a depressed area. Setation very dense ventrally, but essentially lacking dorsally, except for five rigid macrosetae on depressed area of manus: two anterior (the shortest), two posterior and one in the center on a rounded and elevated base (Fig. 16).

Pedipalps orthobothriotaxic A-α; moderately elongated (length/width ratio of femur and patella = 4.8 and 3.6, respectively). Femur with dorsal, external and ventral intercarinal spaces finely and densely granulose (Fig. 17); internal face with with many scattered coarser granules, some of which are large and conical; carinae: dorsal internal, dorsal external and ventral internal well developed, dentate; ventral external carina strong, serrate. Patella sparsely setose, with intercarinal spaces finely and densely granulose; dorsal, external and ventral carinae crenulate to subcrenulate, internal surface with five very large and sharp tubercles (Fig. 18). Hand evenly ovate (Figs 9, 19, 20), 1.1 times as

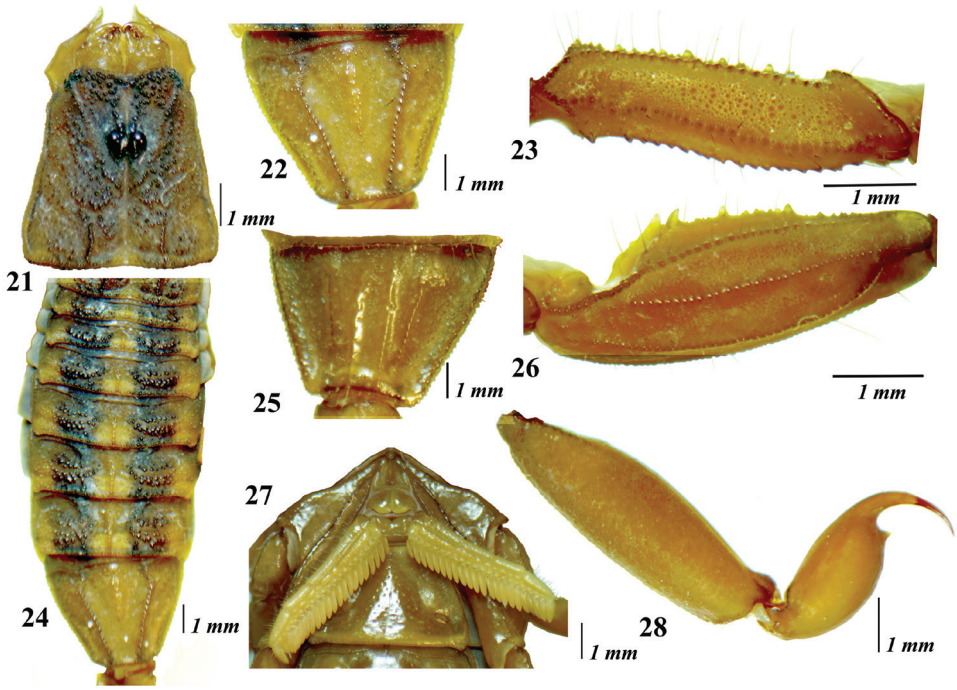

Figures 21–28. *Centruroides romeroi* sp. nov., female paratype: **21** carapace **22** mesosoma **23** tergite VII **24** sternite VII **25** coxoesternal region **26** femur **27** pedipalp patella in dorsal aspect **28** metasomal segment V and telson.

wide as the patella; intercarinal spaces coriaceous; ventral accessory carina and external secondary carina indistinct, with obsolete small granules (Figs 19, 20); digital carina feebly to moderately granulose; dorsal secondary carina and dorsal external carina poorly developed, subgranulose; ventral external carina and ventral internal carina strong and rather subcrenate. Fixed finger long, slender and evenly curved, with a basal notch, eight principal rows of denticles, rows 3 to 7 are flanked by two outer accessory denticles and two inner accessory denticles, whereas in row 8 there is no outer accessory denticle nor an inner accessory denticle; movable finger with eight principal rows of denticles and one apical subrow of three denticles (Fig. 20), basal lobe moderately developed, rows 3 to 7 are flanked by two outer accessory denticles and two inner accessory denticles, whereas row 8 has a single outer accessory denticle and one inner accessory denticle.

Legs. Slender, with carinae granulose to subserrate and intercarinal tegument coriaceous to minutely granulose. Prolateral and retrolateral pedal spurs strong and somewhat curved in all legs. Ventral surface of tarsomere II densely covered by long macrosetae irregularly arranged into two longitudinal, broad, dense rows converging basally. Claws rather short and curved.

Female. Differs from males as follows: color pattern somewhat darker. Metasoma and pedipalps shorter and robust (Figs 21–28, Table 2). Telson with vesicle more globose

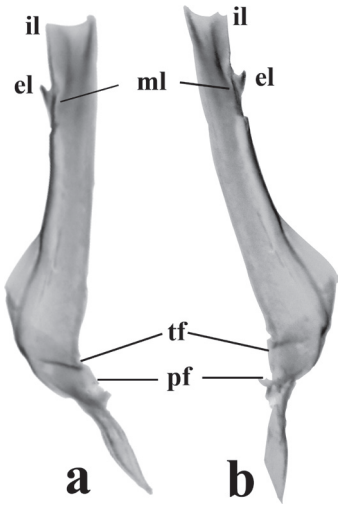

Figure 29. *Centruroides romeroi* sp. nov., ventral aspect of hemispermatophores of adult ♂ from "La Nieve" of Coalcomán municipality, Michoacán, Mexico. **a** Left side **b** Right side. Abbreviations: il, internal lobe. el, external lobe. ml, medial lobe. pf, pedal flexure. Tf, trunk flexure. Scale bar: 0.5 mm.

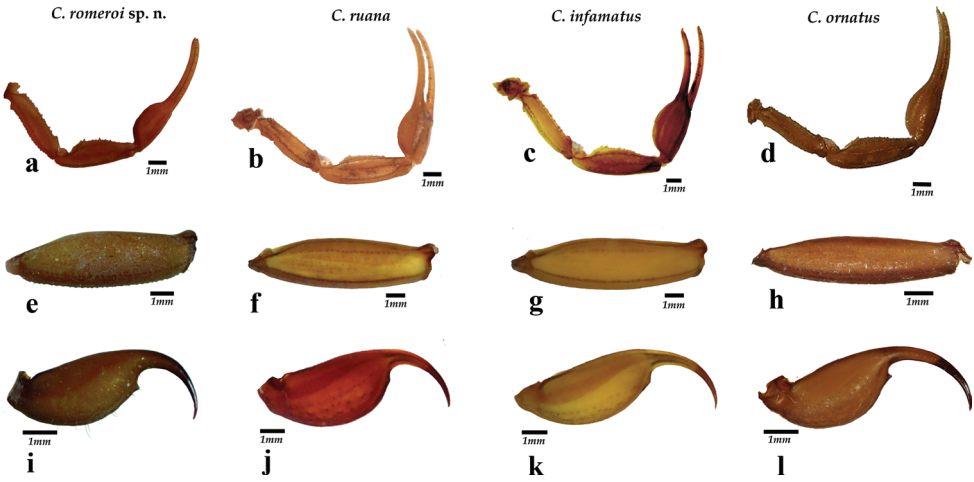

Figure 30. Comparison among pedipalps, metasomal segment V and telson of *Centruroides romeroi* sp. nov. (**a, c, i**); *C. ruana* (**b, f, j**); *C. infamatus* (**c, g, k**) and *C. ornatus* (**d, h, l**).

(Fig. 28). Pectines with 16–21 (mode 18, $N = 90$) teeth in females, whereas in males it is 18–22 (mode 21, $N = 46$) (Table 3). Basal plate of the pectines with anterior margin faintly concave and the posterior margin slightly convex (Fig. 25). Genital papillae absent.

Variation. Pectinal tooth count varies among both sexes (Table 3). Adult males of the type series comprise three size categories and range from 33 to 45 mm in total length. Females: 34–40 mm (Table 1). Most males have pedipalp manus as wide as the patella.

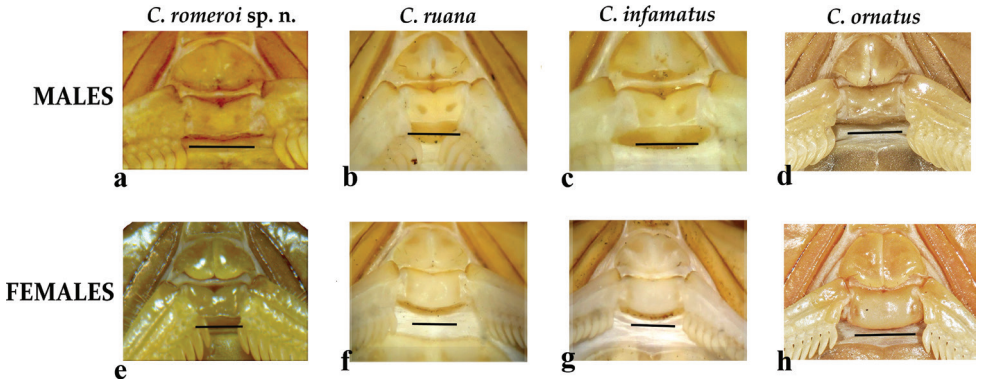

Figure 31. Male and female pectinal plates of *Centruroides romeroi* sp. nov. (**a, e**); *C. ruana* (**b, f**); *C. infamatus* (**c, g**); *C. ornatus* (**d, h**). Scale bar: 1.0 mm.

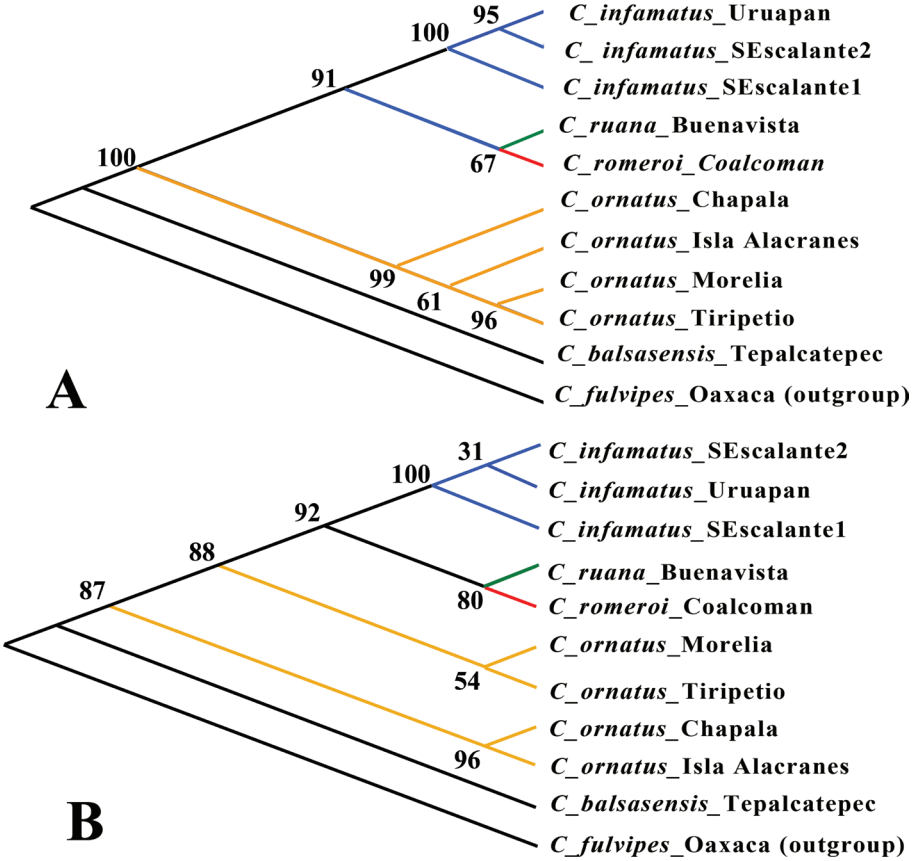

Figure 32. Phylogenetic trees of the *Centruroides infamatus* subgroup obtained by **A** maximum parsimony and **B** maximum likelihood analysis from 500 replicates bootstrap consensus. The specimens used as terminal belong to populations of the species that inhabit localities near the Coalcomán Range. Population identifications are represented by different colors.

Natural history. La Nieve (2030 to 2260 m a.s.l.) belongs to the Coalcomán Range, the predominant vegetation is pine forest, and the climate is temperate sub humid (*Cw*). The scorpions were collected at night, with portable U.V. lights, under stones and fallen rotten trees, under bark of *Pinus* sp., in the yards and walls of the local school and houses of the village. During the collection the temperature and relative humidity of the air were 10−12 °C and 90%, respectively. *Centruroides romeroi* sp. nov. is sympatric with *Vaejovis coalcoman* Contreras-Félix & Francke, 2014.

Molecular analysis. The 16S mitochondrial marker was used successfully by several authors for delimiting several species in the genus *Centruroides* such as the cryptic species *C. exilicauda* (Wood) and *C. sculpturatus* (Ewing) (Gantenbein et al. 2001), and *C. limpidus* Karsch and *C. tecomanus* Hoffmann (Ponce-Saavedra et al. 2009), and for delimiting new species such as *C. ruana* which was separated from *C. ornatus* and *C. infamatus* (Quijano-Ravell and Ponce-Saavedra 2016). For this reason, in addition to the morphological diagnostic characters, a molecular analysis using sequences of the mitochondrial gene mRNA 16S was carried out.

The results showed stronger genetic divergence (measured as p-distance and the Jukes-Cantor model) between the population of *C. romeroi* sp. nov. and populations of *C. ornatus* at two localities of the municipality of Morelia, Michoacán (p-distance = 0.076–0.079), and with two populations at Chapala, Jalisco (p-distance = 0.093–0.098), with one population of *C. balsasensis* (p-distance = 0.128) rather than to *C. infamatus* from two localities of Michoacán (p-distance = 0.463) and with the type population of *C. ruana* (p-distance = 0.049). These differences were consistent both using p-distance and the Jukes-Cantor model (Table 4). The trees obtained by the different phylogenetic hypothesis models were topologically consistent; the bootstrapping consensus tree is showed in the Figure 32. The

Table 4. Genetic distances among different populations of four species of *Centruroides* from Michoacán and Jalisco state including *Centruroides romeroi* sp. nov. The outgroup was *Centruroides fulvipes* from Puerto Ángel, Oaxaca. The evolutionary distances were computed using the Jukes-Cantor method [2] and are in the units of the number of base substitutions per site. p-distance (Nucleotide). This distance is the proportion (p) of nucleotide sites at which two sequences being compared are different. Distances with *C. infamatus* in blue, distances with *C. ornatus* in green.

Especie localidad	1	2	3	4	5	6	7	8	9	10	11
1. *C fulvipes* Oaxaca**		0.8883	0.9837	0.9492	0.8840	0.8973	0.8706	0.8973	0.8536	0.8533	0.8619
2. *C infamatus* Uruapan	0.5205		0.1259	0.1231	0.0000	0.1008	0.0977	0.0647	**0.0478**	0.0736	0.0825
3. *C balsasensis* Tepalcatepec	0.5479	0.1159		0.1690	0.1263	0.1753	0.1652	0.1652	**0.1404**	0.1453	0.1552
4. *C infamatus* SEscalante1	0.5205	0.0000	0.1159		0.0000	0.1008	0.0977	0.0647	**0.0478**	0.0736	0.0825
5. *C infamatus* SEscalante2	0.5192	0.0000	0.1162	0.0000		0.1011	0.0950	0.0619	**0.0478**	0.0738	0.0828
6. *C ornatus* Chapala	0.5233	0.0943	0.1563	0.0943	0.0946		0.0191	**0.1133**	**0.1051**	0.0275	0.0359
7. *C ornatus* Isla Alacranes	0.5151	0.0916	0.1482	0.0916	0.0892	0.0189		**0.1070**	**0.0989**	0.0247	0.0331
8. *C ruana* Buenavista	0.5233	0.0620	0.1482	0.0620	0.0595	***0.1051***	***0.0997***		**0.0507**	0.1008	0.1039
9. *C romeroi* sp. nov. Coalcomán	0.5097	**0.0463**	**0.1281**	**0.0463**	**0.0463**	***0.0981***	***0.0926***	**0.0490**		**0.0805**	**0.0835**
10. *C ornatus* Morelia	0.5096	0.0701	0.1321	0.0701	0.0703	0.0270	0.0243	**0.0943**	***0.0763***		0.0081
11. *C ornatus* Tiripetío	0.5123	0.0782	0.1402	0.0782	0.0784	0.0350	0.0323	**0.0970**	***0.0790***	0.0081	

** Outgroup

Table 5. Localities and sequences used to obtain genetic distances and bootstrap consensus tree for five species and one outgroup including *C. romeroi* sp. nov.

Species	Locality	Code	GenBank registration	Author	Museum where is deposited the voucher specimen
Centruroides fulvipes (Pocock, 1898)	Puerto Ángel, Oaxaca, Mex.	*C. fulvipes* Oaxaca	MK876846	Quijano-Ravell, et al.	CAFBUM
Centruroides infamatus (C. L. Koch, 1844)	Zumpimito, Uruapan del Progreso, Michoacán, Mex.	*C. infamatus* Uruapan	AF439753	Towler et al. 2001	CAFBUM
Centruroides balsasensis Ponce-Saavedra & Francke, 2004	Tepalcatepec, Michoacán, Mex.	*C. balsasensis* Tepalcatepec	MK787193	Quijano-Ravell and Ponce-Saavedra.	CAFBUM
Centruroides infamatus (C. L. Koch, 1844)	Salvador Escalante, Michoacán, Mex.	*C. infamatus* SEscalante1	MK877232	Quijano-Ravell, et al.	CAFBUM
Centruroides infamatus (C. L. Koch, 1844)	Salvador Escalante, Michoacán, Mex.	*C. infamatus* SEscalante2	MK877233	Quijano-Ravell, et al.	CAFBUM
Centruroides ornatus Pocock, 1902	Chapala, Jalisco, Mex.	*C. ornatus* Chapala	MK774709	Quijano-Ravell and Ponce-Saavedra.	CAFBUM
Centruroides ornatus Pocock, 1902	Isla de Los Alacranes, Chapala, Jalisco, Mex.	*C. ornatus* Isla Alacranes	MK774710	Quijano-Ravell and Ponce-Saavedra.	CAFBUM
Centruroides ruana Quijano-Ravell & Ponce-Saavedra	Felipe Carrillo Puerto, Buenavista, Michoacán, Mex.	*C. ruana* Buenavista	MK789720	Quijano-Ravell and Ponce-Saavedra.	CAFBUM
Centruroides romeroi sp. nov.	La Nieve, Coalcomán de Vázquez Pallares, Michoacán, Mex.	*C. romeroi* sp. nov. Coalcomán	MK789721	Quijano-Ravell and Ponce-Saavedra.	CAFBUM
Centruroides ornatus Pocock, 1902	Morelia, Michoacán, Mex.	*C. ornatus* Morelia	MK774718	Quijano-Ravell and Ponce-Saavedra.	CAFBUM
Centruroides ornatus Pocock, 1902	Tiripetío, Morelia, Michoacán, Mex.	*C. ornatus* Tiripetío	MK774721	Quijano-Ravell and Ponce-Saavedra.	CAFBUM

topology of the consensus tree shows that *C. romeroi* sp. nov. appears most related to *C. ruana* in a clade formed by the populations of *C. infamatus* and *C. ornatus* (Fig. 32). The results are consistent with the geographic distribution of the new species, which lives in the Coalcomán mountain range in the westernmost region of the Sierra Madre del Sur, with its nearest species *C. ruana,* that inhabit the western region of Balsas Depression, while the other two clades are species occur in the Transverse Volcanic Belt (Fig. 1).

These molecular results support our decision of considering the Coalcomán population as an isolated and taxonomically valid species.

Acknowledgements

The authors thank Dr Omar Chassin Noria for his support with the DNA extraction.

References

Acosta LE, Candido DM, Buckup EH, Brescovit AD (2008) Description of *Zabius gaucho* (Scorpiones, Buthidae), a new species from southern Brazil, with an update about the generic diagnosis. The Journal of Arachnology 36: 491–501. https://doi.org/10.1636/H07-28.1

Armas LF de, Teruel R, Kovařík F (2011) Redescription of *Centruroides granosus* (Thorell, 1876) and identity of *Centrurus granosus simplex* Thorell, 1876 (Scorpiones: Buthidae). Euscorpius 127: 1–11.

Arriaga L, Espinoza JM, Aguilar C, Martínez E, Gómez L, Loa E (2000) Regiones terrestres prioritarias de México. Conabio, México, D.F., 580 pp.

Beutelspacher-Baigts CR (2000) Catálogo de alacranes de México. Universidad Michoacana de San Nicolás de Hidalgo, 310 pp.

Francke OF (1977). Scorpions of the genus *Diplocentrus* Peters from Oaxaca, Mexico. Journal of Arachnology 4: 145–200.

FitzSimmons N (1997) Male Marine Turtles. Gene Flow. Philopatry and Mating Systems of the Green Turtle Chelonia mydas. PhD Thesis, Queensland University, Australia, 241 pp.

Gantenbein B, Fet V, Largiadèr CR, Scholl A (1999) First DNA phylogeny of *Euscorpius* Thorell, 1876 (Scorpiones: Euscorpiidae) and its bearing on taxonomy and biogeography of this genus. Biogeographica 75: 49–65.

Gantenbein B, Fet V, Barker M, Scholl A (2000) Nuclear and mitochondrial markers reveal the existence of two parapatric scorpion species in the Alps: *Euscorpius germanus* (C. L. Koch, 1837) and *E. alpha* Caporiacco, 1950, stat. nov. (Scorpiones, Euscorpiidae). Revue Suisse de Zoologie 107 (4): 843–869. https://doi.org/10.5962/bhl.part.80151

Gantenbein B, Fet V, Barker MD (2001) Mitochondrial DNA reveals a deep, divergent phylogeny in *Centruroides exilicauda* (Wood, 1863) (Scorpiones: Buthidae). In: Fet V, Selden PA (Eds) Scorpions 2001: In Memoriam Gary A (Ed.) Polis. British Arachnological Society, Burnham Beeches, Bucks, 235–244.

Kumar S, Stecher G, Li M, Knyaz C, Tamura K (2018) MEGA X: Molecular Evolutionary Genetics Analysis across computing platforms. Molecular Biology and Evolution 35: 1547–1549. https://doi.org/10.1093/molbev/msy096

Nei M, Kumar S (2000) Molecular Evolution and Phylogenetics. Oxford University Press, 329 pp.

Ponce-Saavedra J, Francke OF, Cano-Camacho H, Hernández-Calderón E (2009) Evidencias morfológicas y moleculares que validan como especie a *Centruroides tecomanus* (Scorpiones, Buthidae). Revista Mexicana de Biodiversidad 80: 71–84.

Ponce-Saavedra J, Francke OF (2013a) Clave para la identificación de especies de alacranes del género *Centruroides* Marx 1890 (Scorpiones: Buthidae) en el Centro Occidente de México Biológicas 15(1): 52–62. https://biologicas.umich.mx/index.php/biologicas/article/download/158/158

Ponce-Saavedra J, Francke OF (2013b) Actualización taxonómica sobre alacranes del centro occidente de México. Dugesiana 20(2): 73–79.

Ponce-Saavedra J, Francke OF (2019) Una nueva especie de alacrán del género *Centruroides* (Scorpiones: Buthidae) del noroeste de México. Revista Mexicana de Biodiversidad 90: e902660. https://doi.org/10.22201/ib.20078706e.2019.90.2660

Ponce-Saavedra J, Moreno-Barajas RJ (2005) El género *Centruroides* Marx 1890 (Scorpiones: Buthidae) en México. Biologicas 7: 42–51.

Ponce-Saavedra J, Francke OF, Quijano-Ravell AF, Cortés Santillán R (2016) Alacranes (Arachnida: Scorpiones) de importancia para la salud pública en México. Folia Entomologica Mexicana (NS) 2(3): 45–70. http://www.socmexent.org/folia/revista/Num%202016_3/45-70.pdf

Quijano-Ravell AF, Ponce-Saavedra J (2016) A new species of scorpion of the genus *Centruroides* (Scorpiones: Buthidae) from the state of Michoacan, Mexico. Revista Mexicana de Biodiversidad, 87: 49–61. https://doi.org/10.1016/j.rmb.2016.01.022

Soleglad ME, Fet V (2003) The scorpion sternum: structure and phylogeny (Scorpiones: Orthosterni). Euscorpius 5: 1–34.

Stahnke HL (1970) Scorpion nomenclature and mensuration. Entomological News 81: 297–316.

Simon C, Frati F, Beckembach A, Crespi B, Liu H, Flook P (1994) Evolution weighting and phylogenetic utility of mitochondrial gene sequences and compilation of conserved polymerase chain reaction primers. Annals of the Entomological Society of America 87: 651–701. https://doi.org/10.1093/aesa/87.6.651

Teruel R, Fet V, Graham MR (2006) The first mitochondrial DNA Phylogeny df Cuban Buthidae (Scorpiones: Buthoidea). Boletín Sociedad Entomológica Aragonesa 1(3): 219–226.

Towler WL, Ponce-Saavedra J, Gantenbein B, Fet V (2001) Mitochondrial DNA reveals a divergent phylogeny in Central Mexican *Centruroides* (Scorpiones: Buthidae). Biogeographica 77 (4): 157–172.

Vachon M (1974) Études des caractères utilisés pour classer les familles et les genres des scorpions (Arachnides). 1. La trichobothriotaxie en arachnologie. Sigles trichobothriaux et types de trichobothriotaxie chez les Scorpions. Bulletin du Muséum national d'Histoire naturelle, 3e série, 140(Zoologie 104): 857–958.

Vachon M (1975) Sur l'utilisation de la trichobothriotaxie du bras des pédipalpes des Scorpions (Arachnides) dans le classement des genres de la famille des Buthidae Simon. Comptes Rendus des Séances de l'Académie des Sciences 281(D): 1597–1599.

ZooKeys 859: 49–61 (2019)
doi: 10.3897/zookeys.859.31720
http://zookeys.pensoft.net

RESEARCH ARTICLE

A peer-reviewed open-access journal
ZooKeys
Launched to accelerate biodiversity research

Two new species of the genus *Microplitis* Förster, 1862 (Hymenoptera, Braconidae, Microgastrinae) from China

Wangzhen Zhang[1,2], Dongbao Song[3], Jiahua Chen[3]

1 *Plant Protection College, Fujian Agriculture and Forestry University, Fuzhou 350002, China* **2** *Fuzhou Airport Inspection and Quarantine Bureau, Changle 350209, China* **3** *Institute of Beneficial Insects, Fujian Agriculture and Forestry University, Fuzhou 350002, China*

Corresponding author: *Jiahua Chen* (jhchen34@163.com); *Dongbao Song* (waspsong@foxmail.com)

Academic editor: *J. Fernandez-Triana* | Received 15 December 2018 | Accepted 3 June 2019 | Published 2 July 2019

http://zoobank.org/98CBB907-5B6C-4C27-AF84-3C6D4018B299

Citation: Zhang W, Song D, Chen J (2019) Two new species of the genus *Microplitis* Förster, 1862 (Hymenoptera, Braconidae, Microgastrinae) from China ZooKeys 859: 49–61. https://doi.org/10.3897/zookeys.859.31720

Abstract

Two new species of *Microplitis* Förster, 1862, *M. bomiensis* Zhang, **sp. nov.**, and *M. paizhensis* Zhang, **sp. nov.** from Tibet, China are described and illustrated. A key to the species of the genus *Microplitis* Förster from China is added.

Keywords

Braconidae, taxonomic key, *Microplitis paizhensis*, *Microplitis bomiensis*

Introduction

The genus *Microplitis* Förster was established by Förster (1862) with the type species *Microgaster sordipes* (Nees von Esenbeck, 1834).

In 1982, van Achterberg examined three male specimens of *Ichneumon deprimator,* and found that the genus *Microplitis* should not be *Microgaster*, but rather *Microplitis* (van Achterberg 1982). Mason (1981) and Whitfield (1987) suggested and recommended to the International Committee of Zoological Nomenclature (ICZN) to abandon *Ichneumon deprimator* as the type species of *Microgaster*, and reassigned *Microgaster australis* Thomson, 1895 as type species of this genus; the original genus names of

Microplitis and *Microgaster* remained unchanged. This recommendation was adopted by ICZN in 1988 (International Commission on Zoological Nomenclature 1988).

Microplitis is a moderately large genus in Microgastrinae, with 190 species known from all over the world, of which 37 species have been reported from China (Fernandez-Triana and Ward 2015; Zhang et al. 2017).

This paper describes and illustrates two new species.

Materials and methods

This study is based on a collection of specimens preserved in the Parasitic Hymenoptera Collection of the Institute of Beneficial Insect, College of Plant Protection, Fujian Agriculture and Forestry University (FAFU; Fuzhou, China). The morphological characters were examined and photographed using a Leica M205C digital stereomicroscope. All specimens described are deposited in the Beneficial Insects Institute, Fujian Agriculture and Forestry University (Fuzhou, China). The morphological terminology used in this paper follows van Achterberg (1988) and Austin and Dangerfield (1992, 1993). Terminology for wing venation is based on the modified Comstock-Needham system (Eady 1974; van Achterberg 1979). Abbreviations used in this paper are as follows: POL, Postocellar line (minimum distance between posterior ocelli); OD, Posterior ocellus maximum diameter; OOL, Ocular-ocellar distance (minimum distance between posterior ocellus and eye); T1, T2, etc., first, second, etc. metasomal tergites.

Taxonomic part

Microplitis Förster, 1862

Microplitis Förster, 1862: 245 [type species, by original designation, *Microgaster sordipes* Nees ab Esenbeck, 1834.] Nixon 1970: 3. Mason 1981: 132. Austin and Dangerfield 1992 [see Shenefelt (1973: 737) for complete bibliography].

Dapsilotoma Cameron, 1906: 101 [type species, by monotypy, *Dapsilotoma testaceipes* Cameron, 1906]. Synonymized by Viereck (1914: 25).

Glabromicroplitis Papp, 1979: 176 [type species, *Glabromicroplitis mahunkai* Papp, 1979]. Synonymized by Austin and Dangerfield (1992).

Diagnosis. Hypopygium usually small, never bearing longitudinal creases along median line. Ovipositor and sheaths usually projecting only a little beyond apex of hypopygium; sheaths bearing a few setae distally. T1 variable from wide to narrow apically and usually moderately sculptured; T2 rarely weakly sculptured and often with a weakly delimited trapezoidal median area; T3 longer than T2, the transverse groove between them poor; remaining tergites nearly smooth. Propodeum usually convexly rounded and often with a distinct percurrent medial keel, never with an areola, surface almost completely rugose, sometimes reticulo-rugose. Mesoscutum

often densely sculptured, sometimes smooth, and with notauli, sometimes strongly defined. Posterior band of scutellum usually smooth but interrupted medially by rugosity. Fore wing usually with a D-shaped areolet, shape variable in some species, subtriangular, rectangular, etc.; 1CU1 much shorter than 2CU1; r short. Hind wing with vannal lobe convex and fringed throughout. Hind coxa small and not longer than T1; hind spurs shorter than half length of basitarsus. Labial palpi 3-jointed, sometimes 4-jointed.

Generally, the genus are clearly distinct from other genera. A detailed description of the genus and references to the revised generic diagnosis and Oriental *Microplitis* species can be made using the most recent data (Mason 1981; Austin and Dangerfield 1993; Ranjith et al. 2015).

Key to species of the genus *Microplitis* Förster from China

1 T1 less than 1.5× as long as maximum width **2**
– T1 more than 1.5× as long as maximum width **4**
2 Hypopygium in ventral view apically emarginated ..... ***M. ocellatae*** **(Bounche)**
– Hypopygium in ventral view not emarginated apically **3**
3 Head 2.1× as wide as long in dorsal view; antennae as long as body ..... ***M. amplitergius*** **Xu & He**
– Head less than 1.9× as wide as long in dorsal view; antennae distinctly longer than body ..... ***M. hirtifacialis*** **Song & You**
4 Notauli virtually absent, indicated only by indentations, or shallow; mesoscutum weakly punctate or simply sculptured **5**
– Notauli impressed, percurrent and meeting posterioly, or deep; mesoscutum roughly punctate or with rugose sculpture **10**
5 Propodeum with basal transverse carina distinct ..... ***M. carinata*** **Ashmead, 1900**
– Propodeum with basal transverse carina indistinct or absent **6**
6 Head in dorsal view broadening behind eye; T1 less than 1.8× as long as maximum width; tegula black **7**
– Head in dorsal view not broadening behind eye; T1 more than 2× as long as maximum width; tegula reddish yellow **9**
7 Areolet approximately triangular; stigma with basal patch semihyaline ..... ***M. basipallescentis*** **Song & Chen**
– Areolet approximately quadrangular or rectangular; stigma without basal patch Semihyaline **8**
8 Mesosoma narrower than head; T1 slightly narrowed in posterior part; 1-R1 1.7× as long as the distance from itself to apex of marginal cell ..... ***M. fujianica*** **Zhang, Song et Chen**
– Mesosoma wider than head; T1 slightly widened in posterior part; 1-R1 2.1× as long as the distance from itself to apex of marginal cell ..... ***M. longwangshanus*** **Xu & He**

9	Vein 1-R1 (metacarpus) 1.6× as long as its distance from apex of marginal cell and 1.3× as long as stigma.....***M. bomiensis*, sp.n.**
–	Vein 1-R1 (metacarpus) 1.1× as long as its distance from apex of marginal cell and 0.7× as long as stigma.....***M. helicoverpae* Xu & He**
10	T1 distinctly broadening posteriorly **11**
–	T1 either weakly broadening posteriorly, or subparallel to parallel sides **17**
11	Scutellum evenly or almost evenly rugose **12**
–	Scutellum anteriorly or antero-medially smooth with weak and rather scattered punctures **13**
12	Flagellomeres thick and dark brown; 1-R1 1.5× as long as the distance from itself to apex of marginal cell.....***M. crassiantenna* Song & Chen**
–	Flagellomeres thin and reddish yellow; 1-R1 2× as long as the distance from itself to apex of marginal cell.....***M. tadzhica* Telenga**
13	T2 rugose or at least shrivelled medially.....***M. menciana* Xu & He**
–	T2 smooth or at most slightly uneven.....**14**
14	Both outer and inner spurs are the same length, only 0.2× as long as basitarsi; propodeum with basal transverse carina distinct..... .....***M. brevispina* Song & Chen**
–	Both outer and inner spurs are equal or unequal length, more than 0.2× as long as basitarsi; propodeum with basal transverse carina indistinct **15**
15	Stigma fully dark or reddish brown, without pale basal spot..... .....***M. borealis* Xu & He**
–	Stigma blackish with a yellow basal spot at its proximal third.....**16**
16	1-R1 almost equal to stigma; tegula reddish yellow..... .....***M. jiangsuensis* Xu & He**
–	1-R1 half as long as stigma; tegula black .....***M. cubitellanus* Xu & He**
17	T1 more than 1.7× as long as maximum width; usually with subparallel or parallel sides.....**18**
–	T1 less than 1.7× as long as maximum width; usually more or less broadening posteriorly, or subquadrate.....**26**
18	Flagellum reddish yellow to yellow white basely, dull apically, or blackish basely, reddish yellow apically **19**
–	Flagellum back or brownish yellow entirely.....**20**
19	Antenna short, clearly shorter than body .....***M. chui* Xu & He**
–	Antenna long, clearly as long as or longer than body.....***M. zhaoi* Xu & He**
20	Head in dorsal view 2 or more than 2× as broad as long **21**
–	Head in dorsal view less than 1.8× as broad as long.....**24**
21	Middle and hind femora mostly or entirely black or blackish brown.....**22**
–	Middle and hind femora mostly or entirely reddish yellow.....**23**
22	Mesonotum antero-medially dull with dense sculpture; fore wing slightly hyaline.....***M. bicoloratus* Xu & He**
–	Mesonotum antero-medially shiny with few fine punctures; fore wing almost opaque.....***M. obscuripennatus* Xu & He**

23 Hind coxa black..... ***M. marshalli*** **Kokujev**
– Hind coxa reddish yellow..... ***M. longiradiusis*** **Xu & He**
24 Metasoma usually reddish yellow or testaceous, or T1 and last 2 or 3 segments blackish; hind coxa reddish yellow..... ***M. pallidipes*** **Szépligeti**
– Metasoma black, or T2–3 reddish yellow to brownish yellow; hind coxa black..... **25**
25 T2–3 reddish yellow to brownish yellow..... ***M. mediator*** **Haliday**
– T2–3 brownish testaceous to black ..... ***M. tuberculifer*** **Wesmael**
26 Hind femora mostly or entirely black..... **27**
– Hind femora mostly or entirely reddish yellow to brownish yellow **30**
27 Wings with pale brown areas over first discal cell and above areolet .... ***M. prodeniae*** **Rao & Kurian**
– Wings without pale brown areas over first discal cell and above areolet, or only with brown area above areolet **28**
28 Tegula reddish yellow; stigma blackish brown; hind tibia with basal white or yellowish white ring..... **29**
– Tegula black; stigma blackish brown with yellow basal spot at its proximal third; hind tibia reddish yellow..... ***M. varipes*** **Ruthe**
29 Antennae distinctly longer than body; hind tibia yellow .... ***M. paizhensis*** **sp. nov.**
– Antennae slightly longer than body; hind tibia yellowish white..... ..... ***M. albotibialis*** **Telenga**
30 Fore wing with areolet approximately triangular ..... ***M. strenuus*** **Reihard**
– Fore wing with areolet approximately quadrangular..... **31**
31 T1 slightly widened towards apex; antennae with flagellomeres 12–15 tightly connected..... ***M. changbaishanus*** **Song & Chen**
– T1 parallel or subparallel-sided; antennae with flagellomeres 12–15 loosely connected..... **32**
32 Penultimate joint of antenna 2.5 times as long as wide, apex of hypopygium ending far beyond apex of abdomen ..... ***M. leucaniae*** **Xu & He**
– Penultimate joint of antenna 1.6–2.0 times as long as wide, apex of hypopygium reach beyond apex of abdomen..... ***M. vitellipedis*** **Li, Tan et Song**

Microplitis paizhensis **Zhang, sp. nov.**
http://zoobank.org/94F03DB7-B4AC-4293-B7D2-D7992DC54AC9
Figs 1–7

Etymology. The specific name is derived from the type locality.

Type material. Holotype: female, Paizhen, Tibet, 94°58'10.57"E, 29°50'45.67"N, 3696 m, 16.vii.2013, leg. Zhang Wangzhen (FAFU).

Comparative diagnosis. This species is similar to *Microplitis fujianica* Song and Zhang, but can be distinguished by its shiny pronotum, which is sparsely punctate (vs

rugose-punctate); fore wing with vein 1R-1 (metacarpus) 1.3× as long as its distance from apex of marginal cell (vs vein 1-R1 1.7× as long as its distance from apex of marginal cell); T2 subrectangular, ratio of apical width: central length = 3.2: 0.7 (vs T2 nearly triangular, ratio of apical width: central length = 3.6: 1.4).

This species (*M. paizhensis*, sp. nov.) is similar to *M. albotibialis* Telenga, but can be distinguished by antennae distinctly longer than body (vs antennae slightly longer than body); hind tibia yellow (vs hind tibia yellowish white). Frons faintly sculptured (vs frons coarsely sculptured). POL: OD = 1.0: 0.4 (vs POL: OD: OOL = 2.0: 2.0).

This species is also similar to *Microplitis bomiensis*, sp. nov. (see below for further diagnosis).

Description. Female (holotype).

Head. Roughly triangular in anterior view, with antennal sockets high above the middle level of the eyes. Face slightly convex, finely micropunctate associated with long setae. Inner margin of the eyes straight to moderately emarginate near antennal sockets. Transverse in dorsal view, 1.7× as wide as long, posterior vertex and temples finely punctate to rugose-punctate, with long sparse setae. Frons faintly sculptured. Ocelli small, in a high triangle, imaginary tangent of posterior margin of anterior ocellus far from posterior ocelli. POL: OD: OOL = 1.0: 0.4: 0.9. Antennae longer than body (14.2: 10.5), flagellomeres thin, setose. Flagellomere proportion: 2 L/W (section 2 length/ width) = 2.3, 8 L/W = 2.4, 14 L/W = 2.6. L 2/14 = 1.2, W 2/14 = 1.4. F12–15 (Flagellomere 12–15) loosely connected.

Mesosoma. Mesosoma almost as wide as head. Pronotum shiny, sparsely punctate. Mesoscutum evenly and densely punctate, setose. Notauli shallow. Scutellar lunules deep, broad, divided by five carinae. Disc of scutellum shiny, weakly convex, evenly punctate, with white setae, its rugose-punctate spot in the middle interrupting the posterior, polished band of scutellum. Propodeum rather evenly curved, coarsely reticulate-rugose, with a median longitudinal carina.

Wings. Fore wing: vein 1-R1 (metacarpus) 1.3 × as long as its distance from apex of marginal cell and 1.1 × as long as stigma. Vein r (1st radius) arising distally from the middle of the stigma and approximately as long as 2-SR. Areolet approximately quadrangular. Stigma 2.9× as long as width. Width of 1st discal cell: height of 1st discal = 20.0: 21.5. 1-CU1: 2-CU1: m-cu = 7.5: 11.0: 10.0. Hind wing vein cu-a slightly incurved.

Legs. Hind coxa small, slightly shorter than T1. Inner hind tibial spur almost as long as outer one, about 0.3× as long as hind basitarsus.

Metasoma. Slightly longer than mesosoma (5.3: 4.8). T1 widening towards apex, then narrowing to the extreme apex, weakly punctured except for moderately depressed base and small apical swelling smooth. T2 subrectangular, smooth, ratio of apical width: central length = 3.2: 0.7, its median field slightly raised. T3 longer than T2 (1.0: 0.7), suture between T3 and T2 weak, T3 and the remaining tergites smooth, shiny, sparsely setose. Hypopygium small, slightly shorter than tip of metasoma; ovipositor sheath short, approximately 1.3× as long as second hind tarsomere.

Color. Black. Antennae dark brown. Maxillary palps, labial palps, and tibial spur pale yellow. Ocelli reddish. Stigma and most veins brown, semitransparent. Wings

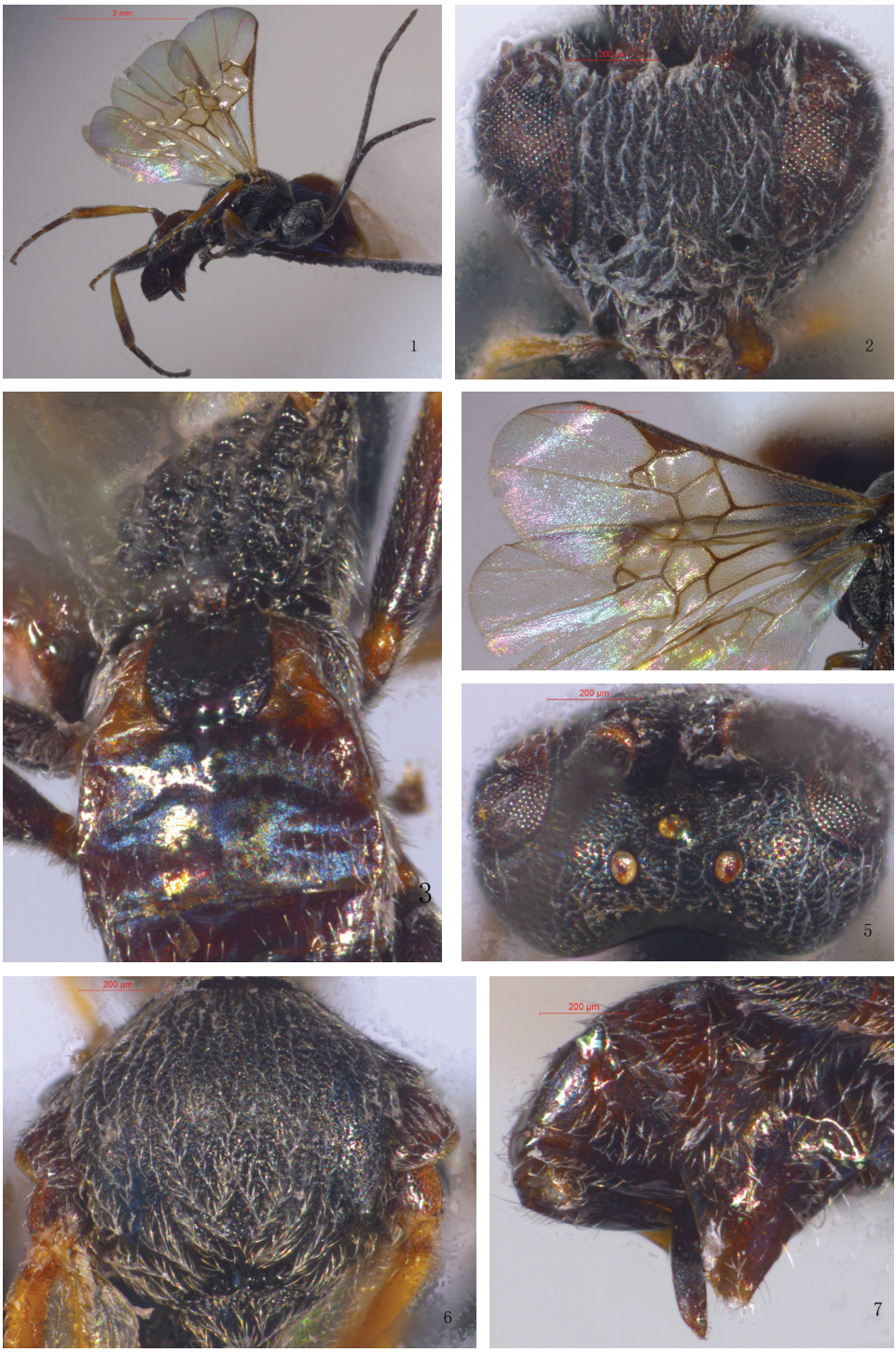

Figure 1–7. *Microplitis paizhensis*, sp. nov. (female) **1** Habitus, lateral view **2** Head, anterior view **3** Propodeum and basal tergites of metasoma **4** Wings **5** Head, dorsal view **6** Mesoscutum **7** Apex of metasoma (showing ovipositor).

hyaline without infuscations, except for light brown central area. Wing setae whitish. Legs yellow except all coxae, basal 2/5 of fore femur, basal 4/5 of mid femur, hind femur black, distal 2/5 of hind tibia and tarsus brown. Metasoma blackish brown except for T1 and T2 which are black.

Body length 3.2 mm; fore wing length 3.8 mm.

Male. Unknown.

Distribution. Tibet, China.

Habitat. Prairie and bushes.

Microplitis bomiensis Zhang, sp. nov.

http://zoobank.org/55F4D31C-13EC-4856-B38A-4B58B7FD92EB
Figs 8–14

Etymology. The specific name "*bomiensis*" is derived from the type locality.

Type material. Holotype: female, Bomi, Tibet, 96°23'23.23"E, 29°36'22.33"N, 3427 m, 28.vii. 2013. Leg. Zhang Wangzhen (FAFU).

Comparative diagnosis. Morphologically this species and *M. paizhensis* Zhang, sp. nov. are very similar; the main points of distinction are to be found in the former having golden setae on mesoscutum and disc of scutellum (vs light grey or colourless setae on mesoscutum and disc of scutellum). Fore vein 1-R1 1.6× as long as its distance from apex of marginal cell and 1.3× as long as stigma (vs. vein 1-R1 1.3× as long as its distance from apex of marginal cell and 1.1× as long as stigma). Mid coxa reddish brown, hind coxa black brown or infuscate (vs all coxae black).

The new species is also similar to *M. helicoverpae* Xu & He with the distinction between them as following: vein 1-R1 1.6× as long as its distance from apex of marginal cell and 1.3× as long as stigma (vs vein 1-R1 1.1× as long as its distance from apex of marginal cell and 0.7× as long as stigma). Areolet approximately quadrangular (vs areolet approximately triangular). T1 2.2× as long as wide (vs T1 1.7× as long as wide).

Description. Female (holotype).

Head. Subcircular in anterior view, lateral temples hidden behind eyes in anterior view. Width of face (at widest) half as wide as head. Face flat to slightly convex, densely punctate, with associated dense setae. Inner margin of eyes straight to moderately emarginate adjacent to antennal sockets. Eyes setose. Transverse in dorsal view, 2.2× as wide as long. Ocelli medium-sized, in a high triangle, imaginary tangent of posterior margin of anterior ocellus distant from posterior ocelli. Vertex shiny, shallowly punctate. Frons depressed, nearly smooth. POL: OD: OOL = 0.9: 0.4: 1.1. Antennae long than body (14.1: 10.3), flagellomeres thin, with bristly setae. Flagellomere proportion: 2 L/W (Flagellomere 2 length/ width) = 2.5, 8 L/W = 2.6, 14 L/W = 2.5. L 2/14 = 1.4, W 2/14 = 1.3. F12–15 (Flagellomere 12–15) loosely connected.

Mesosoma. Thorax slightly wider than head (7.3: 7.8). Pronotum sparsely punctae. Mesoscutum shiny, evenly punctate, with dense setae. Notauli faintly impressed. Scutellar lunules broad, divided by five carinae. Disc of scutellum shiny, weakly convex, evenly punctate, with setae, its rugose spot in the middle interrupting the poste-

Figure 8–14. *Microplitis bomiensis*, sp. nov. (female) **8** Habitus, lateral view **9** Wings **10** Head, anterior view **11** Head, dorsal view **12** Mesoscutum and scutellum **13** Propodeum and basal tergites of metasoma **14** Apex of metasoma (showing ovipositor).

rior, polished band of scutellum. Propodeum rather evenly curved in profile, coarsely reticulate and rugose, with a median longitudinal carina.

Wings. Fore wing: vein 1-R1 (metacarpus) 1.6× as long as its distance from apex of marginal cell and 1.3 × as long as stigma. Vein r (1st radius) emitted distally from middle of stigma and approximately as long as 2-SR. Areolet approximately quadrangular. Stigma 2.9× as long as wide. Ratio of width of 1st discal cell: height of 1st discal = 21.6: 17.5. 1-CU1: 2-CU1: m-cu = 7.4: 11.5: 9.5. Hind wing: vein cu-a incurved.

Legs. Hind coxa small, slightly shorter than T1. Inner hind tibial spur almost as long as outer one, 0.3× as long as hind basitarsus. Metasoma Slightly shorter than mesosoma (4.9: 5.2). T1 2.2× as long as wide, parallel-sided, with broad shallow medial depression on basal 1/3, surface rugulose except for smooth apical swelling. T2 subtrapezoidal, its apical width: medial length ratio = 3.1: 0.9, smooth, shiny, glabrous, with a shield-shaped median field indicated by oblique grooves. T3 longer than T2 (1.3: 0.9), suture between T3 and T2 reduced to slight depression. T3 and the following tergites smooth, each with one or two transverse rows of sparse hairs posteriorly, denser laterally. Hypopygium small. Ovipositor sheath short, 1.3× as long as second hind tarsomere.

Color. Body generally black to dark brown. Palps yellow to white. Setae of mesoscutum and disc of scutellum golden. Lateral edges of T1–T3 reddish yellow. Hypopygium reddish brown. Antennae dark brown or brown. Wings hyaline, venation brown, stigma with pale yellowish patch basally. Legs yellow, except mid coxa which are reddish brown; hind coxa, tibia, and tarsus black brown or infuscate.

Body length 3.4 mm; forewing length 3.9 mm.

Male. Unknown.

Distribution. Tibet, China.

Habitat. Prairie and bushes.

Remarks

Both new species were collected in high-altitude areas in Tibet, China (above 3400 m), which is relatively rare for this group above this altitude. We also collected single male specimen of a third species, which, considering the importance of the females in microgastrine taxonomy and the recommendation of the reviewers, will not be published for the time being.

Acknowledgements

We thank Professor Pubu and her students at Tibet University and Professor Fuping Zhang and her students at the Xizang Agriculture and Husbandry College for their assistance. The National Key Research and Development Program of China (2017YFD0202100) supported this study.

References

Austin AD, Dangerfield PC (1989) The taxonomy of New World microgastrine braconids (Hymenoptera) parasitic on *Diatraea* spp. (Lepidoptera: Pyralidae). Bulletin of Entomological Research 79(1): 131–144. https://doi.org/10.1017/s0007485300018642

Austin AD, Dangerfield PC (1992) Synopsis of Australasian Microgastrinae (Hymenoptera : Braconidae), with a key to genera and description of new taxa. Invertebrate Taxonomy 6(1): 1–76. https://doi.org/10.1071/it9920001

Austin AD, Dangerfield PC (1993) Systematics of Australian and New Guinean *Microplitis* Foerster and Snellenius Westwood (Hymenoptera: Braconidae : Microgastrinae), with a review of their biology and host relationships. Invertebrate Taxonomy 7(5): 1097–1166. https://doi.org/10.1071/it9931097

Cameron P (1906) On the Tenthredinidae and parasitic Hymenoptera collected in Baluchistan by Major C.G. Nurse. Part I. Journal of the Bombay Natural History Society 17: 89–107. https://biodiversitylibrary.org/page/30119169

Chen JH, Ji QE, Song DB (2004) A new species of *Microplitis* Förster from China (Hymenoptera: Braconidae: Microgastrinae). Entomological Journal of East China 13(2): 1–5. http://med.wanfangdata.com.cn/Paper/Detail/PeriodicalPaper_hdkcxb200402001

Eady RD (1974) The present state of nomenclature of wing venation in the Braconidae (Hymenoptera); its origins and comparison with related groups. Journal of Entomology Series B, Taxonomy 43(1): 63–72. https://doi.org/10.1111/j.1365-3113.1974.tb00089.x

Fernandez-Triana J, Ward D (2015) Microgastrinae Wasps of the World. http://microgastrinae.myspecies.info/ [Accessed on: 2019-5-23]

International Commission on Zoological Nomenclature (1988) Opinion 1510. *Microgaster* Latreille, 1804 (Insecta, Hymenoptera): *Microgaster australis* Thomson, 1895 designed as the type species. Bulletin of Zoological Nomenclature 45: 239–240. https://biodiversitylibrary.org/page/12229669

Mason WRM (1981) The polyphyletic nature of *Apanteles* Foerster (Hymenoptera: Braconidae): a phylogeny and reclassification of Microgastrinae. Memoirs of the Entomological Society of Canada 113(S115): 1–147. https://doi.org/10.4039/entm113115fv

Nixon GEJ (1970) A revision of the N.W. European species of Microplitis Förster (Hymenoptera: Braconidae). Bulletin of the British Museum (Natural History) 25(1): 1–30. https://www.biodiversitylibrary.org/item/19402#page/6/

Ranjith AP, Rajesh KM, Nasser M (2015) Taxonomic studies on Oriental *Microplitis* Foerster (Hymenoptera: Braconidae, Microgastrinae) with description of two new species from South India. Zootaxa 3963(3): 369–415. https://doi.org/10.11646/zootaxa.3963.3.4

Song D, Chen J (2004) A study on *Microgaster* Latreille from China with description of a new species (Hymenoptera: Braconidae: Microgastrmae). In: Rajmohana K, Sudheer K, Girish Kumar P, Santhosh S (Eds) Perspectives on Biosystematics and Biodiversity: Prof T C Narendran Commemortive Volume. Systematic Entomology Research Scholars Association, Kerala, 315–325.

Song D, Chen J (2008) Five new species of the genus *Microplitis* (Hymenoptera: Braconidae: Microgastrinae) from China. Florida Entomologist 91(2): 283–293. https://doi.org/10.1653/0015-4040(2008)91[283:fnsotg]2.0.co;2

Tobias VI (1986) Hymenoptera Fauna USSR. Guide to the Insect of European Part of the USSR 4: 344–459

van Achterberg C (1979) A revision of the subfamily Zelinae auct. (Hymenoptera, Braconidae). Tijdschrift voor Entomologie 122: 241–479. https://biodiversitylibrary.org/page/28227686

van Achterberg C (1982) Notes on some type species described by Fabricius of the subfamilies Braconidae, Rogadinae, Microgastrinae and Agathidinae (Hymenoptera: Ichneumonidae). Entomologische Berichten 42: 133–139. https://biodiversitylibrary.org/page/57854343

van Achterberg C (1988) Revision of the subfamily Blacinae Förster (Hymenoptera, Braconidae). Zoologische Verhandelingen 249: 1–324. https://pdfs.semanticscholar.org/d04d/7f072d970e54bd36e28f1c0be8b43b4a98c9.pdf

van Achterberg C (1997) Notes on the types and type depositories of Braconidae (Insecta: Hymenoptera) described by T.C. Narendran and students. Zoologische Mededelingen 71(16): 177–179. https://www.repository.naturalis.nl/document/149965

Whitfield JB (1987) Comment on the proposed designation of Microgaster australis Thomson, 1895 as type of Microgaster Latreille, 1804 (Insecta, Hymenoptera) (Case 2397). Bulletin of Zoological Nomenclature 47(1): 47. https://biodiversitylibrary.org/page/12229352

Whitfield JB (1995) Annotated checklist of the Microgastrinae of North America north of Mexico (Hymenoptera: Braconidae). Journal of the Kansas Entomological Society 68(3): 245–262. https://www.jstor.org/stable/25085593

Wilkinson DS (1930) A revision of the Indo-Australian species of the genus *Microplitis* (Hym. Bracon.). Bulletin of Entomological Research 21(1): 23–27. https://doi.org/10.1017/s0007485300021519

Xu WA, He JH (1999a) A new species of Microplitis Förster (Hymenoptera: Braconidae: Microgastrinae) from Fujian, China. Entomotaxonomia 21(1): 64–68. http://www.cqvip.com/qk/96329X/199901/3424292.html

Xu WA, He JH (1999b) A new species of *Microplitis* Förster from China (Hymenoptera: Braconidae, Microgastrinae). Entomological Journal of East China 8(1): 1–3. http://www.cnki.com.cn/Article/CJFDTotal-HDKC199901000.htm

Xu WA, He JH (2000a) A new species and a new record of *Microplitis* Foerster from China (Hymenoptera:Braconidae:Microgastrinae). Acta Entomologica Sinica 43(2): 193–197. https://doi.org/10.3321/j.issn:0454-6296.2000.02.013

Xu WA, He JH (2000b) A new species and a new record species of *Microplitis* Förster (Hymenoptera: Braconidae: Microgastrinae) from China. Entomological Journal of East China 9(2): 5–8. http://www.cnki.com.cn/Article/CJFDTotal-HDKC200002001.htm

Xu WA, He JH (2000c) A new species of *Microplitis* Förster from China (Hymenoptera, Braconidae, Microgastrinae). Acta Zootaxonomica Sinica 25(2): 195–198. https://doi.org/10.3969/j.issn.1000-0739.2000.02.016

Xu WA, He JH (2000d) Two new species of *Microplitis* Foerster (Hy-menoptera: Braconidae) from China. Insect Science 7(2): 107–112. https://doi.org/10.1111/j.1744-7917.2000.tb00346.x

Xu WA, He JH (2000e) Two new species of *Microplitis* Förster (Hymenoptera: Braconidae: Microgastrinae) from China. Entomotaxonomia 22(3): 204–208. http://xbkcflxb.alljournal.net/xbkcflxb/ch/reader/view_abstract.aspx?file_no=20000354&flag=1

Xu WA, He JH (2002a) Two new species of *Microplitis* Foerster from China (Hymenoptera, Braconidae, Microgastrinae). Acta Zootaxonomica Sinica 27(1): 153–157. https://doi.org/10.3969/j.issn.1000-0739.2002.01.027

Xu WA, He JH (2002b) Two new species of *Microplitis* Förster (Hymenoptera: Braconidae, Microgastrinae) from China. Acta Entomologica Sinica 45(Suppl): 99–102. https://doi.org/10.3321/j.issn:0454-6296.2002.z1.034

Xu WA, He JH (2003) Two new species of *Microplitis* Foerster from China (Hymenoptera, Braconidae, Microgastrinae). Acta Zootaxonomica Sinica 28(4): 724–728. https://doi.org/10.3969/j.issn.1000-0739.2003.04.032

Xu WA, He JH (2006) One new species of *Microplitis* Foerster (Hymenoptera: Braconidae: Microgastrinae) from China. Entomotaxonomia 28(3): 227–230. https://doi.org/10.3969/j.issn.1000-7482.2006.03.009

Xu WA, He JH, Ye BH, Zheng FQ (2000) Two new recorded species of *Microplitis* Foerster from China (Hymenoptera: Braconidae: Microgasterinae). Journal of Shandong Agricultural University (Natural Science) 31(4): 378–380. https://doi.org/10.3969/j.issn.1000-2324.2000.04.007

You LS, Wei M (2006) Fauna Hunan Hymenoptera Braconidae (I). Hunan Press of Science & Technology, Changsha, 16–28 pp.

Zhang W, Song D, Chen J (2017) Revision of *Microplitis* species from China with description of a new species. Zootaxa 4231(2): 296–300. https://doi.org/10.11646/zootaxa.4231.2.12

ZooKeys 859: 63–68 (2019)
doi: 10.3897/zookeys.859.35465
http://zookeys.pensoft.net

RESEARCH ARTICLE

A peer-reviewed open-access journal
ZooKeys
Launched to accelerate biodiversity research

A new species of *Linan* Hlaváč (Coleoptera, Staphylinidae, Pselaphinae) from Shenzhen, China

Qing-Hao Zhao[1], Wang Xu[2], Zi-Wei Yin[1]

1 *College of Life Sciences, Shanghai Normal University, Shanghai 200234, China* **2** *Shenzhen Environmental Monitoring Center, Shenzhen 518049, Guangdong, China*

Corresponding author: *Zi-Wei Yin* (pselaphinae@gmail.com)

Academic editor: *Jan Klimaszewski* | Received 15 April 2019 | Accepted 27 May 2019 | Published 2 July 2019

http://zoobank.org/555B0434-51EC-4788-8E45-383068C0CAE8

Citation: Zhao Q-H, Xu W, Yin Z-W (2019) A new species of *Linan* Hlaváč (Coleoptera, Staphylinidae, Pselaphinae) from Shenzhen, China. ZooKeys 859: 63–68. https://doi.org/10.3897/zookeys.859.35465

Abstract

A new Chinese species of the genus *Linan* Hlaváč, 2003, *L. qiniangmontis* **sp. nov.**, is described based on two male and three female specimens from sifted leaf litter samples at Qiniang Mountain, Shenzhen City, Guangdong. The species can be readily recognized and separated from all congeners based on the forms of the male antennae, the metaventral processes, and the aedeagus.

Keywords

Ant-loving beetles, southern China, taxonomy, Tyrini

Introduction

The Oriental genus *Linan* Hlaváč, 2003 belonging to the '*Pselaphodes* complex' of genera (Hlaváč 2003; Yin et al. 2013a) is a small group containing 16 species distributed in China (16 spp.) and Thailand (1 sp.) (Hlaváč 2003; Yin et al. 2011, 2013b; Yin and Li 2012, 2013; Zhang et al. 2018). An identification key and distributional maps of the genus were recently provided by Zhang et al. (2018). A survey of the local coleopterous fauna in Shenzhen City has resulted in the discovery of the 17th species of *Linan*, which is described here.

Materials and methods

The material used in this paper is housed in the Insect Collection of Shanghai Normal University, Shanghai, China (**SNUC**). The text of the specimen labels is quoted verbatim, with original Chinese names listed in parentheses.

Dissected parts were preserved in Euparal on plastic slides that were placed on the same pins as the respective specimens. The habitus images were taken using a Canon 5D Mark III camera with a Canon MP-E 65mm f/2.8 1–5X Macro Lens, and a Canon MT-24EX Macro Twin Lite Flash used as the light source. Images of the morphological details were produced using a Canon G9 camera mounted to an Olympus CX31 microscope under transmitted light. Zerene Stacker (version 1.04) was used for image stacking. All images were modified and grouped into plates in Adobe Photoshop CS5 Extended.

The abdominal tergites and sternites are numbered following Chandler (2001) in Arabic (starting from the first visible segment) and Roman (reflecting true morphological position) numerals, e.g., tergite 1 (IV), or sternite 7 (IX).

Taxonomy

***Linan qiniangmontis* sp. nov.**
http://zoobank.org/122313A9-AF98-429B-BBBE-D13402160D5C
Figs 1, 2

Type material. Holotype: CHINA: ♂: 'China: Guangdong, Shenzhen City, Mt. Qiniang (七娘山), 23°32'28.73"N, 114°35'8.46"E, mixed leaf litter, sifted, 45 m, 23.III.2019, Tang, Shuai, Zhao, Zhou & Xia leg.' (SNUC). **Paratypes: CHINA:** 1 ♂, 3 ♀♀, same label data as holotype (SNUC).

Diagnosis. Body length slightly less than 2.5 mm. Male: antennal club almost simple, with antennomere IX slightly angulate at anteromesal corner; metaventral processes short and narrowing toward apex; protibiae with small denticle at apex; metacoxae with truncate, curved, ventral projection; aedeagus elongate, median lobe asymmetrically narrowed at apex. Female: identifiable only when in association with a male.

Description. Male (Fig. 1A). Body length (combined length of head, pronotum, elytra, and abdomen) 2.32–2.33 mm. Head longer than wide, length from clypeal anterior margin to head base 0.52–0.54 mm, width across eyes 0.48–0.49 mm; eyes small, each composed of ca. 23 facets. Antennae elongate, 1.78–1.79 mm long, scape elongate, ca. 3.5 times as long as wide, antennomeres 2–8 each sub-moniliform, of similar width, antennal club (Fig. 2A) formed by antennomeres 9–11, antennomere 9 much longer than wide, broadening from base to apex, angulate at anteromesal corner (Fig. 2A, indicated by arrow), antennomere 10 slightly transverse, antennomere 11 truncate and broadest at base and narrowing apically, both antennomeres 10 and 11 simple. Pronotum (Fig. 2B) approximately as long as wide, with rounded lateral margins, length along midline 0.49–0.51 mm, maximum width 0.49–0.52 mm. Elytra

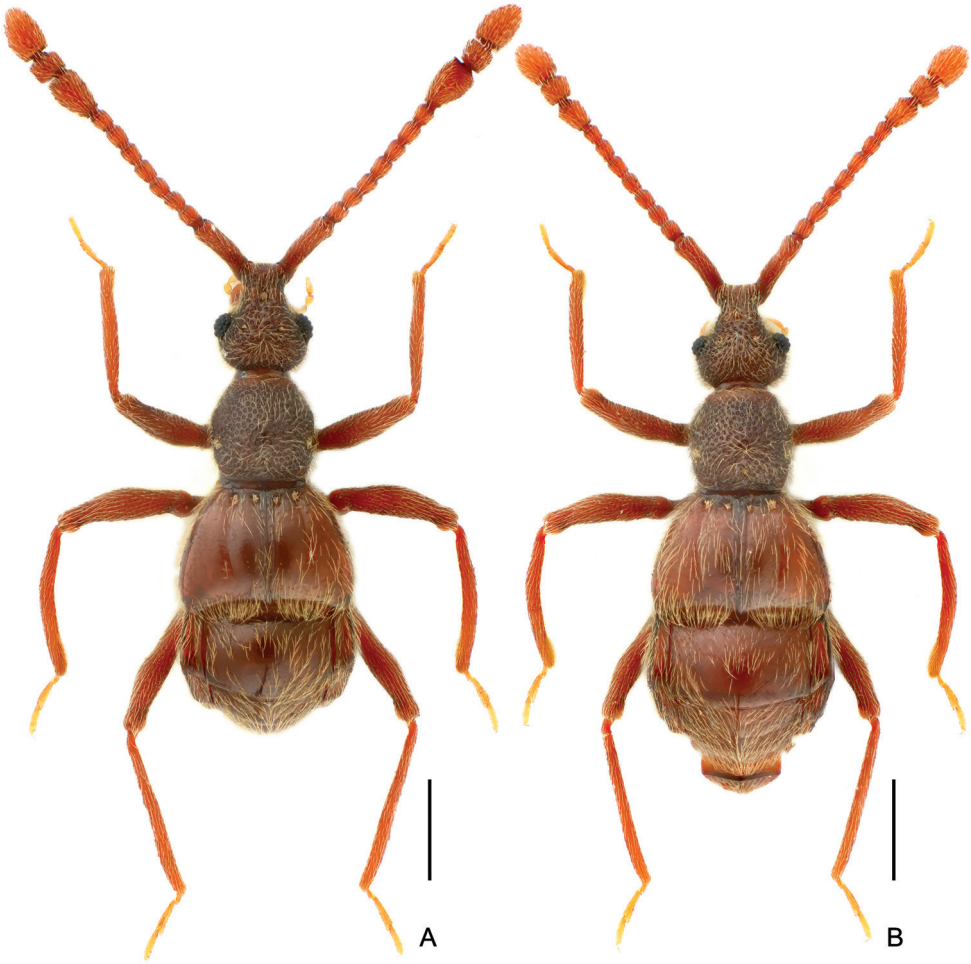

Figure 1. Dorsal habitus of *Linan qiniangmontis* sp. nov. **A** male **B** female. Scale bars: 0.5 mm.

strongly transverse, length along suture 0.56–0.57 mm, maximum width 0.85–0.88 mm. Metaventral processes (Fig. 2C) short, narrowing apically. Protrochanters and profemora (Fig. 2D) simple, protibiae (Fig. 2E) with small but distinct denticle at apex; mesotrochanters, mesofemora, and mesotibiae (Fig. 2F) simple; metacoxae (Fig. 2G) with truncate curved projection on ventral margin; metatrochanters, metafemora, and metatibiae simple. Abdomen approximately as wide as elytra, length of dorsally visible part along midline 0.74–0.77 mm, maximum width 0.86–0.87 mm; tergite 1 (IV) more than twice as long as tergite 2 (V); sternite 7 (IX) (Fig. 2H) semi-membranous, elongate. Length of aedeagus (Fig. 2I–K) 0.38–0.40 mm; median lobe asymmetrical dorso-ventrally, narrowing apically with pointed apex; elongate parameres slightly exceeding apex of median lobe, with rounded apices; endophallus with one broad, rounded triangular sclerite, and one much shorter, elongate sclerite forked at apex.

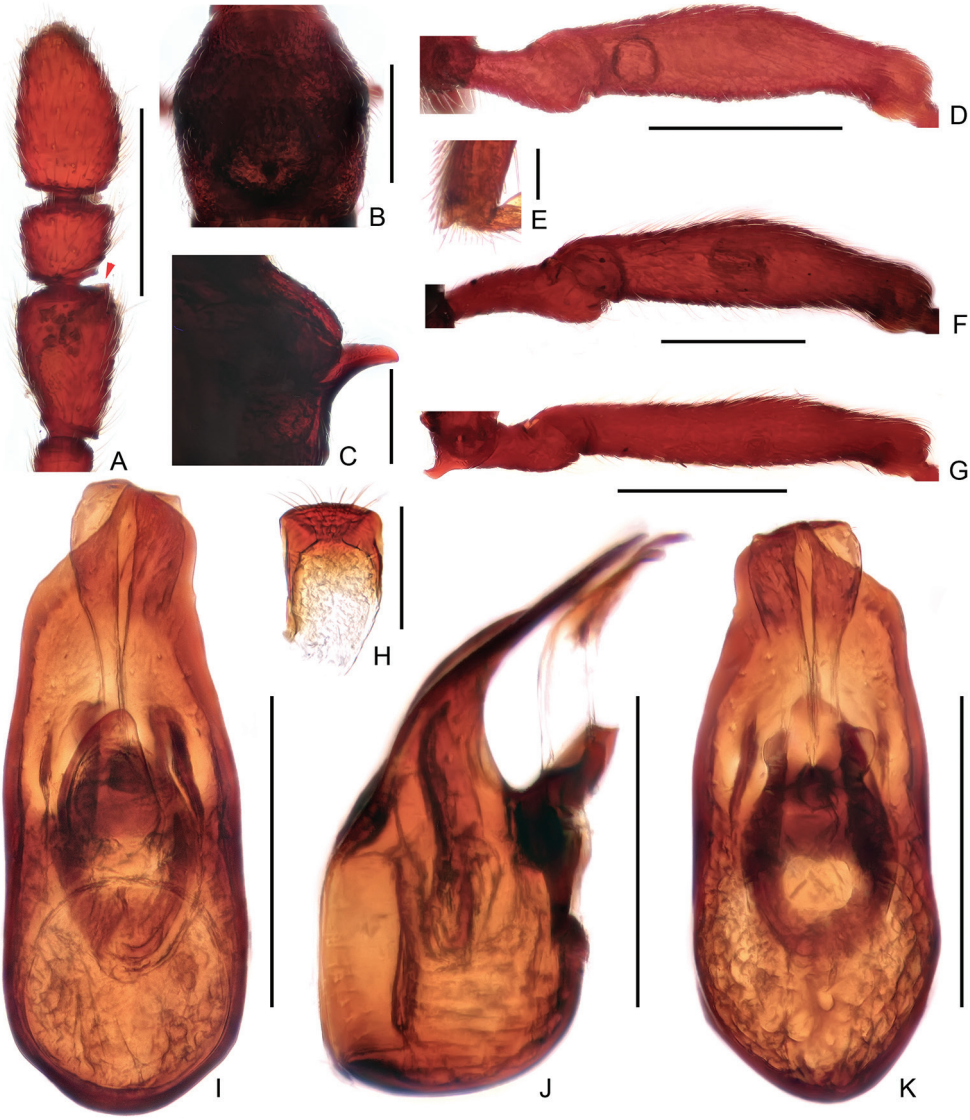

Figure 2. Male diagnostic features of *Linan qiniangmontis* sp. nov. **A** antennal club **B** pronotum **C** metaventral process, lateral **D** protrochanter and profemur **E** apex of protibia **F** mesotrochanter and mesofemur **G** metacoxa, metatrochanter, and metafemur **H** sternite IX **I–K** aedeagus, dorsal (**I**), lateral (**J**), and ventral (**K**). Scale bars: 0.3 mm (**A, B, D, F, G**); 0.2 mm (**C, I, J, K**); 0.1 mm (**H**); 0.05 mm (**E**).

Female. Similar to male in general morphology, with slightly shorter antennae and smaller eyes; antennae and legs simple; lacking metaventral processes. Eyes each composed of approximately 18 facets. Measurements (as of male): Body length 2.33–2.44 mm, length/width of head 0.53–0.55 /0.49–0.51 mm, length of antennae 1.63–1.70 mm, length/width of pronotum 0.50–0.51/0.51 mm, length/width of elytra 0.57/0.89–0.91 mm, length/width of abdomen 0.72–0.81/0.92–0.93 mm.

Distribution. China: Guangdong.

Etymology. The new species epithet refers to the type locality of the new species, Qiniang Mountain.

Comparative notes. The new species is placed as a member of the *L. chinensis* group by the almost unmodified antennal clubs in the male. It is most similar to *L. hujiayaoi* Yin & Li, 2013 and *L. mulunensis* Zhang, Li & Yin, 2018 (both from Guangxi) in sharing modified male metacoxae. *Linan qiniangmontis* differs from both known species in the slightly angulate anteromesal corner of antennomere 9 (rounded in *L. hujiayaoi* and *L. mulunensis*), a different form of the metaventral processes (processes stouter in *L. hujiayaoi* and much more elongate in *L. mulunensis*), the lack of additional projections above the metacoxae (present in *L. hujiayaoi* and *L. mulunensis*), and a more elongate aedeagus with a different configuration of the endophallus.

Acknowledgments

Peter Hlavác (Czech University of Life Sciences Prague, Praha, Czech Republic) and Giorgio Sabella (Geologiche ed Ambientali dell'Università, Catania, Italy) reviewed the draft manuscript and provided helpful comments. The present study was supported by the National Natural Science Foundation of China (No. 31872965), the Shanghai 'Phosphor' Science Foundation, China (19QA1406600), the Shanghai Engineering Research Center of Plant Germplasm Resources (No. 17DZ2252700), and Shenzhen Environmental Monitoring Center, Shenzhen, China.

References

Chandler DS (2001) Biology, morphology and systematics of the ant-like litter beetles of Australia (Coleoptera: Staphylinidae: Pselaphinae). Memoirs on Entomology, International 15, 560 pp.

Hlaváč P (2003) A taxonomic revision of the Tyrini of the Oriental region. II. Systematic study on the genus *Pselaphodes* and its allied genera (Coleoptera: Staphylinidae: Pselaphinae). Annales de la Société Entomologique de France 38: 283–297.

Yin Z-W, Hlaváč P, Li-Zhen Li (2013a) Further studies on the *Pselaphodes* complex of genera from China (Coleoptera, Staphylinidae, Pselaphinae). ZooKeys 275: 23–65. https://doi.org/10.3897/zookeys.275.4571

Yin Z-W, Li L-Z (2012) Notes on Michael Schülke's pselaphine collections from China. – Tyrini. I. genera *Labomimus* Sharp, *Linan* Hlaváč and *Pselaphodes* Westwood (Coleoptera, Staphylinidae, Pselaphinae). ZooKeys 251: 83–118. https://doi.org/10.3897/zookeys.251.4099

Yin Z-W, Li L-Z (2013) Five new species of the genera *Labomimus* and *Linan* from Guangxi, South China (Coleoptera: Staphylinidae: Pselaphinae). Acta Entomologica Musei Nationalis Pragae 53: 141–153.

Yin Z-W, Li L-Z, Zhao M-J (2011) A review of the genus *Linan* (Coleoptera: Staphylinidae: Pselaphinae). Acta Entomologica Musei Nationalis Pragae 51: 123–135.

Yin Z-W, Nomura S, Li L-Z (2013b) New species and new records of the *Pselaphodes* complex of genera (Staphylinidae: Pselaphinae: Tyrini) from China. Annales Zoologici 63: 343–356. https://doi.org/10.3161/000345413X669595

Zhang Y-Q, Li L-Z, Yin Z-W (2018) Six new species and a new record of *Linan* Hlaváč in China, with a key to species (Coleoptera, Staphylinidae, Pselaphinae). ZooKeys 793: 115–133. https://doi.org/10.3897/zookeys.793.27661

ZooKeys 859: 69–115 (2019)
doi: 10.3897/zookeys.859.32624
http://zookeys.pensoft.net

RESEARCH ARTICLE

A peer-reviewed open-access journal
ZooKeys
Launched to accelerate biodiversity research

Morphological differences between species of the sea bass genus *Lateolabrax* (Teleostei, Perciformes), with particular emphasis on growth-related changes

Kōji Yokogawa[1]

1 *13-5 Higashihama, Tadotsu-cho, Nakatado-gun, Kagawa 764-0016, Japan*

Corresponding author: *Kōji Yokogawa* (gargariscus@ybb.ne.jp)

Academic editor: *Nina Bogutskaya* | Received 22 December 2018 | Accepted 19 March 2019 | Published 2 July 2019

http://zoobank.org/456E5144-1FC0-4382-876A-39182E0F7EC7

Citation: Yokogawa K (2019) Morphological differences between species of the sea bass genus *Lateolabrax* (Teleostei, Perciformes), with particular emphasis on growth-related changes. ZooKeys 859: 69–115. https://doi.org/10.3897/zookeys.859.32624

Abstract

Morphological differences, including growth-related changes, were examined in three morphologically similar East Asian sea bass species, *Lateolabrax japonicus*, *L. maculatus* and *L. latus*. In many cases, body measurements indicated specific patterns of growth-related proportional changes. *Lateolabrax latus* differed from the other two species in having greater body depth, caudal peduncle depth, caudal peduncle anterior depth, snout length, and upper and lower jaw length proportions. In particular, scatter plots for caudal peduncle anterior depth relative to standard length (SL) in that species indicated complete separation from those of the other two species, being a new key character for identification. Comparisons of *L. japonicus* and *L. maculatus* revealed considerable proportional differences in many length-measured characters, including fin lengths (first and second dorsal, caudal and pelvic), snout length, post-orbital preopercular width (POPW) and post-orbital length. In particular, snout length (SNL) and POPW proportions of the former were greater and smaller for specimens >200 and ≤ 200 mm SL, respectively. Because the scatter plots of these proportions for the two species did not overlap each other in either size range, identification of the species was possible using a combination of the two characters. In addition, scatter plots of the POPW / SNL proportion (%) of *L. japonicus* and *L. maculatus* were almost completely separated throughout the entire size range examined (border level 90%), a further aid to identification. The numbers of pored lateral line scales and scales above the lateral line tended to increase and decrease with growth, respectively, in *L. japonicus*, whereas scales below the lateral line and gill raker numbers tended to increase with growth in *L. maculatus*. Because the ranges of these meristic characters may therefore vary with specimen size, they are unsuitable for use as key characters. Accordingly, a new key is proposed for the genus *Lateolabrax*.

Keywords
Lateolabrax japonicus, *Lateolabrax maculatus*, *Lateolabrax latus*, morphology, growth, new key

Introduction

The sea basses of the genus *Lateolabrax* (Lateolabracidae) are common East Asian coastal marine fishes (occasionally also occurring in fresh water). Bleeker (1854–57) established the genus for a single species, *Lateolabrax japonicus* (Cuvier, 1828), Katayama (1957) later describing a second species, *Lateolabrax latus*, from Japan. More recently, Yokogawa and Seki (1995) concluded that differences between the Japanese and Chinese forms of "*L. japonicus*" were sufficient for the Chinese form to be recognized as a distinct species, being referred to as "spotted sea bass" by Yokogawa and Tajima (1996). Finally, it was formally redescribed as *Lateolabrax maculatus* (McClelland, 1844) in Yokogawa's (2013b) revision, where *Lateolabrax lyiuy* (Basilewsky, 1855), which is incorrectly treated as valid and applied to the Chinese form (Kottelat 2013; Eschmeyer 2019), was regarded as a junior synonym of *L. maculatus*. At this point, three valid species of *Lateolabrax* are recognized (Fig. 1).

Lateolabrax latus has been distinguished from *L. japonicus* by having greater proportions of body and caudal peduncle depth (BD and CPD), more dorsal and anal fin rays (≥15 and ≥9, respectively), fewer scales below the lateral line (≤16) and possessing ventromandibular scale rows (VSRs) (Katayama 1957). Furthermore, the range of dorsal fin ray (DFR) counts in *L. latus*, which had been considered to not overlap that of *L. japonicus*, had become established as a key identification character (e.g., Katayama 1960a, 1965, 1984; Hatooka 1993). However, subsequent finding of *L. latus* individuals with 14 DFRs [overlapping the range in *L. japonicus* (12–14 DFRs)] (Hatooka 2000, 2013; Murase et al. 2012) made this character an incomplete key for identification. In addition, VSRs have not been adopted in recent keys proposed for *Lateolabrax* (Hatooka 2000, 2013), because they have been found in some specimens of the other two *Lateolabrax* species (Paxton and Hoese 1985; Hirota et al. 1999; Kang 2000; Murase et al. 2012). On the other hand, recent keys have included "caudal fin notch depth," being shallower in *L. latus* than in the other two species (Hatooka 2000, 2013), although the lack of any proportional information means that verification following examination of possible growth-related changes is necessary. Furthermore, proportional differences in BD and CPD appear to be based on the premise that their proportions are stable (isometric growth), although this has not been verified to date.

Lateolabrax maculatus has been characterized by many clear black spots on the body, but this character is also problematic as a few individuals of the species lack such spots (Yokogawa and Seki 1995), whereas some individuals of the other two *Lateolabrax* species have dots (Fig. 2). Although Yokogawa and Seki (1995) revealed differences between *L. japonicus* and *L. maculatus* in some meristic characters, including counts of lateral line scales, gill rakers and vertebrae, overlapping ranges between the two species result in no single character separating them completely. Proportional snout length

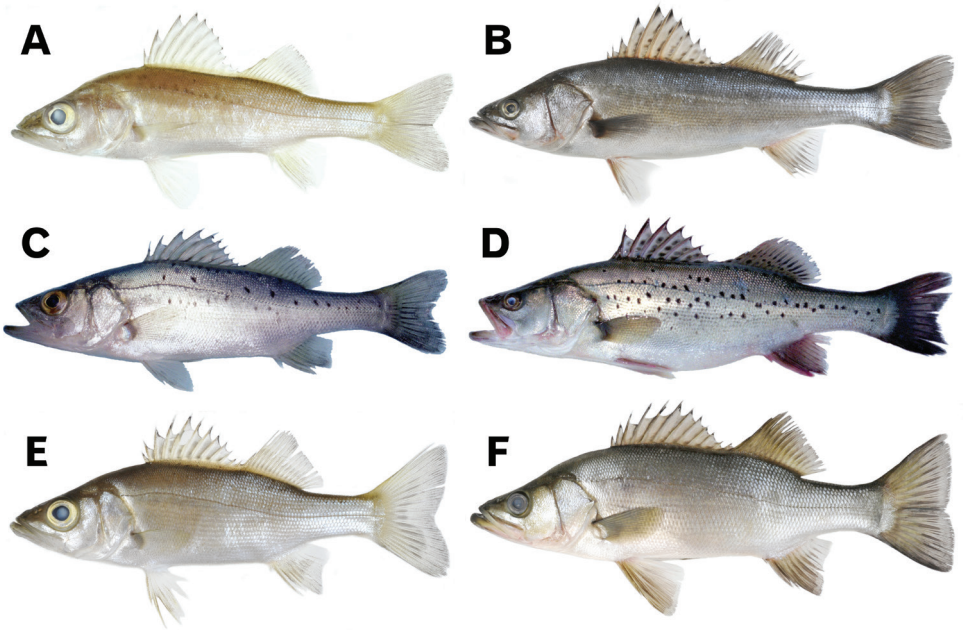

Figure 1. General aspects of small (fingerling) and large (adult) individuals of *Lateolabrax japonicus* (**A, B**), *L. maculatus* (**C, D**) and *L. latus* (**E, F**) in fresh condition. **A** KPM-NI 27449 (91.9 mm SL) **B** KPM-NI 30671 (331.0 mm SL) **C** uncatalogued specimen (94.3 mm SL) **D** BSKU 100776 (265.0 mm SL) **E** KPM-NI 29044 (97.1 mm SL) **F** KPM-NI 24656 (369.0 mm SL). **A, B, E** and **F** were photographed by Hiroshi Senou (KPM), **C** and **D** were photographed by K. Yokogawa.

(SNL), also recently used to separate the two species [SNL of *L. maculatus* relatively shorter than in *L. japonicus* (Hatooka 2000, 2013; Yamada et al. 2007)], may also be problematic due to lack of proof of isometric growth. Furthermore, morphology of the first anal pterygiophore (arched and straight in *L. japonicus* and *L. maculatus*, respectively), proposed by Kang (2000), still needs to be validated due to possible growth-related changes.

Thus, morphological identifications of the three *Lateolabrax* species remain problematic, although genetic studies have shown them to be independent species (Yokogawa 1998; Shan et al. 2016). Accordingly, the present study investigated the morphology of the three *Lateolabrax* species in detail, emphasizing growth-related changes, which have received little previous attention, in a search for clear and unequivocal key characters. Concerning this, although the potential of sexual dimorphism is an important issue, *Lateolabrax* species have no reported visual traits to distinguish the gender. Although sex determination requires observations on gonads by dissection, it could not be performed on the catalogued specimens, which represented most of the materials examined in the present study (see Materials and methods), therefore sexual dimorphism was not considered.

Materials and methods

Specimens examined

Measurements were based on the following *Lateolabrax* specimens, which have been deposited in the Laboratory of Marine Biology, Faculty of Science, Kochi University (BSKU), Kanagawa Prefectural Museum of Natural History (KPM), the Kagoshima University Museum (KAUM) and Tokushima Prefectural Museum (TKPM), together with some uncatalogued ones. Because presence of some specialized sea bass populations, which resulted from introgressive hybridization between *Lateolabrax japonicus* and *L. maculatus*, have been reported from Japan (Ariake and Yatsushiro Seas) (Yokogawa et al. 1997; Yokogawa 2002, 2004; Nakayama 2002; Han et al. 2015) and Korea (Yokogawa 2004; Bae et al. 2017), specimens from such areas were not adopted. Further, most specimens of these two species examined in the present study had been previously genetically recognized to be from the pure strains, using isozyme analysis (Yokogawa and Seki 1995).

Lateolabrax japonicus (229 specimens). BSKU 100789–100804 (16), 100826, KPM-NI 9697, 9698, KAUM–I. 82683–82703 (21), 93431–93439 (9), uncatalogued specimens (54) – all Kagawa Pref.; BSKU 101505–101541 (37), Hyogo Pref., Seto Inland Sea; BSKU 100739–100769 (31), 100788, Yamaguchi Pref., Seto Inland Sea; BSKU 66400, KPM-NI 9699 – both Uwajima, Ehime Pref., TKPM-P 352 (20), Tokushima Pref.; KPM-NI 27449, Mie Pref.; KPM-NI 30671, Sagami Bay; BSKU 100837, 100839, 100842, 100845, 100846, 100852, 100854, 100855, 100859–100862 (4), 100865, 100867, 100873, 100874, 100876, 100878, 100879, 100882, 100883, 100886, 100888, 100891, 100893, 100897, 100898, 100900–100902 (3), 100904, 100906, 100907 – all Ishikawa Pref.

Lateolabrax maculatus (170 specimens). BSKU 100770–100787 (18), 101787–101826 (40), a wild strain imported from Yantai, China and cultured in Kagawa, Japan; TKPM-P 1655 (40), uncatalogued specimens (33), a wild strain imported from China (locality unknown) as aquacultural seeds; BSKU 66398, 66399, 66401–66406 (6), TKPM-P 6114, 6140, KPM-NI 9686–9689 (4), 9691–9694 (4), uncatalogued specimens (17) – all Uwajima, Ehime Pref. (presumed escapees from nurseries); TKPM-P 16897, KPM-NI 9696, uncatalogued specimens (2) – all eastern Seto Inland Sea (presumed escapees from nurseries).

Lateolabrax latus (136 specimens). BSKU 101827, Awaji I., Seto Inland Sea; BSKU 100553, 100554, 100556–100561 (6), 101835, TKPM-P 372 – all Tokushima Pref.; KAUM–I. 1895 (4) locality unknown; KAUM–I. 25203, 29117, KPM-NI 24246–24248 (3), 24252–24256 (5), 24648–24656 (9), 24935–24940 (6) – all Yakushima I.; KAUM–I. 33778, Ikarajima I., Yatsushiro Sea.; KAUM–I. 39049–39051 (3), 39055–39058 (4), 39128, 39129, 61956, 64737, 64738, 66393, 66394, 67090, Tanegashima I.; KAUM–I. 42043, 42044, 51058–51068 (11), 54112, 54668, 57963, 58161, 58162, 61406, 61407, 61577, 63162–63169 (8), 63625, 65483–65485 (3), 65671, 80441–80444 (4), Kagoshima Pref. (mainland); KAUM–I. 66081, 75375, 75660,

75815, 75816, Nagasaki Pref.; KPM-NI 21869, 22433, 23429, Shizuoka Pref.; KPM-NI 24566, 24579, 24615, 35333, Miyazaki Pref.; KPM-NI 26185, 26186, 26992, 28599 (3), 29040, Chiba Pref.; KPM-NI 26973, 26975–26979 (5), 26988–26991 (4), Uwajima, Ehime Pref.; KPM-NI 29041–29048 (8), 31568, Kochi Pref.; KPM-NI 29279, 37509, 37919, 37920, Kanagawa Pref.

Morphological measurements

Methods of measurements and counts followed Hubbs and Lagler (1970). Dimensions were taken with calipers (minimum scale 0.1 mm), with particular care for smaller specimens due to the effect of even a small error on the calculated proportion. The characters examined are listed with abbreviations in Table 1 and illustrated in Figure 3. New or uncommon length-measured characters included: post-orbital preopercular width (horizontal distance from orbit posterior edge to preopercle posterior margin), post-orbital length (distance from orbit posterior edge to opercle posterior angle), caudal peduncle anterior depth (distance between posterior ends of dorsal and anal fin bases), caudal fin notch depth (horizontal distance from bottom of notch to margin of naturally spread fin) and pectoral scaly area length (defined by Yokogawa and Seki 1995) (see Figure 3).

Scale row and paired fin ray counts were made on the left side of the body, whereas gill rakers were counted on the first gill arch on the right side by separating the upper and lower limbs of the gill arch. Because counts of pelvic fin-spine (P_2FS) and soft rays (P_2FRs) showed no variation (P_2FS: 1, P_2FRs: 5 in all specimens), these counts were omitted from the statistical analyses. Abdominal and caudal vertebrae were counted, and first anal fin pterygiophore morphology observed from radiographs.

Total numbers of recognizable black or faint spots / dots on the left side of the body and mid-dorsal aspect of the caudal peduncle (Fig. 2) were counted. Dorsal head squamation [reported as differing between *L. japonicus* and *L. maculatus* (Yokogawa and Seki 1995)], was examined in all three species. Ventromandibular scale rows were also examined on the left side by separating the anterior and posterior parts following Murase et al. (2012), and their status recorded as present, vestigial or absent.

Statistical computations

For a length-measured dimension (LD), a growth-related proportional change pattern is given by the relationship between base dimension [e.g., standard length (SL) or head length (HL)] and the LD proportion (LD / SL or LD / HL). Because the relationship between SL (or HL) and LD is generally expressed by a power regression formula ($LD = a\ SL^{b}$) (allometric growth), the following formula was used ($LD / SL = a\ SL^{b-1}$). Accordingly, power regressions were applied for the relationships between SL (or HL) and the LD proportions (Table 2).

Table 1. Characters considered for the analysis.

	Abbreviation		Abbreviation
Length-measured body characters		Post-orbital preopercular width	POPW
Standard length	SL	Upper jaw length	UJL
Pre-anus length	PAL	Lower jaw length	LJL
Body depth	BD	**Meristic characters**	
Body width	BWT	Dorsal fin spine	DFS
Caudal peduncle depth	CPD	Dorsal fin soft ray	DFR
Caudal peduncle anterior depth	CPAD	Anal fin spine	AFS
Caudal peduncle length	CPL	Anal fin ray	AFR
Pre-dorsal length	PDL	Pectoral fin ray	P_1FR
First dorsal fin (longest spine) length	FDFL	Pelvic fin spine	P_2FS
Second dorsal fin (longest ray) length	SDFL	Pelvic fin ray	P_2FR
Caudal fin length	CFL	Pored scale on lateral line	LLS
Caudal fin notch depth	CFND	Scale above lateral line	SAL
Anal fin (longest ray) length	AFL	Scale below lateral line	SBL
Pectoral fin length	P_1FL	Upper-limb gill raker	UGR
Pelvic fin length	P_2FL	Lower-limb gill raker	LGR
Pectoral scaly area length	PSAL	Total gill raker	TGR
Head length	HL	Abdominal vertebra	AV
Length-measured cephalic characters		Caudal vertebra	CV
Snout length	SNL	Total vertebra	TV
Orbital diameter	OD	**Others**	
Inter-orbital width	IOW	Dorsocephalic scale row	DSR
Sub-orbital width	SOW	Ventromandibular scale row	VSR
Post-orbital length	POL	First anal pterygiophore	FAP

Characteristics that changed with growth were evaluated so as to determine if the changes were isometric or allometric, i.e., regressions between SL (or HL) and LD were transformed into natural logarithms (ln) ($\ln LD = a \ln SL + b$), and a t test was used to examine slope significance for the null hypothesis ($a = 1$), according to Zar (2010). When a differed significantly from 1, the character was considered to have changed allometrically, i.e., its proportion had increased or decreased with growth. Meristic counts (MC) were regressed using SL ($MC = a\ SL + b$), and a t test used to examine slope significance for the null hypothesis ($a = 0$) (Zar 2010). When a differed significantly from 0, the character was considered to have changed with growth. In addition, standard errors, which indicated data variation from the regression lines, were calculated during the above analyses (Zar 2010).

To examine inter-specific differences in length-measured characters, regressions between SL (or HL) and LD were also logarithm-transformed ($\ln LD = a \ln SL + b$), since most characters showed allometric growth (Table 3). Parameters of the regressions (a and b) were compared by analysis of covariance (ANCOVA) (t test), following the methods of Yamada and Kitada (2004).

Because some meristic counts tended to increase significantly with growth (Table 4), they were compared using the Mann-Whitney U test (Iwasaki 2006). Example numbers for the U test being >20 for all species, z values (instead of U values) for the

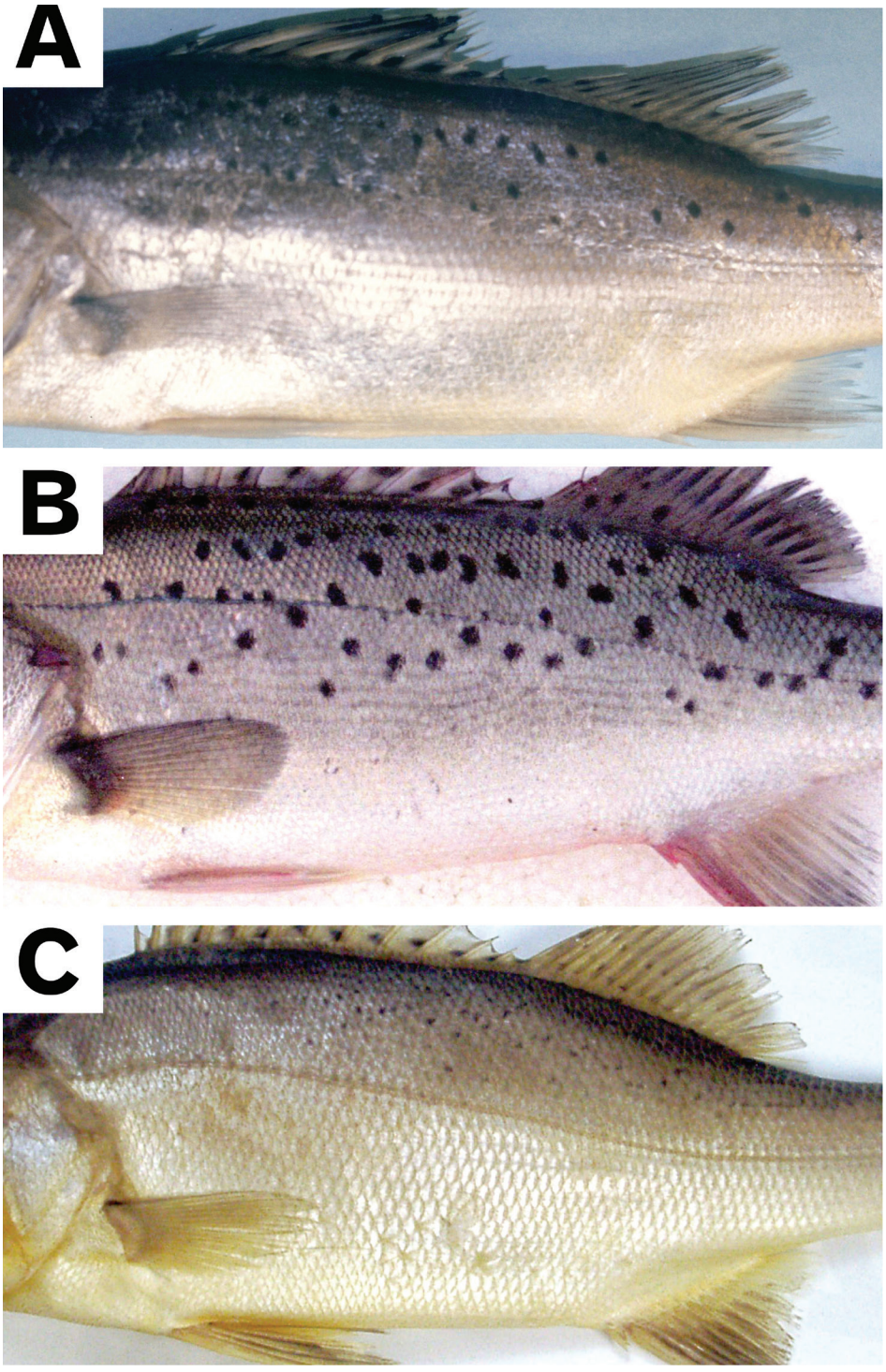

Figure 2. Dots / spots on lateral body regions of *Lateolabrax japonicus* (**A**), *L. maculatus* (**B**) and *L. latus* (**C**). **A** uncatalogued specimen (168.4 mm SL) **B** BSKU 100773 (254.2 mm SL) **C** KAUM–I. 29117 (219.7 mm SL).

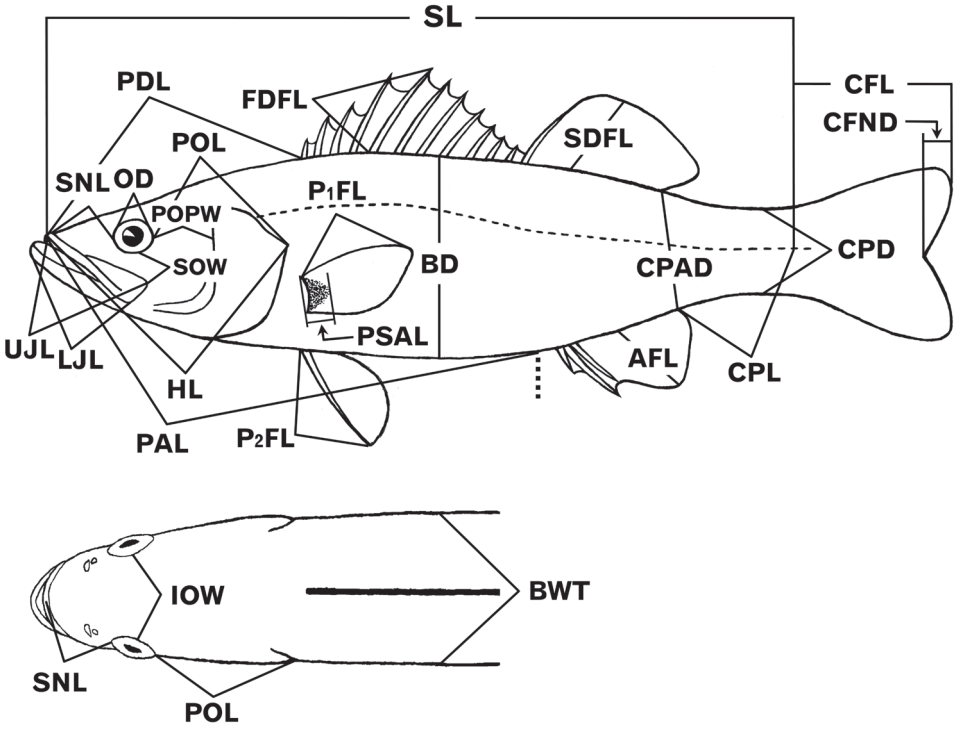

Figure 3. Illustrations of *Lateolabrax* body measurements taken. For abbreviations, see Table 1.

normal distribution were calculated after correction for distribution continuity, following Iwasaki (2006).

In the above statistical inferences, due to multiple tests being applied simultaneously in each case, multiple comparisons were introduced for the *t* test results, risk percentages for the *t* values being corrected according to total test counts, using the Holm-Bonferroni method (Holm 1979).

Results

Growth-related proportional changes

Body characters

In the three *Lateolabrax* species, slopes of the logarithm-transformed regressions were significantly different from 1 (allometric growth) for most characters (Table 3), indicating that most of the body proportions changed with growth. Relationships between standard length (SL) and length-measured body proportions are shown graphically by species in Figure 4, those with prominent plot separation between species being shown with multiple specific plots in Figure 5.

Table 2. Regression parameters and correlation between standard length (SL) or head length (HL) and proportions of length-measured dimensions (LD) [SL = a (LD/SL)^b, HL = a (LD/HL)^b] of three *Lateolabrax* species.

Regression	*Lateolabrax japonicus*			*Lateolabrax maculatus*			*Lateolabrax latus*		
	a	***b***	***r***	***a***	***b***	***r***	***a***	***b***	***r***
SL–PAL/SL	64.42	0.004	0.092	74.89	-0.026	-0.524	63.90	0.008	0.270
SL–BD/SL	44.23	-0.108	-0.735	29.94	-0.029	-0.379	33.03	-0.021	-0.240
SL–BWT/SL	8.78	0.075	0.471	10.71	0.048	0.455	8.43	0.079	0.466
SL–CPD/SL	16.55	-0.100	-0.749	11.48	-0.025	-0.353	11.32	0.002	0.034
SL–CPL/SL	22.33	-0.007	-0.069	19.83	0.019	0.216	21.55	-0.010	-0.115
SL–CPAD/SL	21.12	-0.091	-0.686	14.36	-0.014	-0.220	15.05	0.009	0.140
SL–PDL/SL	44.01	-0.041	-0.574	39.76	-0.029	-0.513	45.07	-0.039	-0.711
SL–FDFL/SL	22.72	-0.081	-0.407	12.40	0.008	0.065	22.22	-0.086	-0.541
SL–SDFL/SL	36.65	-0.201	-0.762	17.05	-0.068	-0.443	23.31	-0.091	-0.485
SL–CFL/SL	32.62	-0.085	-0.472	17.40	0.008	0.056	28.45	-0.055	-0.445
SL–CFND/SL	9.30	-0.115	-0.220	2.87	0.077	0.176	25.10	-0.296	-0.781
SL–AFL/SL	28.14	-0.142	-0.713	18.56	-0.061	-0.474	24.60	-0.096	-0.553
SL–P_1FL/SL	25.19	-0.070	-0.581	16.98	-0.010	-0.109	19.79	-0.024	-0.270
SL–P_2FL/SL	31.24	-0.101	-0.701	25.47	-0.073	-0.682	23.84	-0.040	-0.357
SL–HL/SL	42.88	-0.054	-0.677	38.39	-0.036	-0.629	46.25	-0.066	-0.836
SL–SNL/SL	8.23	0.002	0.047	11.42	-0.087	-0.664	10.91	-0.027	-0.456
SL–OD/SL	65.54	-0.431	-0.958	42.67	-0.364	-0.945	55.60	-0.368	-0.963
SL–IOW/SL	7.55	-0.020	-0.173	9.31	-0.064	-0.601	7.75	-0.010	-0.082
SL–SOW/SL	2.26	0.067	0.232	1.80	0.135	0.513	2.04	0.070	0.246
SL–POPW/SL	5.47	0.045	0.423	13.03	-0.094	-0.741	7.21	-0.008	0.066
SL–POL/SL	15.94	0.016	0.170	13.46	0.060	0.691	19.07	-0.027	-0.373
SL–UJL/SL	19.09	-0.061	-0.706	20.81	-0.083	-0.778	22.01	-0.071	-0.778
SL–LJL/SL	20.51	-0.058	-0.700	22.29	-0.084	-0.782	21.66	-0.052	-0.629
SL–PSAL/SL[1]							8.14	-0.130	-0.203
SL–POPW/SNL	71.07	0.030	0.314	90.56	0.031	0.222	65.79	0.020	0.149
HL–SNL/HL	20.42	0.057	0.530	28.48	-0.054	-0.453	24.50	0.040	0.533
HL–OD/HL	109.60	-0.400	-0.946	79.68	-0.338	-0.945	93.74	-0.323	-0.950
HL–IOW/HL	18.38	0.033	0.246	23.83	-0.031	-0.292	17.72	0.057	0.359
HL–SOW/HL	5.90	0.127	0.397	5.55	0.178	0.625	4.98	0.143	0.432
HL–POPW/HL	14.81	0.090	0.690	26.66	-0.022	-0.240	16.41	0.061	0.418
HL–POL/HL	39.87	0.073	0.729	38.83	0.099	0.873	42.78	0.041	0.498
HL–UJL/HL	44.57	-0.009	-0.139	51.77	-0.049	-0.667	47.53	-0.006	-0.109
HL–LJL/HL	48.01	-0.005	-0.092	55.24	-0.049	-0.713	47.36	0.014	0.237

[1] Simple patterned regressions could not be applied for complicated fluctuations in L. japonicus and L. maculatus.

Similar patterns of growth-related proportional changes common to the three species were observed for some characters, viz., significant positive allometric growth (proportions increased with growth) in body width and significant negative allometric growth (proportions decreased with growth) in head (HL) and pre-dorsal length (PDL), and second dorsal, anal and pelvic fin (longest ray) lengths (SDFL, AFL and P_2FL), although patterns of the regression curves or plot distributions for the three spe-

Table 3. Regression parameters (slope and intercept) and correlation between logarithm-transformed length-measured characters, together with results of *t* tests to examine significance of slopes for three *Lateolabrax* species (null hypothesis, slope = 1).

Regression	*Lateolabrax japonicus*			*Lateolabrax maculatus*			*Lateolabrax latus*		
	Slope	Intercept	*t*	Slope	Intercept	*t*	Slope	Intercept	*t*
ln SL–ln PAL	1.004	-0.44	1.39	0.974	-0.29	-7.97***	1.008	-0.45	3.25*
ln SL–ln BD	0.892	-0.82	-16.35***	0.971	-1.21	-5.31***	0.979	-1.11	-2.87*
ln SL–ln BWT	1.075	-2.43	8.05***	1.048	-2.23	6.62***	1.079	-2.47	6.10***
ln SL–ln CPD	0.900	-1.80	-17.04***	0.975	-2.16	-4.89***	1.002	-2.18	0.40
ln SL–ln CPL	0.993	-1.50	-1.05	1.019	-1.62	2.86*	0.990	-1.53	-1.33
ln SL–ln CPAD	0.909	-1.55	-14.28***	0.986	-1.94	-2.92*	1.009	-1.89	1.63
ln SL–ln PDL	0.959	-0.82	-10.56***	0.971	-0.92	-7.71***	0.961	-0.80	-11.72***
ln SL–ln FDFL	0.919	-1.48	-6.72***	1.008	-2.09	0.85	0.914	-1.50	-7.45***
ln SL–ln SDFL	0.794	-0.97	-17.15***	0.932	-1.77	-6.31***	0.909	-1.46	-6.42***
ln SL–ln CFL	0.914	-1.11	-7.84***	1.008	-1.75	0.70	0.974	-1.35	-2.55
ln SL–ln CFND	0.880	-2.35	-3.41**	1.077	-3.55	2.22	0.704	-1.38	-13.88***
ln SL–ln AFL	0.858	-1.27	-15.17***	0.939	-1.68	-6.97***	0.904	-1.40	-7.67***
ln SL–ln P_1FL	0.930	-1.38	-10.73***	0.990	-1.77	-1.41	0.976	-1.62	-3.25*
ln SL–ln P_2FL	0.899	-1.16	-14.81***	0.927	-1.37	-12.06***	0.960	-1.43	-4.42***
ln SL–ln HL	0.946	-0.85	-13.87***	0.964	-0.96	-10.46***	0.934	-0.77	-17.67***
ln SL–ln SNL	1.002	-2.50	0.67	0.913	-2.17	-11.57***	0.973	-2.22	-5.94***
ln SL–ln OD	0.569	-0.42	-50.25***	0.636	-0.85	-37.39***	0.632	-0.59	-41.41***
ln SL–ln IOW	0.980	-2.58	-2.64	0.936	-2.37	-9.71***	0.990	-2.56	-0.95
ln SL–ln SOW	1.067	-3.79	3.60**	1.135	-4.02	7.73***	1.070	-3.89	2.94*
ln SL–ln POPW	1.033	-2.84	5.68***	0.943	-2.26	-7.72***	0.993	-2.63	-0.69
ln SL–ln POL	1.014	-1.82	2.10	1.060	-2.00	12.25***	0.974	-1.66	-4.56***
ln SL–ln UJL	0.939	-1.66	-15.04***	0.917	-1.57	-16.02***	0.929	-1.51	-14.34***
ln SL–ln LJL	0.942	-1.58	-14.74***	0.916	-1.50	-16.11***	0.948	-1.53	-9.34***
ln SNL–ln POPW	1.026	-0.26	4.37***	1.020	0.01	1.71	1.017	-0.36	4.19***
ln HL–ln SNL	1.057	-1.59	9.41***	0.946	-1.26	-6.65***	1.040	-1.41	7.28***
ln HL–ln OD	0.600	0.09	-44.06***	0.662	-0.23	-37.38***	0.677	-0.06	-35.28***
ln HL–ln IOW	1.033	-1.69	3.82**	0.969	-1.43	-3.94**	1.057	-1.73	4.45***
ln HL–ln SOW	1.127	-2.83	6.52***	1.178	-2.89	10.36***	1.143	-3.00	5.55***
ln HL–ln POPW	1.090	-1.91	14.36***	0.978	-1.32	-3.19*	1.061	-1.81	5.32***
ln HL–ln POL	1.073	-0.92	15.93***	1.099	-0.95	23.15***	1.041	-0.85	6.62***
ln HL–ln UJL	0.991	-0.81	-2.11	0.951	-0.66	-11.57***	0.994	-0.74	-1.27
ln HL–ln LJL	0.995	-0.73	-0.19	0.952	-0.59	-13.19***	1.014	-0.75	2.81*

Asterisks indicate significance of t values; single, double and triple asterisks indicate 5%, 1% and 0.1% levels, respectively, after Holm-Bonferroni correction by species.

cies sometimes varied from one another (Figs 4, 5, Table 3). Differing specific growth-related proportional changes were evident for some other characters, e.g., pre-anus length (PAL), isometric growth in *L. japonicus*, negative and positive allometric growth in *L. maculatus* and *L. latus*, respectively (Fig. 4A–C, Table 3); and caudal fin notch depth (CFND), modestly and highly negative allometric growth in *L. japonicus* and *L. latus*, respectively, and isometric growth in *L. maculatus* (Fig. 4G–I, Table 3). In the latter, however, despite specific growth-related patterns, ranges of the CFND / SL proportions taken over the entire range of SLs were similar to one another, viz., 2.0–8.4%, 1.9–7.4% and 2.9–7.9%, in *L. japonicus*, *L. maculatus* and *L. latus*, respectively (Fig. 4J–L).

Table 4. Regression parameters (slope and intercept) and correlation between standard length (SL) and meristic counts of three *Lateolabrax* species (null hypothesis, slope = 0).

Regression	Slope	Intercept	*r*	*t*
Lateolabrax japonicus				
SL–DFS counts	-0.00008	12.87	-0.019	-0.28
SL–DFR counts	-0.00081	13.13	-0.130	-2.05
SL–AFR counts	0.00048	7.56	0.089	1.34
SL–P_1FR counts	-0.00047	16.96	-0.086	-1.30
SL–LLS counts	0.01207	77.01	0.343	5.50***
SL–SAL counts	-0.00258	15.84	-0.258	-3.98**
SL–SBL counts	0.00057	18.57	0.046	0.68
SL–UGR counts	0.00111	8.63	0.126	1.90
SL–LGR counts	-0.00025	17.93	-0.027	-0.41
SL–TGR counts	0.00086	26.56	0.073	1.10
SL–AV counts	0.00017	16.00	0.073	0.93
SL–CV counts	-0.00068	20.02	-0.108	-1.38
SL–TV counts	-0.00051	36.02	-0.083	-1.80
SL–Dot counts	-0.02297	12.69	-0.198	-2.90*
Lateolabrax maculatus				
SL–DFS counts	-0.00046	12.95	-0.153	-2.00
SL–DFR counts	-0.00028	13.03	-0.066	-0.86
SL–AFS counts	0.00008	2.98	0.104	1.36
SL–AFR counts	0.00097	7.34	0.217	2.88
SL–P_1FR counts	0.00079	16.33	0.190	2.50
SL–LLS counts	0.00261	73.45	0.099	1.30
SL–SAL counts	0.00008	15.52	0.009	0.24
SL–SBL counts	0.00477	18.17	0.409	5.72***
SL–UGR counts	0.00139	6.40	0.173	2.24
SL–LGR counts	0.00330	14.70	0.507	7.49***
SL–TGR counts	0.00469	21.11	0.408	5.68***
SL–AV counts	-0.00026	15.97	-0.135	-1.67
SL–CV counts	0.00022	19.00	0.089	1.09
SL–TV counts	0.00003	34.97	-0.012	-0.02
SL–Spot counts	0.02333	33.89	0.126	1.62
Lateolabrax latus				
SL–DFS counts	-0.00026	13.05	-0.092	-1.08
SL–DFR counts	-0.00041	15.11	0.011	-1.20
SL–AFS counts	-0.00002	3.00	0.001	-0.34
SL–AFR counts	0.00026	9.06	0.002	0.55
SL–P_1FR counts	-0.00026	16.20	0.004	-0.73
SL–LLS counts	0.00264	72.91	0.169	1.99
SL–SAL counts	-0.00063	13.86	-0.079	-0.92
SL–SBL counts	-0.00013	15.79	-0.014	-0.16
SL–UGR counts	-0.00045	6.83	-0.072	-0.83
SL–LGR counts	-0.00109	17.11	-0.176	-2.07
SL–TGR counts	-0.00154	23.94	-0.166	-1.95
SL–AV counts	0.00004	16.03	0.018	0.22
SL–CV counts	-0.00005	19.92	-0.014	-0.17
SL–TV counts	0.00001	35.95	-0.004	-0.05
SL–Dot counts	-0.06278	24.74	-0.365	-4.53***

Asterisks indicate significance of t values; single, double and triple asterisks indicate 5%, 1% and 0.1% levels, respectively, after Holm-Bonferroni correction by species.

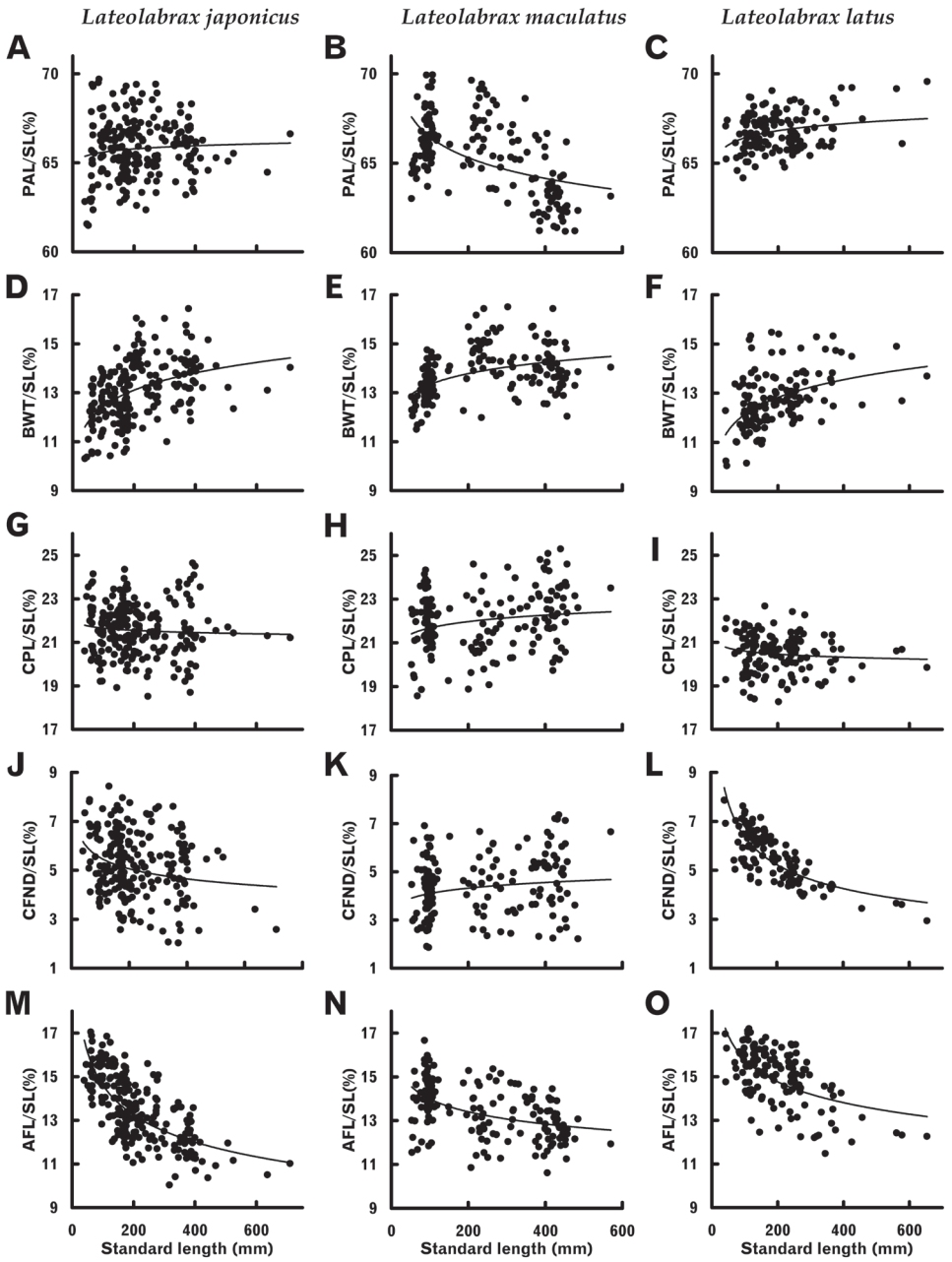

Figure 4. Relationships between standard length and proportions of some length-measured body characters of three *Lateolabrax* species. For character abbreviations, see Figure 3 and Table 1. Solid lines indicate power regression curves (parameters given in Table 2).

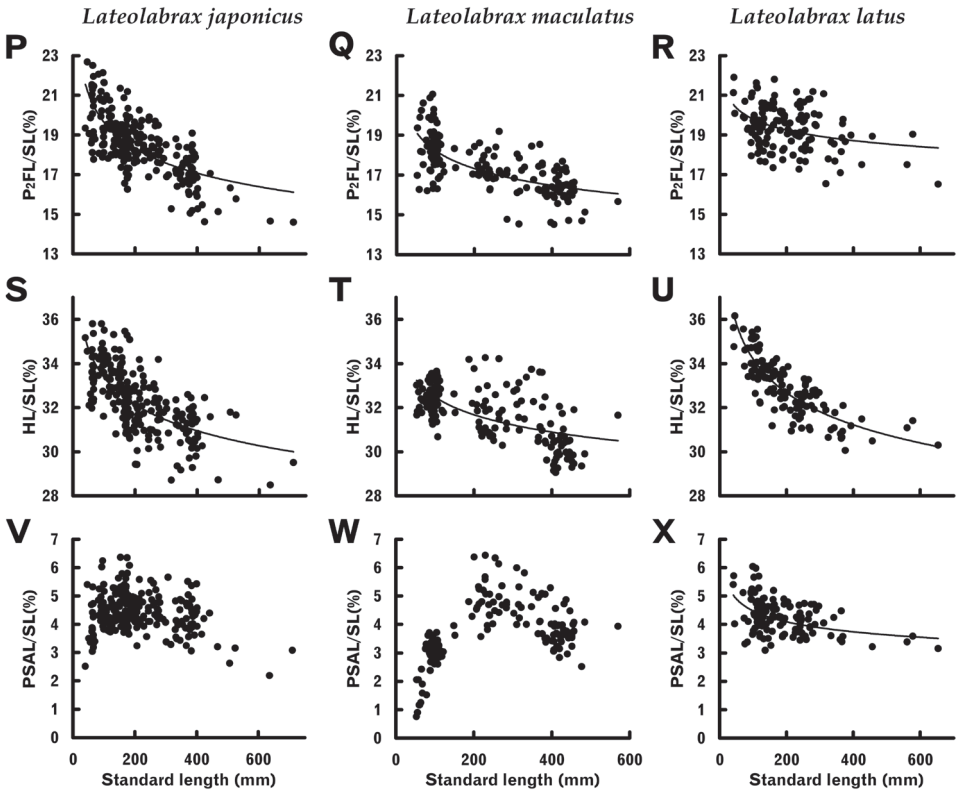

Figure 4. (Continued) Relationships between standard length and proportions of some length-measured body characters of three *Lateolabrax* species. For character abbreviations, see Figure 3 and Table 1. Solid lines indicate power regression curves (parameters given in Table 2).

Cephalic characters

For length-measured dimensions (LD) of cephalic characters, SL-based (SL–LD / SL) and HL-based relationships (HL–LD / HL) are illustrated in pairs with multiple specific plots in Figure 6. In each species, significant allometric growth was recognized in most length-measured cephalic characters as well as length-measured body characters (Table 3). In particular, negative allometric growth was so significant for orbital diameter (OD) (very high *t* values, see Table 3) that the plots for each all formed typical arched curves (Fig. 6C, D), indicating rapid decrement of OD proportions with growth. Such acute relative OD decrement in the three species was clearly apparent from photographs (Fig. 1).

Growth-related proportional change patterns based on SL and HL were inconsistent with each other for some characters in *L. japonicus* and *L. latus*, e.g., snout length (SNL) of *L. japonicus* was isometric and positively allometric for SL and HL,

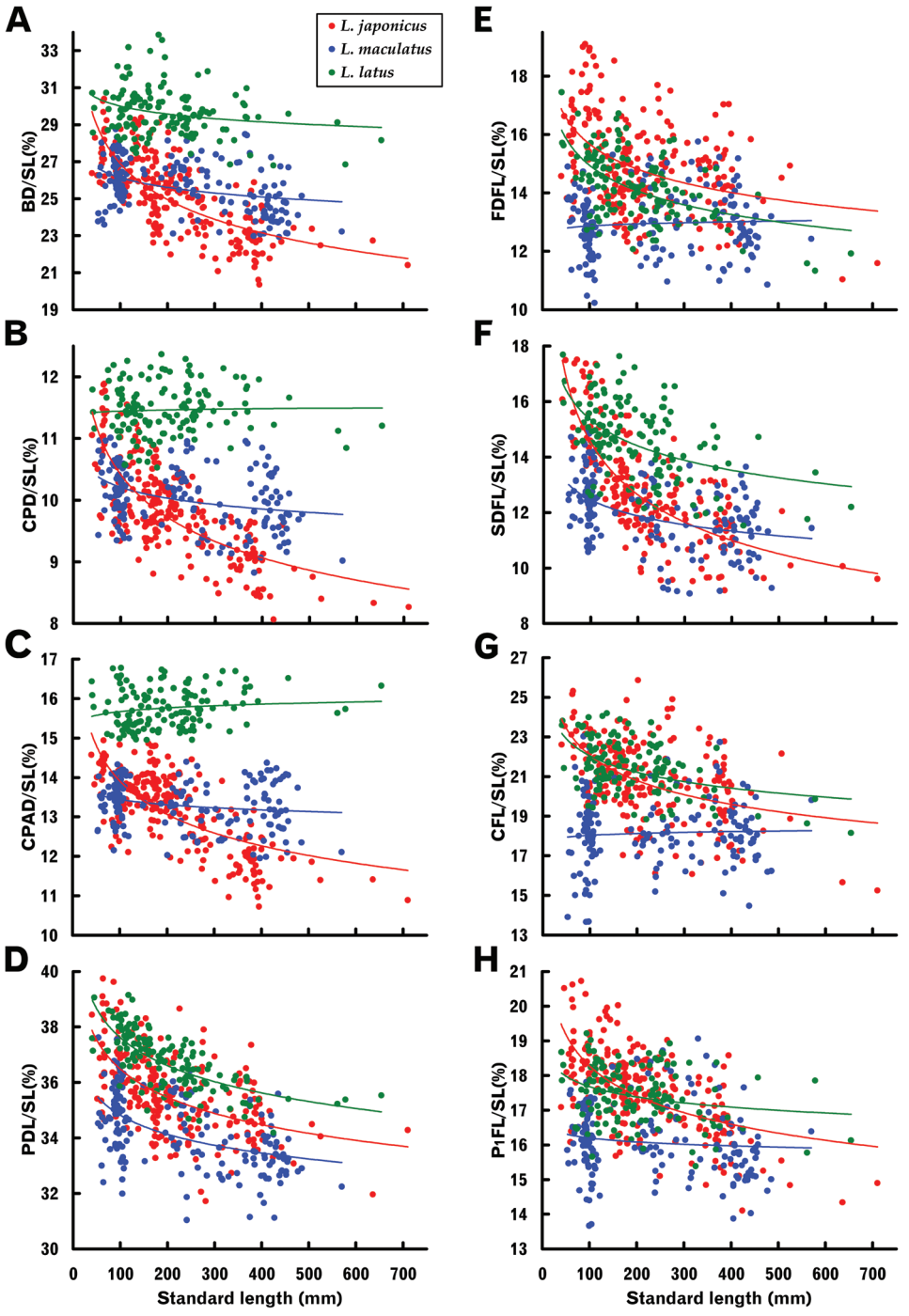

Figure 5. Relationships between standard length and proportions of some length-measured body characters which exhibited prominent plot separation among three *Lateolabrax* species. For character abbreviations, see Figure 3 and Table 1. Solid lines indicate power regression curves (parameters given in Table 2) for each species.

respectively; that of *L. latus* was negatively and positively allometric for SL and HL, respectively (Fig. 6A, B, Table 3). While the patterns were consistent between the SL- and HL-based relationships in *L. maculatus* for all cephalic characters (Fig. 6A–P, Table 3), allometric increment / decrement rates varied in the two-way relationships e.g., proportions of post-orbital preopercular width (POPW) decreased with growth acutely and slightly for SL and HL, respectively (Fig. 6I, J, Table 3).

As well as some body characters, specific proportional change patterns were recognized for some characters, e.g., SL-based relationships of POPW, exhibiting isometric growth in *L. japonicus*, and positive and negative allometric growth in *L. maculatus* and *L. latus*, respectively (Fig. 6K, Table 3); and SNL, exhibiting isometric growth in *L. japonicus*, and high and modest negative allometric growth in *L. maculatus* and *L. latus*, respectively (Fig. 6A, Table 3).

Pectoral scaly area length

The relationship between SL and pectoral scaly area length (PSAL) in *L. latus* was well fitted to a power regression (like many other body and cephalic length-measured characters), the PSAL / SL proportion gradually decreasing with growth (Fig. 4X, Table 2). In the other two species, however, proportional PSAL rapidly increased from the smallest specimens to a peak and thereafter gradually decreased (Fig. 4V, W), therefore being unsuitable for simple patterned regressions. Synchronous plotting for the two species showed the proportional PSAL of *L. maculatus* to be distinctly less than that of *L. japonicus* during the initial stage (< ca. 150 mm SL), although plots of the two species largely overlapped during the subsequent decreasing stage (Fig. 7). The proportional PSAL of *L. latus* during the former stage was much greater than in the other two species (Fig. 4V–X).

Inter-specific differences

Length-measured body and cephalic characters

Plot separation of *L. latus* from the other two species was prominent for vertical body dimensions of body depth (BD), caudal peduncle depth (CPD) and caudal peduncle anterior depth (CPAD), *L. japonicus* and *L. maculatus* both showing significant negative allometric growth, the degree of relative decrease being especially acute in the former. Although BD of *L. latus* showed slight negative allometric growth, CPD and CPAD were regarded as isometric (Fig. 5A–C, Table 3). However, despite considerable plot separation of BD and CPD between *L. latus* and the other species, plots of the three species overlapped for the smaller size class (< ca. 200 mm SL) (Fig. 5A, B). CPAD plots for *L. latus* were entirely separated from those of the other two species (border level 15%) (Fig. 5C). Although similar plot separation for caudal peduncle length (CPL) in *L. latus* was

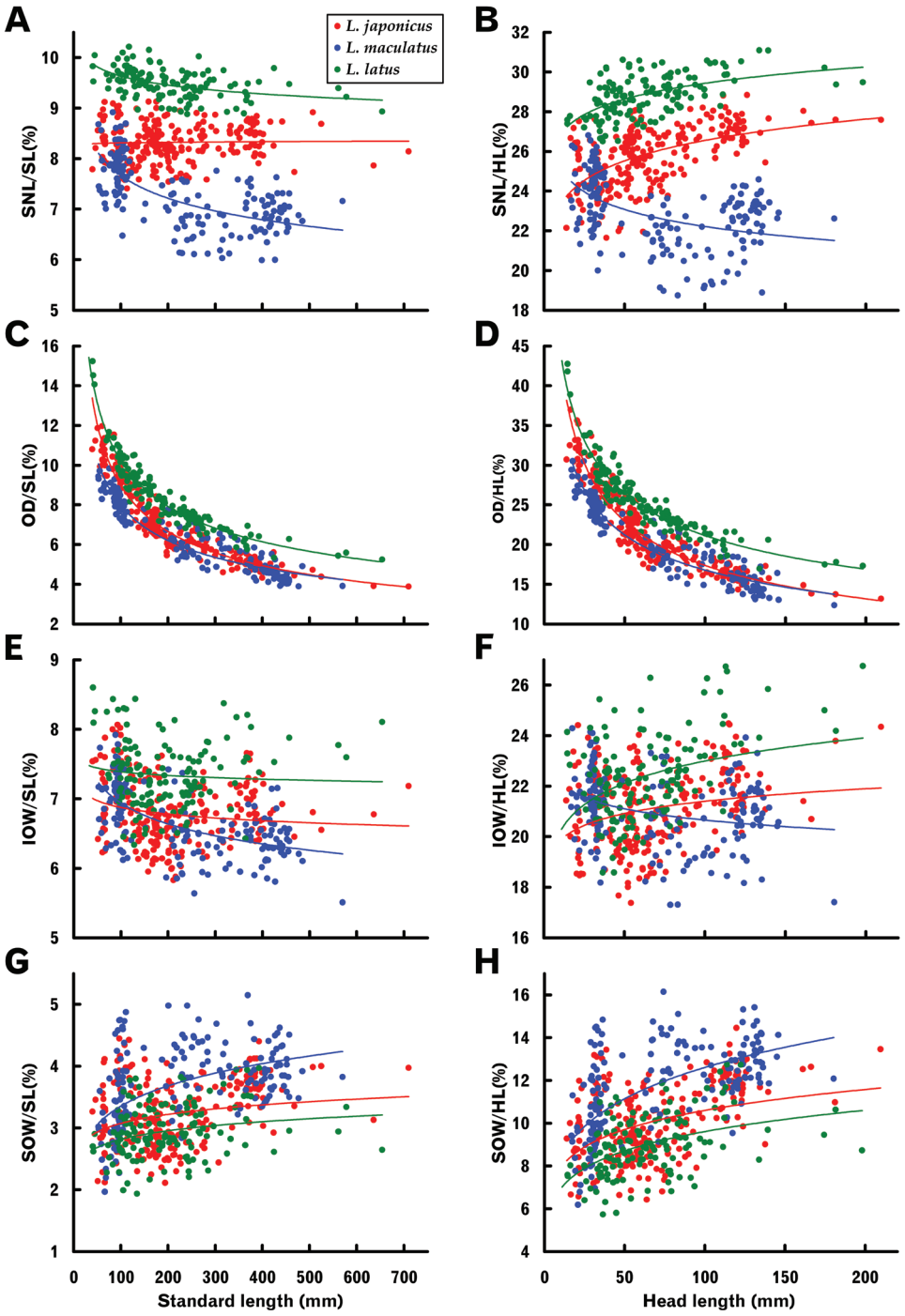

Figure 6. Relationships between standard length or head length and proportions of length-measured cephalic characters of three *Lateolabrax* species. For character abbreviations, see Figure 3 and Table 1. Solid lines indicate power regression curves (parameters given in Table 2) for each species.

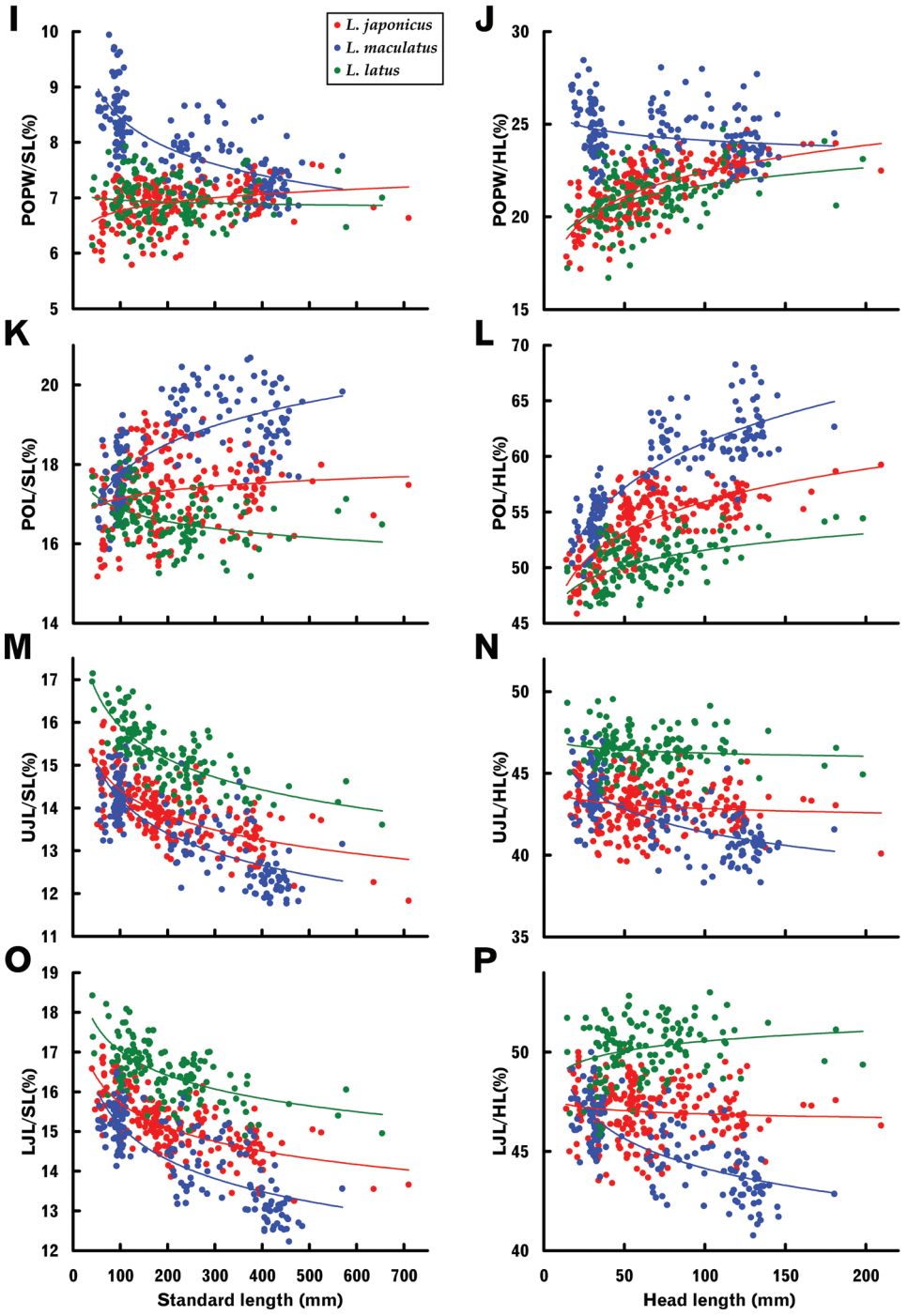

Figure 6. (Continued) Relationships between standard length or head length and proportions of length-measured cephalic characters of three *Lateolabrax* species. For character abbreviations, see Figure 3 and Table 1. Solid lines indicate power regression curves (parameters given in Table 2) for each species.

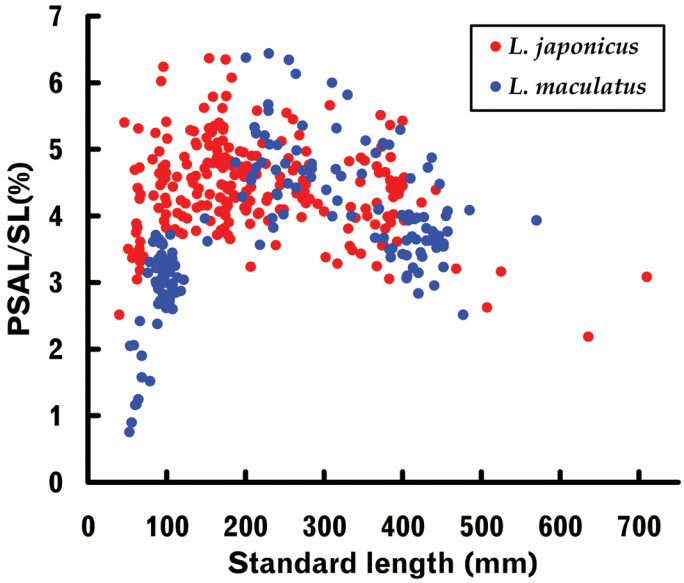

Figure 7. Relationships between standard length (SL) and pectoral scaly area length (PSAL) proportions for *Lateolabrax japonicus* and *L. maculatus*.

also apparent, ranges of proportional CPL of the three species almost overlapped due to considerable variation in plot distribution in *L. japonicus* and *L. maculatus* (Fig. 4G–I).

Plot separation of first and second dorsal (FDFL and SDFL), caudal (CFL) and pectoral (P_1FL) fin lengths was also apparent between *L. japonicus* and *L. maculatus* (Fig. 5E–H), the former showing significant negative allometric growth of each feature, whereas the latter exhibited isometric growth for all, except SDFL (Table 3). Proportions in the former were distinctively greater than in the latter in the smaller size class (< ca. 200 mm SL), although plots of the two species overlapped in the larger size class (> ca. 200 mm SL), since fin length proportions decreased and did not change with growth, respectively (Fig. 5E, G, H). Such proportional differences in fin length in the smaller size class between the two species were clearly apparent from photographs (Fig. 1A, C).

Upward plot separation of *L. latus* from the other two species was prominent for SNL and upper and lower jaw lengths (UJL and LJL), there being almost no overlap with *L. maculatus* and only modest overlap with *L. japonicus* (Fig. 6A, B, M–P). Plots of OD for *L. latus* were similarly upwardly separated from those of the other two species (Fig. 6C, D), especially in the HL-based graph (Fig. 6D). Post-orbital length (POL) plots for *L. latus* were shifted downward from those of the other two species (Fig. 6K, L), plot separation being more prominent in the HL-based graph (Fig. 6L).

On the other hand, plot separation between *L. japonicus* and *L. maculatus* was prominent for SNL, POPW and POL (Fig. 6A, B, I–L). SNL plots for the two species overlapped in the smaller size class (< ca. 200 mm SL), subsequently progressively separating with growth due to the proportional SNL of *L. maculatus* decreasing with growth (negative allometry), to a border level of ca. 7.7% (Fig. 6A) in the larger

size class (> ca. 200 mm SL). This phenomenon was more apparent in the HL-based relationship because proportional SNL in *L. japonicus* increased with growth (positive allometry) (Fig. 6B, Table 3), unlike that for the SL-based relationship (isometric growth) (Fig. 6A, Table 3). Similar patterns were observed for POL, plots of the two species overlapping in the smaller size class (< ca. 200 mm SL), but subsequently separating to a certain extent with growth due to a proportional POL increase in *L. maculatus* (positive allometry) (Fig. 6K, L). In contrast, POPW plots of the two species were completely separated from each other in the smaller size class (< ca. 200 mm SL), having a border level of ca. 7.5%, but progressively overlapped with growth due to the proportional POPW of *L. japonicus* and *L. maculatus* increasing and decreasing with growth, respectively (Fig. 6I, J).

POPW proportional to SNL is shown graphically in Figure 8. The SL–POPW / SNL regressions were positively allometric for *L. japonicus* and *L. latus*, and isometric for *L. maculatus* (Table 3). Plots for *L. japonicus* and *L. maculatus* were separated from each other almost entirely throughout all size ranges (border level 90%), following a slight plot overlap at ca. 100 mm SL (Fig. 8). In addition, plots for *L. latus* were displaced well downward from the other two species, despite some overlap with *L. japonicus* (Fig. 8).

Meristic characters

The *t* tests of regressions between SL and meristic counts (null hypothesis, slope = 0) proved significant for scales on (LLS) and above the lateral line (SAL) in *L. japonicus*, and scales below the lateral line (SBL) and gill raker counts [lower limb and total (LGR and TGR, respectively)] in *L. maculatus* (Table 4). Whereas SAL counts in *L. japonicus* tended to decrease with growth (Fig. 9), having negative slope values (Table 4), the remaining characters tended to increase (Fig. 9, Table 4). No significant differences in any meristic characters were found in *L. latus* (Table 4), indicating that none changed with growth in that species.

Figure 10 shows multiple specific frequency histograms for all meristic characters, *L. latus* clearly differing from the other two species in dorsal (DFR) and anal fin ray (AFR) counts (there being only slight range overlaps), as well as in pectoral fin ray (P_1FR) and SBL counts, again with some range overlaps. Notably, DFRs (14) in *L. latus* had only a 7.4% overlap of the ranges of the other two species, the latter differing significantly in vertebral counts [caudal and total (CV and TV, respectively)] and ranges of LLS, LGR and TGR. However, no species had a meristic character count range that was entirely separated from those of the other species.

Spots / dots on lateral body region

Some examples of *L. japonicus* and *L. latus* had small and fine dots, respectively, on the lateral body region (Fig. 2A, C), whereas *L. maculatus* usually had many clear black spots (Fig. 2B). In both of the former, dots appeared to be limited to some smaller specimens (Fig. 11A, C), the maximum sizes of specimens with dots being 260.6 mm

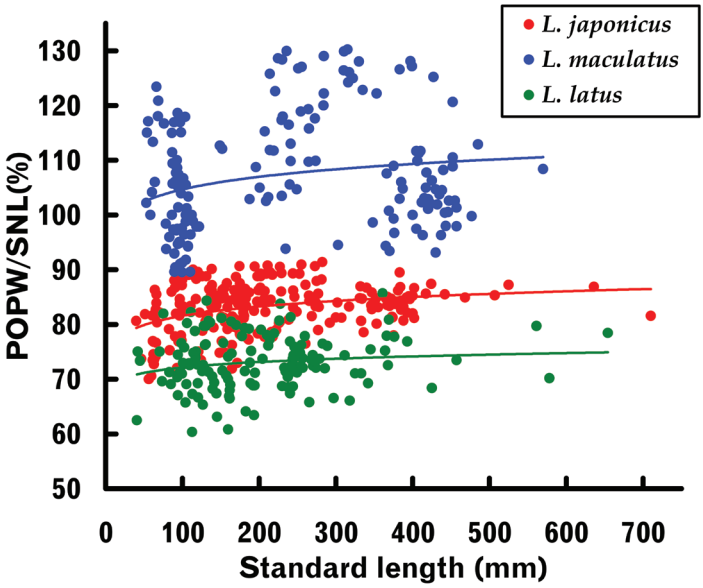

Figure 8. Relationships between standard length and (post-orbital preopercular width) / (snout length) proportions of three *Lateolabrax* species. Solid lines indicate power regression curves (parameters given in Table 2) for each species.

SL (BSKU 100765) and 254.8 mm SL (KAUM–I. 66393), respectively. The *t* tests indicated significant regressions between SL and dot counts for the two species (null hypothesis, slope = 0 rejected), both indicating negative correlations (minus slope values) (Fig. 11A, C, Table 4). The proportions of dotted specimens of the total material examined were 35.6% and 46.3% (51.9 and 60.0% for specimens <250 mm SL) in *L. japonicus* and *L. latus*, respectively. In *L. maculatus*, spot counts were typically abundant (ca. 40 on average), but variable (absent in 4.9% of specimens) (Fig. 11B) and not related to body size, a *t* test (null hypothesis, slope = 0) indicating no significant regression between SL and spot counts (Table 4).

Squamation on dorsal head region

Post-juvenile specimens (> ca. 70 mm SL) of the three *Lateolabrax* species had a pair of scale rows (dorsocephalic scale rows, DSRs) extending forward from the inter-orbital area, which was densely covered with fine scales (Fig. 12). DSRs in *L. japonicus* and *L. latus* were well developed distally, with anterior edges always beyond the anterior nostril position (ANP) (Fig. 12A, B, E, F), and almost reaching the upper lip in large specimens of *L. latus* (Fig. 12F). On the other hand, DSRs in small specimens of *L.*

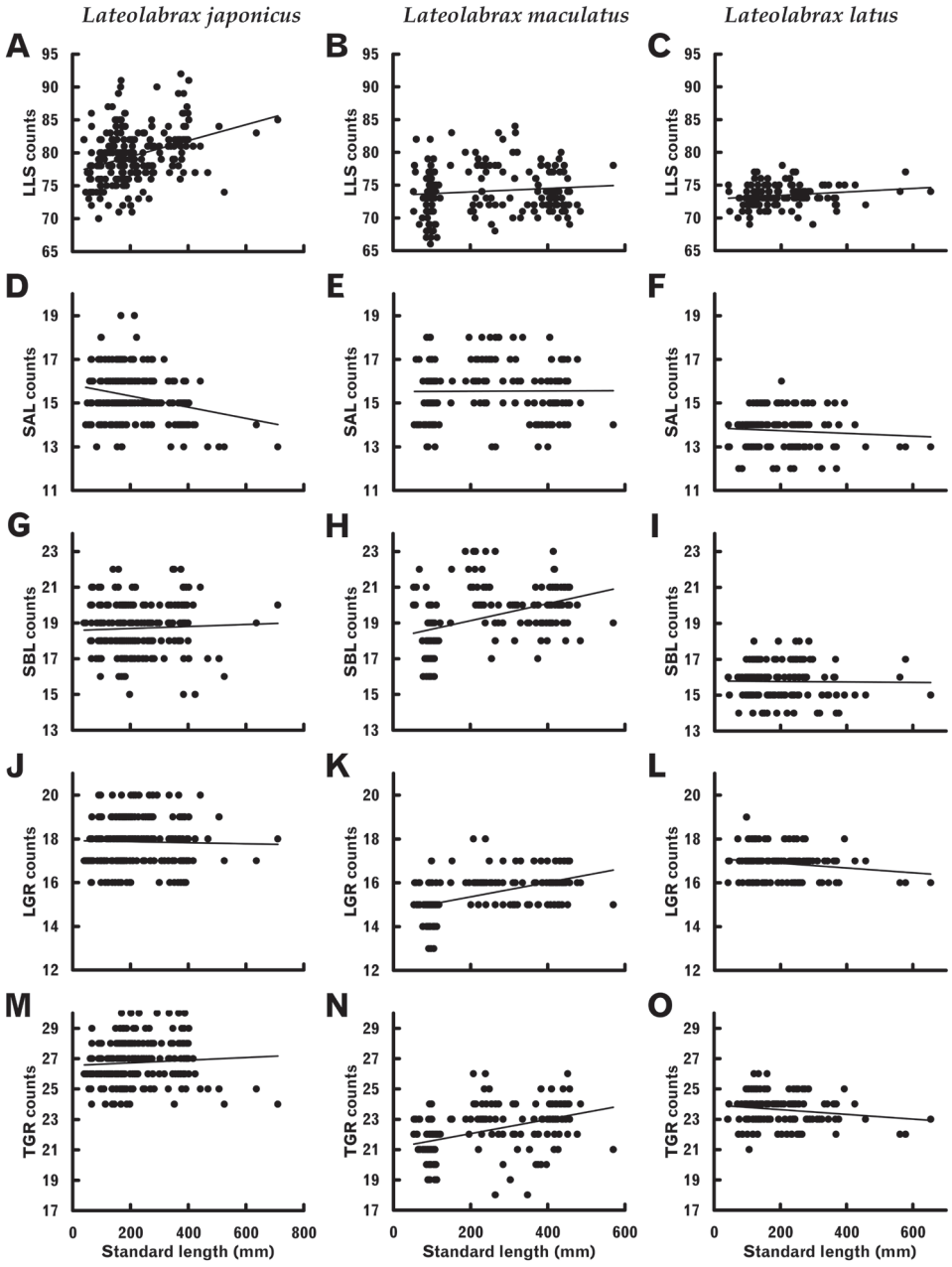

Figure 9. Relationships between standard length and some meristic characters which exhibited growth-related changes in some *Lateolabrax* species. For character abbreviations, see Figure 3 and Table 1. Solid lines indicate linear regressions (parameters given in Table 4).

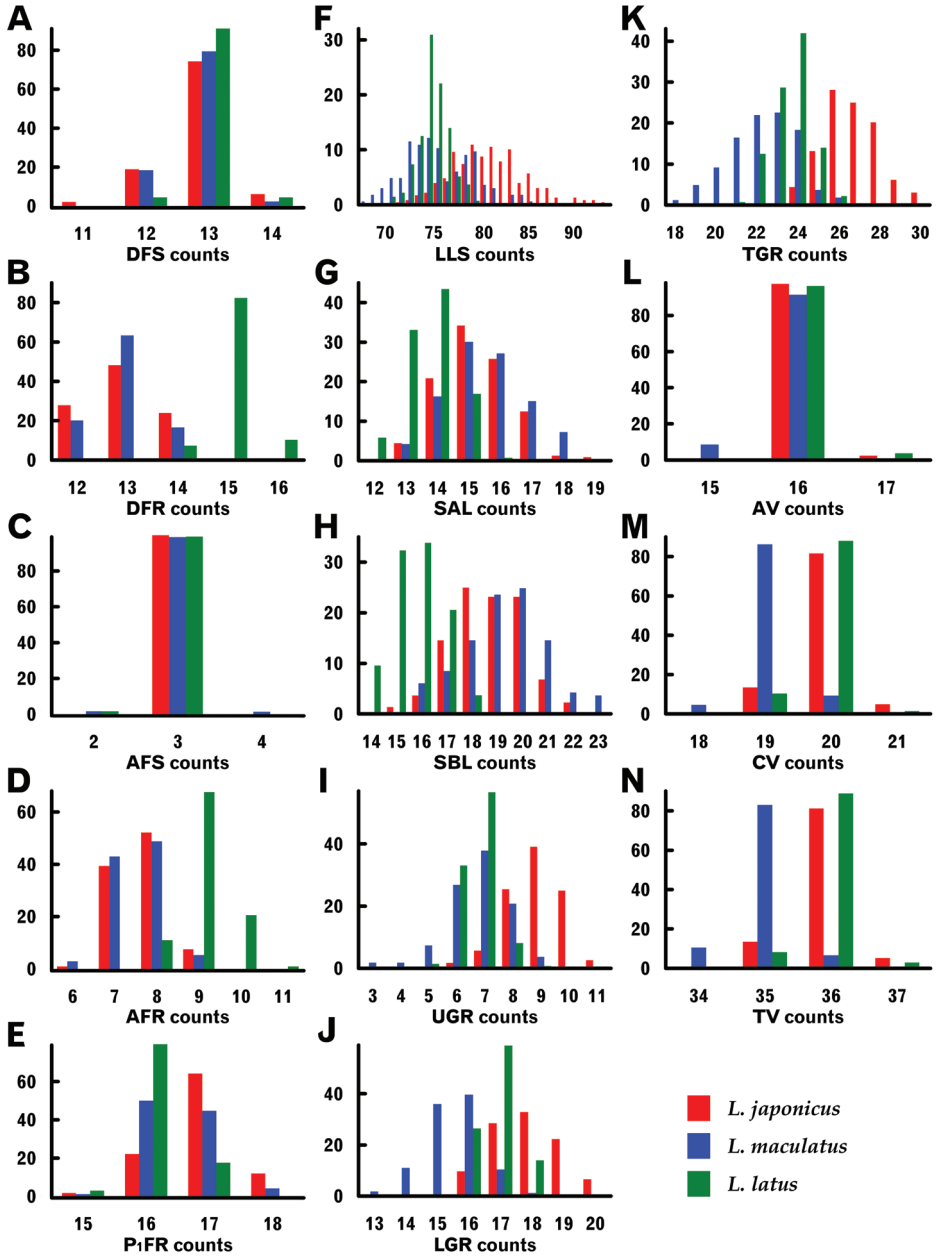

Figure 10. Histograms of meristic characters of three *Lateolabrax* species. For character abbreviations, see Figure 3 and Table 1. Vertical axes indicate frequencies (%).

maculatus were almost entirely restricted to the inter-orbital region, not extending beyond ANPs (Fig. 12C), although gradual development with growth resulted in DSRs extending beyond the ANP in specimens > ca. 150 mm SL (Fig. 12D).

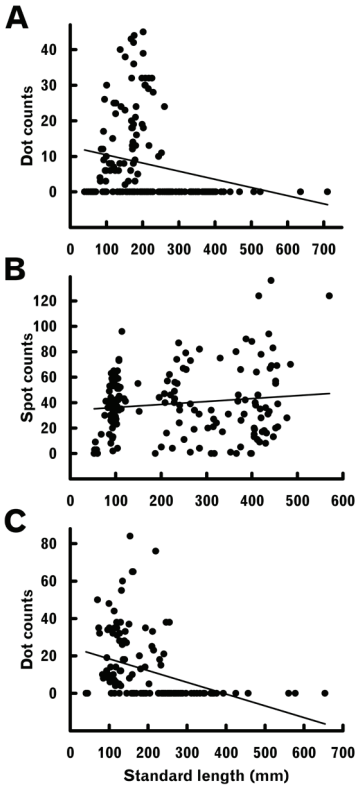

Figure 11. Relationships between standard length and dot / spot counts on lateral body regions of *Lateolabrax japonicus* (**A**), *L. maculatus* (**B**) and *L. latus* (**C**). Solid lines indicate linear regressions (parameters given in Table 4).

Squamation on ventral head region

Some individuals of the three *Lateolabrax* species had a pair of ventromandibular scale rows (VSRs), VSR status by body size being summarized in Table 5. In *L. japonicus*, although VSRs were entirely absent in specimens ≤ 100 mm SL, a few ca. 150 mm SL had vestigial VSRs. Subsequently, the proportion of specimens with VSRs gradually increased with growth, those lacking anterior and posterior VSRs comprising 25.0% and 0%, respectively, of the largest size class (> 400 mm SL). VSRs were entirely absent in *L. maculatus* specimens < 200 mm SL, appearing in a few just over 200 mm SL. Subsequently, the proportion of specimens with VSRs gradually increased with growth, those without anterior and posterior VSRs comprising 36.4% and 0%, respectively, of the largest size class (> 400 mm SL). Although VSRs were absent in most *L. latus* specimens ≤ 100 mm SL, a few over 90 mm SL had incipient or established VSRs. Subsequently, the proportion of specimens with VSRs rapidly increased with growth, including most up to 300 mm SL and all > 300 mm SL. Notably, 100–200 mm SL specimens with VSRs showed greater development of the

Table 5. Frequencies (%) of ventromandibular scale row status in three Lateolabrax species.

SL range (mm)	Anterior part			Posterior part		
	Present	Vestigial	Absent	Present	Vestigial	Absent
Lateolabrax japonicus						
≤100	0.0	0.0	100.0	0.0	0.0	100.0
100–200	0.0	14.3	85.7	10.7	21.4	67.9
200–300	5.0	25.0	70.0	35.0	30.0	35.0
300–400	5.3	26.3	68.4	31.6	57.9	10.5
>400	25.0	50.0	25.0	37.5	62.5	0.0
Lateolabrax maculatus						
≤100	0.0	0.0	100.0	0.0	0.0	100.0
100–200	0.0	0.0	100.0	0.0	0.0	100.0
200–300	0.0	18.2	81.8	22.7	54.5	22.7
300–400	5.6	55.6	38.9	55.6	27.8	16.7
>400	12.1	51.5	36.4	84.8	15.2	0.0
Lateolabrax latus						
≤100	0.0	13.3	86.7	6.7	13.3	80.0
100–200	70.5	18.0	11.5	49.2	19.7	31.1
200–300	95.1	4.9	0.0	97.6	2.4	0.0
300–400	100.0	0.0	0.0	100.0	0.0	0.0
>400	100.0	0.0	0.0	100.0	0.0	0.0

anterior portion, contrary to the developmental pattern displayed by the other two species. The prominence of VSR appearance was ranked: 1 *L. latus*, 2 *L. japonicus*, 3 *L. maculatus*.

Morphology of first anal pterygiophore

All three *Lateolabrax* species had a well-developed first anal pterygiophore (FAP), which comprised a short thin plate-like anterior part and a long thick spiny posterior part (Fig. 13). In *L. japonicus*, although the FAPs were straight in small specimens (< ca. 90 mm SL) (Fig. 13A), they became modestly arched in larger specimens (Fig. 13B–D), suggesting a growth-related morphological change. In contrast, the FAPs in *L. maculatus* remained straight (morphologically stable) regardless of body size (Fig. 13E–H). In *L. latus*, on the other hand, although the FAPs were straight in some specimens (Fig. 13I, K), they were slightly arched distally in others (Fig. 13J, L), thus showing neither growth-related morphological change nor morphological stability. As such, relationships between body size and FAP morphology were specifically unique.

Statistical differences

Analyses of covariance (ANCOVA) for regressions of logarithm-transformed length-measured characters by pairwise comparisons for the three *Lateolabrax* species indi-

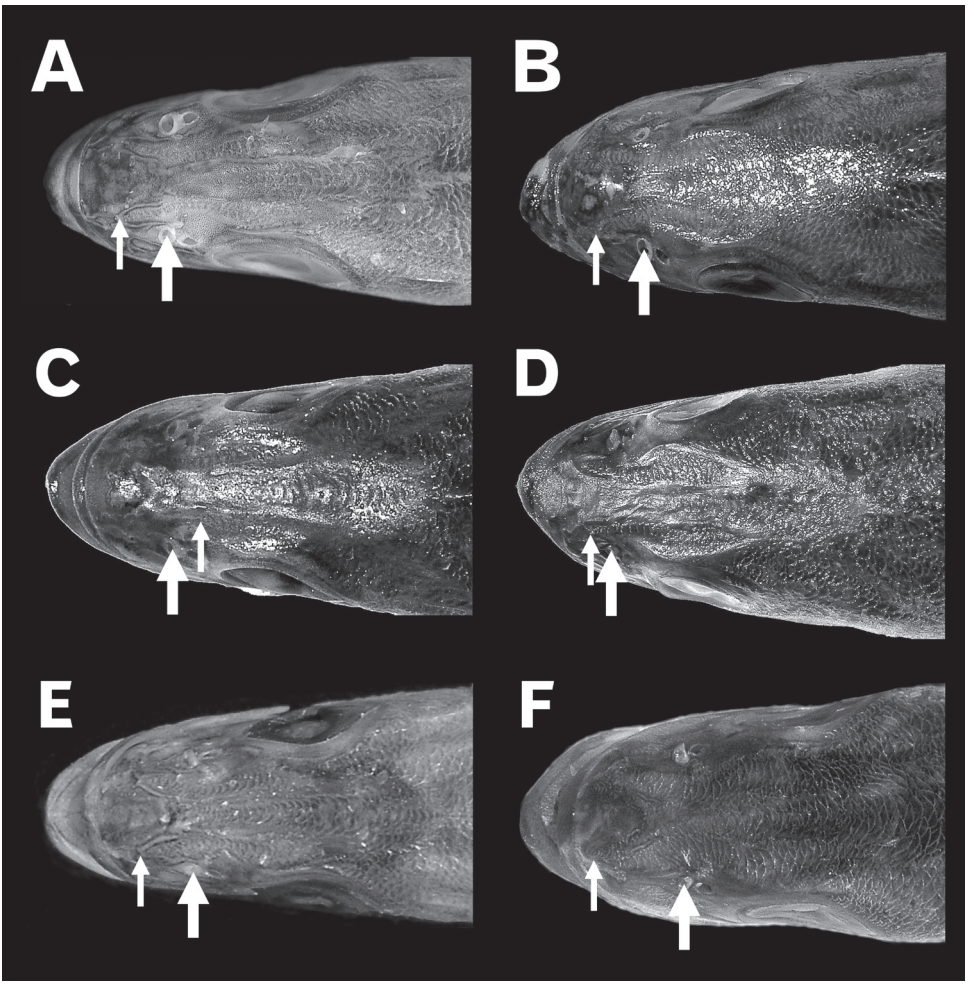

Figure 12. Squamation on dorsal head regions of *Lateolabrax japonicus* (**A, B**), *L. maculatus* (**C, D**) and *L. latus* (**E, F**). Thick arrows indicate anterior nostrils, thin arrows indicate anterior edges of dorsocephalic scale rows. **A** KAUM–I. 93435 (137.0 mm SL) **B** BSKU 100803 (265.2 mm SL) **C** uncatalogued specimen (104.9 mm SL) **D** BSKU 100773 (254.2 mm SL) **E** KAUM–I. 39058 (114.2 mm SL) **F** KPM-NI 24255 (240.1 mm SL).

cated significant differences in the slopes or intercepts of all such characters (Table 6). In general, significance (*t* values) between *L. japonicus* and *L. latus*, and *L. maculatus* and *L. latus* were greater than those between *L. japonicus* and *L. maculatus*, suggesting that *L. latus* exhibited greater morphological differences from the other two species (Table 6). High significance levels between the species were apparent for the SNL–POPW relationship (*t* values for intercepts ca. 28–44), in which the scatter plots were almost entirely separated from one another (Fig. 8). The next highest significance levels between the species were for vertical body dimensions (BD, CPD and CPAD), which

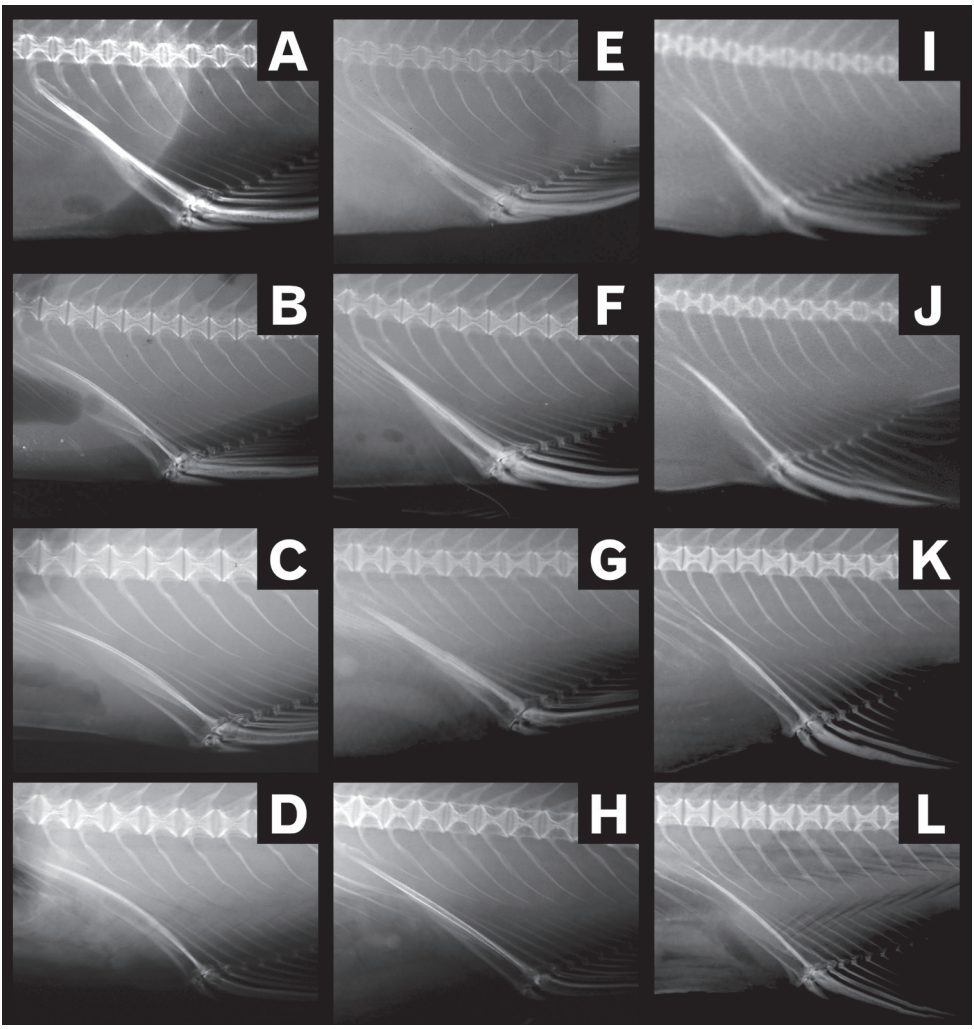

Figure 13. Radiographs of first anal pterygiophores in *Lateolabrax japonicus* (**A–D**), *L. maculatus* (**E–H**) and *L. latus* (**I–L**), according to body size by species. **A** KAUM–I. 82683 (65.6 mm SL) **B** BSKU 100883 (96.8 mm SL) **C** BSKU 100756 (252.4 mm SL) **D** KPM-NI 9697 (317.0 mm SL) **E** uncatalogued specimen (58.4 mm SL) **F** TKPM-P 1655-6 (95.2 mm SL) **G** BSKU 100771 (250.8 mm SL) **H** KPM-NI 9686 (364.0 mm SL) **I** KAUM–I. 1895-4 (70.3 mm SL) **J** KAUM–I. 64737 (SL 94.2 mm) **K** KPM-NI 24650 (265.4 mm SL) **L** KAUM–I. 57963 (342.0 mm SL).

also exhibited considerable plot separation from one another (Fig. 5) (*t* values of ca. 10 for slopes between *L. japonicus* and *L. maculatus* and between *L. japonicus* and *L. latus* and ca. 27–37 for intercepts between *L. maculatus* and *L. latus*) (Table 6).

Although the Mann-Whitney *U* tests for pairwise comparisons of meristic characters of the three species found significant differences in many, significance was not apparent for others, including counts of vertical fin rays [dorsal fin spines (DFSs), DFRs and AFRs] between *L. japonicus* and *L. maculatus*, and vertebrae [abdominal vertebrae (AVe), CVe and TVe] between *L. japonicus* and *L. latus* (Table 7).

Table 6. Results of analysis of covariance (ANCOVA) (*t* test) to compare regression parameters of logarithm-transformed length-measured characters between three *Lateolabrax* species.

Regression	*L. japonicus* × *L. maculatus*		*L. japonicus* × *L. latus*		*L. maculatus* × *L. latus*	
	Slope	Intercept	Slope	Intercept	Slope	Intercept
ln SL–ln PAL	7.00***	–	1.03	6.61***	7.08***	–
ln SL–ln BD	9.03***	–	8.16***	–	0.91	26.57***
ln SL–ln BWT	2.34	6.92***	0.22	2.58*	2.22	9.23***
ln SL–ln CPD	9.51***	–	10.97***	–	3.26	26.59***
ln SL–ln CPL	2.81	2.97*	0.29	9.35***	2.69	11.00***
ln SL–ln CPAD	9.41***	–	10.18***	–	2.91	36.84***
ln SL–ln PDL	2.22	11.60***	0.25	10.07***	1.83	21.83***
ln SL–ln FDFL	5.75***	–	0.30	5.13***	5.99***	–
ln SL–ln SDFL	8.52***	–	6.02***	–	1.23	18.51***
ln SL–ln CFL	6.05***	–	3.45*	–	1.86	16.84***
ln SL–ln CFND	3.99**	–	3.49*	–	7.37***	–
ln SL–ln AFL	6.28***	–	2.88	12.25***	2.25	11.23***
ln SL–ln P_1FL	6.17***	–	4.24**	–	1.26	12.21***
ln SL–ln P_2FL	3.07	9.89***	5.18***	–	2.96	16.28***
ln SL–ln HL	3.45*	–	1.82	5.42***	5.30***	–
ln SL–ln SNL	9.97***	–	3.68*	–	5.53***	–
ln SL–ln OD	5.26***	–	4.66***	–	0.26	28.99***
ln SL–ln IOW	4.29**		0.73	10.95***	4.27**	–
ln SL–ln SOW	2.64	7.96***	0.08	5.20***	2.15	12.35***
ln SL–ln POPW	10.37***	–	3.61*	–	4.15**	–
ln SL–ln POL	5.43***	–	3.90**	–	10.54***	–
ln SL–ln UJL	3.42*	–	1.44	25.97***	1.55	26.46***
ln SL–ln LJL	4.05**	–	0.79	22.93***	3.76*	–
ln SNL–ln POPW	0.48	33.61***	0.76	27.56***	0.18	44.42***
ln HL–ln SNL	11.07***	–	1.82	23.86***	7.76***	–
ln HL–ln OD	4.84***	–	5.29***	–	1.02	28.82***
ln HL–ln IOW	5.47***	–	1.52	7.78***	5.92***	–
ln HL–ln SOW	1.95	9.36***	0.46	6.42***	1.14	15.08***
ln HL–ln POPW	12.17***	–	2.40	2.74*	6.34***	–
ln HL–ln POL	4.04**	–	4.15**	–	7.64***	–
ln HL–ln UJL	6.89***	–	0.38	22.63***	6.19***	–
ln HL–ln LJL	7.92***	–	2.84	3.37**	9.71***	–

Numbers indicate t values given by ANCOVA. Asterisks indicate significance of t vales; single, double and triple asterisks indicate 5%, 1% and 0.1% levels, respectively, after Holm-Bonferroni correction. Bars indicate that calculation was not demonstrated because significance was recognized for the slope and ANCOVA was therein terminated.

Table 7. Results of the Mann-Whitney *U* test (*z* values) to compare meristic counts between three *Lateolabrax* species.

Character	*L. japonicus* × *L. maculatus*	*L. japonicus* × *L. latus*	*L. maculatus* × *L. latus*
DFS counts	0.37	3.00*	3.64**
DFR counts	0.12	16.22***	15.60***
AFS counts	0.00	1.29	0.64
AFR counts	1.39	14.64***	14.11***
P_1FR counts	5.69***	10.62***	5.77***
LLS counts	11.53***	13.74***	0.89
SAL counts	2.04	11.50***	11.47***
SBL counts	3.57**	14.43***	13.88***
UGR counts	14.31***	14.58***	0.65
LGR counts	15.45***	8.83***	11.76***
TGR counts	16.54***	15.13***	7.81***
AV counts	4.23***	0.64	4.15***
CV counts	13.58***	0.01	13.45***
TV counts	14.82***	0.73	14.09***

Asterisks indicate significance of z vales; single, double and triple asterisks indicate 5%, 1% and 0.1% levels, respectively, after Holm-Bonferroni correction.

Table 8. Standard errors for morphological character regressions of three *Lateolabrax* species.

Regression	*L. japonicus*	*L. maculatus*	*L. latus*
ln SL–ln PAL	0.024	0.029	0.015
ln SL–ln BD	0.057	0.050	0.043
ln SL–ln BWT	0.080	0.064	0.077
ln SL–ln CPD	0.051	0.046	0.036
ln SL–ln CPL	0.055	0.060	0.044
ln SL–ln CPAD	0.055	0.044	0.031
ln SL–ln PDL	0.033	0.033	0.020
ln SL–ln FDFL	0.103	0.084	0.068
ln SL–ln SDFL	0.094	0.096	0.084
ln SL–ln CFL	0.085	0.095	0.068
ln SL–ln CFND	0.273	0.299	0.119
ln SL–ln AFL	0.079	0.079	0.074
ln SL–ln P_1FL	0.056	0.063	0.045
ln SL–ln P_2FL	0.058	0.053	0.054
ln SL–ln HL	0.034	0.031	0.022
ln SL–ln SNL	0.044	0.067	0.027
ln SL–ln OD	0.074	0.087	0.053
ln SL–ln IOW	0.066	0.059	0.065
ln SL–ln SOW	0.160	0.155	0.140
ln SL–ln POPW	0.050	0.058	0.060
ln SL–ln POL	0.057	0.044	0.035
ln SL–ln UJL	0.035	0.046	0.029
ln SL–ln LJL	0.034	0.046	0.033
ln SNL–ln POPW	0.052	0.097	0.068
SL–DFS counts	0.515	0.424	0.299
SL–DFR counts	0.649	0.607	0.420
SL–AFS counts	0.000	0.109	0.086
SL–AFR counts	0.626	0.629	0.581
SL–P_1FR counts	0.624	0.589	0.432
SL–LLS counts	3.828	3.725	1.623
SL–SAL counts	1.117	0.614	0.837
SL–SBL counts	1.394	1.516	1.009
SL–UGR counts	1.020	1.131	0.659
SL–LGR counts	1.073	0.804	0.644
SL–TGR counts	1.366	1.507	0.963
SL–AV counts	0.155	0.279	0.191
SL–CV counts	0.420	0.370	0.336
SL–TV counts	0.426	0.414	0.333

Standard errors (SEs) for regression lines between logarithm-transformed SL and length-measured characters, and between SL and meristic characters are summarized in Table 8. For many characters, *L. latus* had the lowest SE values among the three species, followed by *L. japonicus* (Table 8). In general, degrees of SE could be ranked: 1 *L. maculatus*, 2 *L. japonicus*, 3 *L. latus*.

Discussion

Growth-related morphological changes

The present study revealed that most body proportions of the three *Lateolabrax* species change with growth (Table 3). Although such proportional changes with growth have been reported for a number of fishes, including two black-and-white snappers of the genus *Macolor* (Kishimoto et al. 1987), Spanish mackerel, *Scomberomorus niphonius* (Yokogawa 1996), giraffe catfish, *Auchenoglanis occidentalis* (Chioma et al. 2007), red porgy, *Pagrus pagrus* (Minos et al. 2008), bluegill, *Lepomis macrochirus* (Yokogawa 2013a; Bell and Jacquemin 2017), largemouth bass, *Micropterus salmoides* (Yokogawa 2014), two flatfishes of the genus *Pleuronichthys* (Yokogawa 2015), and some sea banjofishes of the genus *Banjos* (Matsunuma and Motomura 2017), such have been frequently neglected, particularly in taxonomic studies.

On the other hand, taxonomic and related literature on *Lateolabrax* have commonly noted the diagnostic importance of ranges and / or averages of body proportions (e.g., Katayama 1960a, b; Yokogawa and Seki 1995; Kim and Jun 1997; Yamada et al. 2007; Murase et al. 2012), although such, being commonly subject to allometric growth, are largely biased by the body sizes of specimens examined. For example, Figure 14 summarizes proportional body depth (BD) and orbital diameter (OD) ranges previously reported for *L. japonicus* and *L. maculatus*, respectively, compared with the present study. The smaller proportional ranges previously reported were all less than those presented here, representing many variously-sized specimens, suggesting that the former were based on relatively few specimens. Also, the variations in published proportional ranges, in some cases showing no range overlap (e.g., Fig. 14J vs K; L vs M), suggested differing body size ranges of the material studied. Although such proportional data has often been included in taxonomic diagnoses, the inherent inconsistencies have made specimen comparisons and specific identifications problematic. In fact, the use of proportions subject to isometric growth in species diagnoses is a legitimate procedure, although such proportions are rare in both *Lateolabrax* species (Table 3) and the other species listed above. However, the use of non-isometric proportional data, traditionally under the premise of (presumed) isometric growth, in species diagnoses is inappropriate.

Differing growth-related proportional change patterns in the three *Lateolabrax* species include pre-anus length (PAL) (Fig. 4A–C, Table 3) and post-orbital preopercular width (POPW) (Fig. 6K, Table 3). Similarly, the very similar East Asian frog flounders *Pleuronichthys lighti* and *P. cornutus* have the caudal fin, and dorsal and anal fins shortened with growth in the former and latter, respectively (Yokogawa 2015), indicating the potential for differing specific patterns, even between closely related species. Comparisons of black bass congeners (genus *Micropterus*) have shown the upper jaw length proportion to increase with growth in *M. salmoides* (Yokogawa 2014), while remaining stable in *M. dolomieu* (Senou 2002). Although the three *Lateolabrax* species share a similar "bass shape" with *M. salmoides*, the upper and lower jaw length (UJL and LJL) / standard length (SL) proportions decreased with growth in the former (Fig. 6M, O,

Table 3), unlike the latter (Yokogawa 2014). Also, it is notable that BD and head length (HL) proportions of the three *Lateolabrax* species decreased with growth (Fig. 5A, Table 3), in contrast to the centrarchids *M. salmoides* and *L. macrochirus* (Yokogawa 2013a), in which BD and HL increased with growth (Yokogawa 2014). This suggests that some phylogenetic factors may be responsible for growth-related proportional change patterns.

As in many other fishes (Okiyama 1988), BD of *L. japonicus* increased relatively with growth during the larval stage (from 13–16 to 26–30% of SL) until ca. 25 mm SL, thereafter being "stable," according to Tanaka and Matsumiya (1982) and Tamura et al. (2013), although subsequently decreasing from ca. 30 to ca. 21% of SL (Fig. 5A). Similarly, HL of *L. japonicus* and *L. latus* increased relatively with growth during the larval stage (Kinoshita 1988), in contrast to the growth-related acute decrement of HL during the juvenile and adult stages (Fig. 4S, U). During the larval stage of *L. japonicus* and *L. latus* (11–19 mm SL), the greater HL / SL proportion of the latter compared with the former in same-sized larvae, enabled ready distinction of the two species from each other (Kinoshita 1988). Although a similar distinction was observed in juvenile fishes (ca. 40–100 mm SL), very similar growth-related HL decreasing patterns between the two species in the adult stage (Fig. 4S, U) made it clear that Kinoshita's (1988) criterion for separation was applicable only for larvae of the two species.

Growth-related proportional change patterns of length-measured cephalic characters (based on SL and HL) were sometimes inconsistent in *L. japonicus* and *L. latus* (Fig. 6, Table 3), possibly due to HL being negatively allometric with SL (decreasing with growth) (Fig. 4S, U, Table 3) and paralleling or exceeding the change rate of some cephalic characters, resulting in negative allometry and isometry in SL-based relationships appearing as isometry and positive allometry in the HL-based ones, respectively. However, OD was negatively allometric relative to both SL and HL (Fig. 6C, D, Table 3), due to their degree of allometry relative to SL exceeding that of HL to SL. On the other hand, the consistency of the growth patterns between the two-way relationships in *L. maculatus* (Fig. 6A–P, Table 3) may be due to the growth-related decreasing rate of proportional HL being less apparent in this species (Fig. 4T) than in the others (Fig. 4S, U) and therefore less influential on the relative growth of the cephalic characters. Although HL-based proportions of cephalic characters have been frequently used for cephalic characters in taxonomic studies on *Lateolabrax* (e.g., literature cited in Fig. 14), it should be recognized that the base dimension (HL) is not a stable character.

The proportional values (percentages) of proportions subject to allometric growth are correlated with the base dimension (e.g., SL and HL). In Figure 14, because both BD and OD were negatively allometric in both *L. japonicus* and *L. maculatus* (Figs 5A, 6D, Table 3), high and low proportional values are regarded as representing small and large size specimens, respectively. McClelland (1844) noted in the original description of *L. maculatus* (as *Holocentrum maculatum*) that the eyes were large, indicating that his description was based on a small specimen(s). The OD / SL proportion taken from his specimen illustration (pl. 21, fig. 1) was 6.4%, whereas the SL calculated by the inverse function of the SL–OD / SL regression (Fig. 6C, Table 2) was ca. 184 mm, agreeing with the above suggestion. This suggests that length-measured characters (including OD) subject to allometric growth can be utilized for estimation of body size.

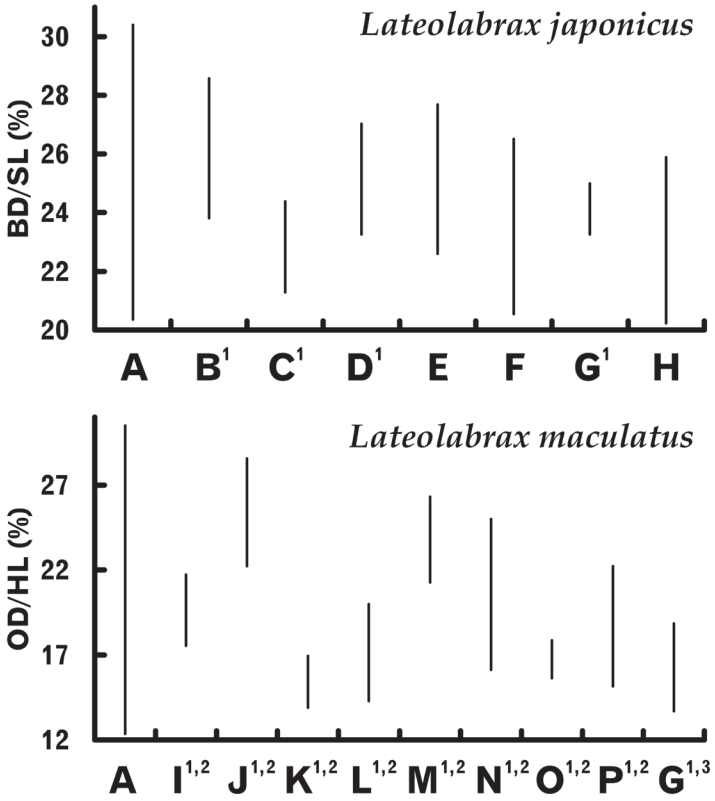

Figure 14. Proportional range comparisons of head length [HL, % of standard length (SL)] in *Lateolabrax japonicus* (upper graph, axis labelled BD / SL) and orbital diameter (OD, % of HL) in *L. maculatus* (lower graph, axis labelled OD / HL) in the present study and previous literature. Data based on **A** present study **B** Katayama (1960a) **C** Lindberg and Krasyukova (1969) **D** Chyung (1977) **E** Yokogawa (1995) **F** Nozaka (1995) **G** Yamada et al. (2007) **H** Bae et al. (2016) **I** Chu et al. (1962) **J** Chu (1985) **K** Chen (1987) **L** Zheng (1987) **M** Chen et al. (1990) **N** Mao et al. (1991) **O** Gao (1991) **P** Cheng and Zhou (1997). [1] Proportional percentages were calculated as reciprocal numbers from proportional data (multiple numbers) therein given. [2] Despite descriptions as "*L. japonicus*," synonymized as *L. maculatus* by Yokogawa (2013b). [3] Provisionally referred to as *Lateolabrax* sp., which was identical with *L. maculatus*.

Hirota et al. (1999) compared their morphometric data for *L. maculatus* (as *Lateolabrax* sp.) from Kanto region, Japan [*n* = 6, 151–451 (average 298.3) mm SL] with those examined by Yokogawa and Seki (1995) [*n* = 62, 76.3–121.8 (average 97.6) mm SL], recording lower OD proportions (% of HL) for their specimens [18.5–25.3 (average 20.8) vs 21.3–30.5 (average 24.8)] (Hirota et al. 1999, table 1). Such inconsistency was clearly due to body size differences of the specimens examined in the two studies, i.e., the larger specimens in the former study provided lower OD proportions (Fig. 6D). Nevertheless, Hirota et al. (1999) suggested that the different OD proportions resulted from Yokogawa and Seki (1995) having measured eye diameter rather than OD, which was incorrect. Kim and Jun (1997) examined the morphology of Korean

L. japonicus specimens from Kohung [*n* = 69, 77.4–353.0 (average 175.0) mm SL] and Puan [*n* = 6, 465.0–640.0 (average 582.0) mm SL], giving similar average proportional values (% of SL) for BD (25.8 and 24.3), caudal peduncle depth (CPD) (31.6 and 32.1), HL (31.4 and 31.8) and OD (19.7 and 19.8) for the respective lots (Kim and Jun 1997, table 1). However, those degrees of proportional similarity between such different-sized specimens is extremely unlikely due to the highly negatively allometric proportions of those characters in this species (Figs 5A, B, 4S, 6C, Table 3).

Because most of the length-measured characters of the three *Lateolabrax* species were subject to allometric growth (Table 3), raw dimension measurement data were logarithm-transformed in order to transform the data distribution to be symmetric for statistical analysis, including canonical discriminant analysis (Bae et al. 2016) and analysis of covariance (ANCOVA), performed in the present study. Although Wang et al. (2016) provided multiple-regression analyses between body weight (BW) and some body dimensions for *L. maculatus* using raw data, the approach was problematic, because the raw dimension data (including BW) needed to have been logarithm-transformed before analysis, as done for *M. salmoides* by Yokogawa (2014).

Counts of pored scales on the lateral line (LLSs) and scales above the lateral line (SALs) tended to increase and decrease with growth, respectively, in *L. japonicus* (Fig. 9A, D, Table 4), those of scales below the lateral line (SBLs) and lower-limb and total gill rakers (LGRs and TGRs) tending to increase with growth in *L. maculatus* (Fig. 9H, K, N, Table 4). By contrast, overall meristic counts (except dots) did not change with growth in *L. latus* (Table 4), implying some phylogenetic determination of growth-related meristic characters, as in the case of PSAL change patterns. Although the mechanism by which such counts increase or decrease with growth is uncertain, an SBL count increase with growth has been reported for *L. macrochirus* (Yokogawa 2013a), *M. salmoides* (Yokogawa 2014) and *P. cornutus*, in which gill raker numbers also increased with growth (Yokogawa 2015), suggesting that such phenomena are not so rare in fishes. Although meristic characters have been frequently used as important keys in taxonomic studies on the premise that they are stable at any body size, the potential for growth-related changes should be considered and actively assessed in taxonomic studies.

Nozaka (1995) examined the morphology of *L. japonicus* fingerlings from the eastern Seto Inland Sea (*n* = 112, average 141.1 mm SL), comparing his data with Yokogawa and Seki (1995) [*n* = 65, 122.8–417.0 (average 301.4) mm SL] and noting differences in LLS and gill raker numbers (average LLSs = 76.4 and 83.1, average TGRs = 24.9 and 27.2, in the former and latter, respectively). Inconsistency in LLS counts may have resulted from body size differences in specimens examined, larger specimens resulting in higher LLS counts (Fig. 9A, Table 4). On the other hand, the difference in gill raker counts, which do not change with growth in *L. japonicus* (Fig. 9J, M, Table 4), may have resulted from the non-inclusion of rudiments located on the gill arch edges, since low gill raker counts as reported by Nozaka (1995) have not been found in the many other *L. japonicus* samples examined from around Japan (Yokogawa, unpublished data).

The growth-related status of dots / spots on the lateral body region also varied among the three *Lateolabrax* species. In *L. japonicus* and *L. latus*, although dots appeared in some smaller specimens (up to 260.6 and 254.8 mm SL, respectively), they disappeared with growth (Fig. 11A, C), a well-known phenomenon in the former species (e.g., Katayama 1960a, 1960b; Yokogawa 1995; Kim and Jun 1997; Kim et al. 2004; Ishikawa and Senou 2010), but barely noted in taxonomic descriptions of the latter species, other than Katayama (1957, 1960a) and Murase et al. (2012). This may have been due to such dots being so fine or faint (Fig. 2C) that they were overlooked, or because descriptions were based only on large specimens. However, spot counts were not related to body size in *L. maculatus*, which typically had many clear spots in both large and small specimens (Fig. 2B, Table 4). Although many taxonomic descriptions of this species have incorrectly noted that spot counts decreased gradually with growth (Tchang et al. 1955; Chu et al. 1962, 1963; Chu 1985; Chen 1987; Chen et al. 1990; Li and Zhang 1991; Feng and Jiang 1998; Chen and Fang 1999; Wang et al. 2001; Zhao and Zhong 2006), such may have been based only on subjective observations without statistical analysis, unlike the present study. On the other hand, large individuals of this species tend to have smaller and more rounded (non-jagged) spots than in small individuals [e.g., Katayama 1984, plate 108-I, 52 cm, as a variation of *L. japonicus*; Yokogawa et al. 1996, fig. 1, 600 mm in total length (TL), as *L.* sp.], which may have provided some grounds for the above views. Descriptions of *L. maculatus* (as *L. japonicus*) from Hong Kong noted that in young specimens, spots were larger and fewer in number, whereas with advancing fish age the large spots become smaller and more numerous (Chan and Tang 1968; Sadovy and Cornish 2000). However, although growth-related spot size decrement is correct, growth-related spot number increment is not.

The proportional growth-related change pattern of pectoral scaly area length (PSAL) in *L. latus* closely fitted a power regression (Fig. 4X, Table 2). However, simple patterned regressions could not be applied to *L. japonicus* and *L. maculatus* since they exhibited inverted V-shaped changes (Fig. 4V, W). This may reflect the phylogenetic status of the three species, *L. latus* being genetically further from the other two species (Yokogawa 1998; Song et al. 2008; Shan et al. 2016). A similar growth-related change pattern was also observed for the maximum blotch diameter on the dorsal fin (% of SL) in *Banjos banjos banjos* (Matsunuma and Motomura 2017, fig. 8d), inferring that such non-linear patterns arise in some characters in which dimensions are not determined by internal bony structure, rather than in normal body portions. Although PSAL, as defined by Yokogawa and Seki (1995) (see above), was examined in *L. japonicus* and *L. maculatus*, overall growth-related change patterns were limitedly revealed for both at that time due to size-biased samples. Accordingly, Nozaka's (1995) examination of *L. japonicus* fingerlings (see above) resulted in a much smaller proportional PSAL range and average than those given by Yokogawa and Seki (1995) for larger examples of that species. Such disagreement was regarded as arising from body size differences in the material specimens between the two studies.

Inter-specific differences and taxonomy

Lateolabrax latus is typically characterized by a deeper body, represented by BD and CPD. However, neither character provides unequivocal identification due to the range overlap for proportional BD and CPD between *L. latus* and *L. japonicus* (Katayama 1957, 1965). In the present study, although the scatter plots for proportional BD and CPD of *L. latus* were well separated from those of the other two species, some overlap occurred in the smaller size class (< ca. 200 mm SL) (Fig. 5A, B). However, the newly defined dimension caudal peduncle anterior depth (CPAD), located between BD and CPD (Fig. 3), is suitable for distinguishing *L. latus* from the other two species, there being no plot overlap with the latter (border level 15%) (Fig. 5C).

The CPAD proportion may be a useful feature for specific identification, since it can also be determined from illustrations and photographs of *Lateolabrax* species. For instance, an illustration of "*L. japonicus* (as *Perca-labrax japonicus*)" in Fauna Japonica (Temminck and Schlegel 1846, pl. II, fig. 1, drawn by Keiga Kawahara) may, in fact, be *L. latus*, because the proportional CPAD (% of SL) measured from the illustration was 15.4%, falling within the range of the latter (Fig. 5C). Because the SL of the illustrated specimen estimated by the earlier-described procedure (use of an inverse function of SL–OD / SL regression for *L. latus*) was ca. 336 mm, proportional BD and CPD (% of SL), which had no plot overlap with the larger size classes (>200 mm SL) of the other two *Lateolabrax* species, may also be used for specific identification. The proportional BD and CPD of the illustrated specimen were 29.3 and 12.1%, respectively, corresponding with the ranges of *L. latus* (Fig. 5A, B). Although Katayama (1960b) also recognized the greater BD and CPD proportions of Temminck and Schlegel's (1846) specimen, he identified it as *L. japonicus* because the dorsal and anal fin ray counts (xiv, 13 and iii, 8, respectively) corresponded to the ranges for *L. japonicus*. In fact, he may have counted 12 spines in the first dorsal fin, and 2 spines plus 13 rays in the second (SDF). However, the SDF should be regarded as comprising 1 spine and 14 rays, the ray next to the first SDF spine having a distal branch. Specimens examined in the present study included 6 *L. latus* with 14 dorsal fin rays (DFRs) and 8 anal fin rays (AFRs), supporting the opinion that Temminck and Schlegel's (1846) illustration was of *L. latus*. Similarly, illustrations of *L. japonicus* and *L. latus* in Katayama (1965, figs 520 and 521) should actually be reversed, since their proportional CPAD (% of SL) values were 15.1 and 13.5%, respectively, falling within the respective ranges of *L. latus* and *L. japonicus*.

In addition to caudal peduncle stoutness in *L. latus*, Hatooka (2000, 2013) proposed peduncle shortness as a diagnostic character of the species. Similarly, Murase et al. (2012) recorded proportions of caudal peduncle length (CPL) (% of SL) for *L. latus* (*n* = 27, 18.7–20.9), *L. japonicus* (*n* = 25, 20.0–23.4), and *L. maculatus* (*n* = 7, 20.7–22.3), indicating a clear difference between *L. latus* and the other two species. However, despite the distinctly downward shift in plot distribution in *L. latus* from the other two species found here, the CPL proportion range (*n* = 136, 18.3–22.7) largely overlapped those of *L. japonicus* (*n* = 229, 18.5–24.6) and *L. maculatus* (*n* = 170, 18.6–

25.3), owing to considerable variation in plot distribution in the latter two species (Fig. 4G–I). The disagreement between the above two studies and the present one is likely to have resulted from differing numbers of specimens examined. In conclusion, although the proportional CPL of *L. latus* tended to be lower than in the other species, adoption of the feature as a diagnostic key for *L. latus* is problematic.

Caudal fin notch depth (CFND) has been recently proposed as a new character for distinguishing *L. latus* from the other two species, the former having a shallower CFND than the others (Hatooka 2000, 2013). However, although growth-related patterns of proportional CFND (% of SL) differed from one another among the three species (Fig. 4J–L) and ANCOVA for the logarithm-transformed regressions indicated significant differences of the slopes between any two species (Table 6), the ranges relative to overall SL (2.9–7.9, 2.0–8.4 and 1.9–7.4% for *L. latus*, *L. japonicus* and *L. maculatus*, respectively) were similar (Fig. 4J–L) and unable to distinguish between species. In fact, the proportional CFND of *L. latus* decreased acutely with growth, with relatively little variation owing to high correlation with SL (Fig. 4L, Table 3), being almost stable at low values (around 4–5%) in specimens > ca. 200 mm SL (Fig. 4L). In contrast, the other two species had highly variable proportional CFND, up to ca. 8% at any body size (Fig. 4J, K). Therefore, individual specimens of *L. japonicus* and *L. maculatus* with greater CFND may give the impression that *L. latus* has a shallower CFND than the others, as emphasized by some photographs of *L. latus* in which the caudal fins are so well opened that CFND decreases considerably (nearly truncate) (e.g., Masuda et al. 1975, pl. 42E; Ishikawa and Senou 2010; Murase et al. 2012, fig. 2C). It is possible that the caudal fin of *L. latus* may spread more than that of the other two species owing to broader membrane between the fin rays (Fig. 1E, F), particularly when fresh (when specimens were photographed). Notwithstanding, the results herein clearly indicate that CFND is problematic as a key character. Although Shimose et al. (2011) made underwater observations of and photographed a single *Lateolabrax* fish at Ishigaki Island, Okinawa, Japan, suggesting it to likely be *L. latus* based on some visually-recognized features, including CFND, the influence of such a key in the popular media is unfortunate.

Among the length-measured cephalic characters of *L. latus*, plot separation of that species from the others was marked for snout length (SNL) (Fig. 6A, B), post-orbital length (POL) (Fig. 6K, L), and upper and lower jaw lengths (UJL and LJL) (Fig. 6M–P). In particular, SNL may be a practical means of distinguishing *L. latus* from the others because plots were vertically separated for both in the SL- and HL-based relationships (border levels ca. 9 and 28%, respectively) (Fig. 6A, B), which were similar to Murase et al.'s (2012) results. However, POL may not be practical for identification because the plots and vertical axis ranges overlapped considerably with those of *L. japonicus* (Fig. 6K, L). Although Murase et al. (2012) showed an unequivocal difference in POL (% of SL) between *L. latus* (n = 27, 14.1–15.8) and the other species [*L. japonicus* (n = 25, 16.1–18.5), *L. maculatus* (n = 7, 16.4–20.2)], such may have been due to the low numbers specimens examined, as in the case of CPL. The fact that SNL and POL of *L. latus* are greater and shorter, respectively, than in the other species infers that the eyes of *L. latus* are located more posteriorly than in the latter.

The UJL and LJL plots for all three species (SL-based relationships) were well clustered around their regression curves (high negative allometry), but could not be distinguished from one another vertically (Fig. 6M, O). On the other hand, since the UJL and LJL plots of *L. latus* in the HL-based relationships formed almost horizontal clusters, they could be vertically distinguished from those of the other two species (border levels of ca. 45 and 49%, respectively) (Fig. 6N, P). Despite Murase et al.'s (2012) proposal of some diagnostic characters for *L. latus* including greater SNL and shorter POL, they excluded UJL, despite having measured that dimension. Although Hirota et al.'s (1999) (see above) examination of *L. maculatus* recorded SNL and UJL proportions (% of HL) [23.2–30.0 (average 26.3) and 39.4–46.4 (average 42.5), respectively], the maximum values of both fell within the ranges peculiar to *L. latus* (Fig. 6B, N). Assuming correct calculations, their catalogued "*L. maculatus*" specimens (whereabouts unknown) may have included *L. latus*. This possibility is also suggested by their higher counts of DFRs [13–14 (average 13.3)] and AFRs [8–9 (average 8.2)], including a small proportion of specimens (n = 6) with minor counts in *L. maculatus* [14 DFRs (16.6%) and 9 AFRs (5.3%)] (Fig. 10B, D).

The original description of *L. latus* included several diagnostic meristic characters, including counts of DFRs, AFRs and SBLs (Katayama 1957). In particular, DFR numbers =15, considered peculiar to the species, have subsequently been noted as an important diagnostic key (Katayama 1960a, 1965, 1984; Masuda et al. 1975; Araga 1981; Hatooka 1993). However, because some *L. latus* specimens with 14 DFRs (overlapping the ranges of the other two *Lateolabrax* species) have been recognized (Sakai et al. 1998; Hatooka 2000, 2013; Murase et al. 2012), including 7.4% of *L. latus* specimens in the present study, DFR counts alone cannot absolutely distinguish *L. latus* from the others, although higher DFR counts may be useful (Fig. 10B). In contrast, AFR and SBL counts have rarely been adopted as diagnostic for *L. latus*, inferring that the count range overlaps between *L. latus* and the other two species are problematic for specific identification. In the present study, *L. latus* was well separated from the other species by AFRs (Fig. 10D) and DFRs, whereas SBL counts broadly overlapped (Fig. 10H). On the other hand, pectoral fin ray (P_1FR) counts, which have not been emphasized as having taxonomic significance for *L. latus*, showed a strong modal shift between *L. latus* and *L. japonicus* (16 and 17, respectively) (Fig. 10E). Although the large range overlap of P_1FR counts in *L. japonicus* and *L. maculatus* preclude their diagnostic use, they may be useful in the case of *L. latus*. For example, the two *Lateolabrax* specimens collected from Tanegashima Island both having 16 P_1FRs (Sakai et al. 1998) are likely referable to *L. latus*.

In addition to length-measured and meristic characters in the original description of *L. latus* a further diagnostic feature proposed was the possession of ventromandibular scale rows (VSRs) (Katayama 1957). Although frequently noted as diagnostic for *L. latus* until recent years (e.g., Katayama 1960a, 1965, 1984; Masuda et al. 1975; Araga 1981; Hatooka 1993), the possession of such scales has subsequently been omitted from keys to the genus *Lateolabrax* (Hatooka 2000, 2013) owing to the presence of VSRs in some specimens of *L. japonicus* and *L. maculatus* (Table 5) (Paxton and Hoese

1985; Hirota et al. 1999; Kang 2000; Murase et al. 2012). Furthermore, the lack of VSRs in some small *L. latus* (mainly ≤100 mm SL) (Table 5) underlines the unsuitability of this feature as a diagnostic character for *L. latus*. It was clear in the present study that VSRs did not exist in larvae and juveniles of all *Lateolabrax* species, but first appeared in *L. latus* at ca. 90 mm SL, thereafter rapidly developing with growth until present in almost all large individuals. In *L. japonicus* and *L. maculatus*, the appearance of VSRs was delayed, beginning from around 150 and 200 mm SL, respectively, and thereafter gradually developing with growth, although still absent in some large individuals. Such specific differences in squamation development may be common for PSAL (Fig. 4X) and dorsocephalic scale rows (DSRs) (Fig. 12), development being greatest in *L. latus* and least in *L. maculatus*, as indicated by Murase et al. (2012).

The diagnosis accompanying the original description of *L. latus* included ventral (pelvic fins) generally dusky, unlike in *L. japonicus* (Katayama 1957), followed by Katayama (1965) and Araga (1981). Although such coloring was infrequent in preserved *L. latus* specimens examined here, it has been noted in some large fresh adult specimens [e.g., photographs in Araga (1981) and Ishikawa and Senou (2010)]. However, non-dusky (pale) pelvic fins have been commonly observed in small *L. latus* (to fingerling size) (Fig. 1E, Murase et al. 2012, fig. 2A, B) and some large fresh condition specimens (Fig. 1F, Murase et al. 2012, fig. 2C). Possibly based on this supposed feature, the English name "blackfin sea bass" has been employed for *L. latus* (e.g., Matsuyama et al. 2002; Arakaki et al. 2014; FishBase 2018), however, such naming is not suitable, because it suggests that all fins were black, and many *L. latus* specimens including the large individual (915 mm TL) figured in FishBase (2018) do not have dusky ("black") pelvic fins. Instead, "flat sea bass," which describes the deeper body, a common feature of the species, should be applied for *L. latus*, following Yokogawa and Kishimoto (2012).

Recent keys for identification of *L. japonicus* and *L. maculatus* have adopted SNL, that of *L. maculatus* supposedly being relatively shorter than that of the former (Yamada et al. 2007; Hatooka 2000, 2013). However, plots of proportional SNL largely overlapped in smaller size classes (< ca. 200 mm SL) of the two species, although plots for *L. maculatus* shifted downward (highly negative allometry) and were clearly separated from those of *L. japonicus* in specimens > ca. 200 mm SL (border levels ca. 7.7% and 24% for SL- and HL-based relationships, respectively) (Fig. 6A, B). Accordingly, SNL proportions enable separation only of large specimens (> ca. 200 mm SL) of the two species; e.g., Wakabayashi and Nakamura's (2003) *L. maculatus* specimen (as *L.* sp.) from Shima Peninsula, Japan (381 mm SL) was identifiable by its SNL proportions (7.1 and 22.8% of SL and HL, respectively).

On the other hand, post-orbital preopercular width (POPW) is a notable dimension, showing a contrasting pattern to SNL, i.e., plots of proportional POPW in small (< 200 mm SL) *L. maculatus* shifted upward and separated completely from those of similar sized *L. japonicus* (border levels ca. 7.5% and 23% for SL- and HL-based relationships, respectively), although larger specimens (> 200 mm SL) of the two species had some overlap due to the relative decrease of POPW with growth

(highly negative allometry) in the former (Fig. 6I, J). Thus, a combination of SNL and POPW proportions [for small (< ca. 200 mm SL) and large (> ca. 200 mm SL) specimens, respectively] enables the two species to be separated unequivocally for their entire size range. Furthermore, the POPW / SNL proportion, which largely separates the two species throughout their entire size range (border level 90%) (Fig. 8), can also be adopted.

Proportional differences between *L. japonicus* and *L. maculatus* were also apparent in many of the fin lengths (first and second dorsal, caudal and pectoral), proportions of the former being distinctly greater than those of the latter in smaller specimens (< ca. 200 mm SL), although plots of the two species overlapped in the larger size class (> ca. 200 mm SL), due to the relative fin lengths decreasing and not changing with growth in the former and latter species, respectively (Fig. 5E–H). That this means of distinguishing between small specimens of *L. japonicus* and *L. maculatus* has largely gone unrecognized is probably due to a lack of morphological examination of small *Lateolabrax* specimens. The benchmark size of 200 mm SL being common to SNL, POPW and fin lengths of the two species suggests some synchronization of specific growth-related morphological changes.

Although Yokogawa and Seki (1995, figs 6, 7) proposed that considerable differences in LLS and gill raker numbers were sufficient for unequivocal differentiation of *L. japonicus* and *L. maculatus* when used in combination, the present study has demonstrated greater count range overlaps between the two species (70–84 LLSs and 24–26 TGRs, vs 76–82 LLSs and 24 TGRs) (Fig. 10F, K), due to LLS and gill raker counts increasing with growth in *L. japonicus* and *L. maculatus*, respectively (Fig. 9A, M, Table 4). Similarly, Kang's (2000) comparable frequency distributions of LLS and gill raker counts between the two species from Korean waters may have resulted from a size bias in specimens examined, his *L. maculatus* material including only very large specimens (ca. 500–750 mm SL). Accordingly, counts of LLSs and gill rakers, which can be biased by specimen size, are now likely to be unsuitable for distinguishing between the two species. In fact, Lou et al. (2002), who compared morphology between *L. japonicus* (1 sample lot from Tokyo, Japan) and *L. maculatus* (5 sample lots from Beihai, Xiamen, Fuzhou, Zhoushan and Weihai, China), showed considerable range overlaps for LLS and TGR counts, although the average values of those counts for *L. maculatus* were unequivocally lower than those for *L. japonicus*. Although Iseki et al. (2010) identified 263 *Lateolabrax* specimens from western Japan as *L. maculatus* (as *L.* sp.) based on LLS and gill raker counts proposed by Yokogawa and Seki (1995), some difficulties in identification may have been encountered due to some of their specimens being very large (up to 1130 mm SL), with gill raker counts that approached or overlapped the range for *L. japonicus*.

On the other hand, caudal and total vertebral counts (CV and TV, respectively), in which dominant counts were almost completely replaced between *L. japonicus* and *L. maculatus* (20 and 19 CVe, 36 and 35 TVe, for the former and latter, respectively) (Fig. 10M, N), may be useful for specific identification because they do not change with growth (Table 4). A modal count of 35 TVe in *L. maculatus* was indicated by

Lou et al. (2002) (see above), who recorded average TV counts for 5 sample lots from China, viz., 34.75 (Beihai, *n* = 40), 34.64 (Xiamen, *n* = 19), 34.90 (Fuzhou, *n* = 10), 34.98 (Zhoushan, *n* = 27) and 35.07 (Weihai, *n* = 50), in spite of a geographic cline that suggested a trend towards lower and higher TVe in sample lots from southern and northern regions, respectively. Notwithstanding, Chen et al. (2001) recorded an average TV count of 35.31 (*n* = 98) for a sample lot from Laizhou, China, inferring that approximately 30% of their specimens had 36 TVe, which largely contradicts the present results (Fig. 10N). However, the former average count is suspect, differing considerably from the sample lot from Weihai (Lou et al. 2002), located close to Laizhou. In fact, such a high average TV value has not been recorded elsewhere at any time for *L. maculatus* (Yokogawa and Seki 1995; Yokogawa et al. 1996; Lou et al. 2002). Although vertebral counts [abdominal (AV), CV and TV, respectively] of *L. japonicus* and *L. latus* are similar to each other, those of *L. maculatus* stand apart (Fig. 10L–N, Table 7), in contrast to their phylogenetic relationship (Yokogawa 1998; Song et al. 2008; Shan et al. 2016). In this case, since the difference in *L. maculatus* was primarily due to a difference in CV counts, which generally reflect inter-specific differences or lower, unlike AV counts which may reflect differences at a higher taxonomic level (Takahashi 1962), the vertebral count peculiarity in *L. maculatus* may not have phylogenetic significance.

Although *L. maculatus* typically possessed many black spots on the body, individual spot counts and patterns varied considerably (Yokogawa 2013b, fig. 2), a few specimens (4.9% of total) entirely lacking spots. In addition, the proportion of dotted *L. japonicus* specimens (35.6% of total) made visual separation of the two species difficult, the use of color pattern for specific identification being of value only as an accessory character. Youn's (2002) key, however, distinguished between the two species on the presence or absence of black spots, may causing mis-identification.

Yokogawa and Seki (1995) demonstrated differences between *L. maculatus* and *L. japonicus* in some newly-demonstrated characters, including PSAL and DSRs (scale development in these characters being poorer in *L. maculatus*). However, because their examined material was size-biased (see above), overall growth-related change patterns were still unclear. Examination of PSAL and DSR in the present study have overcome that problem. Although differences between the two species were apparent in specimens < ca. 150 mm SL, squamation developed thereafter with growth in *L. maculatus*, the two species consequently having similar degrees of squamation in large specimens (Figs 7, 12). Notwithstanding, specific differences in specimens < ca. 150 mm SL can be used to identify *Lateolabrax* individuals up to fingerling size. Growth-related squamation development has been examined in laboratory-reared larval and juvenile *L. japonicus* (Fukuhara and Fushimi 1982) and *L. maculatus* (Kang 2000). Although squamation initially occurred on the caudal peduncle at ca. 19 mm SL in both species, body squamation was completed earlier in the former (ca. 35 mm SL vs 47 mm SL) (Fukuhara and Fushimi 1982; Kang 2000), indicating delayed development in *L. maculatus*. The slower development in PSAL and DSRs in *L. maculatus* might be an extension of such squamation delay, which is a characteristic peculiar to that species.

A morphological difference in the first anal pterygiophore (FAP) between *L. japonicus* and *L. maculatus* was initially noted by Kang (2000) during his detailed osteological observations of the three *Lateolabrax* species, and included in one of his keys (for adults) to the genus *Lateolabrax*; FAPs were arched and straight in *L. japonicus* and *L. maculatus*, respectively (Kang 2000). However, FAPs of small *L. japonicus* specimens (< ca. 90 mm SL) were found here to be straight (Fig. 13A), a condition not found by Kang (2000) due to his examining only larger specimens (minimum size 185.5 mm TL). Although Kang (2000) also described FAP in *L. latus* as straight, some examples of that species examined here had the FAP slightly arched distally (Fig. 13J, L). Because Kang (2000) examined only three *L. latus* specimens, ontogenetic morphological variations were not considered at that time. However, despite the growth-related morphological changes now apparent in *L. japonicus*, morphological differentiation of FAP is stable in specimens of *L. japonicus* and *L. maculatus* > 90 mm SL (Fig. 13B–D, F–H), enabling separation of the two species. Yokogawa and Kishimoto's (2012) identification of a long-finned *Lateolabrax* specimen from Japan (SPMN-h 40001, 331 mm SL) as *L. japonicus* was based on its genetic characteristics, although morphological identification of the specimen was equivocal, the TV count of 35 being suggestive of *L. maculatus* (Fig. 10N). However, identification of the specimen as *L. japonicus* was settled by the FAP being arched (Yokogawa and Kishimoto 2012, fig. 2a).

Standard errors (SEs) for the length-measured and meristic character regressions, which indicated degrees of morphological variation, were generally lowest in *L. latus* (Table 8), suggesting less morphological variation in that species. This may be due to less genetic variation, average observed heterozygosity for 28 isozymic loci in *L. latus* being 0.033, much lower than that of *L. japonicus* (0.095) and *L. maculatus* (0.103) (Yokogawa 1998). Usually, lower genetic diversity occurs in a small or reduced population, but the *L. latus* specimens examined in the present study were from a broad area around southern Japan. Possibly, in spite of the species' broad distribution, *L. latus* resources may not be so abundant, since the species is much less popular than *L. japonicus* in Japanese commercial markets. In contrast, SEs were generally highest in *L. maculatus* (Table 8), inferring considerable morphological variation. The significant geographical differences in otolith morphology among some *L. maculatus* samples from China (Ye et al. 2007) may have also resulted from its genetic diversity. This is supported by *L. maculatus* being broadly distributed along the east Asian coast, with some local populations being so genetically divergent from one another as to form a genetic / geographic cline, unlike *L. japonicus*, which is genetically stable (Yokogawa 2004; Liu et al. 2006; Han et al. 2015). In this regard, Zhao et al. (2018) reasonably considered that the Leizhou Peninsula, Hainan Island and Shandong Peninsula were major physical barriers, substantially blocking gene flow and genetic admixture among local *L. maculatus* populations.

The present study demonstrated a number of growth-related morphological changes in the three *Lateolabrax* species, including some new key characters for identification. Despite the number of taxonomic descriptions and studies of *Lateolabrax*, such features have remained obscure due to the limited numbers of specimens examined and an inherent belief that fish morphology is stable regardless of growth, notwithstanding some

recent unique allometric approaches to fish morphology and taxonomy (e.g., Sidlauskas et al. 2011). The importance of investigating possible growth-related morphological changes, as well as meristic characters, is emphasized herein, as an understanding of proportional changes throughout the overall size range of a species may provide certain criteria which can distinguish between species and become keys for identification. Although such examinations need to be based on many specimens of various sizes, it may not be so difficult for commercial fishes, including *Lateolabrax*. Based on the results of the present study, a new key to the genus *Lateolabrax* is proposed.

Key to *Lateolabrax* species

a[1] Caudal peduncle anterior depth [% of standard length (SL)] > 15%. Snout length (% of SL) > 9%. Upper and lower jaw length [% of head length (HL)] > 45% and 49%, respectively. Dorsal fin rays 15–16 [rarely 14 (7.4%)]. Anal fin rays 9 (usually)–11 [rarely 8 (11.0%)] ..... ***Lateolabrax latus***

a[2] Caudal peduncle anterior depth (% of SL) ≤ 15%. Snout length (% of SL) ≤ 9%. Upper and lower jaw length (% of HL) ≤ 45% and 49%, respectively. Dorsal fin rays 14 or fewer. Anal fin ray counts 8 or fewer (rarely 9) ..... **b**

b[1] Post-orbital preopercular width (POPW) [% of snout length (SNL)] < 90% [POPW (% of SL) < 7.5% in specimens ≤ 200 mm SL; SNL (% of SL) > 7.7% in specimens > 200 mm SL]. Caudal vertebrae 20 (usually)–21 [rarely 19 (13.5%)]; total vertebrae 36 (usually)–37 [rarely 35 (13.5%)]. First anal pterygiophore modestly arched in specimens ≥ 90 mm SL. Spots / dots absent on body in specimens > 260 mm SL (although some specimens ≤ 260 mm SL have some dots restricted to upper part than lateral line) ..... ***Lateolabrax japonicus***

b[2] Post-orbital preopercular width (POPW) [% of snout length (SNL)] ≥ 90% [POPW (% of SL) ≥ 7.5% in specimens ≤ 200 mm SL; SNL (% of SL) ≤ 7.7% in specimens > 200 mm SL]. Caudal vertebrae 18–19 (usually) [rarely 20 (9.2%)]; total vertebrae 34–35 (usually) [rarely 36 (6.6%)]. First anal pterygiophore straight. Usually many clear black spots on lateral and dorsal body regions (usually even on lower part than lateral line) ..... ***Lateolabrax maculatus***

Acknowledgments

The author is grateful to Drs. Hiroshi Senou (KPM), Hiroyuki Motomura (KAUM) and Hiromitsu Endo (BSKU) for the loan of registered specimens of *Lateolabrax* species. Dr. Motomura also enabled registration of additional *L. japonicus* specimens to KAUM. Dr. Senou provided some photographs of fresh KPM specimens. Mr. Taiga Naito (BSKU) assisted with radiography and some measurements. Dr. Shi Dong (Tianjin Normal University) advised on translation of some Chinese literature. Dr.

Endo, Mr. Hirokazu Kishimoto (Shizuoka City, Japan), Mr. Taiji Kurozumi (Natural History Museum and Institute, Chiba), Dr. Brian L. Sidlauskas (Oregon State University) and Mr. Ikuo Wakabayashi (Wildlife Research Society of Shima Peninsula) helped with provision of literature. Finally, I wish to thank Dr. Graham S. Hardy (Ngunguru, New Zealand) for checking the manuscript.

References

Araga C (1981) *Lateolabrax latus*. In: Ochiai A (Ed.) Gakken Illustrated Nature Encyclopedia, the Fishes of Japan. Gakushu-kenkyusha, Tokyo, 82, 258–259. [In Japanese]

Arakaki S, Hutchinson N, Tokeshi M (2014) Foraging ecology of a large opportunistic predator (adult *Lateolabrax latus*) on a temperate-subtropical rocky shore. Coastal Ecosystems 1: 14–27. http://www.scesap.org/ce_archive/ce2014/arakaki2014a.pdf

Bae S, Kim J, Kim J (2016) Evidence of incomplete lineage sorting or restricted secondary contact in *Lateolabrax japonicus* complex (Actinopterygii: Moronidae) based on morphological and molecular traits. Biochemical Systematics and Ecology 66: 98–108. https://doi.org/10.1016/j.bse.2016.03.006

Basilewsky S (1855) Ichthyographia Chinae borealis. Nouveaux mémoires de la Société impériale des naturalistes de Moscou, Tome 10, Impremerie de l'Université Impériale, Moscou, 215–263. [pls. 1–9; in Latin]

Bell Jr AJ, Jacquemin SJ (2017) Evidence of morphological and functional variation among Bluegill *Lepomis macrochirus* populations across Grand Lake St Mary's watershed area. Journal of Freshwater Ecology 32(1): 1–18 https://doi.org/10.1080/02705060.2017.1319429

Bleeker P (1854–57) Nieuwe nalezingen op de ichthyologie van Japan. Verhandelingen van het Bataviaasch Genootschap van Kunsten en Wetenschappen 26: 1–132. [8 pls.; in Dutch]

Chan W, Tang Y (1968) Marine Fishes of Hong Kong, Part I. Hong Kong Government Press, Hong Kong, 129 pp.

Chen J (1987) Family Serranidae. In: Liu C, Qin K (Eds) Fauna Liaoningica, Pisces. Liaoning Science and Technology Publishing House, Shenyang, 232–235. [In Chinese]

Chen D, Gao T, Zeng X, Ren Y, Ruan S (2001) Study on the fishery biology of Laizhou population of *Lateolabrax* sp. Acta Oceanologica Sinica 23(4): 81–86. [In Chinese with English abstract]

Chen I, Fang L (1999) The Freshwater and Estuarine Fishes of Taiwan. National Museum of Marine Biology & Aquarium, Checheng, 287 pp. [In Chinese]

Chen M, Yu T, Tong H (1990) Fish Resources of Qiantang Jiang. Shanghai Scientific and Technical Publishers, Shanghai, 267 pp. [In Chinese]

Cheng Q, Zhou C (1997) The Fishes of Shandong Province. Shandong Science and Technology Press, Jinan, 549 pp. [In Chinese]

Chioma GN, Adejumo AO, Olumoh S (2007) Allometric and isometric growth of external body parts of *Auchenoglanis occidentalis* (Pisces: Bagridae). Science Focus 12(2): 76–82.

Chu Y (1985) The Fishes of Fujian Province, Part 2. Fujian Science and Technology Publishing House, Fuzhou, 700 pp. [In Chinese]

Chu Y, Tchang T, Cheng Q (1962) Fishes of the South Sea. Science Press, Beijing, 1184 pp. [In Chinese]

Chu Y, Tchang T, Cheng Q (1963) Fishes of the East Sea. Science Press, Beijing, 642 pp. [In Chinese]

Chyung M (1977) The fishes of Korea. Iljisa, Seoul, 727 pp. [In Korean]

Cuvier G (1828) Des poissons de la famille des perches, ou des percoïdes. Histoire Naturelle des Poissons, Tome II, Livre 3, F. G. Levrault, Paris, 490 pp. [In French]

Eschmeyer WN (2019) Eschmeyer's Catalog of Fishes, Online Version. California Academy of Sciences, San Francisco. http://researcharchive.calacademy.org/research/Ichthyology/catalog/fishcatmain.asp

Feng Z, Jiang Z (1998) Spotted Sea Bass Research. China Ocean Press, Beijing, 119 pp. [In Chinese]

FishBase (2018) *Lateolabrax latus* Katayama, 1957, blackfin seabass. http://www.fishbase.org/summary/23379

Fukuhara O, Fushimi T (1982) Development of fins and squamation in the percichthyid fish, *Lateolabrax japonicus*. Japanese Journal of Ichthyology 29(2): 173–178. https://www.jstage.jst.go.jp/article/jji1950/29/2/29_2_173/_pdf

Gao G (1991) Serranidae. In: Pan J, Zhong L, Zheng C, Wu H, Liu J (Eds) The Freshwater Fishes of Guangdong Province. Guangdong Science and Technology Press, Guangzhou, 363–371. [In Chinese]

Han Z, Han G, Wang Z, Shui B, Gao T (2015) The genetic divergence and genetic structure of two closely related fish species *Lateolabrax maculatus* and *Lateolabrax japonicus* in the Northwestern Pacific inferred from AFLP markers. Genes & Genomics 37(5): 471–477 https://doi.org/10.1007/s13258-015-0276-3

Hatooka K (1993) Percichthyidae. In: Nakabo T (Ed.) Fishes of Japan with Pictorial Keys to the Species, 1st ed. Tokai University Press, Tokyo, 594–599. [In Japanese]

Hatooka K (2000) Moronidae. In: Nakabo T (Ed.) Fishes of Japan with Pictorial Keys to the Species (2nd edn). Tokai University Press, Tokyo, 683 pp. [In Japanese]

Hatooka K (2013) Lateolabracidae. In: Nakabo T (Ed.) Fishes of Japan with Pictorial Keys to the Species (3rd edn). Tokai University Press, Hadano, 748 pp. [In Japanese]

Hirota Y, Ikeda M, Setokuma T, Mochizuki K (1999) New record of Chinese sea bass, *Lateolabrax* sp., from the coastal area of Kanto, central Japan. Journal of the Natural History Museum and Institute, Chiba 5: 103–108. [In Japanese with English abstract]

Holm S (1979) A simple sequentially rejective multiple test procedure. Scandinavian Journal of Statistics 6: 65–70.

Hubbs CL, Lagler KF (1970) Fishes of the Great Lakes Region (3rd edn). The University of Michigan Press, Ann Arbor, 213 pp. [44 pls]

Iseki T, Mizuno K, Ohta T, Nakayama K, Tanaka M (2010) Current status and ecological characteristics of the Chinese temperate bass *Lateolabrax* sp., an alien species in the western coastal waters of Japan. Ichthyological Research 57(3): 245–253. https://doi.org/10.1007/s10228-010-0161-7

Ishikawa H, Senou H (2010) Grand Illustrated Encyclopedia of Marine Fishes. Nitto Shoin Honsha Co.,Ltd., Tokyo, 399 pp. [In Japanese]

Iwasaki M (2006) A Guide to Statistical Data Analysis, Non-Parametric Methods. Tokyo-tosho Co, Tokyo, 110 pp. [In Japanese]

Kang C (2000) Taxonomical studies on the genus *Lateolabrax* (Pisces, Perciformes) from the Korean Waters. PhD Thesis, Pukyung National University, Pusan. [In Korean with English abstract]

Katayama M (1957) Four new species of serranid fishes from Japan. Japanese Journal of Ichthyology 6(4–6): 153–159. https://doi.org/10.11369/jji1950.6.153

Katayama M (1960a) Fauna Japonica, Serranidae. Tokyo News Service, Tokyo, 189 pp. [86 pls]

Katayama M (1960b) Studies of the serranid fishes of Japan (II). Bulletin of the Faculty of Education, Yamaguchi University 9: 63–96.

Katayama M (1965) *Lateolabrax latus*. In: Okada K, Uchida S, Uchida T (Eds) New Illustrated Encyclopedia of the Fauna of Japan. Hokuryu-kan Publishing Co.Ltd., Tokyo, 278. [In Japanese]

Katayama M (1984) Percichthyidae. In: Masuda H, Amaoka K, Araga C, Uyeno T, Yoshino T (Eds) The Fishes of the Japanese Archipelago (1st edn). Tokai University Press, Tokyo, 121. [pl 108; in Japanese]

Kim C, Jun J (1997) Provisional classification of temperate sea bass, the genus *Lateolabrax* (Pisces: Moronidae) from Korea. Korean Journal of Ichthyology 9(1): 108–113.

Kim Y, Han K, Kang C, Kim J (2004) Commercial Fishes of the Coastal and Offshore Waters in Korea (2nd edn). National Fisheries Research and Development Institute, Pusan, 333 pp. [In Korean]

Kinoshita I (1988) Genus *Lateolabrax*. In: Okiyama M (Ed.) An Atlas of Early Stage Fishes in Japan, 1st ed. Tokai University Press, Tokyo, 402–404. [In Japanese]

Kishimoto H, Amaoka K, Kohno H (1987) A revision of the black-and-white snappers, genus *Macolor* (Perciformes: Lutjanidae). Japanese Journal of Ichthyology 34(2): 146–156. https://www.jstage.jst.go.jp/article/jji1950/34/2/34_2_146/_pdf

Kottelat M (2013) The fishes of the inland waters of southeast Asia: a catalogue and core bibiography of the fishes known to occur in freshwaters, mangroves and estuaries. Raffles Bulletin of Zoology Supplement 27: 1–663.

Li M, Zhang H (1991) Fish Biology in the Bohai Sea. Science and Technology of China Press, Beijing, 141 pp. [In Chinese]

Lindberg GU, Krasyukova ZV (1969) Fishes of the Sea of Japan and of adjacent areas of the Sea of Okhotsk and the Yellow Seas, Part 3, Teleostomi XXIX Perciformes. Opredeliteli Faune SSSR 99: 1–479. [In Russian]

Liu J, Gao T, Yokogawa K, Zhang Y (2006) Differential population structuring and demographic history of two closely related fish species, Japanese sea bass (*Lateolabrax japonicus*) and spotted sea bass (*Lateolabrax maculatus*) in northwestern Pacific. Molecular Phylogenetics and Evolution 39(3): 799–811. https://doi.org/10.1016/j.ympev.2006.01.009

Lou D, Gao T, Zhang X (2002) The comparison of morphological characteristics among six sea bass populations [sic]. Journal of Ocean University of Qingdao 32(suppl): 85–89. [In Chinese with English abstract]

Mao J, Xu S, Jia G (1991) Fauna of Zhejiang, Freshwater Fishes. Zhejiang Science and Technology Publishing House, Hangzhou, 250 pp. [In Chinese]

Masuda H, Araga C, Yoshino T (1975) Coastal Fishes of Southern Japan. Tokai University Press, Tokyo, 379 pp. [In English and Japanese]

Matsunuma M, Motomura H (2017) Review of the genus *Banjos* (Perciformes: Banjosidae) with descriptions of two new species and a new subspecies. Ichthyological Research 64(3): 265–294. https://doi.org/10.1007/s10228-016-0569-9

Matsuyama H, Atsumi S, Takase S (2002) Spawning of the blackfin sea bass *Lateolabrax latus* in a tank. Bulletin of the Shizuoka Prefectural Fisheries Experiment Station 37: 45–48. [In Japanese]

McClelland J (1844) Description of a collection of fishes made at Chusan and Ningpo in China, by Dr. G. R. Playfair, surgeon of the Plegethon, war steamer, during the late military operations in that country. Calcutta Journal of Natural History 4: 390–413. [pls. 21–25]

Minos G, Kokokiris L, Kentouri M (2008) Allometry of external morphology and sexual dimorphism in the red porgy (*Pagrus pagrus*). Belgian Journal of Zoology 138(1): 90–94.

Murase A, Miyazaki Y, Senou H (2012) Redescription of the temperate seabass *Lateolabrax latus* from Yaku-shima Island, Kagoshima Prefecture, southern Japan with notes on riverine habitats. Japanese Journal of Ichthyology 59(1): 11–20. [In Japanese with English abstract] https://doi.org/10.11369/jji.59.11

Nakayama K (2002) Intra-structure of the Ariake population. In: Tanaka M, Kinoshita I (Eds) Temperate Bass and Biodiversity–New Perspective for Fisheries Biology. Koseishakoseikaku, Tokyo, 127–139. [in Japanese]

Nozaka M (1995) Morphology of fingerling sea bass (*Lateolabrax japonicus*) in waters around Okayama Prefecture]. Proceedings of the Annual Conference of Marine Resources in the Seto Inland Sea 1: 41–46. [In Japanese]

Okiyama M (1988) An Atlas of Early Stage Fishes in Japan (1st edn). Tokai University Press, Tokyo, 1154 pp. [In Japanese]

Paxton JR, Hoese DF (1985) The Japanese sea bass, *Lateolabrax japonicus* (Pisces, Percichthyidae), an apparent marine introduction into Australia. Japanese Journal of Ichthyology 31(4): 369–372. https://doi.org/10.11369/jji1950.31.369

Sadovy Y, Cornish AS (2000) Reef Fishes of Hong Kong. Hong Kong University Press, Hong Kong, 321 pp.

Sakai H, Satou M, Nakamura M (1998) A record of the temperate sea bass, *Lateolabrax latus*, from a freshwater habitat of Tanegashima Island. Japanese Journal of Ichthyology 45(2): 107–109. [In Japanese with English abstract] https://doi.org/10.11369/jji1950.45.107

Senou H (2002) Taxonomy of fishes of the genus *Micropterus* imported into Japan. In: Goto A, Senou H (Eds) Black Bass, an Invader in Rivers and Lakes. Koseishakoseikaku, Tokyo, 11–30. [In Japanese]

Shan B, Song N, Han Z, Wang J, Gao T, Yokogawa K (2016) Complete mitochondrial genomes of three sea basses *Lateolabrax* (Perciformes, Lateolabracidae) species: Genome description and phylogenetic considerations. Biochemical Systematics and Ecology 67: 44–52. https://doi.org/10.1016/j.bse.2016.04.007

Shimose T, Nanami A, Senou H (2011) First record of *Lateolabrax* from the Yaeyama Islands, Japan, based on underwater photographs from Ishigaki Island. Japanese Journal of Ichthyology 58(2): 211–213. [In Japanese]

Sidlauskas B, Mol JH, Vari RP (2011) Dealing with allometry in linear and geometric morphometrics: a taxonomic case study in the *Leporinus cylindriformis* group (Characiformes: Anostomidae) with description of a new species from Suriname. Zoological Journal of the Linnean Society 162(1): 103–130. https://doi.org/10.1111/j.1096-3642.2010.00677.x

Song L, Xiao Y, Gao T (2008) Studies on the phylogeny of *Lateolabrax* species based on sequence variations of the S7 ribosomal protein gene. Transactions of Oceanology and Limnology 2008(2): 152–158. [In Chinese with English abstract]

Takahashi Y (1962) Study for the identification of species based on the vertebral column of Teleostei in the Inland Sea and its adjacent waters. Bulletin of Naikai Regional Fisheries Research Laboratory 16: 1–197. [In Japanese with English résumé] https://agriknowledge.affrc.go.jp/RN/2010841491.pdf

Tamura Y, Moteki M, Yokoo T, Kohno H (2013) Occurrence patterns and ontogenetic intervals based on the development of swimming- and feeding-related characters in larval and juvenile Japanese sea bass (*Lateolabrax japonicus*) in Tokyo Bay. La Mer 51(1–2): 13–29. http://www.sfjo-lamer.org/la_mer/51-1_2/51-1-2.pdf

Tanaka M, Matsumiya Y (1982) Early life history of Japanese sea bass, *Lateolabrax japonicus*, with particular emphasis on transitional process to juvenile stage. Technical Reports of Japanese Sea Ranching Programs 11: 49–65. [In Japanese]

Tchang T, Cheng Q, Zheng B (1955) Survey Report of Fishes from the Yellow and Bohai Seas. Science Press, Beijing, 353 pp. [In Chinese]

Temminck CJ, Schlegel H (1846) Pisces, Part 10. In: von Siebold PF (Ed.) Fauna Japonica. Lugduni Batavorum, Leiden, 173–188. [In French] https://rmda.kulib.kyoto-u.ac.jp/item/rb00000002

Wakabayashi I, Nakamura M (2003) A record of spotted sea bass, *Lateolabrax* sp., from coastal waters of the Shima Peninsula, Japan. Wildlife News from Mie 16: 2–3. [In Japanese]

Wang S, Wang Z, Li G, Cao Y, et al. (2001) The Fauna of Hebei, China, Pisces. Hebei Science and Technology Publishing House, Shijiazhuang, 366 pp. [In Chinese]

Wang W, Ma C, Chen W, Ma H, Zhang H, Meng Y, Ni Y, Ma L (2016) Optimization of selective breeding through analysis of morphological traits in Chinese sea bass (*Lateolabrax maculatus*). Genetics and Molecular Research 15(3): 1–11. https://doi.org/10.4238/gmr.15038285

Yamada S, Kitada S (2004) *Handbook of Biostatistics*. Seizando Book Co., Tokyo, 262 pp. [In Japanese]

Yamada U, Tokimura M, Horikawa H, Nakabo T (2007) Fishes and Fisheries of the East China and Yellow Seas. Tokai University Press, Hadano, 1262 pp. [In Japanese]

Ye Z, Meng X, Gao T, Yang Y, Wang Y (2007) The geographical differentiation in otolith morphology of sea bass: *Lateolabrax japonicus* and *L. maculates* [sic]. Oceanologia et Limnologia Sinica 38(4): 356–360. [In Chinese with English abstract]

Yokogawa K (1995) Morphological and genetic features of Japanese sea bass *Lateolabrax japonicus* with black dots on lateral body region. Fish Genetics and Breeding Science 22: 67–75. [In Japanese with English abstract]

Yokogawa K (1996) Growth and condition factor of Spanish mackerel *Scomberomorus niphonius* in the eastern waters of the Seto Inland Sea. Census Report for Fisheries Affected by Honshu-Shikoku Bridge Construction 67: 179–198. [In Japanese]

Yokogawa K (1998) Genetic divergence of fishes in genus *Lateolabrax* (Perciformes: Percichthyidae). Suisanzoshoku 46(3): 315–320. https://doi.org/10.11233/aquaculturesci1953.46.315

Yokogawa K (2002) Genus *Lateolabrax* distributed in the east Asian coastal waters. In: Tanaka M, Kinoshita I (Eds) Temperate Bass and Biodiversity–New Perspective for Fisheries Biology. Koseishakoseikaku, Tokyo, 114–126. [in Japanese]

Yokogawa K (2004) Biological characteristics and specific divergence in genus *Lateolabrax* (Perciformes: Percichthyidae). PhD Thesis, Ehime University, Matsuyama. https://doi.org/10.13140/RG.2.1.2471.4324

Yokogawa K (2013a) Morphological variations in bluegill, *Lepomis macrochirus*, with particular emphasis on growth-related changes. Ichthyological Research 60(1): 48–61. https://doi.org/10.1007/s10228-012-0310-2

Yokogawa K (2013b) Nomenclatural reassessment of the sea bass *Lateolabrax maculatus* (McClelland, 1844) (Percichthyidae) and a redescription of the species. Biogeography 15: 21–32.

Yokogawa K (2014) Morphological variations in the largemouth bass *Micropterus salmoides* with particular emphasis on growth-related changes. Aquaculture Science 62(4): 361–374. https://doi.org/10.11233/aquaculturesci.62.361

Yokogawa K (2015) Morphological differences between two closely related East Asian flatfish species of the genus *Pleuronichthys*, with particular emphasis on growth-related changes. Ichthyological Research 62(4): 474–486. https://doi.org/10.1007/s10228-015-0462-y

Yokogawa K, Seki S (1995) Morphological and genetic differences between Japanese and Chinese sea bass of the genus *Lateolabrax*. Japanese Journal of Ichthyology 41(4): 437–445. https://doi.org/10.11369/jji1950.41.437

Yokogawa K, Tajima T (1996) Morphological and genetic characters of artificially propagated sea bass in Taiwan. Fisheries Science 62(3): 361–366. https://doi.org/10.2331/fishsci.62.361

Yokogawa K, Kishimoto H (2012) A long-finned variant of the Japanese sea bass *Lateolabrax japonicus* from Enshu-nada, Japan. Ichthyological Research 59(1): 86–93. https://doi.org/10.1007/s10228-011-0253-z

Yokogawa K, Taniguchi N, Seki S (1997) Morphological and genetic characteristics of sea bass, *Lateolabrax japonicus* from the Ariake Sea, Japan. Ichthyological Research 44(1): 51–60. https://doi.org/10.1007/BF02672758

Yokogawa K, Suetomo K, Murakami K, Shibuya R, Seki S, Tsujino K, Miyagawa M (1996) Morphological and genetic features of sea bass, so-called "hoshisuzuki", from waters around Shikoku, Japan. Japanese Journal of Ichthyology 43(1): 31–37. [In Japanese with English abstract] https://doi.org/10.11369/jji1950.43.31

Youn C (2002) Fishes of Korea with Pictorial Key and Systematic List. Academy Book, Seoul, 747 pp. [In Korean]

Zhao S, Zhong J (2006) Colored Encyclopedia of Fishes in Zhoushan Waters. Zhejiang Science and Technology Press, Hangzhou, 200 pp. [In Chinese]

Zhao Y, Peng W, Guo H, Chen B, Zhou Z, Xu J, Zhang D, Xu P (2018) Population genomics reveals genetic divergence and adaptive differentiation of Chinese sea bass (*Lateolabrax maculatus*). Marine Biotechnology 20(suppl): 45–59. https://doi.org/10.1007/s10126-017-9786-0

Zar JH (2010) Biostatistical Analysis (5th edn). Pearson Education Inc., Upper Saddle River, 944 pp.

Zheng B (1987) Illustrated Encyclopedia of Animals in China, Fishes (2nd edn). Science Publishing, Beijing, 295 pp. [In Chinese]

ZooKeys 859: 117–130 (2019)
doi: 10.3897/zookeys.859.32869
http://zookeys.pensoft.net

RESEARCH ARTICLE

A peer-reviewed open-access journal
ZooKeys
Launched to accelerate biodiversity research

Amphibian diversity in Serranía de Majé, an isolated mountain range in eastern Panamá

Daniel Medina[1,2], Roberto Ibáñez[2,3,4,5], Karen R. Lips[2,6], Andrew J. Crawford[2,3,7]

1 *Laboratório de História Natural de Anfíbios Brasileiros (LaHNAB), Departamento de Biologia Animal, Universidade Estadual de Campinas, Campinas, SP 13083-862, Brazil* **2** *Smithsonian Tropical Research Institute, Apartado Postal 0843-03092, Panamá, República de Panamá* **3** *Círculo Herpetológico de Panamá, Estafeta Universitaria, Apartado Postal 10762, Panamá, República de Panamá* **4** *Departamento de Zoología, Universidad de Panamá, Panamá, República de Panamá* **5** *Sistema Nacional de Investigación, Panamá, República de Panamá* **6** *Department of Biology, University of Maryland, College Park, MD 20742, USA* **7** *Departamento de Ciencias Biológicas, Universidad de los Andes, Bogotá, 111711, Colombia*

Corresponding author: *Roberto Ibáñez* (ibanezr@si.edu)

Academic editor: *Anthony Herrel* | Received 4 January 2019 | Accepted 29 March 2019 | Published 2 July 2019

http://zoobank.org/57338B9B-D249-47EE-B152-9828A8B446AA

Citation: Medina D, Ibáñez R, Lips KR, Crawford AJ (2019) Amphibian diversity in Serranía de Majé, an isolated mountain range in eastern Panamá. ZooKeys 859: 117–130. https://doi.org/10.3897/zookeys.859.32869

Abstract

Eastern Panamá is within the Mesoamerican biodiversity hotspot and supports an understudied amphibian fauna. Here we characterize the amphibian diversity across an elevational gradient in one of the least studied mountain ranges in eastern Panamá, Serranía de Majé. A total of 38 species were found, which represent 17% of all species reported for Panamá. Based on expected richness function and individual-based rarefaction curves, it is estimated that this is an underestimate and that at least 44 amphibian species occur in this area. Members of all three amphibian orders were encountered, represented by ten families and 22 genera, including five species endemic to Central America. Estimated species richness decreased with elevation, and the mid-elevation site supported both lowland and highland species. Our study provides a baseline for understanding the distribution pattern of amphibians in Panamá, for conservation efforts, and for determining disease-induced changes in amphibian communities.

Keywords

Altitudinal diversity, amphibian species inventory, Panamá

Introduction

Mesoamerica is a global biodiversity hotspot (Johnson et al. 2015). Within this region, Panamá has the second greatest number of reptile and amphibian species, containing 26% of all amphibian species reported for Mesoamerica (Jaramillo et al. 2010). However, a substantial portion of eastern Panamá has been understudied. Geographically, eastern Panamá comprises the northernmost part of the Chocó biogeographical region (Duque-Caro 1990), and it is part of the Tumbes-Chocó-Magdalena global biodiversity hotspot (Mittermeier et al. 1999). This region includes a number of relatively low mountain ranges, including the Serranía de San Blas + Serranía del Darién on Caribbean side, the inland Serranía de Pirre + Altura de Nique + Altos de Quía, Serranía de Majé, and the Serranía de Sapo + Serranía de Jingurudó + Altos de Aspavé + Cordillera de Juradó along the Pacific Ocean (Duque-Caro 1990; Batista et al. 2016).

Whitfield et al. (2016) analyzed regional trends and reported that eastern Panamá has a very small number of recognized species in relation to its geographic area, which reflects the limited number of field surveys in the area. A sharp increase in the number of field surveys during the last decade has led to the discovery of several new amphibian species with restricted distribution ranges (e.g., Ibáñez and Crawford 2004; Crawford et al. 20104a; Batista et al. 2014a, 2014b, 2016) supporting the hypothesis that eastern Panamá is a region with a high endemic amphibian diversity. This is in contrast to the claim that it was mainly a dispersal route during the Great American Biotic Interchange (Webb 2006), and was colonized by species groups from the north and South America (Vanzolini and Heyer 1985; Pinto-Sánchez et al. 2012).

One reason to establish baseline estimates of amphibians is to assess changes following loss caused by disease epidemics. The pathogenic fungus *Batrachochytrium dendrobatidis* (*Bd*) causes population declines and extinctions of many amphibian species worldwide, particularly in the Neotropics (James et al. 2015, Lips 2016). *Bd* has caused dramatic declines of amphibian communities in the highlands of western and central Panamá (Lips 1999; Lips et al. 2006; Crawford et al. 2010b). Importantly, to our knowledge, at the time of sampling there were no published data reporting the presence of *Bd* in the region – though the amphibian species present at this region can either represent the original community or a subset as a consequence of an undetected *Bd* epidemic. Here, we describe the results from field surveys to characterize α and β diversity along an altitudinal gradient in the isolated Serranía de Majé of eastern Panamá.

Materials and methods

Study sites

During the wet season, from June 23 to July 2 2007, we conducted field surveys at three study sites located at a low, middle, and high elevations in the Serranía de Majé. This mountain range is located on the Pacific coast, previously known as Serranía de Cañazas (Myers 1969), and is isolated from others mountainous areas by the Chepo

and Chucunaque Rivers (Figure 1; Angher and Christian 2000). Its highest point, Cerro Chucantí (1,489 m), stands on the eastern end of the mountain range, at the boundary of the Panamá and Darién provinces (Angher and Christian 2000).

The three study sites were located in Lowland Wet/Moist Forest (LWM) below 600 m, and Premontane Rain Forest/Wet Forest (PRW) above 600 m (Holdridge 1967). The sites were: a low elevation site, Centro Cristo Misionero (8.96N, 78.457W) at 120–150 m elevation; a mid-elevation site, located within the Reserva Natural Privada Cerro Chucantí (8.79N, 78.451W) at 797 m elevation; and, the high elevation site, also located in the Cerro Chucantí private natural reserve (8.80N, 78.462W), near the top of the Cerro Chucantí, at 1,240–1,365 m elevation. The approximate airline distances between the study sites were 19, 18, and 2 km for lowland-mid-elevation, lowland-highland and mid-elevation-highland sites, respectively.

Data collection

The surveys were conducted using the sampling technique "free and unrestricted search", which is considered to be one of the most efficient methods to record a high number of species in a relatively short amount of time (Rueda et al. 2006). Different types of habitat such as forest, streams, ponds, and open areas with grass were surveyed during the day and night. Species identification and individual counts were performed using the techniques 'visual encounter survey' (VES) and 'acoustic encounter survey' (AES). In addition, the search effort invested (in person-hours) at each sampling site was calculated by multiplying the search time by the number of observers, and the catch per unit of search effort for each site was calculated by dividing the number of post-metamorphic amphibians encountered by the search effort at the respective site as estimated by Kilburn et al. (2011).

A few specimens of each species were collected as voucher specimens (Suppl. material 1: Table S1), photographed, and deposited in the reference Collection of Herpetology (specimen tags CH and AJC) at the Smithsonian Tropical Research Institute, and in the Museo de Vertebrados de la Universidad de Panamá (tags MVUP). Amphibians to be preserved were first euthanized using Orajel (benzocaine 20%) or occasionally 10% ethanol. Before fixation, liver samples were taken from each specimen and preserved for future phylogenetic and phylogeographic analyses (Seutin et al. 1991). Vouchers were then fixed in 10% formalin in a position that facilitates examination. To verify the identification of specimens we used all relevant literature available on the amphibians of Panamá (e.g., Ibáñez et al. 1999a), and compared specimens with those in the CH reference collection. The identification of anuran advertisement calls was facilitated by audio recordings of Panamanian frogs (Ibáñez et al. 1999b).

Data analyses

We calculated α diversity based on all post-metamorphic amphibians captured at each site (Hortal et al. 2006), using the software EstimateS 8.0.0 (Colwell 2006). We calcu-

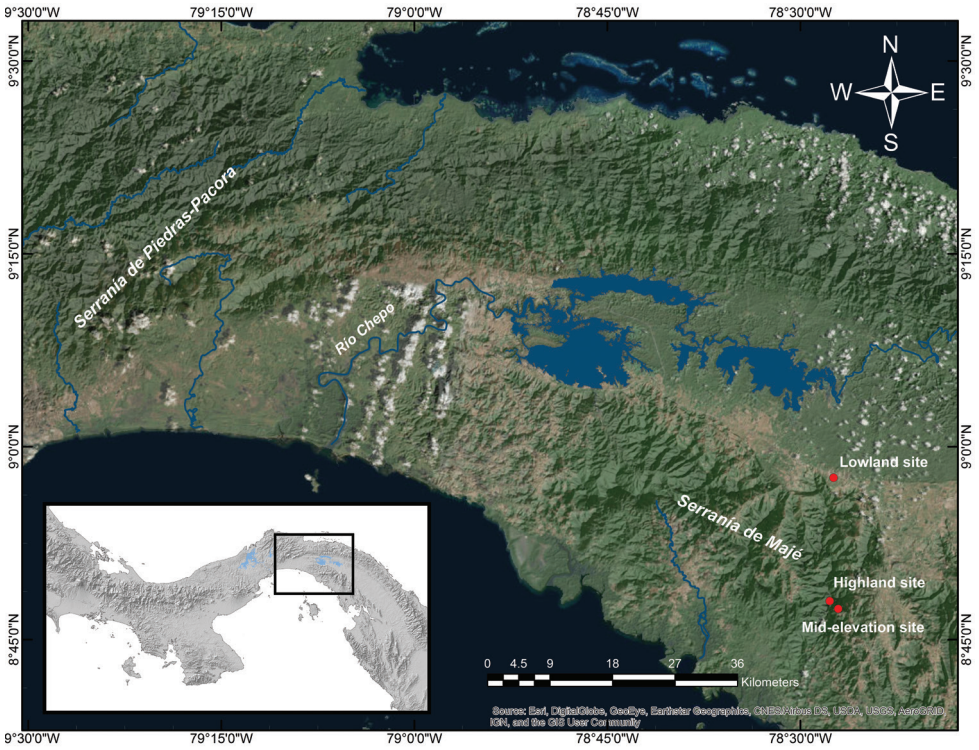

Figure 1. Map showing the location of the study sites in the Serranía de Majé and the Serranía de Piedras-Pacora across the valley of the Chepo River.

lated Mao Tau (Colwell et al. 2004) and plotted sample-based rarefaction curves with 95% confidence intervals.

To determine β diversity for assessing the variation in species composition across sites, we also used all post-metamorphic amphibians captured at each site, and conducted a cluster analysis based on Jaccard dissimilarity measures estimated with the R function vegdist from the *vegan* package (Oksanen et al. 2017). In order to identify clusters, we built a dendrogram using the unweighted pair-group method based on arithmetic averages (UPGMA), using function hclust from the default R package *stats*. This analysis was completed in the R version 3.3.3 (R Core Team, 2017).

Results

Our team conducted 280 person-hours of surveys (lowland site: 125; mid-elevation site: 96; highland site: 59) and identified 38 amphibian species from all three amphibian orders, ten families, and 22 genera (Table 1). The total number of species for the surveyed area within the Serranía de Majé was estimated as 44 species based on the upper 95% confidence interval of the Mao Tau function (Table 2).

Table 1. List of species and number of post-metamorphic individuals found at the three surveyed sites across the elevational gradient in the Serranía de Majé. The letter 'L' refers to a species that was recorded by its larvae and 'V' by its vocalizations. The IUCN conservation status is based on the IUCN (2018). 'E' represents a species that is endemic to Central America (CA) based on Johnson et al. (2015).

Order	Family	Genus	Species	Lowland	Mid-elevation	Highland	IUCN status	Endemic to CA
Anura	Aromobatidae	*Allobates*	*talamancae*	2	1		LC	
	Bufonidae	*Rhaebo*	*haematiticus*		9	11	LC	
		Rhinella	*alata*	13	1	1	LC	
		Rhinella	*horribilis*	2	1		LC	
	Centrolenidae	*Espadarana*	*prosoblepon*	L	8	V	LC	
		Cochranella	*euknemos*		3		LC	
		Hyalinobatrachium	*colymbiphyllum*	1			LC	
		Hyalinobatrachium	*fleischmanni*	3			LC	
		Hyalinobatrachium	*vireovittatum*		1		DD	E
	Craugastoridae	*Craugastor*	*crassidigitus*	1	9	1	LC	
		Craugastor	*fitzingeri*	5	3		LC	
		Craugastor	*raniformis*	15	3		LC	
		Pristimantis	aff. *latidiscus*			4	–	–
		Pristimantis	*caryophyllaceus*			57	NT	E
		Pristimantis	*cruentus*		1	71	LC	
		Pristimantis	*gaigei*	1			LC	
		Pristimantis	*moro*			10	LC	
		Pristimantis	*pardalis*			1	NT	E
		Pristimantis	*ridens*		1		LC	
		Pristimantis	*taeniatus*		V		LC	
		Strabomantis	*bufoniformis*	2			LC	
	Dendrobatidae	*Colostethus*	aff. *pratti*	11	9	4	–	–
		Dendrobates	*auratus*	8	19		LC	
		Silverstoneia	aff. *nubicola*	3	12	4	–	–
	Eleutherodactylidae	*Diasporus*	aff. *diastema**	21			–	–
		Diasporus	*majeensis***			1	–	E
	Hylidae	*Agalychnis*	*callidryas*	L	4		LC	
		Dendropsophus	*microcephalus*	10			LC	
		Boana	*rosenbergi*	4			LC	
		Scinax	*rostratus*	2			LC	
		Scinax	*ruber*	3			LC	
		Smilisca	*phaeota*	6			LC	
		Smilisca	*sila*		12		LC	
	Leptodactylidae	*Engystomops*	*pustulosus*	13	1		LC	
		Leptodactylus	*fragilis*	3			LC	
		Leptodactylus	*savagei*	1	V		LC	
Caudata	Plethodontidae	*Oedipina*	*complex*			1	LC	
Gymnophiona	Caeciliidae	*Caecilia*	*isthmica*		1		DD	E
3	**10**	**22**	**38**	**130**	**99**	**166**		

* This species refers to the *Diasporus* aff. *diastema* from the Serranía de Majé as suggested by Batista et al. (2016).
** Described by Batista et al. (2016), only known from Panamá; therefore, considered endemic to CA.

Table 2. Total number of post-metamorphic individuals and species per site, and the site-level estimated richness as a function of the 95% confidence intervals (CI) calculated by the function Mao Tao.

Site	Number of Individuals	Number of species observed (Sobs)	Expected 95% CI upper limit
Lowland	130	22	24.64
Mid-elevation	99	19	25.58
Highland	166	12	16.57
All sites	395	37	44.08

The greatest number of species was found at the lowland site (24 spp., Table 2; individuals catch per unit of search effort: 1.04), where the search effort was the highest, and where multiple aquatic habitats were available (i.e. ponds and forest streams). The most abundant species at this site were *Diasporus* aff. *diastema* (sensu Batista et al. 2016), *Craugastor raniformis* and *Engystomops pustulosus* (Table 1). *Espadarana prosoblepon* and *Agalychnis callidryas* were detected at this site with larval surveys. The mid-elevation site had fewer species than the lowland site (22 spp., Table 2; individuals catch per unit of search effort: 1.03); however, despite lower search effort at this site, the upper 95% confidence intervals of the Mao Tau function estimated very similar species number (i.e., 25 spp. at the lowland site and 26 spp. at the mid-elevation site). The most abundant species at the mid-elevation site were *Dendrobates auratus*, *Silverstoneia* aff. *nubicola* and *Smilisca sila* (Table 1). In addition, at this site two species were detected only by their vocalizations: *Pristimantis taeniatus* and *Leptodactylus savagei*. The lowest richness was observed at the highland site (13 spp., Table 2; frog catch per unit of search effort: 2.81), because of limited searching effort, fewer habitats, and the lower diversity of the upland area. The estimated number of species for this site based on the upper 95% confidence intervals of the Mao Tau function was 17 spp., and the most abundant species at this site were *Rhaebo haematiticus*, *Pristimantis caryophyllaceus*, *P. cruentus*, and *P. moro* (Table 1). Moreover, the glassfrog, *Espadarana prosoblepon*, was detected at this site only by its vocalization.

The individual-based rarefaction curves for the total area surveyed (Figure 2A) and at the site level (Figure 2B) showed a substantial decrease in the slope as the number of individuals increased with search effort. Thus, while the upper 95% confidence interval of the Mao Tau function suggests that not all species present in the area were observed, the amphibian community determined in these surveys might be representative of the extant community in Serranía de Majé.

Based on the Jaccard dissimilarity coefficients calculated, the community composition was more similar between the low and mid-elevation sites relative to the high elevation site (Table 3, Figure 3). As expected, the sites that most differed were the low versus high elevation sites. However, six species were consistently present across all three elevation sites: *Rhinella alata*, *Espadarana prosoblepon*, *Craugastor crassidigitus*, *Colostethus* aff. *pratti*, and *Silverstoneia* aff. *nubicola*.

Table 3. Number of species shared between pairs of sites along an elevational transect of the Serranía de Majé (below the diagonal); total number of species per site including the species registered by post-metamorphic stages, vocalization, or larval stage (**diagonal**); and Jaccard similarity coefficients (1 - dissimilarity estimate) for each pair of sites (*above the diagonal*).

	Lowland	Mid-elevation	Highland
Lowland	**24**	*0.32*	*0.13*
Mid-elevation	13	**22**	*0.24*
Highland	5	7	**13**

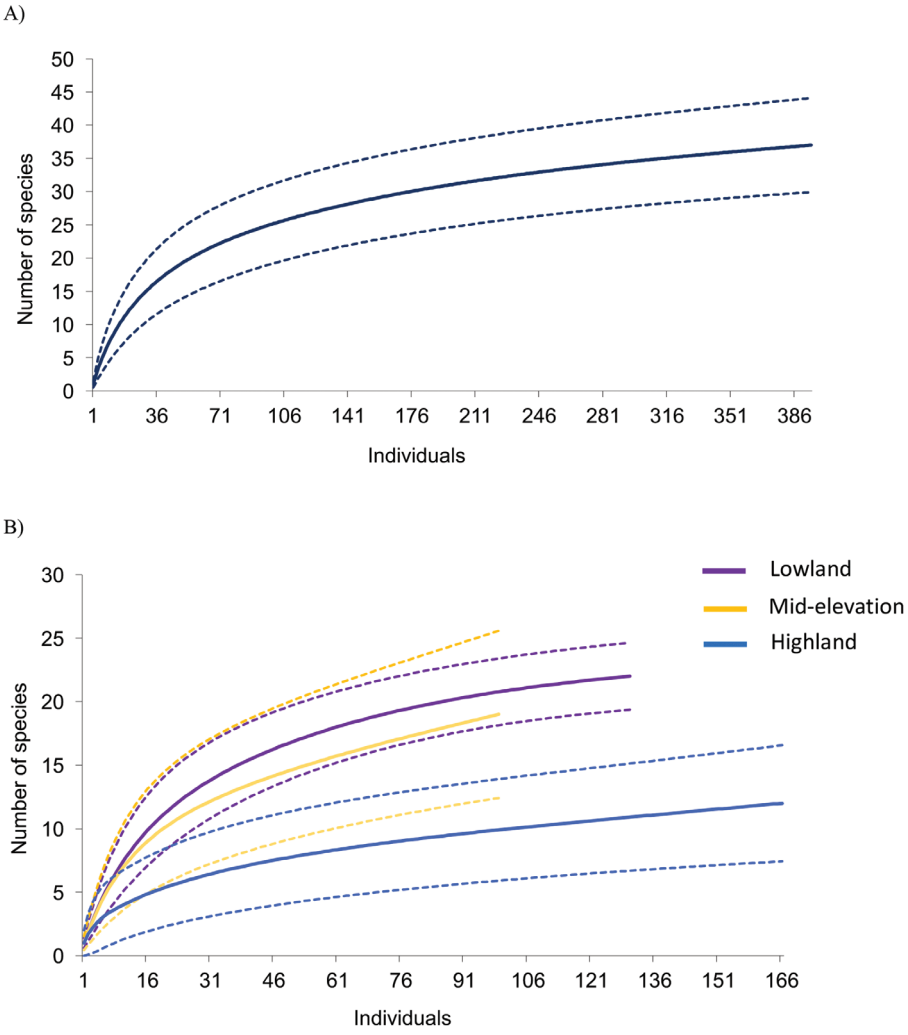

Figure 2. Individual-based rarefaction curves showing the estimated richness as a function of the upper 95% confidence interval (CI) calculated by the function Mao Tao. **A** Rarefaction curve combining all data obtained for the Serranía de Majé transect **B** rarefaction curves for low (120 – 150 m), intermediate (797 m), and high elevation (1,240–1,365 m) survey sites.

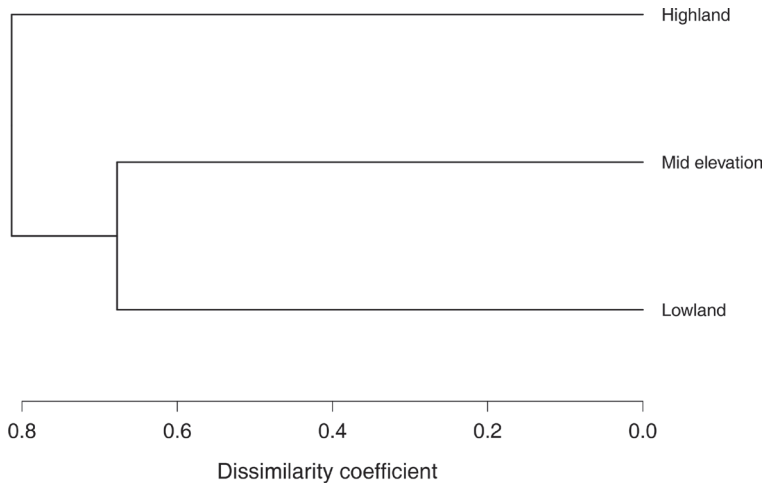

Figure 3. Site-level dendrogram based on Jaccard dissimilarities and built with the unweighted pair-group method based on arithmetic averages (UPGMA). This analysis was based on all post-metamorphic amphibians captured at each site.

Discussion

The present study represents the first attempt to characterize the composition and altitudinal diversity pattern of the amphibian community from the isolated Serranía de Majé of eastern Panamá. We determined that the composition of the species community across the altitudinal gradient was comprised by species from both Mesoamerican and South American groups, and that taxonomic genera from South America dominated the composition of the community (South American genera: 82%; Mesoamerican genera: 18%). In addition, the observed proportion in the composition of genera is consistent with the diversity pattern determined by Savage (2002) for eastern Panamá, where genera from South American groups represented over 50% of the genera comprising the amphibian assemblage.

The species found during this study represent 17% of the native amphibian species of Panamá (AmphibiaWeb 2018). However, the estimated total number of species based on the rarefaction analysis suggests that the richness of the study area is slightly higher than what we observed. In addition, the recent discovery of two new amphibian species from the Serranía de Majé, *Bolitoglossa chucantiensis* and *Diasporus majeensis* (see Batista et al. 2014b, 2016), suggest that this region might be high in endemism, as previously suggested for eastern Panamá (Crawford et al. 2010a).

Amphibians, occurring in Central America, have their highest species richness at intermediate elevations (Savage 2002, Wiens et al. 2006, Whitfield et al. 2016). This general altitudinal diversity pattern might also apply to the Serranía de Majé considering that, despite the relatively lower search effort and lower number of individuals encountered at the mid-elevation site, we observed and estimated a species richness simi-

lar to that of the lowland site (i.e., site with the highest observed richness). In addition, we determined similar estimates of individuals catch per unit of search effort (lowland site: 1.04 vs. mid-elevation site:1.03) between the lowland and mid-elevation sites. Hence, these results suggest that an increase in sampling effort at the mid-elevation site will potentially increase the number of species detected. Lastly, the observed altitudinal pattern of species richness could have been influenced by the variation across sites in the area covered during the surveys and the habitat types present at the sampling sites. In particular, the number of observed species at the highland site was potentially affected by the absence of streams and ponds, and the reduced patch size of the cloud forest.

In terms of β diversity, the higher similarity in the community composition between the mid-elevation and highland sites compared to that between the lowland and highland sites, suggests that the composition at intermediate elevations in Serranía de Majé might result, in part, by an overlap in the altitudinal distribution of the species associated with higher and lower altitudes; a pattern previously observed for the anuran communities from the Panamá Canal watershed (Ibáñez et al. 2002). In addition, despite the mid-elevation and highland sites being closer to each other (i.e., ~2 km apart) than to the lowland site, the community composition between the mid-elevation and highland sites was less similar than the composition between the mid-elevation and lowland sites. The higher similarity in the community composition between the mid-elevation and lowland sites compared to that with the highland site suggests that the highland site might be comprised by species with restricted altitudinal distributions. For instance, the dissimilarity associated with the highland site in our study was potentially influenced by the observation of species with restricted altitudinal ranges, such as: *Pristimantis* aff. *latidiscus*, *P. caryophyllaceus*, *P. moro*, *P. pardalis* and *Diasporus majeensis*.

The Serranía de Majé is isolated from the other mountain ranges in the region by the valleys of the Chepo and Chucunaque Rivers (Figure 1), which could have represented physical barriers leading to genetic isolation of populations that could have resulted in allopatric speciation (Cadena et al. 2011). Preliminary results from a comparison between the amphibian communities from the Serranía de Majé and Serranía de Piedras-Pacora (Ibáñez et al. 1994, Sosa and Guerrel 2013), located across the valley of the Chepo River (Figure 1), showed a lower species diversity at the Serranía de Majé and a decrease in the similarity of species composition as elevation increases (Figure 4). In addition, the highest elevations studied at these two mountain ranges are about 106 km apart (airline distance), and their dissimilarity is largely due to the disproportionate number of species that are present in Serranía de Piedras-Pacora but potentially absent in Serranía de Majé. Hence, thus far, seems that dispersal limitation has potentially played a major role in shaping the amphibian community at Serranía de Majé; nonetheless, more studies would be necessary to address this. Lastly, the decrease in similarity in species composition as elevation increases is consistent with the general pattern of amphibians endemism observed in Central America, that shows that a substantial portion of endemic species in the region are associated with upland regions (Whitfield et al. 2016).

Central America, while being a hotspot for amphibian diversity, is a region with a high proportion of threatened amphibian species. For instance, 41% of the regional

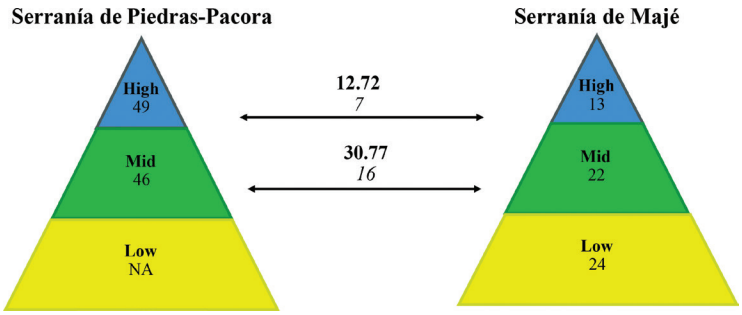

Figure 4. Diagram showing a decrease with elevation in the similarities of amphibian species assemblages associated with sites from the Serranía de Piedras-Pacora mountain range and the isolated Serranía de Majé mountain range. The numbers represent the shared species between sites (*N*), Jaccard similarity coefficients (**N**) and total number of species at the site level (N). Each color represents an elevation category, where the lowlands (< 400 m) are represented in yellow, mid-elevation sites (400–800 m) in green, and highlands (> 800 m) in blue. NA = no data available.

pool of species that have been assessed by the IUCN (International Union for Conservation of Nature) are under one of the following categories of the Red List of Threatened Species: critically endangered, endangered or vulnerable (reviewed in Whitfield et al. 2016). Within this context, the amphibian community of the Serranía de Majé does not seem, at first, to be comprised of species of high conservation concern given that 76% of the species registered in this study are under the category 'least concern' of the IUCN Red List of Threatened Species (IUCN 2018). However, the Serranía de Majé harbors amphibian species that could be regarded as threatened species, as well as poorly known species lacking an evaluation of their conservation status. For example, based on the IUCN criteria, two of the recorded species are considered near threatened (i.e., *Pristimantis caryophyllaceus* and *P. pardalis*), and two others are data deficient (i.e., *Caecilia isthmica*, and *Hyalinobatrachium vireovittatum*). Importantly, these two species that are considered near threatened and the two data deficient ones are endemic to Central America (Johnson et al. 2015). Notably, in this study we also found four species, which include one species from the genus *Pristimantis* (*P.* aff. *latidiscus*), two dendrobatids (*Colostethus* aff. *pratti* and *Silerstoneia* aff. *nubicola*) and one species from the *Diasporus diastema* species group (i.e., *Diasporus* aff. *diastema* suggested by Batista et al. 2016), that are potential new species and, together with the recently described *Diasporus majeensis*, lack an assessment by the IUCN.

Our survey provides baseline information for exploration and conservation efforts by identifying species in the area requiring immediate assessment and conservation action (Table 1). Importantly, this study might also inform the delimitation of protected areas based on species with restricted distribution ranges. This is particularly relevant given the absence of biological reserves within this mountain range that are recognized by the national system of protected areas (Jaramillo et al. 2010), and the increasing deforestation pressure in the region (Parker et al. 2004). Lastly, considering the arrival of *Bd* to the Serranía de Majé some years after this study (Küng et al. 2014), the

baseline information provided by this inventory could potentially serve to determine *Bd*-induced changes in the amphibian community. In particular, at mid and high elevations, where disease-induced losses of amphibian diversity have been substantial in Central America, including Panamá (Lips 2016).

Acknowledgements

Thanks to Arquimedes Batista, Roberto Brenes, Jhoana De Alba, Edgardo J Griffith, Susanne Lanckowsky, Kirsten Nicholson, and Daedre Craig for their field assistance. To Guido C Berguido for his support with the logistics to work at the Reserva Natural Privada Cerro Chucantí, and to Fr Wally Kasuboski for providing housing at the Centro Cristo Misionero. This survey was possible thanks to the Committee for Research and Exploration of the National Geographic Society (grant number 8133-06). Also, thanks to the Autoridad Nacional del Ambiente (now, Ministerio de Ambiente) for the collecting/research permit No. SE/A-37-07. RI was supported by the Sistema Nacional de Investigación of Panamá, the Panamá Amphibian Rescue and Conservation Project, and Minera Panamá, during the preparation of the manuscript. The reviewers Raoni Rebouças Santos and Jiri Moravec helped to improve the manuscript.

References

AmphibiaWeb (2018) AmphibiaWeb. University of California, Berkeley. http://amphibiaweb.org [Accessed 17 September 2018]

Angher GR, Christian DG (2000) Distributional records from the highlands of the Serranía de Majé, an isolated mountain range in eastern Panamá. Bulletin-British Ornithologists Club 120: 173–178.

Batista A, Hertz A, Mebert K, Köhler G, Lotzkat S, Ponce M, Vesely M (2014a) Two new fringe-limbed frogs of the genus *Ecnomiohyla* (Anura: Hylidae) from Panamá. Zootaxa 3826: 449–25. https://doi.org/10.11646/zootaxa.3826.3.2

Batista A, Köhler G, Mebert K, Vesely M (2014b) A new species of *Bolitoglossa* (Amphibia: Plethodontidae) from eastern Panamá, with comments on other species of the *adspersa* species group from eastern Panamá. Mesoamerican Herpetology 1: 97–121. https://doi.org/10.11646/zootaxa.4039.1.2

Batista A, Köhler G, Mebert K, Hertz A, Vesely M (2016) An integrative approach to reveal speciation and species richness in the genus *Diasporus* (Amphibia: Anura: Eleutherodactylidae) in eastern Panamá. Zoological Journal of the Linnean Society 178: 267–311. https://doi.org/10.1111/zoj.12411

Cadena CD, Kozak KH, Gomez JP, Parra JL, McCain CM, Bowie RCK, Carnaval AC, Moritz C, Rahbek C, Roberts TE, Sanders NJ, Schneider ChJ, VanDerWal J, Zamudio KR, Graham CH (2011) Latitude, elevational climatic zonation and speciation in New World vertebrates. Proceedings of the Royal Society B: Biological Sciences 279: 194–201. https://doi.org/10.1098/rspb.2011.0720

Colwell RK, Mao CX, Chang J (2004) Interpolating, extrapolating, and comparing incidence-based species accumulation curves. Ecology 85(10): 2717–2727. https://doi.org/10.1890/03-0557

Colwell RK (2006) EstimateS: Statistical Estimation of Species Richness and Shared Species from Samples (Software and User´s Guide), Version 8.0. http://viceroy.eeb.uconn.edu/estimates

Crawford AJ, Ryan MJ, Jaramillo CA (2010a) A new species of *Pristimantis* (Anura: Strabomantidae) from the Pacific Coast of the Darien Province, Panamá, with a molecular analysis of its phylogenetic position. Herpetologica 66: 192–206. https://doi.org/10.1655/09-018R1.1

Crawford AJ, Lips KR, Bermingham E (2010b) Epidemic disease decimates amphibian abundance, species diversity, and evolutionary history in the highlands of Central Panamá. Proceedings of the National Academy of Sciences USA 107: 13777–13782. https://doi.org/10.1073/pnas.0914115107

Duque-Caro H (1990) The Choco Block in the northwestern corner of South America: structural, tectonostratigraphic, and paleogeographic implications. Journal of South American Earth Sciences 3: 71–84. https://doi.org/10.1016/0895-9811(90)90019-W

Holdridge LR (1967) Life Zone Ecology. Tropical Science Center, San Jose, 206 pp.

Hortal J, Borges PAV, Gaspar C (2006) Evaluating the performance of species richness estimators: sensitivity to simple grain size. Journal of Animal Ecology 75: 274–287. https://doi.org/10.1111/j.1365-2656.2006.01048.x

Ibáñez R, Arosemena FA, Solís FA, Jaramillo CA (1994) Anfibios y reptiles de la Serranía Piedras-Pacora, Parque Nacional Chagres. Scientia 9: 17–31.

Ibáñez R, Rand AS, Jaramillo CA (1999a) Los Anfibios del Monumento Natural Barro Colorado, Parque Nacional Soberanía y Areas Adyacentes / The Amphibians of Barro Colorado Nature Monument, Soberanía National Park and Adjacent Areas. Editorial Mizrachi & Pujol, Panamá, 187 pp. https://doi.org/10.1643/0045-8511(2000)000[0628:br]2.0.co;2

Ibáñez R, Rand AS, Ryan MJ, Jaramillo CA (1999b) Vocalizaciones de Ranas y Sapos del Monumento Natural Barro Colorado, Parque Nacional Soberanía y Areas Aledañas / Vocalizations of Frogs and Toads from Barro Colorado Nature Monument, Soberanía National Park and Adjacent Areas. Compact Disc. Sony Music Entertainment, Costa Rica. https://doi.org/10.1643/0045-8511(2000)000[0628:br]2.0.co;2

Ibáñez R, Condit R, Angehr G, Aguilar S, García T, Martínez R, Sanjur A, Stallard R, Wright SJ, Rand AS, Heckadon S (2002) An ecosystem report on the Panama Canal: monitoring the status of the forest communities and the watershed. Environmental Monitoring and Assessment 80: 65–95. https://doi.org/10.1023/a:1020378926399

Ibáñez R, Crawford AJ (2004) A new species of *Eleutherodactylus* (Anura: Leptodactylidae) from the Darién Province, Panamá. Journal of Herpetology 38: 240–243. https://doi.org/10.1670/12-03A

IGNTG (Instituto Geográfico Nacional "Tommy Guardia") (2007) Atlas Nacional de la República de Panamá. Novo Art, Panamá, 290 pp.

James TY, Toledo LF, Rödder D, Leite DS, Belasen AM, Betancourt-Román CM, Jenkinson TS, Lambertini C, Longo AV, Ruggeri J, Collins JP, Burrowes PA, Lips KR, Zamudio KR, Longcore JE (2015) Disentangling host, pathogen, and environmental determinants of a recently emerged wildlife disease: lessons from the first 15 years of amphibian chytridiomycosis research. Ecology and Evolution 5: 4079–4097. https://doi.org/10.1002/ece3.1672

Jaramillo CA, Wilson LD, Ibáñez R, Jaramillo F (2010) The herpetofauna of Panamá: Distribution and conservation status. In: Wilson LD, Twonsend JH, Johnson JD (Eds) Conservation of Mesoamerican Amphibians and Reptiles. Eagle Mountain Press, Eagle Mountain, Utah, 604–671.

Johnson JD, Mata-Silva V, Wilson LD (2015) A conservation reassessment of the Central American based on the EVS measure. Amphibian & Reptile Conservation 9: 1–94.

Kilburn VL, Ibáñez R, Sanjur O, Bermingham E, Suraci JP, Green DM (2011) Ubiquity of the pathogenic chytrid fungus, *Batrachochytrium dendrobatidis*, in anuran communities in Panamá. EcoHealth 7: 537–548. https://doi.org/10.1007/s10393-010-0634-1

Kozak KH, Wiens JJ (2010) Niche conservatism drives elevational diversity patterns in Appalachian salamanders. The American Naturalist 176: 40–54. https://doi.org/10.1086/653031

Küng D, Bigler L, Davis LR, Gratwicke B, Griffith E, Woodhams DC (2014) Stability of microbiota facilitated by host immune regulation: informing probiotic strategies to manage amphibian disease. PloS One 9(1): e87101–11. https://doi.org/10.1371/journal.pone.0087101

Lips KR (1999) Mass mortality and population declines of anurans at an upland site in western Panamá. Conservation Biology 13: 117–125. https://doi.org/10.1046/j.1523-1739.1999.97185.x

Lips KR, Brem F, Brenes R, Reeve JD, Alford RA, Voyles J, Carey C, Livo L, Pessier AP, Collins JP (2006) Emerging infectious disease and the loss of biodiversity in a Neotropical amphibian community. Proceedings of the National Academy of Sciences 103: 3165–3170. https://doi.org/10.1046/j.1523-1739.1999.97185.x

Lips KR (2016) Overview of chytrid emergence and impacts on amphibians. Philosophical Transactions of the Royal Society B 317: 20150465. https://doi.org/10.1098/rstb.2015.0465

Mittermeier RA, Myers N, Gil PR, Mittermeier CG (1999) Hotspots. CEMEX, Mexico City.

Myers CW (1969) The ecological geography of cloud forest in Panamá. American Museum Novitates 2396: 1–52.

Oksanen J, Blanchet FG, Friendly M, Kindt R, Legendre P, McGlinn D, Minchin PR, O'Hara RB, Simpson GL, Solymos P, Stevens MHH, Szoecs E, Wagner H (2017) vegan: Community Ecology Package. R package version 2.4–3. https://CRAN.R-project.org/package=vegan

Parker T, Carrion J, Samudio R (2004) Environment, biodiversity, water, and tropical forest conservation, protection, and management in Panamá: assessment and recommendations (biodiversity and tropical forestry assessment of the USAID/PANAMÁ Program). Washington, PA: Chemonics International Inc. Task Order# 824, BIOFOR IQC No. I-00-99-00014-00.

Pinto-Sánchez NR, Ibáñez R, Madriñán S, Sanjur OI, Bermingham E, Crawford AJ (2012) The Great American Biotic Interchange in frogs: multiple and early colonization of Central America by the South American genus *Pristimantis* (Anura: Craugastoridae). Molecular Phylogenetics and Evolution 62: 954–972. https://doi.org/10.1016/j.ympev.2011.11.022

R Core Team (2017) R: A language and environment for statistical computing. R Foundation for Statistical Computing, Vienna, Austria. URL https://www.R-project.org/

Rebollar EA, Hughey MC, Harris RN, Domangue RJ, Medina D, Ibáñez R, Belden LK (2014) The lethal fungus *Batrachochytrium dendrobatidis* is present in lowland tropical forests of far eastern Panamá. PLoS ONE 9: e95484–8. https://doi.org/10.1371/journal.pone.0095484

Rodríguez-Brenes S, Rodríguez D, Ibáñez R, Ryan MJ (2016) Spread of amphibian chytrid fungus across lowland populations of Túngara frogs in Panamá. PLoS ONE 11: e0155745–8. https://doi.org/10.1371/journal.pone.0155745

Rueda JV, Castro F, Cortez C (2006) Técnicas para el inventario y muestreo de anfibios: Una compilación. In: Angulo A, Rueda-Almonacid JV, Rodríguez-Mahecha JV, La Marca E (Eds) Técnicas de Inventario y Monitoreo para los Anfibios de la Región Tropical Andina. Conservación Internacional. Serie Manuales de Campo N°2. Panamericana Formas e Impresos SA, Bogotá, 135–171. https://doi.org/10.5479/10088/31959

Savage JM (2002) The Amphibians and Reptiles of Costa Rica: a Herpetofauna between Two Continents, between Two Seas. University of Chicago Press, Chicago, 934 pp. https://doi.org/10.1080/10635150490424619

Seutin G, White WN, Boag PT (1991) Preservation of avian blood and tissue samples for DNA analyses. Canadian Journal of Zoology 69: 82–90. https://doi.org/10.1139/z91-013

Sosa A, Guerrel J (2013) Riqueza, diversidad, y abundancia de anfibios en el bosque nuboso de Cerro Azul, sector Alto Chagres, Parque Nacional Chagres, Panamá. Tecnociencia 15: 57–75.

The IUCN Red List of Threatened Species (2018) Version 2018-1. www.iucnredlist.org [Downloaded on 23 September 2018]

Vanzolini PE, Heyer WR (1985) The american herpetofauna and the interchange. In: Stehli FG, Webb SD (Eds) The Great American Biotic Interchange. Plenum Press, New York, 475–487. https://doi.org/10.1007/978-1-4684-9181-4_18

Webb DS (2006) The Great American Biotic Interchange: patterns and processes. Annals of the Missouri Botanical Garden 93: 245–257. https://doi.org/10.3417/00266493(2006)93[245:tgabip]2.0.co;2

Whitfield SM, Lips KR, Donnelly MA (2016) Amphibian decline and conservation in Central America. Copeia 104: 351–379. https://doi.org/10.1643/CH-15-300

Wiens JJ, Graham CH, Moen DS, Smith SA, Reeder TW (2006) Evolutionary and ecological causes of the latitudinal diversity gradient in hylid frogs: treefrog trees unearth the roots of high tropical diversity. The American Naturalist 168: 579–596. https://doi.org/10.2307/3873455

Supplementary material 1

Table S1. List of voucher specimens collected at the three surveyed sites along the altitudinal gradient in the Serranía de Majé

Authors: Daniel Medina, Roberto Ibáñez, Karen R. Lips, Andrew J. Crawford

Data type: specimen list.

Explanation note: The list includes taxonomy of voucher specimens and collection number, date and locality data. CH = Collection of Herpetology, AJC = Andrew J. Crawford field tag, and MVUP = Museo de Vertebrados de la Universidad de Panamá.

Link: https://doi.org/10.3897/zookeys.859.32869.suppl1

ZooKeys 859: 131–158 (2019)
doi: 10.3897/zookeys.859.33634
http://zookeys.pensoft.net

RESEARCH ARTICLE

A peer-reviewed open-access journal
ZooKeys
Launched to accelerate biodiversity research

Call a spade a spade: taxonomy and distribution of *Pelobates*, with description of a new Balkan endemic

Christophe Dufresnes[1,2,3], Ilias Strachinis[4], Elias Tzoras[5], Spartak N. Litvinchuk[6,7], Mathieu Denoël[8]

1 *Laboratory for Conservation Biology, University of Lausanne, 1015 Lausanne, Switzerland* **2** *Hintermann & Weber SA, Avenue des Alpes 25, 1820 Montreux, Switzerland* **3** *Department of Animal and Plant Sciences, University of Sheffield, Alfred Denny Building, Western Bank, S10 2TN Sheffield, United Kingdom* **4** *School of Biology, Aristotle University of Thessaloniki 54124 Thessaloniki, Greece* **5** *26442 Patra, Achaia, Greece* **6** *Institute of Cytology, Russian Academy of Sciences, Tikhoretsky pr. 4, St. 194064 Petersburg, Russia* **7** *Department of Zoology and Physiology, Dagestan State University, Gadzhiyev str. 43-a, 336700 Makhachkala, Dagestan, Russia* **8** *Laboratory of Fish and Amphibian Ethology, Behavioural Biology Group, Freshwater and OCeanic science Unit of reSearch (FOCUS), University of Liège, Liège, Belgium*

Corresponding author: *Christophe Dufresnes* (christophe.dufresnes@hotmail.fr)

Academic editor: *Angelica Crottini* | Received 4 February 2019 | Accepted 10 June 2019 | Published 2 July 2019

http://zoobank.org/5E2B8623-A309-4EF6-9123-B95F04C5A88E

Citation: Dufresnes C, Strachinis I, Tzoras E, Litvinchuk SN, Denoël M (2019) Call a spade a spade: taxonomy and distribution of *Pelobates*, with description of a new Balkan endemic. ZooKeys 859: 131–158. https://doi.org/10.3897/zookeys.859.33634

Abstract

The genomic era contributes to update the taxonomy of many debated terrestrial vertebrates. In an accompanying work, we provided a comprehensive molecular assessment of spadefoot toads (*Pelobates*) using genomic data. Our results call for taxonomic updates in this group. First, nuclear phylogenomics confirmed the species-level divergence between the Iberian *P. cultripes* and its Moroccan relative *P. varaldii*. Second, we inferred that *P. fuscus* and *P. vespertinus*, considered subspecies until recently, feature partial reproductive isolation and thus deserve a specific level. Third, we evidenced cryptic speciation and diversification among deeply diverged lineages collectively known as *Pelobates syriacus*. Populations from the Near East correspond to the Eastern spadefoot toad *P. syriacus* sensu stricto, which is represented by two subspecies, one in the Levant (*P. s. syriacus*) and the other in the rest of the range (*P. s. boettgeri*). Populations from southeastern Europe correspond to the Balkan spadefoot toad, *P. balcanicus*. Based on genetic evidence, this species is also polytypic: the nominal *P. b. balcanicus* inhabits the Balkan Peninsula; a new subspecies *P. b. chloeae* **ssp. nov.** appears endemic to the Peloponnese. In this paper, we provide an updated overview of the taxonomy and distribution of all extant *Pelobates* taxa and describe *P. b. chloeae* **ssp. nov.**

Keywords
Amphibian, Palearctic, *Pelobates balcanicus*, *Pelobates balcanicus chloeae*, *Pelobates vespertinus*, Pelobatidae, phylogenomics, phylogeography, spadefoot toad

Introduction

The revolution initiated by high-throughput sequencing techniques has reached the field of phylogeography (Coates et al. 2018), where it lifts the veil on cryptic species and solves long-term taxonomic issues (e.g. Rodriguez et al. 2017; Psonis et al. 2018; Dufresnes et al. 2018, 2019a). We conducted such study in spadefoot toads from the monotypic family Pelobatidae Bonaparte, 1850 (genus *Pelobates* Wagler, 1830) endemic to the Western Palearctic (Dufresnes et al. 2019b). These grassland species typically inhabit soft (e.g. sandy) soils with freshwater ponds for breeding and have a semi-fossorial lifestyle, thanks to well-known adaptations such as metatarsal spades (to dig themselves in) and a strongly ossified skull (to dig themselves out) (Székely et al. 2017; Dufresnes 2019). They are threatened in many parts of their fragmented ranges due to land-use changes, wetland destruction, pollution, species introduction, and ongoing changes in climate, which already led to population extinctions and contractions of geographic ranges (Nyström et al. 2002, 2007; Džukić et al. 2005; Eggert et al. 2006). Mediterranean regions, where most of the diversity is located (Litvinchuk et al. 2013; Dufresnes et al. 2019b), could be particularly threatened (Iosif et al. 2014).

Until recently, *Pelobates* included four recognized extant species. First, the sister taxa *P. cultripes* (Cuvier, 1829) and *P. varaldii* Pasteur & Bons, 1959 are found north and south of the Strait of Gibraltar, respectively (Busack et al. 1985). Second, the western and eastern sister taxa *P. fuscus* (Laurenti, 1768) and *P. vespertinus* (Pallas, 1771) were long considered subspecies (e.g. Crottini et al. 2007), but their narrow transition is rather consistent with a species level (Litvinchuk et al. 2013). Third, Mediterranean populations from the Near East and the Balkans are commonly referred to as *P. syriacus* Boettger, 1889 and split as two subspecies: *P. syriacus syriacus* in Asia Minor and *P. syriacus balcanicus* Karaman, 1928 in the Balkans, based on morphological (Uğurtas et al. 2002) and scattered phylogenetic data (Veith et al. 2006; Litvinchuk et al. 2013; Ehl et al. 2019).

Our accompanying paper (Dufresnes et al. 2019b) revisits the evolution of this group, with several taxonomic implications. First, phylogenomics confirmed the old split between *P. cultripes* and *P. varaldii*, previously identified with mtDNA (Garcia-Paris et al. 2003; Veith et al. 2006; Crottini et al. 2007) and allozyme markers (Busack et al. 1985; Litvinchuk et al. 2013). Second, hybrid zone analyses support the conclusions of Litvinchuk et al. (2013) that *P. fuscus* and *P. vespertinus* deserve a specific status. Third, *P. syriacus* represents two cryptic species respectively distributed in the Near East and the Balkans, then corresponding to *P. syriacus* and *P. balcanicus*. Fourth, these species feature deep intraspecific divergence, worthy of subspecific status. This is the case between Levantine and Anatolian/Caucasian populations in *P. syriacus*, and between the northern Balkans and Peloponnese in *P. balcanicus*.

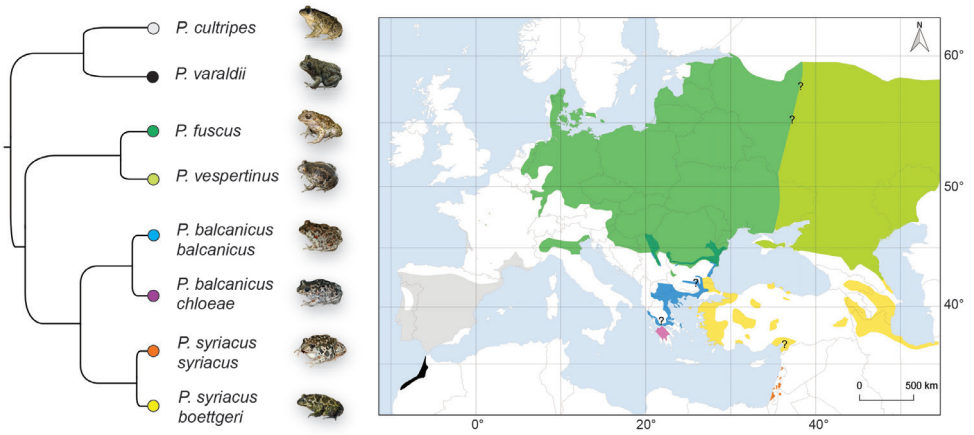

Figure 1. Phylogeny and distribution of *Pelobates* taxa. The tree is adapted from the phylogenomic analysis of Dufresnes et al. (2019b), and the map was built from known records updated with genetic data (see accounts). Note that the distribution of *P. vespertinus* extends further east to Kazakhstan and Siberia. Photo credits: CD (*P. cultripes*, *P. b. chloeae*), SNL (*P. s. boettgeri*), IS (*P. b. balcanicus*), A Sanchez Vialas (*P. varaldii*), A Nöllert (*P. fuscus*), N Suriadna (*P. vespertinus*).

In this paper, we integrate these recent findings into an updated overview of the *Pelobates* radiation, including comparative diagnosis, current taxonomy, distribution, and diversity of the resulting eight extant taxa (Fig. 1). Last but not least, we describe the newly discovered clade from Peloponnese as a subspecies of *P. balcanicus*.

Material and methods

Nomenclatural search

In order to attribute names to the newly documented *Pelobates* species and subspecies, we examined nomina available in the literature. To this end, we first referred to the Amphibian Species of the World online database (Frost 2019) and subsequently reviewed all the original references available.

Diagnosis

We reviewed phenotypic (coloration, morphology) and genetic (genome size, karyotype, and sequence divergence) variation of the considered taxa. Coloration is illustrated by high-quality photographs of known geographic origins, taken by us and credited photographers. Besides detailing general characteristics, we compiled a dataset of snout-vent length (SVL) from published studies (Suppl. material 1, Table S1), consisting of average SVL (computed separately for males and females) from 82 populations, totaling

6,004 individuals at least, and representing all taxa expect the narrowly distributed *P. s. syriacus* and *P. b. chloeae* (Suppl. material 1, Table S1). We report the ranges (minimum-maximum) and average values for each sex separately, and illustrate interpopulation variation by boxplots. We statistically tested differences among taxa and sex by a two way analysis of variance (ANOVA) in *R*. We then performed comparisons between species using a Tukey test. Finally, we tested sex-specific differences within taxa for which measures of both sexes were available in at least five populations, by paired *t*-tests.

We briefly described the karyotype of each taxon based on the literature and further report nuclear DNA content as a proxy to genome size, obtained from flow cytometry. In addition, sequence divergence, available from our phylogeographic study (Dufresnes et al. 2019b), are provided between each pair of taxa, based on mitochondrial (*cyt-b* + 16S, 1.2 kb) and nuclear DNA (63.5 kb of RAD tags).

Distribution

We detailed the distribution of each *Pelobates* taxon, based on available literature, i.e. national and regional atlas, as well as scientific articles informative of distribution. Boundaries between cryptic taxa were inferred from genetic studies, and thus remain unclear for parapatric ranges for which no molecular survey has been conducted. Distribution layers were originally obtained from the IUCN Red List of Threatened Species (https://www.iucnredlist.org/), and meticulously reshaped with the drawing tools of ArcMap 10.3.

Description of *Pelobates balcanicus chloeae* sp. nov.

In order to describe the new *P. balcanicus* subspecies from southern Greece, we conducted a short fieldwork expedition to the only recently confirmed locality of this taxon, Strofylia meadows in Peloponnese (38.1239°N, 21.3858°E) on December 2018. Collection of live animals was authorized by permit ΑΔΑ: ΩΣΜ34653Π8-9ΣΟ issued by the Greek Ministry of Environment, Energy and Climate Change. *Pelobates* usually breed during spring (March–April) in this area but are active all-year round providing proper weather conditions. A total of 18 individuals could be captured in the evening of December 10th, under heavy rains. The largest 12 individuals (putatively adults) were measured for 11 standard morphometric variables, i.e. SVL: snout-vent length; HW: head width; HL: head length; ED: eye diameter; EE: inter-eye distance; NN: inter-nostril distance; EN: eye-nostril distance; ML: metatarsal tubercle length; MH: metatarsal tubercle height; HLL: hind leg length; TTL: tibia + tarsus length. HLL and TTL were measured with a ruler (1 mm precision); all other variables were measured with a digital caliper (0.1 mm precision). For the sake of comparison, only one of us (IS) measured all individuals. Note that we did not discriminate the sex of individuals as it was unclear whether all specimens were adults.

Toads were subsequently released at their place of capture, except for two females that were chosen as holotype and paratype, sent to the Natural History Museum of Crete (NHMC). Our choice for a small type series was bounded by the rarity of this taxon, so far confirmed from a single locality, with unknown population trends.

Results and discussion

We updated the distributions and taxonomy of Eurasian spadefoot toads (genus *Pelobates*). Following recent molecular results (Dufresnes et al. 2019b), a total of eight extant clades are distinguished. Six of them correspond to species level divergences, given their confirmed or putative reproductive isolation, as inferred from hybrid zone analyses, which make ad hoc tests to evaluate where two lineages stand along the speciation continuum (Singhal and Moritz 2013; Dufresnes et al. 2019b). The remaining intraspecific lineages are accordingly treated as subspecies, because they featured extensive admixture and thus seem to lack reproductive barriers.

From our SVL dataset, there was a significant global effect of species ($P < 0.001$) but not of sex ($P = 0.08$), neither of their interaction ($P = 0.42$) (two way ANOVA). The species effect was mainly due to differences between the large *P. cultripes*, *P. syriacus*, and *P. balcanicus* versus the smaller *P. varaldii*, *P. fuscus*, and *P. vespertinus*: all pairwise comparisons between these two groups were significant ($P < 0.001$), but none within groups ($P > 0.05$) (Tukey test). Females were significantly larger than males in *P. cultripes* ($P = 0.002$, $n = 16$ populations with both sexes), *P. fuscus* ($P < 0.001$, $n = 21$), but not in *P. balcanicus* ($P = 0.58$, $n = 15$) (paired *t*-test). Sample size precluded similar analyses in the remaining taxa.

The following present accounts for each taxon. We could successfully access the original literature for all but one description, and herein report the primary information as it was published. The only exception is *Pelobates praefuscus* Khosatzky, 1985, and we rely on Frost (2019) for its information. Phylogeny and distributions of extant *Pelobates* are shown in Figure 1, sizes and color variation are displayed in Figure 2, and Figures 3 and Figures 4, respectively.

Pelobates cultripes (Cuvier, 1829)

Western spadefoot

Diagnosis. The largest *Pelobates* species, *P. cultripes* differs from the other Eurasian spadefoots by metatarsal spades being entirely black and a flat skull. Sizes largely overlap between sexes although males are generally smaller than females (Fig. 2). The background coloration can be yellow, gray, or brown, reticulated by dark patches; it typically lacks orange spots (Fig. 3). Average SVL = 74 mm (range: 32–105 mm) for females ($n = 16$ populations) and 71 mm (34–93 mm) for males ($n = 17$ populations) (Suppl. material 1, Table S1; Fig. 2). The karyotype consists of six large and seven small (i.e. <

6% of total length) pairs of two-armed chromosomes (Morescalchi 1967, 1971; Morescalchi et al. 1977; Schmid et al. 1987; Herrero and Talavera 1988). Large centromeric C-bands appears in pairs 1, 2, 4, 9, and 12; pericentric bands in the short arm of pair 1 and the long arm of pair 8; telomeric bands in the long arms of pairs 1, 2, and 11; the short arm of pair 7 is almost heterochromatic (Herrero and Talavera 1988). Nucleolus organizers (NORs) are in the short arm of pair 7 (Schmid et al. 1987). The nuclear DNA content averages 7.4 pg (Litvinchuk et al. 2013).

Taxonomy. First named ***Rana cultripes*** **Cuvier, 1829**; holotype: MNHNP 0.4554; type locality: "notre midi", corresponds to southern France, as noted by Mertens and Müller (1928). Two junior synonyms. ***Rana calcarata*** **Michahelles, 1830**; type locality: "prope Malagam" (near Malagam), probably Malaga, Spain; type(s): not mentioned. ***Cultripes provincialis*** **Müller, 1832**; type locality: "Provence" (meridional France), France; type(s): not designated, but the author refers to *Rana cultripes* from Paris (MNHN). First mentioned as *Pelobates cultripes* by Tschudi (1838).

Distribution. The species inhabits south-western Europe (0–1770 m elevation a.s.l.) (Sillero et al. 2014; Beja et al. 2009) (Fig. 1). Its main distribution spans across the Iberian Peninsula, where it occurs roughly everywhere in suitable habitats south of the Cantabrian Mountains and Pyrenees (Lizana 1997; Malkmus 2004). It is yet absent from the south-eastern tip of Spain (Lizana 1997). In France, it is present only along the Atlantic coast, from the Landes region to the Loire River, and along the Mediterranean Sea, from the Spanish border to the Var Department, reaching the area of Valence in the Rhone Valley. Some isolates exist also in south-western France (Thirion and Cheylan 2012). IUCN status: Near Threatened (Beja et al. 2009).

Diversity. Combining mtDNA and microsatellite data, Gutiérrez-Rodriguez et al. (2017) identified three closely-related mtDNA haplogroups (see also Crottini et al. 2010) in the southern, western / northwestern, and northeastern parts of the range, which are mirrored by equivalent nuclear clusters that widely admix. Most of the genetic diversity of this species is found in southern ranges, where climate conditions remained stable through the last ice ages (Gutiérrez-Rodriguez et al. 2017).

Pelobates varaldii Pasteur & Bons, 1959

Moroccan spadefoot

Diagnosis. A smaller version of *P. cultripes* (Fig. 2) differing by a few phenotypic features. Unlike *P. cultripes*, the black coloration of the spades is often concentrated on the edges (Pasteur and Bons 1959; Busack et al. 1985). The cranial braincase is high and narrow in *P. varaldii*, while it is low and wide in *P. cultripes* (Pasteur and Bons 1959; Roček 1981). The background coloration can be yellow, gray, and brown, with dark reticulate patches, and the dorsal surface is abundantly covered by orange dots, most pronounced on the eyelids (usually absent in *P. cultripes*; Pasteur and Bons 1959; Beukema et al. 2013; Fig. 3). Males are usually smaller than females (Fig. 2). Average SVL = 53 mm (range: 36–66 mm) for females (n = 4 populations) and 51 mm

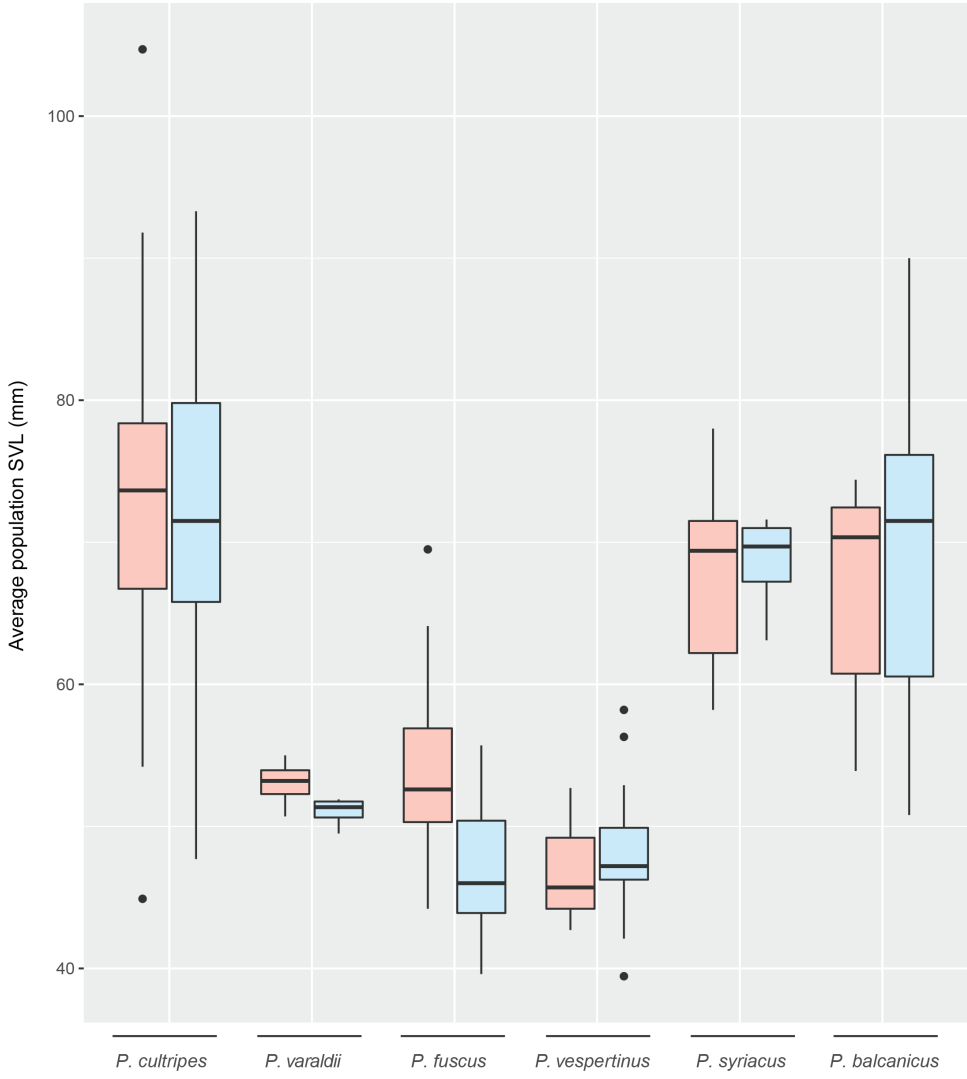

Figure 2. Between-population variation of average size (snout–vent length – SVL) for each *Pelobates* species, measured separately for females (pink) and males (blue). This compiles average size-data from 82 populations, representing at least 6,004 individuals (Suppl. material 1, Table S1). For *P. balcanicus*, it only includes populations from the nominal *P. b. balcanicus*. For *P. syriacus*, it only includes populations from *P. s. boettgeri*.

(33–65 mm) for males (n = 4 populations) (Suppl. material 1, Table S1; Fig. 2). The karyotype includes six large and seven small pairs of two-armed chromosomes. Large centromeric C-bands appears in the pairs 1, 2, 4, 9, and 12; pericentric bands in the short arms of pair 1 and long arm of pair 8; telomeric bands in the long arms of pairs 1, 2, and 11; the short arm of pair 7 is almost heterochromatic (Herrero and Talavera 1988). The nuclear DNA content averages 7.3 pg (Litvinchuk et al. 2013). As shown

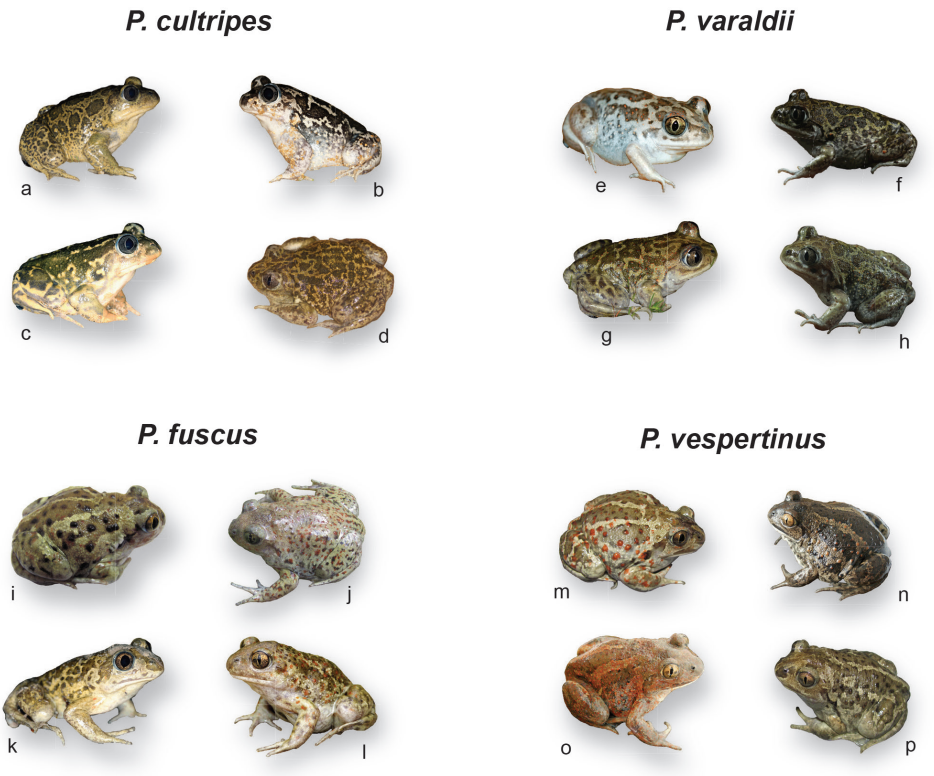

Figure 3. Color variation in *Pelobates cultripes*, *P. varaldii*, *P. fuscus* and *P. vespertinus*. Photo credits and origins as follows **a** CD (Hérault, France) **b, c** CD (Algarve, Portugal) **d** A Sanchez Vialas (Spain) **e** G Martinez (Kenitra, Morocco) **f–h** A Sanchez Vialas (Tanger, Morocco) **i, j** N Suriadna (Ukraine) **k** CD (Wojewodztwo podkarpackie, Poland) **l** A Nöllert (Burgenland, Austria) **m–p** N Suriadna (Ukraine).

in Table 1, *P. varaldii* differs from *P. cultripes* by 6.0% at mtDNA and 0.40% at nuclear DNA (Dufresnes et al. 2019b).

Taxonomy. The nomen ***Pelobates varaldii* Pasteur & Bons, 1959** is the only one ever proposed for the Moroccan populations of spadefoot toads; holotype: MNHN-RA-1959.1; type locality: Merja Samora, Morocco. The ancient split of *P. varaldii*, dating back to the Messinian Salinity Crisis (5.3 My), supports its specific distinction from *P. cultripes* (Busack et al. 1985; Crottini et al. 2007).

Distribution. It is endemic to north-western Morocco (0–350 m elevation a.s.l.), found along the Atlantic coast, from the south of Tanger to Oualidia, where it is rare (de Pous et al. 2012; Beukema et al. 2013; Frost 2019). IUCN status: Endangered (Salvador et al. 2009).

Diversity. To our knowledge, *P. varaldii* has not been the focus of any phylogeographic or population genetic work.

***Pelobates fuscus* (Laurenti, 1768)**
Common spadefoot

Diagnosis. Small spadefoot characterized by pale grayish metatarsal spades and a domed skull. The webbing of the hindfeet is well developed. Males are smaller than females (Fig. 2). The species can be found in a spectrum of gray, brown, or yellowish colors, but rarely greenish (P. Székely pers. comm.), and features patterns such as stripes or blotches of varying sizes; variable presence of orange dots, from almost absent to very abundant (Fig. 3). In Eastern Europe, it differs from its sister species *P. vespertinus* by most individuals having numerous dark rounded spots on a light dorsum (Suriadna et al. 2016) and lacking a dark stripe between the eyes (Lada et al. 2005). Average SVL = 54 mm (range: 37–78 mm) for females (n = 21 populations) and 47 mm (36–65 mm) for males (n = 21 populations) (Suppl. material 1, Table S1; Fig. 2). The karyotype consists of seven large and six small pairs of two-armed chromosomes (Mészáros 1973; Schmid et al. 1987; Manilo and Radchenko 2004; Manilo and Manuilova 2013; Suriadna 2014). Centromeric C-bands are obvious in pairs 2, 6, and 7–13 (Schmid et al. 1987). NORs are in the short arm of pair 7 (Schmid 1980, 1982). The nuclear DNA content (calculated from flow cytometry) averages 8.7–9.0 pg (Litvinchuk et al. 2013).

Taxonomy. Originally described as ***Bufo fuscus* Laurenti, 1768**; type locality: not specifically designated ("in paludibus, rarissime hospitantur in continenti", in swamps, rarely on the land); type(s): the specimens depicted by Rösel von Rosenhof (1758: pls XVII, XVIII), expressively cited by Laurenti (1768); although controversial (see Nöllert et al. 2012; Frost 2019), the additional mention of pl. XV (p. 122), a drawing of a dissected *Pelophylax*, could simply be an error. Rösel depicted the amphibians of Germany, and Shaw (1802) accordingly mentioned that Rösel found his specimens in the neighborhood of "Nurenberg" (Nürnberg), Germany, which could then apply as the type locality. Seven junior synonyms. ***Rana alliacea* Shaw, 1802**; type locality: not specifically designated, but Shaw (1802) refers to Rösel's toads from Nürnberg, Germany; type(s): the toad illustrated by the author (pl. 41), which may very well corresponds to the amplexed female on the top right of pl. XVII in Rösel von Rosenhof (1758), of identical posture and color patterns. ***Bombinator marmorata* Sturm, 1828**; type locality: near Penig, Germany; holotype: the frog illustrated by the author. ***Cultripes minor* Müller, 1832**; type locality: "unbekannt" (unknown); type(s): not mentioned. ***Pelobates fuscus* var. *lividis* Koch, 1872**: type locality: "von den Wiesen in der Nähe des Röder-Wäldchens bei Frankfurt" (the meadows in the Röder groove near Frankfurt), Germany; type(s): not mentioned; ***Pelobates insubricus* Cornalia, 1873**; type locality: nearby Milano, Italy; type(s): not mentioned, most likely deposited at MSNM, but presumably lost since (Blackburn and Scali 2014). ***Pelobates latifrons* Herón-Royer, 1888**; type locality: "environ de Turin" (nearby Torino), Italy; type(s): not mentioned. ***Pelobates praefuscus* Khosatzky, 1985**; type locality: Etuliya, Moldova; holotype: ZISP 21N RNA M-1, a Pliocene fossil (according to Frost 2019).

The Italian populations, for long considered as a subspecies *P. f. insubricus*, have been a matter of debate until recently because they bear private mtDNA haplotypes (Crottini et al. 2007). Litvinchuk et al. (2013) synonymized this taxon with *P. fuscus*, given the weak divergence of these haplotypes, together with the lack of differentiation of allozyme and genome content. As it stands, *P. fuscus* should thus be considered a monotypic taxon.

Distribution. Widespread distribution in western, central and eastern Europe (0–810 m elevation a.s.l.), but absent from the northern European countries and most of southern Europe (Sillero et al. 2014; Nöllert at al. 2012) (Fig. 1). In the west, it reaches the eastern edge of the Netherlands (Creemers and Van Delft 2009), the eastern part of Flanders in Belgium (Bauwens and Claus 1996), the western parts of Nordrhein-Westfalens and the south-east of Rheinland-Pflaz in Germany (Bitz et al. 1996; Chmela and Kronshage 2011), the north-eastern side of France (particularly along the Rhine River, Eggert and Vacher 2012). In the north, it extends to northern Netherlands (Creemers and Van Delft 2009), the North Sea coastline of Germany (Nöllert and Günther 1996) and Denmark, the south of Sweden, as well as the coastline of the Baltic Sea from Germany to Estonia, and eastward until it reaches *P. vespertinus* in Russia (Kuzmin 1999; Nyström et al. 2007; Litvinchuk et al. 2013; Sillero et al. 2014). The contact zone with the latter is well delineated from the Kursk region in Russia to the Black Sea coast (Dufresnes et al. 2019b). From there, it is present westward along the Black Sea coast of Ukraine to north-eastern Bulgaria (Kuzmin 1999; Stojankov et al. 2011). The southern edges extend along the Danube at the borders of Romania and Bulgaria (Stojankov et al. 2011) and across Serbia (Vukov et al. 2013), eastern Croatia, northern Bosnia and Herzegovina, Slovenia (Džukić et al. 2008, Curić et al. 2018), northern and eastern Austria around the Alps (Cabela et al. 2001), and southern Germany (Nöllert and Gunther 1996). The species is also present in a large area of northern Italy, especially in the Po Valley (Andreone 2006). Last, isolated populations persist in central France (Indre, Loiret, Indre-et-Loire: Eggert and Vacher 2012) and western Bulgaria (around Sofia: Stojankov et al. 2011). IUCN Status: Not Evaluated, considered Least Concern when grouped with *P. vespertinus* (Agasyan et al. 2009a). Declines have been reported for more than a century in various parts of Europe, which have caused a regression of the distribution limits (Džukić et al. 2005; Eggert et al. 2006).

Diversity. The phylogeographic work by Crottini et al. (2007) and Litvinchuk et al. (2013) characterized two refugial groups for this species (as the "western lineage of *P. fuscus*"), based on shallow mtDNA divergence and allozyme differentiation: in the Balkans/northern Italy and on the western shores of the Black Sea coast. This seems supported by weak genomic differentiation among Central-European samples (Dufresnes et al. 2019b). The refugial areas bear nearly all the genetic diversity of the species, which was lost in the derived northern populations, following post-glacial colonizations (Eggert et al. 2006).

***Pelobates vespertinus* (Pallas, 1771)**
Pallas' spadefoot

Diagnosis. Morphologically close to its sister species *P. fuscus*, it similarly features pale metatarsal spades and a domed skull. The coloration also spans the gray-yellowish-brownish spectrum, including reddish individuals (Fig. 3); orange dots can be heavily marked or absent (Fig. 3). It differs from *P. fuscus* by most individuals having three light longitudinal stripes on the dorsum (Suriadna et al. 2016), as well as a dark stripe between the eyes (Lada et al. 2005). Sexes of similar size (Fig. 2). Average SVL = 47 mm (range: 29–59 mm) for females (n = 3 populations) and 48 mm (29–61 mm) for males (n = 12 populations) (Suppl. material 1; Table S1, Fig. 2). The karyotype consists of seven large and six small pairs of two-armed chromosomes (Manilo and Manuilova 2013; Suriadna 2014). NORs (secondary constrictions) are in the short arm of pair 7 (Manilo and Radchenko 2008). The nuclear DNA content averages 9.2–9.4 pg (Litvinchuk et al. 2013). As shown in Table 1, *P. vespertinus* differs from *P. fuscus* by 2.5% at mtDNA and 0.13% at nuclear DNA (Dufresnes et al. 2019b). The genome of *P. vespertinus* is about 5% larger than *P. fuscus* (Borkin et al. 2001; Litvinchuk et al. 2013; Suriadna 2014).

Taxonomy. Originally named ***Rana vespertina* Pallas, 1771**; type locality: not specifically designated, but the author mentioned this taxon in Zarbay Creek ("Bach Sarbei", Samara oblast), Russia, which can be considered as the type locality; type(s): not mentioned. Three junior synonyms. ***Pelobates fuscus* var. *orientalis* Severtsov, 1855**; type locality: "Voronezhskaya Gubernia" (Voronezh governorate), Russia; type(s): not mentioned. ***Pelobates campestris* Severtsov, 1855**; type locality: between Bityug, Don and Ikorets rivers in today's Voronezh province, Russia; type(s): not mentioned. ***Pelobates borkini* Zagorodniuk, 2003**; proposed for the eastern form of *P. fuscus* but nomen nudum because neither a type specimen nor a type locality were designated (Zagorodniuk 2003). *Pelobates vespertinus* was previously considered a subspecies of the common spadefoot, as *Pelobates fuscus vespertinus* (Crochet and Dubois 2004). The significant divergence (~2–3 My) and restricted admixture with *P. fuscus*, consistent with reproductive isolation, both support the distinction of *P. vespertinus* as a separate species (Litvinchuk et al. 2013; Dufresnes et al. 2019b), as also proposed from genome size differences (Suriadna 2014).

Distribution. A lowland species (0–830 m elevation a.s.l.) widespread from the contact zone with *P. fuscus*, to western Siberia and Kazakhstan, and along the Ural River (Kuzmin 1999) (Fig. 1). However, the exact limits with *P. fuscus* are not known in the northern 700 km of the distribution range. Detailed genetic data showed that the transition extends between the Kursk region to southern Ukraine (Litvinchuk et al. 2013; Dufresnes et al. 2019b). In the south, it is present along the Sea of Azov coast to the northern Caucasus (Kuzmin 1999; Suriadna et al. 2016). Spadefoot populations in the Crimea are attributed to *P. vespertinus* (Litvinchuk et al. 2013). The southernmost

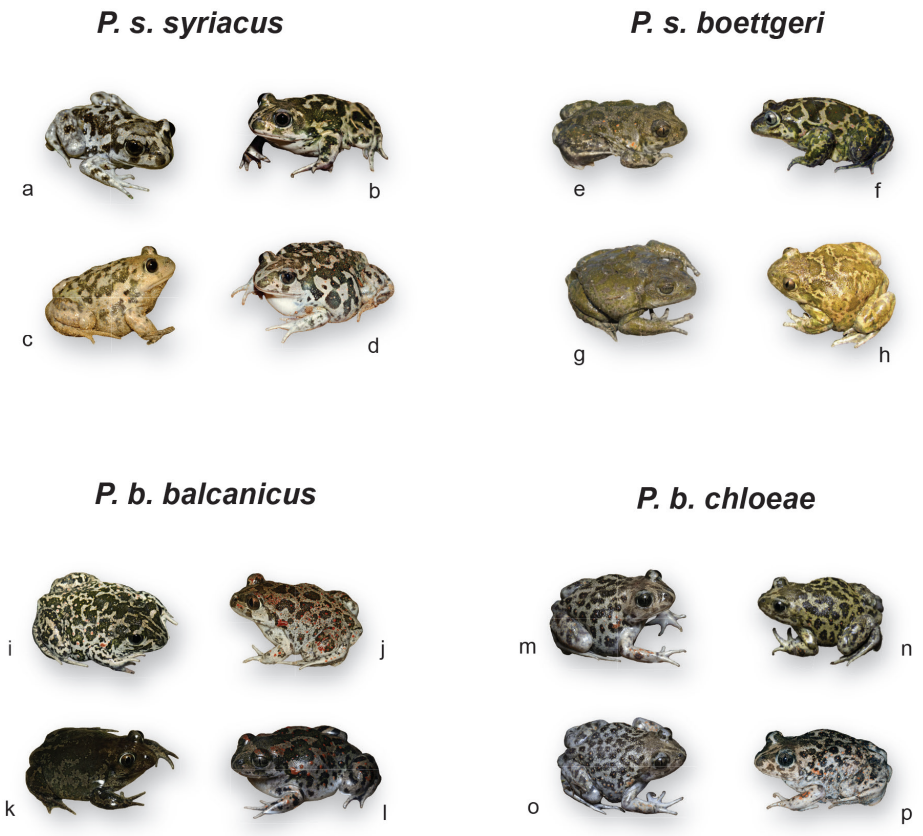

Figure 4. Color variation in *Pelobates syriacus* and *P. balcanicus*. Photo credits and origins as follows **a, b** G Hamoivitch (Israël) **c** R Winkler (Israël) **d** G Martinez (Israël) **e** IS (Limnos, Greece) **f** SNL (European Turkey) **g** IS (Limnos, Greece) **h** A Nöllert (Dagestan, Russia) **i** MD (Danube Delta, Romania) **j** IS (Thrace, Greece) **k** IS (Macedonia, Greece) **l** IS (Evia, Greece) **m–o** IS (Peloponnese, Greece) **p** CD (Peloponnese, Greece).

populations are in Dagestan, where it is sympatric with *P. syriacus* (Mazanaeva and Askenderov 2007). IUCN Status: Not Evaluated, as *P. vespertinus* was previously included in the *P. fuscus* assessment.

Diversity. Crottini et al. (2007) and Litvinchuck et al. (2013) provided detailed phylogeographic accounts for this species (as the "eastern lineage of *P. fuscus*"), which consists of a homogenous clade that expanded from a single glacial refugia located in the eastern shores of the Sea of Azov. *Pelobates vespertinus* forms a narrow hybrid zone (< 20 km) with *P. fuscus* in eastern Ukraine/western Russia (Litvinchuk et al. 2013; Dufresnes et al. 2019b).

***Pelobates syriacus* Boettger, 1889**
Eastern spadefoot

Diagnosis. Large spadefoot with whitish metatarsal spades and a flat skull. Webbing of the hind feet less developed than in *P. fuscus* and *P. vespertinus*. Sexes of similar size (Fig. 2). Coloration can be gray, yellow, greenish but rarely brown; orange dots often present, but not as abundant and marked as in some individuals of *P. fuscus*, *P. vespertinus*, or *P. balcanicus* (Fig. 4). Based on populations of *P. syriacus boettgeri*, average SVL = 68 mm (range: 40–92) for females (n = 5 populations) and 69 mm (57–83 mm) for males (n = 4 populations) (Suppl. material 1, Table S1; Fig. 2). The karyotype consists of seven large and six small pairs of two-armed chromosomes (Uğurtaş et al. 2001, from *P. s. boettgeri*). Centromeric C-bands are obvious in pairs 8 and 10 and telomeric Q-bands in the long arms of pairs 9 and 10 (Schmid 1979; Schmid et al. 1987). NORs are in the short arm of pair 7 (Schmid 1982; Schmid et al. 1987). The nuclear DNA content averages 8.2 pg (Litvinchuk et al. 2013; data from *P. s. boettgeri*).

Taxonomy. Described from the Levant region as ***Pelobates syriacus* Boettger, 1889**; type locality: "Haiffa in Syrien" (Haifa), Israel; type: SMF 1437.1a (Boettger 1892), subsequently designated as lectotype SMF 1722 (Mertens 1967). Other nomina proposed apply to *P. s. boettgeri* and *P. balcanicus* (see below).

Distribution. Scattered distribution; mainly present in the Middle East with 0–2000 m elevation a.s.l. (Agasyan et al. 2009b; Uğurtas 2001; Džukić et al. 2008; Sofianidou 2012) (Fig. 1). The nominate subspecies *P. syriacus syriacus* inhabits the southern part of the distribution in the Levant, from the Syrian coast at the border of Lebanon to the southern Israeli coast, as well as in south-western Syria (Boettger 1889; Munwes et al. 2010; Sofianidou 2012). It may be extinct from western Jordan (Agasyan et al. 2009b; Disi and Amr 2010). The subspecies *P. syriacus boettgeri* occupies the remaining ranges. In the west, it is present in western Turkey and along the Aegean coastline. It also occurs in European Turkey and probably southeastern Bulgaria. Alternatively, the latter populations could belong to *P. balcanicus*, notably along the Maritsa River, and identification is pending molecular analyses. The presence of *P. syriacus* is also documented on the Greek islands of Limnos, Lesbos, and Kos (Sofianidou 2012; Strachinis and Roussos 2016). Its central distribution is poorly known and therefore not well delineated, with several isolates described in Turkey, both along the Black and Mediterranean sea coasts, as well as the central parts of Anatolia. In the northeast, *P. syriacus* reaches the southern slopes of the Caucasus, from Georgia to Azerbaijan. The northernmost records are in Dagestan, on the west coast of the Caspian Sea, where it meets *P. vespertinus* (Mazanaeva and Askenderov 2007). Further east, it is present along the southern shores of the Caspian Sea in Iran (eastern limit in Golestan; Kamali and Malekzadeh 2013). IUCN status: Not Evaluated; considered Least Concern when grouped with *P. balcanicus* (Agasyan et al. 2009b).

Diversity. Using mtDNA and genomic data, Dufresnes et al. (2019b) evidenced a Pleistocene split between the Levant (*P. s. syriacus*) and the rest of the range (*P. s. boettgeri*; see below). Within both subspecies, populations are weakly differentiated despite their present-day fragmentation (see also Munwes et al. 2010 for *P. s. syriacus*). Populations from the Caucasus (*P. s. boettgeri*) differs from Anatolian ones at nuclear, but not mitochondrial markers. In the Lesser Caucasus and southern Turkey, *P. s. boettgeri* features traces of past gene flow with *P. s. syriacus*. Iranian populations have not been examined with genetic tools and could bear cryptic diversity.

Pelobates syriacus boettgeri Mertens, 1923

Anatolian spadefoot

Diagnosis. Similar to the nominal subspecies, notably in terms of cranial characters (Roček 1981) and coloration patterns (Fig. 4). Most biometric data on *P. syriacus* come from populations of *P. s. boettgeri* (Fig. 2, see above). As shown in Table 1, *P. s. boettgeri* differs from *P. s. syriacus* by 1.7% at mtDNA and 0.01% at nuclear DNA (Dufresnes et al. 2019b).

Taxonomy. The oldest nomen available for Anatolian/Caucasian spadefoots is ***Pelobates syriacus boettgeri* Mertens, 1923**; type locality: Belesuwar, southeastern Azerbaijan; holotype: SMF 1725 (originally 1437.2a, Mertens 1923). A single junior synonym. ***Pelobates transcaucasicus* Delwig, 1928**; type locality: "Tiflis" (Tbilisi), Georgia; types: ten syntypes, nine at ZISP, and one at ZIK (Amph A5/A (2164)). Subspecies level of *P. s. boettgeri* is granted by its phylogenetic divergence from *P. s. syriacus*, but the recent split (~1 My) and the widespread traces of admixture between both subspecies in Armenia, Turkey (Antalya region), and Israel argue against a specific status.

Distribution and diversity. See the accounts for *P. syriacus*.

Pelobates balcanicus Karaman, 1928

Balkan spadefoot

Diagnosis. Resembling *P. syriacus* with which it was previously considered a synonym (Frost 2019). Large toad with whitish metatarsal spades and a flat skull. Sexes of similar size (Fig. 2). Various motifs with gray, yellow or greenish colors, but rarely brown (unlike the sympatric *P. fuscus*, P. Székely pers. comm.); frequently specked with orange dots, sometimes heavily (perhaps more than in *P. syriacus*) (Fig. 4). Based on 25 biometric characters, Uğurtas et al. (2002) showed that the *P. balcanicus* populations from the Balkans are morphologically very variable and differentiated from Asia Minor (*P. syriacus*); yet *P. syriacus* populations from European Turkey (Edirne, genetically confirmed by Dufresnes et al. 2019b) and southeastern Bulgaria (Primorsko) grouped with *P. balcanicus* (Uğurtas et al. 2002). Roček (1981) only found one cranial difference: the *processus posterior parasphenoidei* is present in *P. syriacus* but

Table 1. Pairwise % of genetic differences between *Pelobates* taxa (from the data of Dufresnes et al. 2019b). The estimates below diagonal correspond to mitochondrial DNA (*cyt-b* + 16S, 1.2 kb); the estimates above diagonal correspond to nuclear DNA (63.5 kb of RAD tags).

	P. cultripes	*P. varaldii*	*P. fuscus*	*P. vespertinus*	*P. s. syriacus*	*P. s. boettgeri*	*P. b. balcanicus*	*P. b. chloeae*
P. cultripes	–	0.40	0.66	0.75	0.72	0.70	0.74	0.73
P. varaldii	6.0	–	0.83	0.92	0.89	0.88	0.92	0.90
P. fuscus	10.1	10.0	–	0.13	0.63	0.62	0.65	0.64
P. vespertinus	9.7	9.6	2.5	–	0.71	0.70	0.74	0.73
P. s. syriacus	9.1	8.6	9.1	8.9	–	0.01	0.32	0.30
P. s. boettgeri	9.2	8.9	9.2	9.0	1.7	–	0.31	0.29
P. b. balcanicus	9.2	8.6	8.5	8.5	7.2	7.0	–	0.02
P. b. chloeae	9.2	8.2	8.5	8.6	7.7	7.7	2.8	–

not developed in *P. balcanicus*. Morphometric assessments associated to genetic data are needed. Based on populations of *P. balcanicus balcanicus*, average SVL = 67 mm (48–100 mm) for females (*n* = 16 populations) and 68 mm (46–94 mm) for males (*n* = 15 populations) (Suppl. material 1, Table S1; Fig. 2). The karyotype (*P. b. balcanicus*) consists of six large and seven small pairs of two-armed chromosomes. NORs (secondary constrictions) are in the short arm of pair 7 (Belcheva et al. 1977). The nuclear DNA content (calculated from flow cytometry) averages 7.9 pg (Litvinchuk et al. 2013; data from *P. b. balcanicus*). As shown in Table 1, *P. balcanicus* differs from *P. syriacus* by ~7.4% at mtDNA and ~0.31% at nuclear DNA (Dufresnes et al. 2019b).

Taxonomy. Originally described as a subspecies of the Eastern spadefoot, ***Pelobates syriacus balcanicus* Karaman, 1928**; type locality: Dojran Lake, North Macedonia; type(s): most likely include the skeleton described by Karaman (1928), deposited at MMNH (Skopje, North Macedonia), but destroyed in an earthquake in 1963 (V. Sidorovska pers. comm.); the MMNH currently hosts one specimen from the type locality, MMNH-A-699 (collected in 2001). This taxon represents a distinct species from *P. syriacus*, due its old divergence (>6 My) and the absence of contemporary introgression at their area of contact in European Turkey, consistent with advanced reproductive isolation (Dufresnes et al. 2019b). Therefore, we herein remove *P. balcanicus* from its previous synonymy with *P. syriacus*.

Distribution. *Pelobates balcanicus* is restricted to the Balkan Peninsula, 0–920 m a.s.l. (Džukić et al. 2008) (Fig. 1). In the north, it is present in northern Serbia and northwestern Romania. It follows the Danube River from Serbia to the Black Sea in Romania (Székely et al. 2013; Ţeran et al. 2017). There are yet some possible gaps along the Danube (e.g. around the Iron Gate: Vukov et al. 2013; Ţeran et al. 2017). In the north-west, the Great Morova River in Serbia marks its western margin (Džukić et al. 2008). Northern ranges are currently disconnected from the southern populations (Vukov et al. 2013) of North Macedonia, eastern Albania (a single location), south-west Bulgaria (Strimon River), and Greece (Džukić et al. 2008; Mollov et al. 2006; Szabolcs and Mizsei 2017). In the 1980s, Sofianidou (2012) reported the species along the western coastline of the Adriatic Sea and the northern coastline of the Gulf of Corinth (Greece), but there is no recent observation in this region. Elsewhere

in Greece, it is present in Peloponnese (*P. balcanicus chloeae* ssp. nov., see below), in the eastern parts of the mainland, and along the Aegean Sea shores, from Sterea Ellas to the Evros River, until it reaches *P. syriacus* in Thrace (Džukić et al. 2008; Sofianidou, 2012). The spadefoots known from the Maritsa (Evros) River in southern Bulgaria, and along the western coasts of the Black Sea, may correspond to *P. syriacus* (Stojanov et al. 2011; Dufresnes et al. 2019b). IUCN status: Not Evaluated; previously included in *P. syriacus* assessment.

Diversity. Using mtDNA and genomic data, Dufresnes et al. (2019b) evidenced a Pleistocene split (~2 My) for spadefoots from the Peloponnese (*P. balcanicus chloeae* ssp. nov.). In the rest of the range, at least three glacial lineages (<1 My) were identified: a first one in the eastern ranges, from the Carpathians to the Black Sea and as south as Greek Thrace; a second one in western ranges from Serbia to northern Greece; and a third one on the coastal island of Evia (north-east of Peloponnese). The eastern and western lineages widely admix. Populations from central Greece are yet to be examined.

***Pelobates balcanicus chloeae* ssp. nov.**
http://zoobank.org/A1C08645-8307-49EF-A2EB-7F09D7BCC89D
Chloe's spadefoot

Type locality. Strofylia meadows, near the village of Metochi, Peloponnese, Greece (38.1239°N, 21.3858°E, 1 m a.s.l.). Coastal sandy meadows with shallow ponds (Fig. 5).

Holotype. NHMC 80.2.15.10, adult female captured on December 10th 2018 by CD, IS and ET at Strofylia meadows, Greece (38.1239°N, 21.3858°E, 1 m a.s.l.); subsequently deposited at the Natural History Museum of Crete (NHMC); mitochondrial *cyt-b* haplotype BAL19 (Dufresnes et al. 2019b). Full measurements are available in Table 2 and photographs in Figure 5. Large specimen (SVL = 78.7 mm) with the head narrower than the body, ending by a rounded snout; nostrils closer to each other's than from the eyes; forehead flat, as viewed from the side, with large interorbital; tympanum invisible; vomerine teeth present. Large, bulging eyes (7.2 mm of diameter) with vertical pupil and a dark-golden iris. Legs relatively short (92 mm), 1.2 times the size of the body. Five partially webbed toes; webbing formula: I 1-1+ II 1-2 III 1-2+ IV 3-1+ V; relative lengths from inner to outer toes: 4>3>5>2>1; large and long rounded (blade-shaped) metatarsal tubercle ("spade"), whitish; subarticular tubercles indistinct. Strong arms with four unwebbed fingers; palm tubercles visible, oval. Ventral and dorsal skins smooth, although the latter bears scattered warts. Coloration in life: ventrum glossy white, bluish near the limbs; dorsum light gray with prominent green-brown reticulated patches featuring orange dots, notably at the armpits; head darker, with a horizontal brown line running between the eyes. Changes of coloration in ethanol: dorsum less contrasted; fainted orange dots.

Table 2. Morphometric measurements (mm) of *Pelobates balcanicus chloeae* at the type locality (Strofylia meadows), based on 12 adults (both sexes combined), and detailed for the type specimens. SVL: snout-vent length; HW: head width; HL: head length; ED: eye diameter; EE: inter-eye distance; NN: inter-nostril distance; EN: eye-nostril distance; ML: metatarsal tubercle length; MH: metatarsal tubercle height; HLL: hind leg length; TTL: tibia + tarsus length.

	Strofylia population	Holotype NMHC 80.2.15.10	Paratype NMHC 80.2.15.11
SVL	71.5 ± 3.4	78.7	74.1
HW	23.7 ± 1.1	26.6	25.5
HL	21.8 ± 0.9	23.4	23.1
ED	7.4 ± 0.24	7.2	7.1
EE	15.9 ± 0.7	16.7	17.3
NN	4.4 ± 0.2	4.6	4.2
EN	6.0 ± 0.3	6.7	6.0
ML	6.1 ± 0.4	7.1	6.5
MH	2.6 ± 0.1	2.6	2.8
HLL	83.7 ± 3.6	92	90
TTL	64.2 ± 3.1	72	69

Paratype. NHMC 80.2.15.11, adult female captured on December 10th 2018 by CD, IS and ET at Strofylia meadows, Greece (38.1239°N, 21.3858°E, 1 m a.s.l.); subsequently deposited at the Natural History Museum of Crete (NHMC); mitochondrial *cyt-b* haplotype BAL20 (Dufresnes et al. 2019b). Full measurement and post-mortem pictures are provided in Table 2 and Figure 5, respectively.

Diagnosis. Supposedly similar morphologically to the nominal subspecies and reliably diagnosed only by molecular data. So far studied from the type locality only (Strofylia). Like the nominal subspecies, *Pelobates balcanicus chloeae* is a large spadefoot with whitish metatarsal spades, a flat skull and incomplete webbing on the hind feet (Fig. 4). It also shares general characteristics of the genus, i.e. stocky built, smooth skin and vertical pupil; males bear oval protuberances on the arms, absent in females. The dorsum coloration is generally light gray, sometimes yellow, covered with dark green-brown reticulate patches and variable orange dots (Fig. 4). From our own observations, the color patterns seem to slightly differ from the nominal subspecies (Fig. 4). In *P. b. chloeae*, the green patches are small and numerous (fewer but larger patches in the nominal subspecies); dots are usually orange (more reddish in the nominal subspecies) and located inside the green patches (randomly distributed in the nominal subspecies). The ventrum and limbs are glossy and slightly bluish (rather pale whitish in the nominal subspecies). Moreover the snout of *P. b. chloeae* appears shorter and blunter than the nominal subspecies. These suspicions will need to be assessed by formal phenotypic analyses. At the type locality, the SVL of adults averaged 71.5 mm (range: 62–84; *n* = 12 individuals, both sexes combined). The mating call and the tadpole are yet to be described and diagnosed. The karyotype has not been documented. As shown in Table 1, *P. b. chloeae* differs from the nominal subspecies by 2.8% at mtDNA and 0.02% at nuclear DNA (Dufresnes et al. 2019b).

Figure 5. Description of *Pelobates balcanicus chloeae*. **Top** live photograph of the holotype, NHMC 80.2.15.10 (CD, taken on December 10th 2018); **middle** dorsal and lateral views of the type specimens (**left** NHMC 80.2.15.10; **right** NHMC 80.2.15.11) post-mortem (IS); **bottom** Strofylia meadows, the type locality in Peloponnese, Greece (ET).

Taxonomic status. Following Dufresnes et al. (2019b), we raise the population(s) from the Peloponnese as a distinct *P. balcanicus* subspecies based on nuclear and mitochondrial phylogenetic data, but refrain a specific status from current data, due to the relatively young evolutionary divergence (~2 My) and potential introgression with the nominal subspecies.

Etymology. No name is available for spadefoots from the Peloponnese or Greece in general. We hence attribute it a new nomen, *Pelobates balcanicus chloeae*, as a reference to the young daughter of CD, Chloé, who played a decisive role in guiding his research towards European biogeography and herpetology. Moreover, "Chloé" is an ancient Greek name ("Χλόη") designating the young green grass spurring from the ground in spring, reminiscent of spadefoots unearthing themselves to breed in mass. The name is also associated with Dimitra (Δήμητρα), the Ancient Greek goddess of agriculture who protected traditional farmlands in which so many amphibians used to thrive.

Distribution. From current knowledge, this subspecies is endemic to the Peloponnese in southern Greece (Dufresnes et al. 2019b) (Fig. 1); it was so far genetically confirmed from its type locality only. Historically (1980s), there were records of spadefoots all over the Peloponnese, except in the three southern peninsulas (Böhme 1975; Eiselt 1988; Sofianidou 2012). Nowadays, the two known *Pelobates* localities are restricted to the central (Tripoli) and north-western (Strofylia) areas. Consequently, it is likely that there are only few populations left for this subspecies. It is not excluded that its range extends to Central Greece, where potential populations have not been examined; one sample from Kallithea Elassonos (Thessaly, Greece) bore trace of introgression by *P. b. chloeae*, suggesting past or present contact (Dufresnes et al. 2019b).

Ecology. Never studied as such, but this subspecies most likely shares a similar ecology as the nominal subspecies (*P. b. balcanicus*). Inhabits open, flat, lowland areas with soft sandy soil near shallow ponds or ditches with aquatic vegetation for breeding, as described for *P. balcanicus* (Dufresnes 2019). Mostly nocturnal and semi-fossorial: comes out of the ground for foraging and breeding during / right after heavy rains. Hence it can be observed in high numbers during winter-spring showers; ET counted >70 individuals (mostly juveniles) in 15 min of search in late-October 2018 at the type locality; usually active around 13–20 °C, but also as low as 7 °C (ET pers. obs.).

Diversity. Our *P. b. chloeae* samples featured the lowest nuclear genetic diversity recorded across the entire ranges of *P. balcanicus* and *P. syriacus* (Dufresnes et al. 2019b). This implies that the Strofylia population and perhaps the subspecies as a whole have been heavily bottlenecked. Two mtDNA haplotypes co-occur (Dufresnes et al. 2019b). Genetic studies are urgently needed to assess the range and diversity of this regional endemic.

Conservation Status – Ioannidis and Mebert (2011) mentioned road casualties at the type locality of this taxon, one of few extant populations. Although not evaluated yet, this taxon is clearly threatened according to IUCN criteria; given the narrow extent of occurrence (EOO), it should be listed as Critically Endangered (CR).

Identification key

Based on our updated overview of the taxonomy and distribution of *Pelobates*, we hereby provide a key to summarize the main discriminating features within this group. Because several taxa are cryptic and lack diagnostic phenotypic differences, geographic origin remains an essential information.

1 Black spades on the hind legs **2**
– Spades of light coloration **3**
2 Large body (6–9 cm) without orange dots, spades entirely black; Spain, Portugal and southern France ..... ***P. cultripes***
– Small body (<6 cm) with orange dots, spades bordered with black; Morocco ..... ***P. varaldii***
3 Domed skull, developed webbing, and small body (<6 cm) **4**
– Flat skull, partial webbing, and large body (6–8 cm) **5**
4 Dorsum stripes rare; Central and northwestern Europe, west of a Crimea–Moscow imaginary line ..... ***P. fuscus***
– Three dorsum stripes often present; Eastern Europe and Central Asia, east of a Crimea–Moscow imaginary line ..... ***P. vespertinus***
5 Levantine region (Israel, Lebanon, and Syria) ..... ***P. syriacus syriacus***
– Caucasus and Caspian Sea shores, Anatolia, and European Turkey ..... ***P. syriacus boettgeri***
– Balkan Peninsula, except Peloponnese ..... ***P. balcanicus balcanicus***
– Peloponnese ..... ***P. balcanicus chloeae***

Conclusions

Our phylogeographic analyses of *Pelobates* (Dufresnes et al. 2019b) called for a taxonomic reassessment of this threatened amphibian group. We reviewed the evidence for distinct Moroccan (*P. varaldii*), Iberian (*P. cultripes*), Central (*P. fuscus*), and Eastern European (*P. vespertinus*) species. Furthermore, we revised the taxonomy of *P. syriacus* by distinguishing two cryptic species, *P. syriacus* and *P. balcanicus*, and by considering their strong intraspecific diversity into subspecific divisions, *P. s. syriacus*, *P. s. boettgeri*, *P. b. balcanicus*, and *P. b. chloeae*, the latter as a newly described taxon. Their variation in size and coloration are detailed and illustrated, based on a literature review and high-quality photographs, respectively. Finally, our paper provides up-to-date whole-range distribution maps for all extant *Pelobates* taxa.

Acknowledgements

We thank M. Pajković for translating publications from Serbo-Croatian, P. Lymberakis (NHMC) for processing the type series of *P. b. chloeae*, A. Nöllert, G. Haimovitch, G.

Martinez, and A. Sanchez Vialas for sharing their pictures, P.-A. Crochet for taxonomic advices and Nicolas Perrin for support. We are also grateful to T. Vukov, O. Zinenko, A. Ohler, L. Ceriaco, and A. Crottini, as well as an anonymous reviewer, for their expertise and useful feedback. M.D. is Research Director at Fonds de la Recherche scientifique (FNRS). This study was founded by a grant from the Swiss National Science Foundation (SNSF) to Nicolas Perrin (no. 31003A_166323), and a SNSF fellowship to CD (no. P2LAP3_171818).

References

Agasyan A, Avci A, Tuniyev B, Isailovic JC, Lymberakis P, Andrén C, Cogălniceanu D, Wilkinson J, Ananjeva N, Uzüm N (2009a) *Pelobates fuscus*. The IUCN Red List of Threatened Species: eT16498A5951455. https://doi.org/10.2305/IUCN.UK.2009.RLTS.T16498A5951455.en

Agasyan A, Tuniyev B, Crnobrnja-Isailovic J, Lymberakis P, Andrén C, Cogălniceanu D, Wilkinson J, Ananjeva N, Üzüm N, Orlov N, Podloucky R, Tuniyev S, Kaya U (2009b) *Pelobates syriacus*. The IUCN Red List of Threatened Species 2009: eT58053A11723660. https://doi.org/10.2305/IUCN.UK.2009.RLTS.T58053A11723660.en

Andreone F (2006) *Pelobates fuscus* (Laurenti, 1768). In: Sindaco R, Doria G, Razzetti E, Bernini F (Eds) Atlanti degli anfibi e dei rettili d'Italia Atlas of Italian amphibians and reptiles. Edizioni Polistampa, Firenze, 292–297.

Bauwens D, Claus K (1996) Verspreiding van Amfibieën en Reptielen in Vlaanderen. De Wielewaal Natuurvereniging, Turnhout, 192 pp.

Belcheva R, Ilieva H, Beshkov V (1977) On the karyotype of *Pelobates syriacus balcanicus* Karaman (Amphibia, Pelobatidae, Anura). Annuaire de l'Universite de Sofia, Faculté de Biologie, Livre 1 – Zoologie 68: 15–18.

Beja P, Bosch J, Tejedo M, Lizana M, Martinez Solano I, Salvador A, García París M, Recuero Gil E, Pérez Mellado V, Díaz-Paniagua C (2009) *Pelobates cultripes*. The IUCN Red List of Threatened Species 2009: eT58052A86242868. https://doi.org/10.2305/IUCN.UK.2009.RLTS.T58052A11722636.en

Beukema W, De Pous P, Donaire-Barroso D, Bogaerts S, Garci-Port J, Escoriza D, Arribas OJ, El Mouden EH, Carranza S (2013) Review of the systematics, distribution, biogeography and natural history of Moroccan amphibians. Zootaxa 3661: 1–60. https://doi.org/10.11646/zootaxa.3661.1.1

Bitz A, König H, Simon L (1996) Knaublauchkröte – *Pelobates fuscus* (Laurenti, 1768). In: Bitz A, Fischer K, Simon L, Thiele R, Veith M (Eds) Die Amphibien und Reptilien in Rheinland-Pfalz. GNOR, Landau, 165–182.

Blackburn DC, Scali S (2014) An annotated catalog of the type specimens of Amphibia in the collection of the Museo Civico di Storia Naturale, Milan, Italy. Herpetological Monographs 28: 24–45. https://doi.org/10.1655/HERPETOLOGICA-D-13-00008

Boettger O (1889) Ein neuer *Pelobates* aus Syrien. Zoologischer Anzeiger 12: 144–147.

Boettger O (1892) Katalog der Batrachier-Sammlung im Museum der Senckenbergischen Naturforschenden Gesellshaft in Frankfurt am Main. Gebrüder Knauer, Frankfurt am Main, 48.

Böhme W (1975) Zur Vorkommen von *Pelobates syriacus* in Griechenland. Senckenbergiana Biologica 56: 199–202.

Borkin LJ, Litvinchuk SN, Rosanov JM, Milto KD (2001) Cryptic speciation in *Pelobates fuscus* (Anura, Pelobatidae): evidence from DNA flow cytometry. Amphibia-Reptilia 22: 387–396. https://doi.org/10.1023/A:1018806900399

Busack SD, Maxson LR, Wilson MA (1985) *Pelobates varaldii* (Anura: Pelobatidae): A morphologically conservative species. Copeia 1985: 107–112. https://doi.org/10.2307/1444797

Cabela A, Grillitsch H, Tiedemann F (2001) Atlas zur Verbreitung und Ökologie der Amphibien und Reptilien in Österreich. Umweltbundesamt, Wien, 880 pp.

Chmela C, Kronshage A (2011) Knoblauchkröte – *Pelobates fuscus*. In: Hachtel M, Schlüpmann M, Weddeling K, Thiesmeier B, Geiger A, Willigalla C (Eds) Handbuch der Amphibien und Reptilien Nordrhein-Westfalens Band 1. Laurenti Verlag, Bielefeld, 543–582.

Coates DJ, Byrne M, Moritz C (2018) Genetic diversity and conservation units: dealing with the species-population continuum in the age of genomics. Frontiers in Ecology & Evolution 6: 165. https://doi.org/10.3389/fevo.2018.00165

Cornalia EBM (1873) Observazioni sul *Pelobates fuscus* e sulla *Rana agilis* trovate in Lombardia. Atti della Societa Italiana di Scienze Naturali e del Museo Civico di Storia Naturale di Milano 16: 97–107.

Creemers RCM, van Delft JJCW (2009) De amfibieën en reptielen van Nederland. Nationaal Natuurhistorisch Museum Naturalis, Leiden, 476 pp.

Crochet P-A, Dubois A (2004) Recent changes in the taxonomy of European amphibians and reptiles. In: Gasc J-P, Cabela A, Crnobrnja-Isailovic J, Dolmen D, Grossenbacher K, Haffner P, Lescure J, Martens H, Martínez Rica JP, Maurin H, Oliveira ME, Sofianidou TS, Veith M, Zuiderwijk A (Eds) Atlas of Amphibians and Reptiles in Europe (2nd edn). Societas Herpetologica Europeae and Museum National Histoire Naturelle, Paris, 495–516.

Crottini A, Andreone F, Kosuch J, Borkin L, Litvinchuk SN, Eggert C, Veith M (2007) Fossorial but widespread: the phylogeography of the common spadefoot toad (*Pelobates fuscus*), and the role of the Po Valley as a major source of genetic variability. Molecular Ecology 16: 2734–2754. https://doi.org/10.1111/j.1365-294X.2007.03274.x

Crottini A, Galan P, Vences M (2010) Mitochondrial diversity of western spadefoot toads, *Pelobates cultripes*, in northwestern Spain. Amphibia-Reptilia 31: 443–448. https://doi.org/10.1163/156853810791769527

Curić A, Zimić A, Bogdanović T, Jelić D (2018) New data and distribution of common spadefoot toad *Pelobates fuscus* (Laurenti, 1768) (Anura: Pelobatidae) in Western Balkans. North-Western Journal of Zoology 14: 50–59.

Cuvier G (1829) Le règne animal distribué d'après son organisation, pour servir de base à l'histoire naturelle des animaux et d'introduction à l'anatomie comparée. Vol. 2. Déterville, Paris, 406 pp.

de Pous P, Beukema W, Dingemans D, Donaire D, Geniez P, El Mouden EH (2012) Distribution review, habitat suitability and conservation of the endangered and endemic Moroccan spadefoot toad (*Pelobates varaldii*). Basic and Applied Herpetology 26: 57–71. https://doi.org/10.11160/bah.11015

Delwig, W (1928) Eine neue Art der Gattung *Pelobates* Wagl. aus dem zentralen Transkaukasus. Zoologischer Anzeiger 75: 24–31.

Disi AM, Amr ZS (2010) Morphometrics, distribution and ecology of the amphibians in Jordan. Vertebrate Zoology 60: 147–162.

Dufresnes C (2019) Amphibians of Europe, North Africa and the Middle East. Bloomsbury, London, 224 pp.

Dufresnes C, Mazepa G, Rodrigues N, Brelsford A, Litvinchuk SN, Sermier R, Lavanchy G, Betto-Colliard C, Blaser O, Borzée A, Cavoto E, Fabre G, Ghali K, Grossen C, Horn A, Leuenberger J, Philips BC, Saunders PA, Savary R, Maddalena T, Stöck M, Dubey S, Canestrelli D, Jeffries DL (2018) Genomic evidence for cryptic speciation in tree frogs from the Apennine Peninsula, with description of *Hyla perrini* sp. nov. Frontiers in Ecology and Evolution 6: 144. https://doi.org/10.3389/fevo.2018.00144

Dufresnes C, Beddek M, Skorinov DV, Fumagalli L, Perrin N, Crochet P-A, Litvinchuk SN (2019a) Diversification and speciation in tree frogs from the Maghreb (*Hyla meridionalis sensu lato*), with description of a new African endemic. Molecular Phylogenetics and Evolution 134: 291–299. https://doi.org/10.1016/j.ympev.2019.02.009

Dufresnes C, Strachinis I, Suriadna N, Mykytynets G, Cogălniceanu D, Székely P, Vukov T, Arntzen JW, Wielstra B, Lymberakis P, Geffen E, Gafny S, Kumlutas Y, Ilgaz C, Candan K, Mizsei E, Szabolcs M, Kolenda K, Smirnov N, Geniez P, Lukanov S, Crochet P-A, Dubey S, Perrin N, Litvinchuk S, Denoël M (2019b) Phylogeography of a cryptic speciation continuum in Eurasian spadefoot toads (*Pelobates*). Molecular Ecology. https://doi.org/10.1111/mec.15133

Džukić G, Beškov V, Sidorovska V, Cogălniceanu D, Kalezić M (2005) Historical and contemporary ranges of the spadefoot toads *Pelobates* spp. (Amphibia: Anura) in the Balkan Peninsula. Acta Zoologica Cracoviensia 48A: 1–9. https://doi.org/10.3409/173491505783995699

Džukić G, Beškov V, Sidrovska V, Cogălniceanu D, Kalezić ML (2008) Contemporary chorology of the spadefoot toads (*Pelobates* spp.) in the Balkan Peninsula. Zeitschrift fur Feldherpetologie 15: 61–78.

Eggert C, Cogălniceanu D, Veith M, Džukić G, Taberlet P (2006) The declining spadefoot toad, *Pelobates fuscus* (Pelobatidae): paleo and recent environmental changes as a major influence on current population structure and status. Conservation Genetics 7: 185–195. https://doi.org/10.1007/s10592-006-9124-y

Eggert C, Vacher J-P (2012) *Pelobates fuscus* (Laurenti, 1768). Pélobate brun. In: Lescure J, de Massary JC (Eds) Atlas des amphibiens et reptiles de France. Biotope, Mèze and Muséum national d'Histoire naturelle, Paris, 102–103.

Ehl S, Vences M, Veith M (2019) Reconstructing evolution at the community level: a case study on Mediterranean amphibians. Molecular Phylogenetics & Evolution 134: 211–225. https://doi.org/10.1016/j.ympev.2019.02.013

Eiselt J (1988) Krötenfrösche (*Pelobates* gen., Amphibia Salienta) in Türkisch-Thrakien und Griechenland. Annalen des Naturhistorischen Museums in Wien 90: 51–59.

Frost D (2019) Amphibian Species of the World: an Online Reference. Version 6.0 (30 January 2019). American Museum of Natural History, New York. http://research.amnh.org/herpetology/amphibia/index.html [Accessed on: 2019-3-1]

Garcia-Paris M, Buchholz DR, Parra-Olea G (2003) Phylogenetic relationships of Pelobatidae re-examined using mtDNA. Molecular Phylogenetics and Evolution 28: 12–23. https://doi.org/10.1016/S1055-7903(03)00036-8

Gutiérrez-Rodriguez J, Barbosa AM, Martinez-Solano I (2017) Present and past climatic effects on the current distribution and genetic diversity of the Iberian spadefoot toad (*Pelobates cultripes*): an integrative approach. Journal of Biogeography 44: 245–258. https://doi.org/10.1111/jbi.12791

Herón-Royer L-F (1888) Description du *Pelobates latifrons* des environs de Turin, et d'une conformation particuliere de l'ethmoide chez le batraciens. Bulletin de la Société Zoologique de France 13: 85–91. https://doi.org/10.5962/bhl.part.8060

Herrero P, Talavera RR (1988) Cytotaxonomic studies on Iberian and Moroccan *Pelobates* (Anura: Pelobatidae). Acta Zoologica Cracoviensia 31: 505–508.

Ioannidis Y, Mebert KJM (2011) Habitat preferences of *Natrix tessellata* at Strofylia, northwestern Peloponnese, and comparison to syntopic *N. natrix*. Mertensiella 18: 302–310.

Iosif R, Papes M, Samoila C, Cogălniceanu D (2014) Climate-induced shifts in the niche similarity of two related spadefoot toads (genus *Pelobates*). Organisms Diversity and Evolution 14: 397–408. https://doi.org/10.1007/s13127-014-0181-7

Kamali K, Malekzadeh S (2013) A record of *Pelobates syriacus* Boettger, 1889 (Anura: Pelobatidae) in northern Iran. Russian Journal of Herpetology 20: 238–240.

Karaman S (1928) III Prilog herpetologii Jugoslavije – Contribution a l'Herpètologie de la Jugoslavija. Bulletin de la Société Scientifique de Skoplje, Section des Sciences Naturelles 4: 129–143.

Khosatzky LI (1985) Novy' vyd chesnochnyls iz Pliocena Modavii. In: Negadaev-Niknov KN (Ed.) [Fauna and Flora of Late Caenozoic Moldavia]. Akademia Nauk Moldavkoi SSR Shitiintsa, 59–72.

Koch C (1872) Formen und Wandlungen der ecaudaten Batrachier des Unter-Main und Lahn-Gebietes. Bericht der Senckenbergischen Naturforschenden Gesellschaft in Frankfurt am Main 1871–72: 122–183.

Kuzmin SL (1999) The amphibians of the former Soviet Union. Pensoft Publisher, Sofia, 538 pp.

Lada GA, Borkin LJ, Litvinchuk SN (2005) Morphological variation in two cryptic forms of the common spadefoot toad (*Pelobates fuscus*) from eastern Europe. In: Ananjeva N, Tsinenko O (Eds), Herpetologia Petropolitana, St. Petersburg, 53–56.

Laurenti JN (1768) Specimen medicum exhibens synopsin reptilium emendatam cum experimentis circa venena et antidota reptilium austriacorum. Johann Thomas von Trattner, Vienna, 214 pp. https://doi.org/10.5962/bhl.title.5108

Litvinchuk SN, Crottini A, Federici S, De Pous P, Donaire D, Andreone F, Kalezić ML, Džukić G, Lada GA, Borkin LJ, Rosanov JM (2013) Phylogeographic patterns of genetic diversity in the common spadefoot toad, *Pelobates fuscus* (Anura: Pelobatidae), reveals evolutionary history, postglacial range expansion and secondary contact. Organisms Diversity and Evolution, 13: 433–451. https://doi.org/10.1007/s13127-013-0127-5

Lizana M (1997) *Pelobates cultripes* (Cuvier, 1829). In: Pleguezelos JM (Ed.) Distribucion y biogeografia de los anfibios y reptiles en España y Portugal. Editorial Universidad de Granada, Granada, 140–142.

Malkmus R (2004) Amphibians and reptiles of Portugal, Madeira and the Azores-Archipelago. Ganter Verlag K.G., Ruggell, 448 pp.

Manilo VV, Radchenko VI (2004) Comparative karyological research of the «western» form of the common spadefoot, *Pelobates fuscus* (Amphibia, Pelobatidae), from Kyivska, Chernigivska and Zakarpatska Region of Ukraine. Vestnik Zoologii 38: 91–94.

Manilo VV, Radchenko VI (2008) Karyological research of ecaudatas amphibians faunae of Ukraine. Proceeding of the Ukrainian Herpetological Society 1: 29–38.

Manilo VV, Manuilova ON (2013) Comparative karyological research of two species of spadefoot toads *Pelobates fuscus* and *P. vespertinus* (Pelobatidae, Anura, Amphibia) from territory of Ukraine. Zbirnyk Prac' Zoologichnogo Muzeyu 44: 109–115.

Mazanaeva LF, Askenderov AD (2007) New data on the distribution of eastern spadefoot, *Pelobates syriacus* Boettger, 1889 and common spadefoot, *Pelobates fuscus*, Laurenti, 1768 in Dagestan (the North Caucasus). Russian Journal of Herpetology 14: 161–166

Mertens R (1923) Beiträge zur Kenntnis der Gattung *Pelobates* Wagler. Senckenbergiana, 118–128.

Mertens R, Müller L (1928) Liste der Amphibien und Reptilien Europas. Abhandlungen der Senckenbergischen Naturforschenden Gesellschaft 41: 1–62.

Mertens, R (1967) Die herpetologische Sektion des Natur-Museums und Forschungs-Institutes Senckenberg in Frankfurt a. M. nebst einem Verseichnis ihrer Typen. Senckenbergiana Biologica 48: 1–106.

Mészáros B (1973) Critical studies on karyotypes of eight anuran species from Hungary and some problems concerning the evolution of the Order. Acta Biologica Debrecina 10–11: 151–161.

Michahelles, C (1830) Neue südeuropäische Amphibien. Isis von Oken 23: 806–809.

Milto KD, Barabanov AV (2011) An annotated catalogue of the amphibian types in the collection of the Zoological Institute, Russian Academy of Sciences, St. Petersburg. Russian Journal of Herpetology 18: 137–153.

Mollov I, Popgeorgiev G, Naumov B, Georgiev D (2006) New data on the distribution of the Syrian Spadefoot (*Pelobates syriacus balcanicus* Karaman, 1928) in Bulgaria. Scientific Researches of the Union of Scientists in Bulgaria-Plovdiv, Series B Natural Sciences and the Humanities 8: 132–136. [in Bulgarian]

Morescalchi A (1967) The close karyological affinities between a *Ceratophrys* and *Pelobates* (Amphibia, Salientia). Experientia 23: 1071–1072. https://doi.org/10.1007/BF02136458

Morescalchi A (1971) Comparative karyology of the Amphibia. Bolletino di Zoologia 38: 317–320. https://doi.org/10.1080/11250007109429162

Morescalchi A, Olmo E, Stingo V (1977) Trends of karyological evolution in pelobatoid frogs. Experientia 33: 1577–1578. https://doi.org/10.1007/BF01934007

Müller J (1832) Ueber drey verschiedene Familien der froschartigen Thiere nach dem Bau der Gehörwerkzeuge. Isis von Oken 25: 536–539.

Munwes I, Geffen E, Roll U, Friedmann A, Daya A, Tikochinski Y, Gafny S (2010) The change in genetic diversity down the core-edge gradient in the eastern spadefoot toad (*Pelobates syriacus*). Molecular Ecology 19: 2675–2689. https://doi.org/10.1111/j.1365-294X.2010.04712.x

Nöllert A, Günther R (1996) Knoblauchkröte – *Pelobates fuscus* (Laurenti, 1768). In: Günther R (Ed.) Die Amphibien und Reptilien Deutschlands. Gustav Fisher, Jena, 252–274.

Nöllert A, Grossenbacher K, Laufer H (2012) *Pelobates fuscus* (Laurenti, 1768) – Syrische Schaufelkröte. In: Grossenbacher K (Ed.) Handbuch der Reptilien und Amphibien Europas Bd 51 Froschlurche I. Aula, Wiebelsheim, 465–562.

Nyström P, Birkedal L, Dahlberg C, Brönmark C (2002) The declining spadefoot toad *Pelobates fuscus*: calling site choice and conservation. Ecography 25: 488–498. https://doi.org/10.1034/j.1600-0587.2002.250411.x

Nyström P, Hansson J, Månsson J, Sundstedt M, Reslow C, Broström A (2007) A documented amphibian decline over 40 years: possible causes and implications for species recovery. Biological Conservation 138: 399–411. https://doi.org/10.1016/j.biocon.2007.05.007

Pallas PS (1771) Reise durch verschiedene Provinzen des russischen Reichs. Gedruckt bey der Kayserlichen Academie der Wissenschaften, St. Petersburg, 504 pp.

Pasteur G, Bons J (1959) Les batraciens du Maroc. Travaux de l'Institut Scientifique Chérifien. Série Zoologique 17, Rabat, 241 pp.

Psonis N, Antoniou A, Karameta E, Leaché AD, Kotsakiozi P, Darriba D, Kozlov A, Stamatakis A, Poursanidis D, Kukushkin O, Jablonski D, Crnobrnja-Isailovic J, Gherghel I, Lymberakis P, Poulakakis, N (2018) Resolving complex phylogeography patterns in the Balkan Peninsula using closely related wall-lizard species as a model system. Molecular Phylogenetics and Evolution 125: 100–115. https://doi.org/10.1016/j.ympev.2018.03.021

Roček Z (1981) Cranial anatomy of the frogs of the family Pelobatidae Stannius, 1856, with outlines of their phylogeny and systematics. Acta Univesitatis Carolinae – Biologica 1980: 164 pp.

Rodriguez A, Burgon JD, Lyra M, Irisarri I, Baurain D, Blaustein L, Göcmen B, Künzel S, Mable BK, Nolte AW, Veith M, Steinfartz S, Elmer KR, Philippe H, Vences M (2017) Inferring the shallow phylogeny of true salamanders (*Salamandra*) by multiple phylogenomic approaches. Molecular Phylogenetics and Evolution 115: 16–26. https://doi.org/10.1016/j.ympev.2017.07.009

Rösel von Rosenhof AJ (1758) Historia Naturalis Ranarum Nostratium in Qua Omnes earum Proprietates Præsertim quæ ad Generationem Ipsarum Pertinent, Fusius Enarrantur / Die natürliche Historie der Frösche hiesigen Landes, Albrecht von Haller, Nürnberg, 115 pp. https://doi.org/10.5962/bhl.title.149946

Salvador A, Donaire-Barroso D, Slimani T, El Mouden EH, Geniez P (2009) *Pelobates varaldii*. The IUCN Red List of Threatened Species 2009: eT58054A11723994. https://doi.org/10.2305/IUCN.UK.2004.RLTS.T58054A11723994.en

Schmid M (1979) On the arrangement of chromosomes in the elongated sperm nuclei of Anura (Amphibia). Chromosoma 75: 215–234. https://doi.org/10.1007/BF00292209

Schmid M (1980) Chromosome banding in Amphibia. IV. Differentiation of GC- and AT-Rich chromosome regions in Anura. Chromosoma 77: 83–103. https://doi.org/10.1007/BF00292043

Schmid M (1982) Chromosome banding in Amphibia. VII. Analysis of the structure and variability of NORs in Anura. Chromosoma 87: 327–344. https://doi.org/10.1007/BF00327634

Schmid M, Vitelli I, Batistoni R (1987) Chromosome banding in Amphibia. XI. Constitutive heterochromatin, nucleolus organizers, 18S + 28S and 5S ribosomal RNA genes in

Ascaphidae, Pipidae, Discoglossidae and Pelobatidae. Chromosoma 95: 271–284. https://doi.org/10.1007/BF00294784

Severtsov N (1855) Periodic Phenomena in the Life of Animals of Voronezh Governorate. Moscow, 385-386. [in Russian]

Shaw G (1802) General Zoology or Systematic Natural History. Volume III, Part 1. Amphibia. London: Thomas Davison.

Sillero N, Campos J, Bonardi A, Corti C, Creemers R, Crochet P-A, Crnobrnja Isailović J, Denoël M, Ficetola GF, Gonçalves J, Kuzmin S, Lymberakis P, de Pous P, Rodríguez A, Sindaco R, Speybroeck J, Toxopeus B, Vieites DR, Vences M (2014) Updated distribution and biogeography of amphibians and reptiles of Europe. Amphibia-Reptilia 35: 1–31. https://doi.org/10.1163/15685381-00002935

Singhal S, Moritz C (2013) Reproductive isolation between phylogeographic lineages scales with divergence. Proceedings of the Royal Society B: Biological Sciences 280: 20132246. https://doi.org/10.1098/rspb.2013.2246

Sofianidou T (2012) *Pelobates syriacus* (Boetger, 1899)—Syrische Schaufelkröte. In: Grossenbacher K (Ed.) Handbuch der Reptilien und Amphibien Europas Bd 51 Froschlurche I. Aula, Wiebelsheim, 563–620.

Stojankov A, Tzankov N, Naumov B (2011) Die Amphibien und Reptilien Bulgariens. Chimaira, Frankfurth am Main, 588 pp.

Strachinis I, Roussos SA (2016) Terrestrial herpetofauna of Limnos and Agios Efstratios (Northern Aegean, Greece), including new species records for *Malpolon insignitus* (Geoffroy Saint-Hilaire, 1827) and *Pelobates syriacus* Boettger, 1889. Herpetology Notes 9: 237–248.

Sturm J (1828) Deutschlands Fauna. III. Abtheilung. Die Amphibien. Nürnberg, 36

Suriadna NN (2014) Comparative analysis of karyotypes of two cryptic species of pelobatid frogs (Amphibia, Anura) of Ukraine. Vestnik Zoologii 48: 511–520. https://doi.org/10.2478/vzoo-2014-0061

Suriadna NN, Mikitinets GI, Rozanov YuM, Litvinchuk SN (2016) Distribution, morphological variability and peculiarities of biology of spadefood toads (Amphibia, Anura, Pelobatidae) in the south of Ukraine. Zbirnyk Prac' Zoologichnogo Muzeyu 47: 67–87.

Szabolcs IM, Mizsei E (2017) First record of the eastern spadefoot toad (*Pelobates syriacus* Boettger, 1889) in Albania. NorthWestern Journal of Zoology 13: 175–176.

Székely P, Iosif R, Székely D, Stănescu F, Cogălniceanu D (2013) Range extension for the Eastern spadefoot toad *Pelobates syriacus* (Boettger, 1889) (Anura: Pelobatidae). Herpetology Notes 6: 481–484.

Székely D, Cogălniceanu D, Székely P, Denoël M (2017) Out of the ground: two coexisting fossorial toad species differ in their emergence and movement patterns. Zoology 121: 49–55. https://doi.org/10.1016/j.zool.2016.12.003

Ţeran L, Sos T, Hegyeli Z, Gábos E, Fülöp T, Marton A (2017) New data on the distribution of Eastern spadefoot toad *Pelobates syriacus* Boettger, 1889 (Anura: Pelobatidae) in the Pannonian Plain. North-Western Journal of Zoology 13: 179–182.

Thirion J-M, Cheylan M (2012) *Pelobates cultripes* (Cuvier, 1829). Pélobate cultripède. In: Lescure J, de Massary JC (Eds) Atlas des amphibiens et reptiles de France. Biotope – Muséum national d'Histoire naturelle, Mèze & Paris, France, 100–101.

Tschudi JJ (1838) Classification der Batrachier mit Berücksichtigung der fossilen Thiere dieser Abtheilung der Reptilien. Neuchâtel: Petitpierre, 99 pp. https://doi.org/10.5962/bhl.title.4883

Uğurtas IH (2001) Variation in *Pelobates syriacus* of Turkey. Asiatic Herpetological Research 9: 139–141.

Uğurtaş IH, Tunca B, Aydemir N, Bilaloğlu R (2001) A cytogenetic study on the *Pelobates syriacus* (Amphibia, Anura) in Bursa-Turkey. Turkish Journal of Zoology 25: 159–161. https://doi.org/10.1560/UMHA-6J3N-FUG9-D7EV

Uğurtas IH, Ljubusavljevic K, Sidorovska V, Kalezic ML, Džukić G (2002) Morphological differentiation of eastern spadefoot toad (*Pelobates syriacus*) populations. Israel Journal of Zoology 48: 13–32.

Veith M, Fromhage L, Kosuch J, Vences M (2006) Historical biogeography of Western Palaearctic pelobatid and pelodytid frogs: a molecular phylogenetic perspective. Contribution to Zoology 75: 109–120. https://doi.org/10.1163/18759866-0750304001

Vukov T, Kalezić ML, Tomović L, Krizmanić I, Jović D, Labus N, Džukić G (2013) Amphibians in Serbia: distribution and diversity patterns. Bulletin of the Natural History Museum 6: 90–112. https://doi.org/10.5937/bnhmb1306090V

Zagorodniuk I (2003) Species of the lower tetrapodes from Ukraine: in the nature and on the paper. Visnyk of L'viv University, Biology Series, L'viv, 33: 80–90. [in Ukrainian]

Supplementary material 1

Average snout-vent length in *Pelobates* populations

Authors: Christophe Dufresnes, Ilias Strachinis, Elias Tzoras, Spartak N. Litvinchuk, Mathieu Denoël

Data type: measurement

Link: https://doi.org/10.3897/zookeys.859.33634.suppl1